ELECTROPHYSIOLOGICAL STUDIES OF INTRAMURAL NEURONES FROM THE MAMMALIAN HEART AND AIRWAYS

A thesis submitted to the University of London
for the Degree of Doctor of Philosophy
in the Faculty of Science

by

Timothy G.J. Allen B.Sc. (Hons.), M.Sc. (Dist.)
Department of Anatomy and Developmental Biology
University College London

January 1990

ProQuest LLC.
789 East Eisenhower Parkway
P.O. Box 1346
Ann Arbor, MI 48106 – 1346

ABSTRACT

This thesis reports the electrophysiological and neurochemical characteristics of intramural neurones from ganglia of the rat trachea in situ, and from the atria and interatrial septum of the guinea-pig heart in culture. On the basis of their firing characteristics, three different types of intracardiac neurones could be distinguished. Two of these cell types, consisting of 65-75% of the neurones studied, had tetrodotoxin (TTX) -resistant calcium-dependent components to their action potentials and pronounced after-hyperpolarizations following spike discharge. Both cell types were highly refractory, but could be distinguished by whether they fired a single (AH_s cells) or a short burst of action potentials (AH_m cells) in response to current stimulation. A third type of intracardiac neurone (M cells), consisting of 10-15% of the cells studied, had TTX-sensitive spikes, fired tonically and had no significant after-hyperpolarization. The firing characteristics of paratracheal neurones ranged between two extremes. At one extreme, the cells fired tonically at low frequencies, whilst at the other, cells fired high frequency, repetitive bursts of action potentials. All paratracheal neurones displayed calcium-dependent action potentials and after-hyperpolarizations, however the after-hyperpolarization only became pronounced following a train of action potentials. All paratracheal neurones and many AH type intracardiac neurones displayed marked inward and outward rectification in their current-voltage relationships. This largely resulted from activation of time- and voltage-dependent inward rectifier and M-currents.

The neurochemical differentiation of the cells in the two preparations was examined by exogenous application of various neurotransmitters. In AH type intracardiac neurones, M_1 and M_2 muscarinic receptor activation induced changes in up to four different membrane conductances. These included the inhibition of a

voltage-sensitive calcium conductance; inhibition of the M-current; an increase in resting potassium conductance and an increase in a conductance of unknown ionic nature. The effects of exogenous application of purine compounds to intracardiac neurones were also investigated. Adenosine, acting via P_1-purinoceptors, inhibited the current underlying the after-hyperpolarization in AH type cells. Adenosine 5'-triphosphate (ATP), acting via P_2-purinoceptors, activated a mixed sodium- and calcium-dependent conductance in 41% of M and 43% of AH type cells. In a further 31% of AH type cells, ATP produced a multi-component response consisting of a transient, chloride-dependent inward current, followed by a potassium-dependent outward current and a slow prolonged inward current of unknown ionic nature. The effects of ionophoretic and bath application of γ-aminobutyric acid (GABA) to rat paratracheal neurones were investigated. GABA, acting via $GABA_A$ receptors, induced an increase in membrane chloride conductance resulting in membrane depolarization in over 90% of paratracheal neurones studied.

CONTENTS

LIST OF FIGURES

Page

ACKNOWLEDGEMENTS

I would like to thank my supervisor, Professor G. Burnstock, for his support and infectious enthusiasm and for the considerable degree of scientific freedom he has allowed me during the course of this work. In addition, I would like to thank Dr. Candace Hassall, Miss Doreen Bailey, Miss Miriam Windsor and Mr Eamonn Moules for growing the vast majority of the cultures used in these studies and Mr Kevin Farnan for workshop technical assistance. I would also like to thank other members of the group, past and present, for their friendship which has made working in the department so enjoyable.

Finally, I would like to thank Candace Hassall for all her help and for generally putting up with me during the writing of this thesis.

This work was supported by grants from the British Heart Foundation, the Asthma Research Council and the Medical Research Council.

PUBLICATIONS ARISING FROM THE WORK PRESENTED IN THIS THESIS

Allen, T.G.J. & Burnstock, G. (1987). Intracellular studies of the electrophysiological properties of cultured intracardiac neurones of the guinea-pig. Journal of Physiology 388, 349-366.

Burnstock, G., Allen, T.G.J., Hassall, C.J.S. & Pittam, B.S. (1987). Properties of intramural neurones cultured from the heart and bladder. In Histochemistry and Cell Biology of Autonomic Neurons and Paraganglia, Experimental Brain Research Series 16, ed. Heym, C., pp. 323-328. Berlin, Heidelberg, New York, London, Paris, Tokyo: Springer-Verlag.

Burnstock, G., Allen, T.G.J. & Hassall, C.J.S. (1987). The electrophysiological and neurochemical properties of paratracheal neurones in situ and in dissociated cell culture. American Review of Respiratory Disease 136, 523-526.

Allen, T.G.J. & Burnstock, G. (1990). M_1 and M_2 muscarinic receptors mediate excitation and inhibition of guinea-pig intracardiac neurones in culture. Journal of Physiology (in press).

Allen, T.G.J. & Burnstock, G. (1990). A voltage-clamp study of the electrophysiological characteristics of the intramural neurones of the rat trachea. Journal of Physiology (in press).

Allen, T.G.J. & Burnstock, G. (1990). $GABA_A$ receptor-mediated increase in chloride conductance in rat paratracheal neurones. British Journal of Pharmacology (submitted for publication).

Allen, T.G.J. & Burnstock, G. (1990). The actions of adenosine 5'-triphosphate on guinea-pig intracardiac neurones in culture. British Journal of Pharmacology (submitted for publication).

Allen, T.G.J. & Burnstock, G. α_2-adrenergic receptor-mediated inhibition of a calcium activated potassium conductance in guinea-pig intracardiac neurones in culture (in preparation).

Allen, T.G.J. & Burnstock, G. $GABA_A$ receptor-activated chloride current in guinea-pig intracardiac neurones in culture (in preparation).

PREFACE

The study of mammalian autonomic intramural ganglia, other than those in the gut, has been largely neglected due to their small size and wide distribution within the effector tissue. Often their role has been prejudged to be that of a simple cholinergic relay and in some cases they are totally ignored, with some reports stating that an organ such as the heart has been denervated when only the extrinsic nerves have been cut. The aim of the present thesis was to use intracellular recording techniques to investigate the properties of intramural neurones from the heart and trachea.

A dissociated mixed cell culture preparation containing intracardiac neurones from the atria and interatrial septum of the newborn guinea-pig heart has been developed in our laboratory (Hassall & Burnstock, 1986). Ultrastructural and immunocytochemical studies of these cultures suggested that they might be a good model for the less accessible in situ ganglia (see Chapter 1). The culture preparation is ideally suited for intracellular electrophysiological studies because individual neurones can be clearly visualised and are free from overlying connective tissue. However, with the exception of a few cells (see Chapter 5), most neurones are unsuitable for patch-clamp recording as they have closely associated glial cells (Kobayashi, Hassall & Burnstock, 1986 a, b).

The basic electrophysiological properties of cultured guinea-pig intracardiac neurones were studied and the results are presented in Chapter 3. Multiple types of neurone were distinguished, and the underlying membrane conductances responsible for some of the different characteristics were investigated. In culture, autoradiographic studies have localised muscarinic receptors on all intracardiac

neurones (Hassall, Buckley & Burnstock, 1987). In Chapter 4, the actions of exogenously applied muscarine, a selective muscarinic cholinergic receptor agonist, are reported. These studies revealed that all intracardiac neurones in culture have functional muscarinic receptors. By utilizing a variety of selective antagonists, the muscarinic receptor subtypes present on these neurones were determined. Most neurones displayed both M_1 and M_2 receptor subtypes, activation of which resulted in changes in a variety of different membrane ion conductances. The underlying ionic nature of the different conductance changes were investigated.

In situ, many intracardiac neurones and nerve fibres within and around the ganglia show a positive reaction to quinacrine, a fluorescent compound that binds to adenosine 5'-triphosphate (ATP). Furthermore, many purine compounds have been shown to exert powerful effects upon the heart (Burnstock, 1980). In Chapter 5, the actions of ATP and associated nucleotides and nucleosides on intracardiac neurones were investigated. Large subpopulations of intracardiac neurones were found to exhibit P_1- and/or P_2-purinoceptors. The membrane currents and ionic conductance changes elicited by activation of these receptors has been investigated using intracellular current- and voltage-clamp techniques.

In the trachea, intramural ganglia are largely concentrated over the posterior surface and within the body of the trachealis muscle (see Chapter 1). As part of this thesis, an in situ preparation of the trachea, containing intact intrinsic ganglia was developed for electrophysiological studies (see Chapter 2). This preparation maintains much of the extensive plexus of nerves and paratracheal ganglia, as well as the synaptic interactions between intrinsic neurones and their effector sites. Using this preparation, some of the electrophysiological and neurochemical properties of these neurones were examined (see Chapters 6 & 7).

The basic electrophysiological properties of paratracheal neurones from the rat trachea were studied (see Chapter 6). The nature of the observed spontaneous synaptic activity and the characteristics of the underlying membrane currents were analysed. As with intracardiac neurones, these cells appear to be a heterogeneous population and they have been categorised on the basis of their firing characteristics. γ-Aminobutyric acid (GABA) has been found to exert a number effects upon the trachea, including inhibition of acetylcholine release from intrinsic neurones (Tamaoki, Grafe & Nadel, 1987). The actions of ionophoretic and bath application of GABA, as well as selective $GABA_A$ and $GABA_B$ receptor agonists and antagonists on paratracheal neurones were investigated. Greater than 90% of paratracheal neurones were found to be responsive to exogenous GABA (see Chapter 7). The ionic nature of the underlying ionic conductance change was determined.

The General Introduction which follows this Preface briefly surveys current literature relevant to the work presented in this thesis. This is followed by the Methods section which describes the different techniques employed in this work. The particular findings of each of the five chapters of Results are discussed at the end of each chapter. In the General Discussion (Chapter 8), the implications of these findings are reviewed in a broader context with reference to the possible roles of the ganglia in the heart and trachea. Comparisons are made between neurones from the two different preparations and also with the properties of other sympathetic, parasympathetic and enteric ganglia.

Chapter 1

GENERAL INTRODUCTION

SECTION 1: The autonomic nervous system

The autonomic nervous system is also known as the vegetative, visceral or involuntary nervous system. It is largely involved in homeostasis and regulates the activity of the heart, blood vessels, glands and smooth muscle throughout the body. The term autonomic nervous system was first proposed by Langley in 1898 in order to convey the idea of a system with a degree of local autonomy from the central nervous system (see Langley, 1921). The cell bodies of the autonomic neurones innervating the visceral organs lie outside the central nervous system and are generally formed into ganglia consisting of neurones and glial cells surrounded by connective tissue. Langley divided the autonomic nervous system into sympathetic and parasympathetic systems based on the anatomical location of the cell bodies of the preganglionic fibres supplying the peripheral ganglia. The cell bodies of sympathetic preganglionic axons lie in the lateral horns of the thoracic and upper two or three segments of the lumbar spinal cord, whilst parasympathetic preganglionic axons have their cells bodies located in the nuclei of the III, IV, IX and Xth cranial nerves and in sacral segments of the spinal cord. Langley was unable to show that the neurones of Meissner's and Auerbach's plexuses were part of the bulbar or sacral pathways and this, together with their high degree of autonomy, the presence of local reflexes and their different histological appearance, led to him placing them in a separate class, the enteric nervous system.

Sympathetic division

The myelinated axons of the lateral horn cells leave the cord in the anterior roots and run for a short distance in the mixed spinal nerves before branching off as the white rami communicantes and entering the sympathetic chains. The

sympathetic trunk consists of two chains of ganglia (the paravertebral ganglia) extending from the cervical to the sacral vertebrae which run on either side, and anterior to the vertebral column. Preganglionic sympathetic fibres in the white rami terminate in one of three main ways:

(1) Some fibres synapse with the postganglionic neurones in ganglia of the sympathetic chain. Some may form synapses in the ganglion corresponding to the thoracolumbar segment from which they originate, or they may run for some distance up or down the sympathetic chain before forming a synapse. The postganglionic fibres are non-myelinated. They emerge from the paravertebral ganglia, either in the grey rami communicantes which rejoin the spinal nerves, or run to the organ they innervate as discrete nerve bundles or as nerve plexuses accompanying the blood vessels.

(2) Many preganglionic axons pass straight through the paravertebral ganglia, leaving the cord through thoracolumbar segments T4-L3, to synapse in the prevertebral ganglia in the abdominal cavity. There are three main prevertebral ganglia: the coeliac and the superior and inferior mesenteric ganglia.

(3) Some preganglionic fibres leave the cord via the tenth and eleventh thoracic segments and run in the splanchnic nerve to terminate on chromaffin cells in the medullae of the adrenal glands. Like nervous tissue, the cells of the adrenal medullae are derived embryologically from ectodermal cells of the neural crest and are believed to be analogous to sympathetic ganglion cells.

Parasympathetic division

The preganglionic nerve fibres of the parasympathetic division arise from the cranial and sacral regions of the spinal cord. The parasympathetic preganglionic fibres of the cranial region are carried in the IIIrd (oculomotor), VIIth (facial),

IXth (glossopharyngeal), Xth (vagus) and XIth (accessory) cranial nerves. The preganglionic fibres of the cranial parasympathetic nerves synapse on ganglion cells lying within (intramural ganglia) or near (extramural ganglia) the innervated organ. In the sacral region, the cell bodies of the preganglionic parasympathetic fibres lie in the lateral horns and their axons pass out of the spinal cord in the pelvic nerves. Some pelvic preganglionic nerve fibres terminate on ganglia within the pelvic plexus, the postganglionic fibres then pass on to the effector organs; others continue to the target organ as preganglionic fibres, where they synapse with intramural or extramural ganglia innervating the lower parts of the abdominal cavity.

The enteric nervous system

The enteric nervous system is by far the largest and most complex division of the autonomic nervous system which in man has been estimated to contain as many neurones as the spinal cord (Furness & Costa, 1980). The enteric nervous system consists of two main plexuses: the myenteric (Auerbach's) and the sub-mucosal (Meissner's) plexuses, which are embedded in the muscle layers of the wall of the gut and extend for the entire length of the gastrointestinal tract. The parasympathetic preganglionic innervation of the gut, between the oesophagus and large intestine, is via the Xth cranial (vagus) nerve, whilst innervation of the large intestine from the colon downwards is via sacral preganglionic fibres (S2-S4) carried in the pelvic nerve. Sympathetic fibres innervating the gut arise from thoracic (T4-T12) and lumbar (L1-L3) segments of the spinal cord. The preganglionic fibres pass uninterrupted through the sympathetic chain and then out in the splanchnic nerves to synapse in the prevertebral (coeliac, superior and inferior mesenteric) ganglia of the abdominal cavity (for reviews see Gabella, 1979; Furness & Costa, 1980).

Ultrastructural studies of enteric ganglia reveal a pattern of organisation that is totally different from that of other autonomic ganglia, but it shows several similarities to the organisation of the central nervous system (Gabella, 1979; Jessen & Burnstock, 1982). For example, the ganglia are tightly packed with very little extracellular space between individual elements and consist simply of neurones and glial cells with no connective tissue or capillaries. Furthermore, unlike other autonomic ganglia individual neurones are not tightly ensheathed by glial cells (Baumgarten, Holstein & Owman, 1970; Gabella, 1972, 1976, 1979). There are estimated to be between 10^7 and 10^8 enteric neurones (Furness & Costa, 1980). Contrasting this number of intrinsic neurones with the few thousand preganglionic vagal fibres is strong evidence that the enteric neurones do not simply relay vagal nervous input. In addition, the great neurochemical and synaptic complexity of these ganglia and the high degree of independent regulatory activity that they can sustain in the absence of extrinsic input, all support Langley's original classification of the enteric nervous system as a separate division of the autonomic nervous system (Langley, 1921; for reviews see Gershon, 1981; Furness & Costa, 1987).

SECTION 2: Innervation of the heart

The beating of the heart in mammals has an essentially myogenic origin. It is triggered by pacemaker cells in the nodal regions of the atria and synchronised by the rapid spread of excitation through specialised conducting tissues (Noble, 1979). The inherent rhythmicity of the heart is modulated by the nervous system. The heart receives motor and sensory nerves from both the sympathetic and parasympathetic divisions of the autonomic nervous system. The cell bodies of the preganglionic sympathetic neurones lie in the intermediolateral columns of the upper eight thoracic segments of the spinal cord (Henri & Calaresu, 1972). Their axons pass, via the white rami communicantes (level T1-T6), into the sympathetic chain. The synapses between the preganglionic and postganglionic neurones occur in the cervical, upper thoracic and stellate ganglia, with the postganglionic fibres passing via the superior, middle and inferior cardiac nerves to supply nodal tissue, coronary vessels and the muscle of the atria and ventricles (see review Moravec & Moravec, 1987). A few sympathetic fibres also reach the heart without interruption (Kuntz, 1953; Brown, 1967). As well as efferent fibres, the sympathetic nerves also carry afferent sensory fibres of dorsal root ganglion neurones (Navaratnam, 1980; Vance & Bowker, 1983). The vagus nerves which supply the heart have their cell bodies in the medulla of the dorsal motor nuclei of the vagus (Ciriello & Calaresu, 1982). Preganglionic fibres are distributed in the left and right vagus nerves and synapse with ganglia along the vagal nerves close to or within the heart.

Intracardiac ganglia

The intramural cardiac ganglia of mammals are found throughout the heart, but are most abundant in the atria, particularly subepicardially around the sino-atrial

and atrio-ventricular nodes, near the origins of the great vessels and in the interatrial septum (King & Coakley, 1958). Although there have been conflicting studies, it is generally agreed that intrinsic ganglion cells are extremely sparse or absent from the ventricles of most mammals (for review see Davies, Francis & King, 1952). In the atria, intracardiac neurones form part of the extensive cardiac plexus of nerves and ganglia which innervate the atria and coronary vessels (King & Coakley, 1958; Calaresu & St.Louis, 1967; Ellison & Hibbs, 1976). Ultrastructural studies have revealed that intracardiac ganglia contain small capillaries and are wrapped by the processes of interstitial cells. Individual neurones are enveloped by satellite cells with connective tissue between the different neuronal elements (Ellison & Hibbs, 1976; Shvalev & Sosunov, 1985; Kobayashi et al. 1986a). Three morphologically distinct types of neurone, unipolar, bipolar and multipolar, have been described within the ganglia (Davies et al. 1952; Osborne & Silva, 1970; Ellison & Hibbs, 1976). In addition, both mononucleate and binucleate neurones have been observed both in situ and in culture (Smith, 1970; Tay, Wong & Ling, 1984; Kobayashi et al. 1986a). Intracardiac neurones stain positively for acetylcholinesterase, but the intensity of staining varies markedly (Osborne & Silva, 1970). Fluorescent histochemical methods have detected no catecholamines in neurones within intracardiac ganglia (Jacobowitz, 1967; Ehinger, Falck, Persson & Sporrong, 1968; Osborne & Silva, 1970). However, there are numerous adrenergic fibres running through the cardiac plexus. (Forsgren, 1985; Ehinger et al. 1968; Nielsen & Owman, 1968) and in a number of species, fluorescent terminal varicosities of adrenergic fibres have been observed to impinge upon ganglion cells within the plexus (Jacobowitz, 1967; Forsgren, 1987). It has been suggested that they form axo-somatic and axo-axonic connections with the cholinergic neurones (Ellison & Hibbs, 1976; Shvalev & Sosunov, 1985).

Although no adrenergic neurones have been observed within intracardiac ganglia, small cells exhibiting intense yellow fluorescence (SIF cells; small granule-containing cells), characteristic of catecholamine-containing cells, have been detected (Nielsen & Owman, 1968; Ellison & Hibbs, 1974; Yamauchi, Yokoto & Fujimaki, 1975b). Fibres from intracardiac neurones have been seen projecting onto these SIF cells and it has been suggested that they may form synaptic contacts (Jacobowitz, 1967; Yamauchi, Fujimaki & Yokota, 1975a; Yamauchi et al. 1975b). At present, the function of these SIF cells is unknown, however, they may release catecholamines within the ganglia or into capillaries and thereby modify ganglionic neurotransmission.

Until comparatively recently, autonomic neurotransmission in the heart, as in other organs, was believed to be mediated through the actions of just two neurotransmitters, acetycholine and noradrenaline. Over the past twenty years, our understanding of the complexity of autonomic neurotransmission has been revolutionised as a result of the discovery of a wide variety of peripherally active neurotransmitter and neuromodulator substances (Burnstock, 1986a). Many of these neurochemicals have been localised in nerves and ganglia within the heart, where they have been shown to exert powerful inotropic and chronotropic actions, as well as influencing coronary vascular tone (Said, Bosher, Spath & Kontos, 1972; Lundberg, Hua & Franco-Cereceda, 1984; Urban & Papka, 1985; Eimerl & Feuerstein, 1986; Bachelard, St-Pierre & Rioux, 1986; Franco-Cereceda, Bengtsson & Lundberg, 1987). Although there are considerable species differences, immunohistochemical studies have localised large numbers of neuropeptide Y (NPY)-, C-terminal peptide of NPY (C-PON)- and somatostatin (SOM) -containing intracardiac neurones and also small subpopulations of vasoactive intestinal polypeptide (VIP)-, peptide histidine isoleucine (PHI)-, substance P (SP)- and calcitonin gene-related peptide (CGRP) -

containing neurones in the heart (Hassall & Burnstock, 1984; Reinecke & Forssmann, 1984; Gulbenkian, Wharton, Hacker, Varndell, Bloom & Polak, 1985; Franco-Cereceda, Lundberg & Hökfelt, 1986; Gerstheimer & Metz, 1986; Baluk & Gabella, 1989b).

In addition to neuropeptides, some intracardiac neurones exhibit 5-hydroxytryptamine-like immunoreactivity which is frequently co-localised with NPY in culture (Hassall & Burnstock, 1987a, b). Purine nucleotides and nucleosides have long been known to exert powerful actions upon the mammalian heart (for review see Burnstock, 1980). The possibility that there might be purinergic innervation of the atria and also intrinsic purinergic neurones has been suggested on the basis of positive reactions to quinacrine, a fluorescent compound that binds strongly to ATP in neurones and nerve fibres in the atria of guinea-pigs and rabbits (Da Prada, Richards & Lorez, 1978; Crowe & Burnstock, 1982).

It is clear that there are a wide variety of putative neurotransmitter and neuromodulatory substances in the nerves and ganglia of the cardiac plexus, however, we are still almost totally ignorant of the role of the intramural ganglia and what effects if any, these substances have on neurotransmission within these ganglia. In the rat heart, intracardiac ganglia have been categorised by their localisation in four distinct areas and retrograde labelling studies have shown that a discrete group of ganglion cells, located posterior to the interatrial septum and in the left atrium, project across the atrio-ventricular sulcus to innervate the left ventricle (Pardini, Patel, Schmid & Lund, 1987). Other recent reports have demonstrated that there are differences in the roles and projections of intracardiac ganglia from different areas of the canine heart. Studies revealed that selective vagal denervation of either the sino-atrial or atrio-ventricular nodal regions could be accomplished with minimal interference to the nerve supply of the other (Randall

& Ardell, 1985a, b). Further to this, experiments were performed where epicardial fat pads containing multiple encapsulated intracardiac ganglia were surgically disrupted or destroyed. Disruption of a small epicardial fat pad situated between the inferior vena cava and the inferior surface of the left atrium, interrupts both right and left vagal inhibition of atrio-ventricular conduction, without interfering with vagal modulation of sino-atrial function. (Randall, Ardell, Calderwood, Milosavljevic & Goyal, 1986a; Randall, Milosavljevic, Wurster, Geis & Ardell, 1986b). In contrast, removal of a ganglion in a similar fat pad overlying the right pulmonary vein inlets to the left atrium was found to interrupt both right and left vagal inhibition of sino-atrial function, without interfering with vagal control of atrio-ventricular nodal function (Randall et al. 1986a, b). Together, these findings suggest that even when examined at a fairly gross anatomical level, there are demonstrable differences in the function of intracardiac ganglia from different regions of the heart.

To date, there have been very few reported electrophysiological studies of mammalian intracardiac neurones. Extracellular recordings have been made from ganglia within cat and dog heart (Nozdrachev & Pogorelov, 1982; Gagliardi, Randall, Bieger, Wurster, Hopkins & Armour, 1988). In the dog, recordings have been made in vivo from neurones in ganglia located in the epicardial fat pad overlying the right atrium and pulmonary veins. Almost all neurones were found to be spontaneously active. In approximately 40% of cells, this activity was found to be correlated with the cardiac cycle, whilst in a further 8% of cells, activity was linked to the respiratory cycle. Increases in systolic pressure, induced by positive inotropic agents or aortic occlusion, enhanced firing in neurones that displayed cardiovascular-related activity. Furthermore, these effects persisted even after acute decentralization. A small, but significant population of neurones appeared to be mechanosensitive, with firing being enhanced by gentle stimulation of discrete

areas of the heart, lungs and coronary vasculature. Spike discharge in ganglion cells could be elicited by trains of stimuli delivered to the vagosympathetic complexes, stellate ganglion, or cardiopulmonary nerves in both intact and acutely decentralised preparations (Gagliardi et al. 1988). Cat intracardiac ganglia from the right atrium studied in vitro appear to differ from those of the dog in that there was no observed spontaneous activity, but this may be accounted for by the fact that in this study, the ganglia were totally extrinsically denervated and immobilised. In the cat, as in the dog, a population of ganglion cells were mechanosensitive responding to stimulation by discharging bursts of action potentials (Nozdrachev & Pogorelov, 1982).

Intracellular studies of intracardiac neurones have been largely restricted to the amphibian heart where the ganglia are clearly visible in the transparent interatrial septum (McMahan & Kuffler, 1971). In an elegant series of experiments, the chemosensitivity of individual frog ganglion cells was mapped and the synaptic interactions investigated (Harris, Kuffler & Dennis, 1971). Preganglionic nerve stimulation evoked fast excitatory postsynaptic potentials in the ganglion cells which could be mimicked by ionophoretic application of acetylcholine (Dennis, Harris & Kuffler, 1971). Single vagal fibres were found to innervate several ganglion cells, but no intrinsic synapses between the ganglion cells were observed and it was suggested that these ganglia may simply act as cholinergic relays (Dennis et al. 1971; Sargent & Dennis, 1977). In the mudpuppy, where the ganglia can also be visualised in a transparent sheet, a more complex situation was observed. Two cell types were distinguished, principal cells, which gave rise to postganglionic axons, and catecholamine-containing interneurones, similar to SIF cells in mammalian intracardiac ganglia (McMahan & Purves, 1976). The principal neurones received synaptic input from three sources: vagal preganglionic axons, interneurones and

other principal cells. The presence of these intrinsic synapses suggests that the ganglia may not function purely as relay stations, but may be capable of considerable integrative activity (McMahan & Purves, 1976; Roper, 1976). Subsequent studies of frog and mudpuppy intracardiac ganglia have revealed slow inhibitory and excitatory post-synaptic potentials mediated via muscarinic receptors, as well as a late slow post-synaptic potential believed to be mediated by the peptide, luteinizing hormone releasing hormone (Hartzell, Kuffler, Stickgold & Yoshikami, 1977; Kuffler, 1980). Most recently, another peptide, galanin, which has been localised in the intracardiac neurones and SIF-like cells of the mudpuppy heart (Parsons, Neel, Konopka & McKeon, 1989) has been shown to induce membrane hyperpolarization in intrinsic ganglion cells and has been suggested as a possible inhibitory neurotransmitter in this system (Konopka, McKeon & Parsons, 1989). To date, there has only been one brief report of the properties of intact mammalian intracardiac ganglia. In this study of the properties of a large ganglion in the guinea-pig atrium, repetitive nerve stimulation was reported to evoke both fast and slow postsynaptic responses. Exogenous application of SP evoked a slow depolarization of similar amplitude and duration to that of the slow excitatory postsynaptic potential and was thus suggested as a possible neurotransmitter candidate in the guinea-pig heart (Konishi, Okatomo & Otsuka, 1984).

A dissociated mixed cell culture preparation of the atria and interatrial septum of newborn guinea-pig heart was developed in our laboratory to overcome many of the inherent problems associated with the study of the relatively small, widely spread, and inaccessible mammalian intracardiac ganglia (Hassall & Burnstock, 1986). Several investigations have been carried out to determine whether this dissociated cell culture preparation is a suitable model for studying intracardiac neurones. Detailed observations of these cultures have been made using phase-contrast

(Hassall & Burnstock, 1986) and electron microscopy (Kobayashi et al. 1986a; Kobayashi, Hassall & Burnstock, 1986b). These studies show that all of the cell types that are normally associated with the intracardiac neurones in situ are present in culture and that the ultrastructural integrity of the cells and many of their interrelationships are maintained. The cultured neurones also express a similar, high level of neurochemical differentiation as the in situ cells (Hassall & Burnstock, 1984, 1986, 1987a, b). These results indicate that cultured intracardiac neurones retain many of their properties in culture and that the culture preparation is therefore a good model for electrophysiological studies of the intrinsic innervation of the heart.

SECTION 3: Innervation of the trachea

The autonomic innervation of the airways is derived from the vagus nerves and from the sympathetic chain. In addition, the trachea also receives innervation from branches of the recurrent and superior laryngeal nerves. The laryngeal and vagus nerves enter the trachea, where they divide, rejoin and synapse with the many small intrinsic ganglia to form a dense plexus (Honjin, 1954; Fisher, 1964; Smith & Taylor, 1971). This plexus is particularly prominent on the posterior wall of the trachea, along the trachealis muscle opposite intervals between the tracheal rings. Branches from this network send fibres into the trachealis muscle, to the mucous glands and also contribute to the fine plexuses accompanying tracheal vessels (Larsell, 1922; Smith & Taylor, 1971). The sympathetic nerve supply to the airways originates from the upper six thoracic segments of the spinal cord and the postganglionic fibres synapse in the middle and inferior cervical ganglia and the upper four thoracic paravertebral ganglia. Postganglionic fibres run from these ganglia to the lung and enter the hilum to intermingle with the plexus of cholinergic nerves (Richardson, 1979; Barnes, 1986). In contrast to the dense parasympathetic supply to the airways seen in all species, the sympathetic innervation is generally more sparse, although there is considerable variation between species (Richardson, 1979; Doidge & Satchell, 1982).

Parasympathetic cholinergic excitatory nerves

Stimulation of the peripheral vagus nerves provokes tracheobronchial constriction in all species studied (Nadel, 1980). The response is mimicked by exogenous application of acetylcholine, enhanced by acetylcholinesterases (eg. pilocarpine) and blocked by atropine (for review see Widdicombe, 1987). The

contraction occurs in all cartilaginous airways, but probably not in the bronchioles, since lung compliance does not decrease. Vagal excitatory postganglionic nerves can also be activated by field stimulation of the tracheal muscle in vitro. The induced contractions can be inhibited by tetrodotoxin or atropine, but not by blocking ganglionic synapses with hexamethonium (Coburn & Tomita, 1973; Richardson & Beland, 1976; Ito & Takeda, 1982).

Sympathetic adrenergic inhibitory fibres

Without pharmacological agents, it is very difficult to demonstrate the actions of adrenergic inhibitory fibres as the cholinergic excitatory responses are dominant. Furthermore, if the excitatory responses are inhibited by atropine, the lack of cholinergic tone leaves the airways almost completely relaxed and thus inhibitory responses are very difficult to evoke. Therefore, it is common practice to artificially raise muscle tone with histamine or 5-hydroxytryptamine. Under such conditions, sympathetic nerve stimulation can be shown to result in muscle relaxation in a number of species (Richardson, 1979; Grundström, Anderson & Wikberg, 1981; Doidge & Satchell, 1982). This effect is inhibited by tetrodotoxin and is mainly, or completely, blocked by propranolol, indicating that the response is neurally mediated by noradrenaline acting on β-receptors (Coburn & Tomita, 1973; Richardson & Beland, 1976; Ito & Takeda, 1982; Cameron, Johnston, Kirkpatrick & Kirkpatrick, 1983). Such results suggest the involvement of adrenergic nerves acting directly on the smooth muscle of the airways. Other possibilities exist however, for example, noradrenaline released during stimulation may act at the paratracheal ganglia, to inhibit the release of acetylcholine. Inhibition of the cholinergic pathway in this way would be consistent with the sympathetic/parasympathetic interactions observed in other systems (DeGroat & Saum, 1972; Wood & Mayer, 1979). In the

ferret trachea, noradrenaline has been shown to inhibit vagally-induced action potentials, thus giving support to this idea (Baker, Basbaum, Herbert & Mitchell, 1983). However, in a recent study of rat, mouse and guinea-pig trachea, no detectable noradrenergic fibres have been found in association with the paratracheal ganglia (Baluk & Gabella, 1989a).

Non-adrenergic non-cholinergic innervation

In addition to the adrenergic and cholinergic pathways, the trachea in many species has been shown to be innervated by nerves that are neither adrenergic nor cholinergic (NANC; see Burnstock, 1988). Stimulation of NANC nerves produces a long-lasting relaxation of airway smooth muscle (both in vivo and in vitro), which is independent of adrenergic pathways and is inhibited by ganglion blocking drugs and by tetrodotoxin (Coburn & Tomita, 1973; Coleman & Levy, 1974; Richardson & Beland, 1976; Diamond & O'Donnell, 1980). There are two main neurotransmitter candidates for this pathway, VIP and a purine, both of which have been shown to cause relaxation of airway muscle and may be involved as cotransmitters. At present, evidence is in favour of a neuropeptide as the principal neurotransmitter of the NANC inhibitory nerves, and of the various peptides localised in the airways, only VIP and its sister peptide PHI has been shown to relax airway smooth muscle (Said, 1982; Barnes, 1987). The evidence for VIP as the neurotransmitter in airway NANC nerves is based on the following observations: there are VIP-immunoreactive nerves found in close association with airway smooth muscle (Dey, Shannon & Said, 1981; Polak & Bloom, 1982); VIP mimics the mechanical and electrophysiological changes produced by stimulation of the NANC nerves (Matsuzaki, Hamasaki & Said, 1980; Ito & Takeda, 1982; Diamond, Szarek, Gillespie & Altiere, 1983; Cameron et al. 1983); VIP is released from airway tissues during electrical stimulation (Matsuzaki et

al. 1980); and exogenous VIP reduces the amplitude of the NANC response (Ito & Takeda, 1982). However, VIP does not account for the entire NANC inhibitory response (Ellis & Farmer, 1989) and it is possible that ATP release is responsible for the residual component (Welford & Anderson, 1988).

In addition to NANC inhibitory nerves, there is also evidence to suggest the presence of NANC excitatory nerves. Electrical stimulation of the trachea or bronchi of the guinea-pig has been shown to elicit airway contraction which is atropine resistant. SP, which has been localised in the airways (Wharton, Polak, Bloom, Will & Brown, 1979; Lundberg & Saria, 1982), causes contraction of the guinea-pig trachea (Nilsson, Dalberg, Brodin, Sundler & Strandberg, 1977; Brown, Hayes, Meecham & Tyers, 1983). Both the nerve- and SP-evoked responses were antagonised by the SP antagonists suggesting the possible involvement of SP, released from sensory nerves, in mediating the NANC excitatory response.

Paratracheal ganglia

Morphological studies of the innervation of the trachea have all observed a network of small ganglia interconnected by a plexus of nerves concentrated over the posterior surface of the trachealis muscle (Honjin, 1954; Fisher, 1964; Smith & Taylor, 1971). The overall arrangement of the nerve plexuses and ganglia have been studied in the ferret trachea using acetylcholinesterase histochemistry (Baker, McDonald, Basbaum & Mitchell, 1986). The most distinctive feature of the neural distribution was the presence of longitudinal nerve trunks located near the junction of the trachealis muscle and the ends of the cartilaginous rings. Branches from these longitudinal nerve trunks divide and anastomose to form a superficial muscular plexus above the posterior surface of the trachealis muscle between the larynx and

the tracheal bifurcation. Bundles of axons from the superficial muscular plexus descend onto the trachealis muscle where they divide and form the deep muscular plexus. Anteriorly, the superficial muscular plexus and the longitudinal nerve trunks connect to a banded neural plexus over the submucosal glands in between the cartilage rings (the superficial glandular plexus). This plexus gives rise to a deep glandular plexus consisting of tiny nerve bundles enveloping the submucosal glands. Paratracheal ganglia are found along the longitudinal nerve trunks and in the superficial, but not the deep muscular and glandular plexuses (Baker et al. 1986). The ganglion cells along the longitudinal nerve trunks have a different morphology to those associated with the superficial muscular and glandular plexuses. The neuronal cell bodies along the longitudinal nerve trunks are large (mean diameter 34.3 μm), usually attached to the nerve trunk by a stalk and are loosely clustered into groups of up to 38 cell bodies. By contrast, neurones in the superficial muscular and glandular plexuses are significantly smaller (mean diameter 24.2 μm), are not attached by a stalk and are tightly clustered into ganglia of one to four neuronal cell bodies (Baker et al. 1986).

Ultrastructural studies of paratracheal ganglia in the mouse and guinea-pig trachea have revealed that they are covered by a continuous perineurium with connective tissue between the neuronal elements. Blood vessels inside the ganglia have continuous endothelia and are sometimes accompanied by pericytes and a sheath of perineural cells. Individual neuronal cell bodies and large processes are almost completely covered by a thin layer of satellite cells, whilst all nerve fibres are completely and individually ensheathed in Schwann cell processes (Baluk, Fujiwara & Matsuda, 1985; Chiang & Gabella, 1986). Although the trachea shares the same embryological origins as the foregut, the structure of tracheal ganglia is most similar to that of the parasympathetic ganglia of the head and of the small

sympathetic ganglia and not at all like that seen in the enteric nervous system (Baluk et al. 1985; Chiang & Gabella, 1986).

The large differences in the sizes of the individual ganglion cells and the regional differences in their distribution have been suggested to indicate the presence of multiple neuronal populations (Baluk et al. 1985; Baker et al. 1986). Direct electrophysiological investigation of paratracheal neurones was first carried out in ferret ganglia associated with the longitudinal nerve trunks (Cameron & Coburn, 1984). In this study, two cell types, AH and B cells were distinguished. AH type cells were found to be highly refractory, firing only a single action potential in response to intrasomal current injection, the action potential being followed by a prolonged hyperpolarization lasting several hundred milliseconds. In addition, fast cholinergic excitatory post-synaptic potentials could be evoked by focally stimulating the nerve trunks. B cells exhibited no somal spikes, but did display slow excitatory, and occasionally, fast inhibitory post-synaptic potentials in response to repetitive nerve stimulation. Subsequent studies of ferret paratracheal ganglia have reported similar neuronal properties (Baker et al. 1986; Coburn & Kalia, 1986). However, the majority (approximately 70%) of ferret paratracheal neurones that lie in the superficial glandular and muscular plexuses have not yet been studied. In other species, the characteristics of neurones in the paratracheal ganglia appear to be slightly different from those in the ferret. In a brief report, two cell types were identified in rabbit paratracheal ganglia: one had properties similar to AH type ferret cells, but the second type, unlike ferret B cells, also fired somal action potentials and were capable of sustaining multiple spike discharge (Fowler & Weinreich, 1986). In an in vivo study of cat ganglia, two cell types were also distinguished. One type consisted of predominantly large neurones (mean diameter 63 μm) which fired with an inspiratory rhythm, had a small spike after-

hyperpolarization (mean duration 94 ms) and projected to the tracheal muscle. The other type consisted principally of smaller cells (mean diameter 36 μm) which fired with an expiratory rhythm, had no significant after-hyperpolarization, and projected to the intercartilaginous spaces (Mitchell, Herbert, Baker & Basbaum, 1987).

Many neuropeptides are localised in fibres and neurones within the paratracheal ganglia. These include VIP, PHI, SOM, galanin, CGRP, NPY and SP (Dey et al. 1981; Christofides, Yiangou, Piper, Ghatei, Sheppard, Tatemoto, Polak, & Bloom, 1984; Uddman, Sundler & Emson, 1984; Lundberg, Fahrenkrug, Hökfelt, Martling, Larsson, Tatemoto, & Änggärd, 1984; Cheung, Polak, Bauer, Cadieux, Christofides, Springall & Bloom, 1985; Dayer, DeMey & Will, 1985; Cadieux, Springall, Mulderry, Rodrigo, Ghatei, Terenghi, Bloom & Polak, 1986; Luts, Uddman & Sundler, 1989). However, although many of these peptides have been shown to alter airway function, the possible roles they may play in modulating ganglionic transmission remain almost totally unknown (for review see Barnes, 1989). Other possible ganglionic neuromodulators include noradrenaline (Baker et al. 1983), γ-aminobutyric acid (Tamaoki et al. 1987) and barbiturates (Skoogh, Holtzman, Sheller & Nadel, 1982), all of which have been shown to depress ganglionic neurotransmission in the airways. These findings raise the possibility that the paratracheal ganglia possess a degree of complexity and automaticity, for although it has long been accepted that the enteric nervous system is capable of considerable modulation, integration and local control of gut function, other intramural ganglia have generally been assumed to act as purely passive relay stations for exogenous nervous input from higher centres. There can be no doubt that the level of complexity exhibited by the enteric nervous system far exceeds that of other intramural ganglia. However, most assumptions about the role of other intramural ganglia, such as those in the heart and trachea, have been made on the basis of conjecture rather than experimental evidence.

Chapter 2

MATERIALS AND METHODS

SECTION 1: Studies of guinea-pig intracardiac neurones

Tissue culture

Cultures containing intrinsic neurones dissociated from the atria and interatrial septum of the newborn guinea-pig heart were prepared using the method described by Hassall & Burnstock (1986). The basic technique for preparing cultures was as detailed below.

Under sterile conditions, the hearts were removed from two newborn Dunkin-Hartley guinea-pigs. The atria and interatrial septum were dissected free from the ventricles and rinsed in Hank's balanced salt solution (Gibco Biocult, U.K.) to remove excess blood. The tissue was then rinsed two more times in modified Ca^{2+}- and Mg^{2+}-free Dulbecco's phosphate-buffered saline (DPBS) containing an additional 5 mg/ml of glucose. After rinsing, the tissue was transferred into a petri dish containing 1 ml of DPBS and carefully cut into 1 mm^3 pieces. Following this, 1 ml of 0.25% trypsin was added to the petri dish to give a final trypsin concentration of 0.125%, then it was left overnight at $4^{o}C$ to allow the enzyme to fully permeate into the tissue. After this period, the tissue was then incubated at $37^{o}C$ for 20 mins. Following incubation, it was gently triturated with a large bore (3-4 mm) Pasteur pipette and the mixture was then pipetted up and allowed to settle. The tissue fragments were retained and the supernatant discarded. The tissue was resuspended in 2 ml of modified DPBS and incubated for a further 1 hr at $37^{o}C$. After incubation, the tissue was triturated again and allowed to settle as before. The supernatant cell suspension was retained and was added to a small volume of foetal calf serum (FCS, Northumbria Biochemicals, U.K.) to inactivate the trypsin, then stored at $4^{o}C$ in a centrifuge tube. 2 ml of 0.2% collagenase (Gibco Biocult,

U.K.) was added to the remaining tissue fragments, then it was incubated at 37°C for 40 mins. After incubation the tissue was gently dispersed by trituration with a fine bore (0.5-1 mm) Pasteur pipette before being added to the cell suspension in the centrifuge tube. The final dissociated cell suspension was then spun down at 600 rpm for 5 mins. The supernatant was discarded and the pellet of cells was gently resuspended in medium 199 (Gibco Biocult, U.K.) supplemented with 10% FCS, 5 mg/ml glucose and 100 units/ml penicillin.

Cultures were seeded at approximately 5×10^5 cells/ml on glass coverslips in modified Rose chambers and maintained in a 37°C incubator with a 2% CO_2 environment and high humidity (Flow Laboratories, model 61-500).

After setting up the cultures, the chambers were left for approximately 7-8 hrs to allow the cells to adhere to the coverslip before being inverted to allow debris to fall off. After 24 hrs, the growth medium within the chamber was replaced with fresh medium and thereafter every two-three days.

Figures 2.1 & 2.2 show low- and high-power phase-contrast micrographs of groups of intracardiac neurones from typical cultures. The groups of neurones shown in these figures were the result of partial dissociation of ganglia, no re-aggregation of neurones was ever observed in these cultures.

Fig. 2.1. Low-power phase-contrast micrographs of intracardiac neurones from newborn guinea-pig heart maintained in dissociated cell culture. A, a large group of approximately 36 intracardiac neurones surrounded by other mixed cell types (9 day old culture). The neurones had large nuclei which in many cases contained multiple nucleoli. The majority of cells were mononucleate, but some larger binucleate cells were also visible (bn = binucleate). B, a second smaller group, consisting of large binucleate and smaller mononucleate neurones (10 day old culture). Scale bars 40 μm.

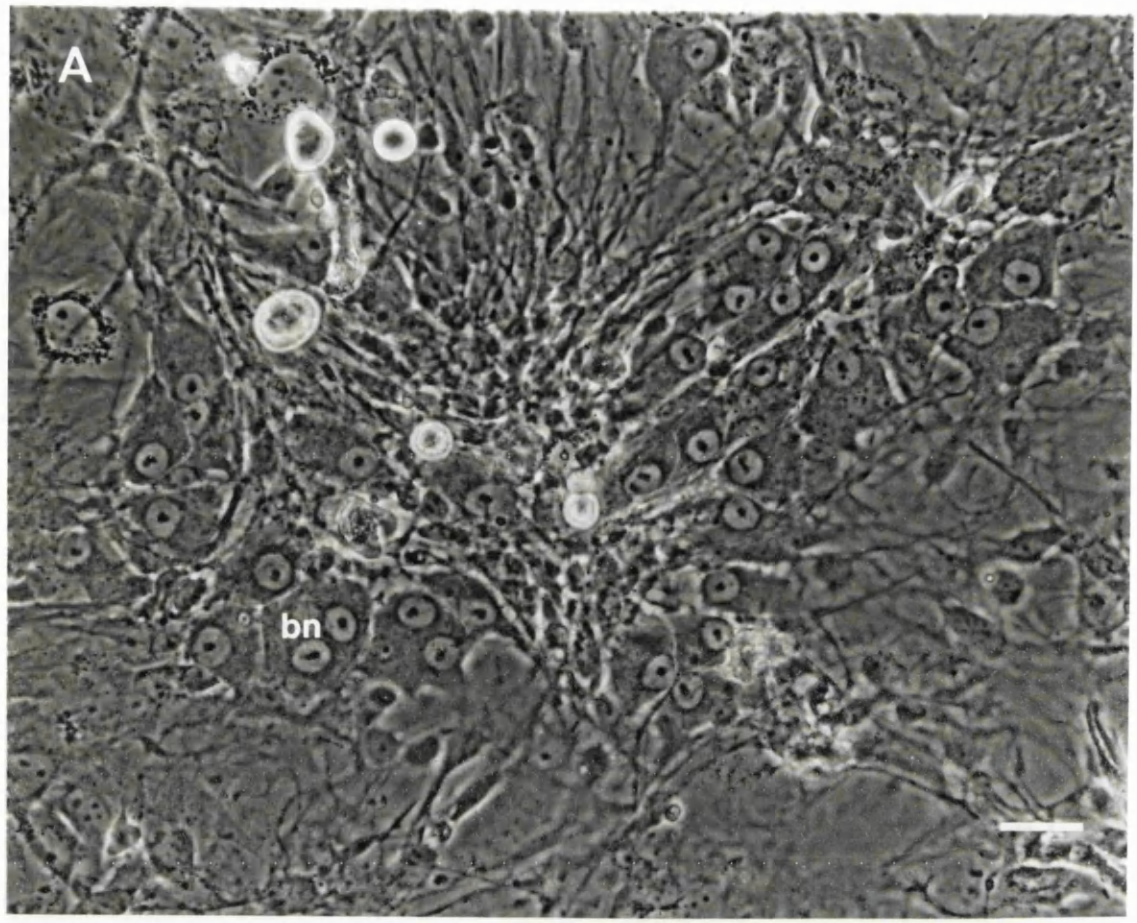
A
bn

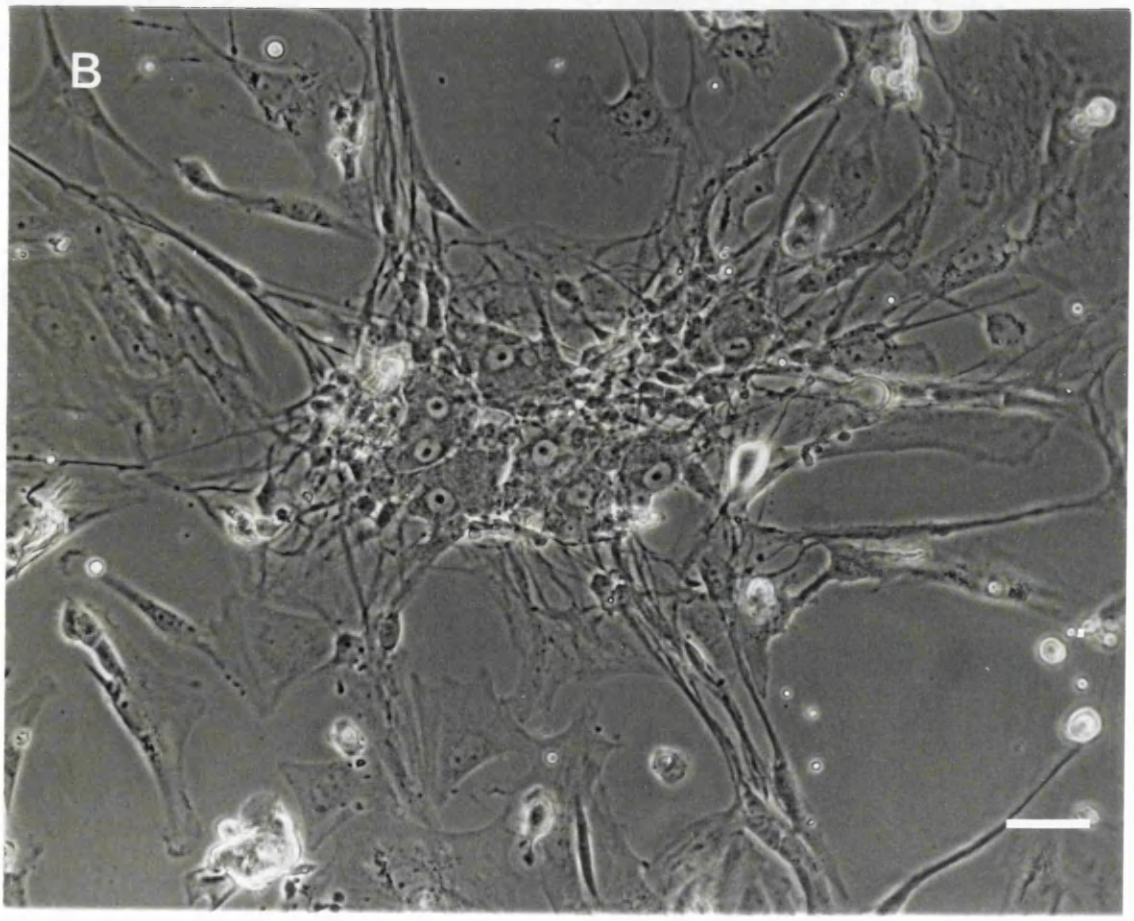
B

Fig. 2.2. High-power phase-contrast micrographs of groups of guinea-pig intracardiac neurones maintained in dissociated mixed cell culture. A, the same group as shown in figure 2.1B. Again clearly distinct mononucleate and binucleate (bn) cells were visible. Small glial cells were also present between the cells (g). The phase-bright neurone on the right of the micrograph is probably an M type cell (see Chapter 3) and shows the typical rounded morphology usually associated with this electrophysiologically distinct cell type. B, a large group of mononucleate neurones (n) and associated glial cells (10 day old culture). Scale bars 20 μm.

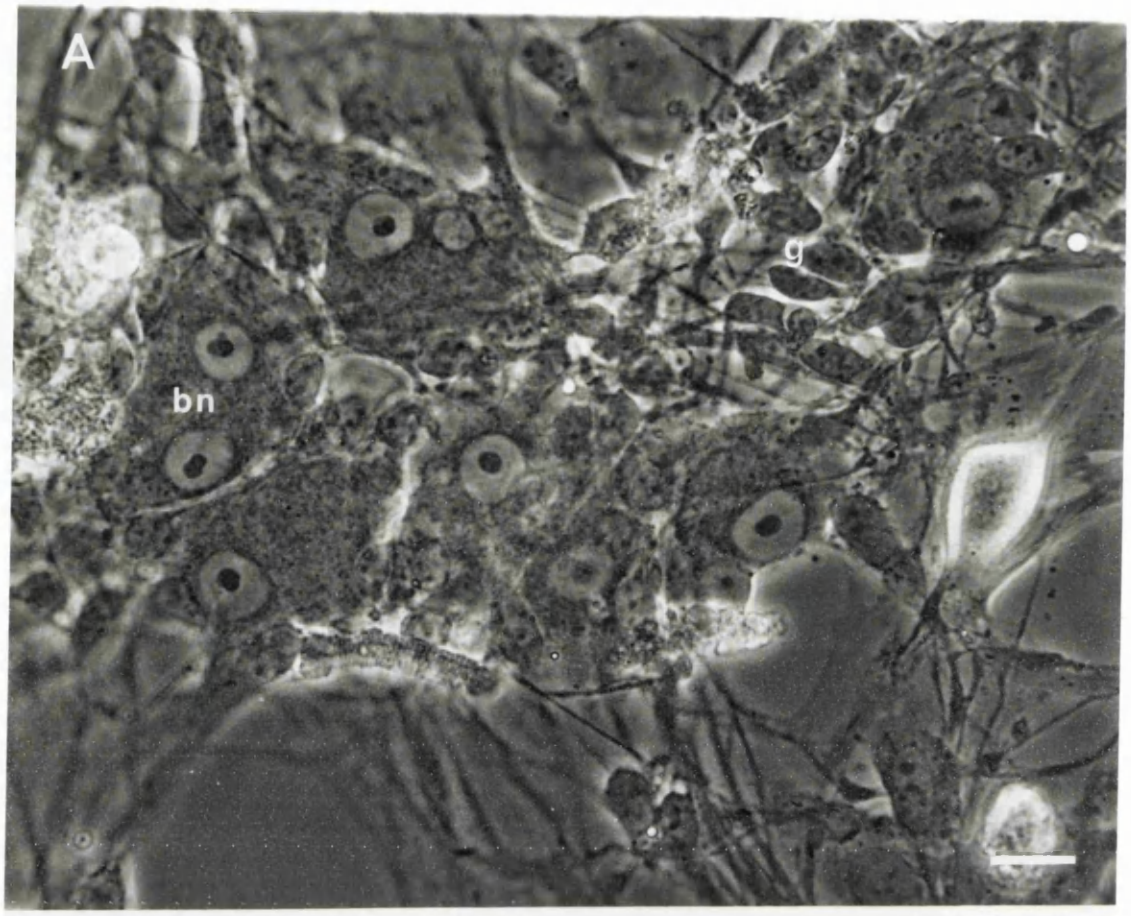
A
g
bn

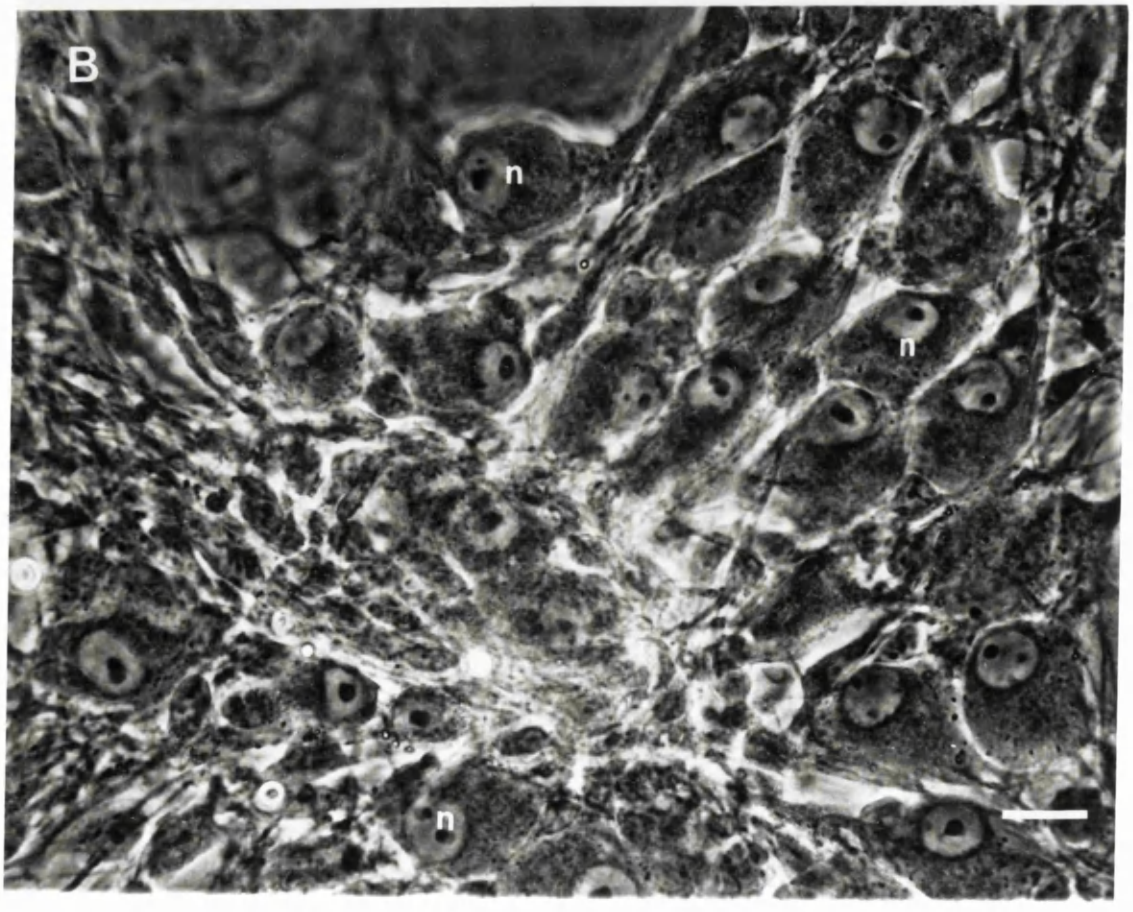
B
n
n
n

Setting up cultures for electrophysiological recording

All experiments were carried out on neurones maintained in culture for between 5 and 14 days. Prior to experiments, the modified Rose chamber in which they were grown was dismantled and the coverslip bearing the culture rinsed in oxygenated Krebs solution. After washing, the coverslip was sealed to the underside of a Perspex recording bath (see Fig. 2.3) using paraffin wax, such that it formed the base of the chamber. The chamber was then positioned over three, threaded metal studs set in a stainless steel plate attached to the stage of an inverted microscope (Zeiss Invertoscope D) and held rigidly in place by three securing nuts. Using this configuration, the edges of the coverslip were firmly sandwiched between the stage and the chamber, thus creating a water tight seal.

Cultures were visualised using conventional phase-contrast optics giving 128- to 512-fold magnification. The preparation was perfused with oxygenated Krebs solution at a rate of 4 ml/min, whilst the temperature was maintained between 36 and 37^{o}C using a remote thermostatically controlled heating coil positioned close to the recording chamber. The Krebs solution was of the following composition (mM): NaCl, 117; KCl, 4.7; $MgCl_2$, 1.2; NaH_2PO_4, 1.2; $CaCl_2$, 2.5; $NaHCO_3$, 25; glucose, 11; gassed with 95% O_2/5% CO_2. Bath volume was 7-8 ml: the large bath volume being dictated by the size of the cover-slips (43 x 50 mm) on which the cultures were grown.

Fig. 2.3. The Perspex recording chamber used for electrophysiological recording from both cultured intracardiac and in situ paratracheal neurones. The coverslip bearing the heart culture, or the slide with the trachea pinned out on a bonded Sylgard block, were sealed to the base of the recording chamber using paraffin wax such that they formed the base of the bath (see text). A, epoxolite embedded sintered silver-silver chloride earth. B, water-tight port for inserting thermistor for monitoring bath temperature. C, a sliding perspex sluice for preventing bubbles in the Krebs from disturbing the liquid in the chamber. D, entry port for Krebs solution. E, one of three anchor points for clamping the recording chamber to the microscope stage (see text), this particular mounting was recessed to prevent it fouling the electrodes. F, the solid Perspex body of the chamber. G & H, adjustable suction port, used to optimally set the depth of the superfusing Krebs when using modulation optics. I, fixed out-flow port used in heart culture experiments. J, plastic encapsulated agar bridge for coupling the recording chamber to the silver-silver chloride earth electrode. K, small reservoir containing the same electrolyte as that used to fill the recording electrodes.

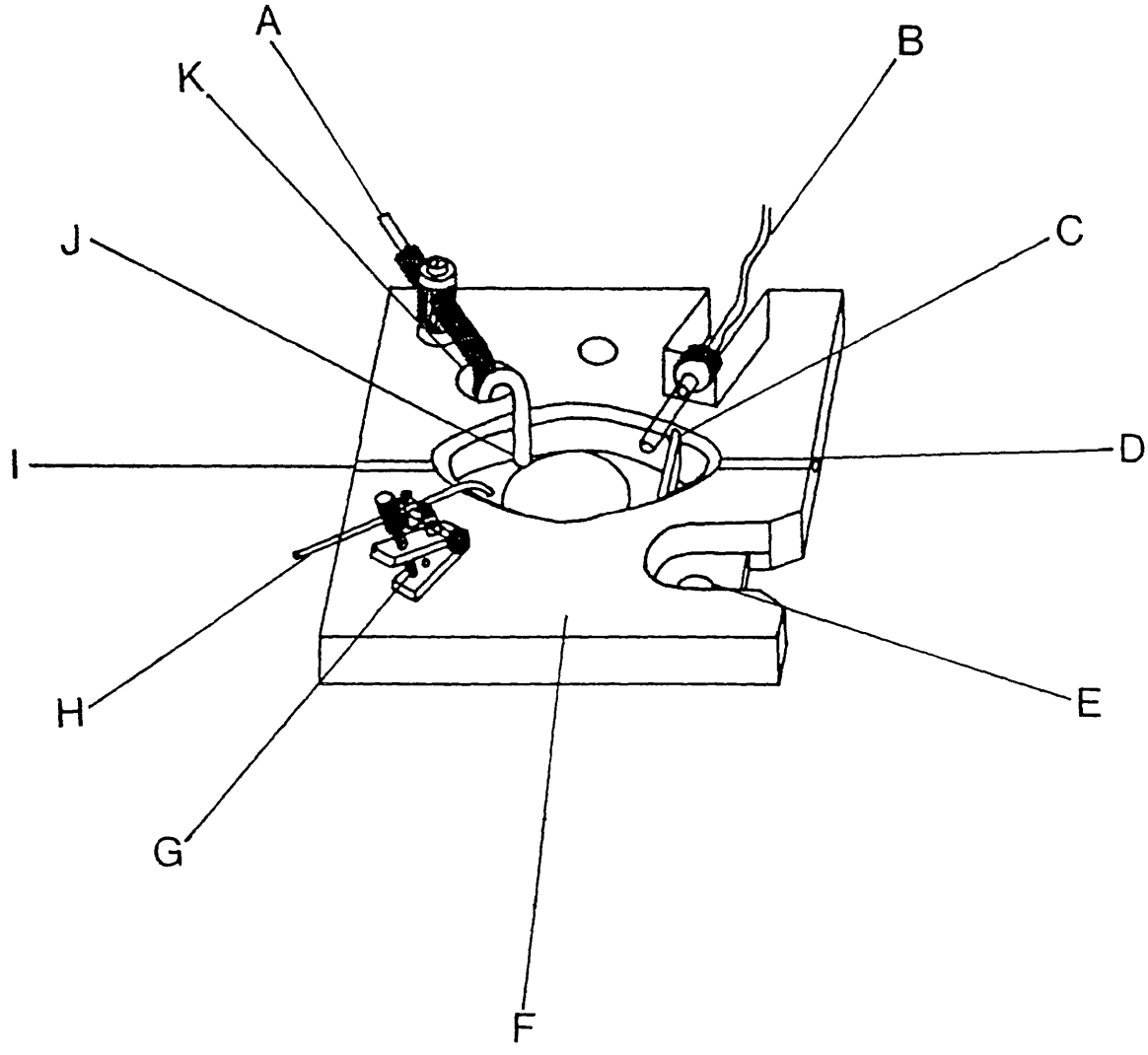
A
B
K
C
J
D
I
H
E
G
F

SECTION 2: Studies of rat paratracheal neurones

Removal and dissection of the trachea

All experiments were performed on 14-18 day old male and female Sprague-Dawley rat pups. Animals were stunned and then killed by cervical dislocation. The trachea between the base of the larynx and the bifurcation of the left and right bronchi was removed and carefully cleared of all superficial fat and connective tissue. The trachea was then cut midline along the length of its ventral surface and pinned out through the cartilage rings onto the surface of a small block of Sylgard (Dow Corning) such that the dorsal surface of the trachealis muscle was uppermost. Figures 2.4 and 2.5 show four views of living paratracheal ganglia viewed using modulation-contrast optics (Hoffman, 1977).

Setting up the trachea for electrophysiological recording

The Sylgard block bearing the trachea was pre-bonded to a glass slide which formed the base of a Perspex recording chamber (see Fig. 2.3). The assembled chamber was then clamped to the moveable stage of a Zeiss Ergoval microscope (in the same manner as described in section 1) equipped with low-power bright-field (x40) and modulation-contrast optics (Hoffman, 1977) giving 320- and 640-fold magnification.

The preparation was perfused at a rate of 6 ml/min with Krebs solution maintained at 33-34^{o}C using a remote thermostatically controlled heating coil. The Krebs solution was of the following composition (mM): NaCl, 117; KCl, 4.7; $MgCl_2$, 1.2; NaH_2PO_4, 1.2; $CaCl_2$, 2.5; $NaHCO_3$, 25; glucose, 11; gassed with 95% O_2 /5% CO_2.

Fig 2.4. Photomicrographs of paratracheal ganglia from a 16 day old rat. A, a small ganglion (G) containing about nine distinct neurones (n) can be seen lying close to a small blood vessel (bv) containing red blood cells (rbc). B, another ganglion (G) lying at the intersection of interganglionic nerve trunks (ign). Scale bars 50 μm.

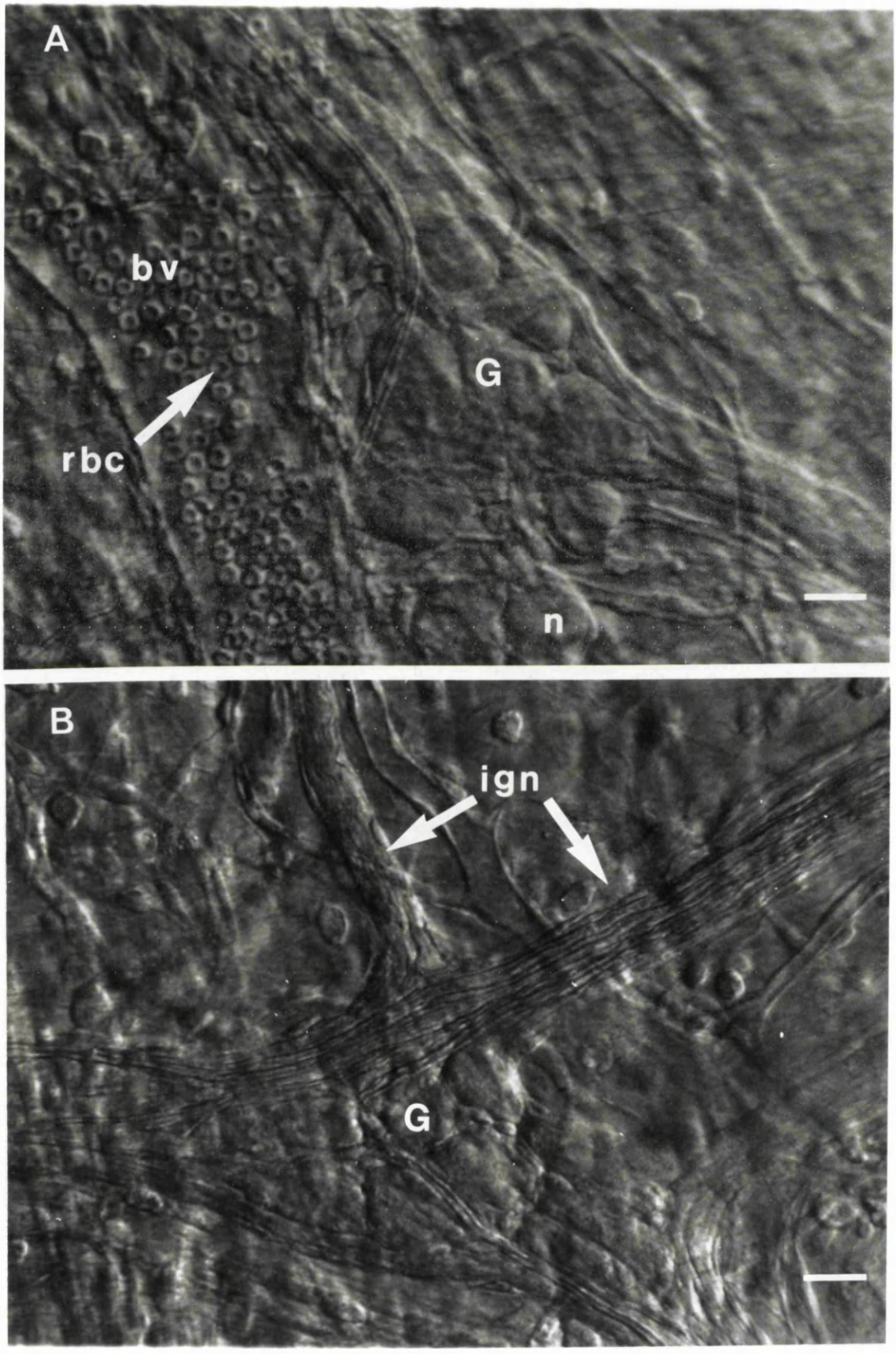
A
bv
rbc
G
n
B
ign
G

Fig. 2.5. Photomicrographs of paratracheal ganglia from A, 17 and B, 14 day old rats. A, one ganglion (G) containing approximately 20 individual cells can be seen lying within the body of a large nerve. This connects with another larger ganglion, top left, the bulk of which is out of view. B, a small ganglion (G) and a number of loosely associated neurones (n) lying close to a nerve. Scale bars 50 μm.

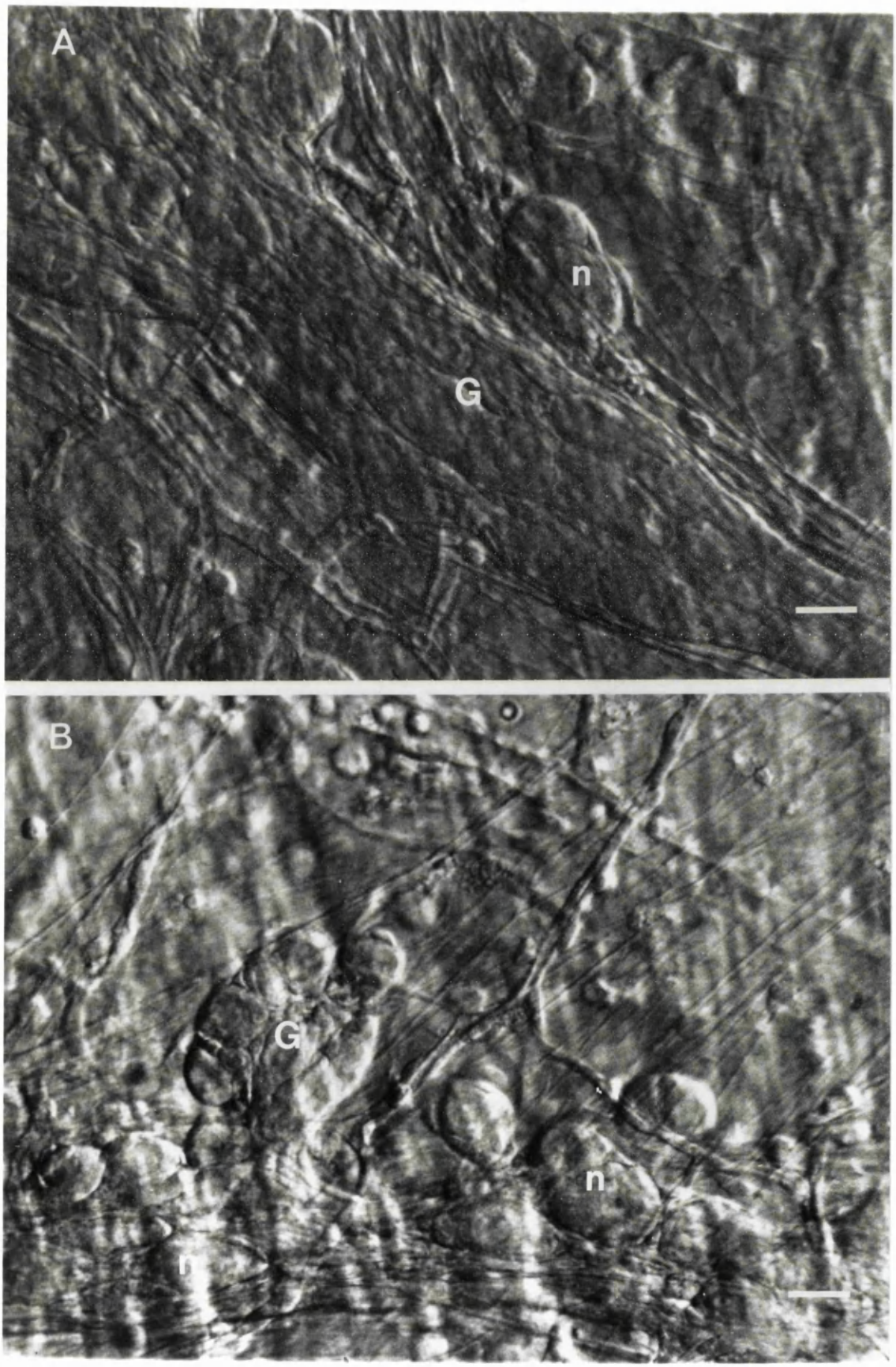
A
n
G
B
G
n
n

SECTION 3: Methods of drug application

Superfusion

Drugs could be perfused into the recording chamber from any one of eight small reservoirs (each of 25 ml volume) by way of a 9-way zero dead space tap. Each reservoir was independently oxygenated with 95% O_2 /5% CO_2. Warming of the drug-containing solutions was achieved by passing the solutions through the thermostatically controlled heating coil in the same way as for the normal Krebs solution.

Ionic substitution

In order to maintain Donnan equilibrium as well as osmolarity, high potassium-containing solutions were made by substituting potassium sulphate and sodium isethionate for sodium choride. Low chloride-containing solutions were produced by direct substitution with either sodium isethionate or sodium gluconate. Low sodium-containing solutions were produced by substituting choline chloride for sodium chloride. Low calcium-containing solutions were produced by direct substitution with magnesium.

Focal pressure application

Direct application of drugs onto the soma of neurones was carried out using blunt microelectrodes placed within 50-100 μm of the cell. Drugs were applied for various periods ranging between 10 ms and 1 s under pressures of 0.5-2 bar (the higher pressures being used when ejecting drugs from fine pipettes). All drugs were

diluted in Krebs solution and, wherever possible, the pH was tested and if necessary adjusted to 7.2. Where problems of desensitization due to drug leakage from pipettes were encountered, the pipettes were backed away from the cell between stimulations. The position of the electrode relative to other cells in the culture was used as a reference to ensure that the electrode was subsequently returned to exactly the same position before the next stimulation.

Ionophoresis

Ionophoretic application of drugs was made using microelectrodes with resistances between 30 and 80 MΩ, placed within 1-5 μm of the cell soma. These were connected to the input of an amplifier with a constant current facility (2nd channel of the Axoclamp-2A). Leakage of drugs from the electrode was prevented by passing a constant "retaining current" with the reverse polarity to that required for drug ejection. Prior to using the ionophoretic pipette, the capacitance cancellation was adjusted to produce the "squarest" current pulse. In order to facilitate ionophoretic application, drugs were made up at high concentrations and the pH was adjusted so that the drug was strongly ionised. Typical ejection currents ranged between 1 and 100 nA (0.01-10 nC).

The concentration, pH and solutions in which the different drugs were made up in are given below.

Acetylcholine	3.0 M	in distilled water	pH 4.5
GABA	0.5 M	in distilled water	pH 4.0
Muscimol	0.05 M	in distilled water	pH 3.0
Baclofen	0.01 M	in 165 mM NaCl	pH 3.0

SECTION 4: Electrical recording

The initial experiments, including all those reported in Chapters 3 and 4 were made using a simple voltage recording amplifier with an active bridge circuit which allowed simultaneous current ejection and voltage recording (Dagan model 8700 cell explorer). Later experiments were performed using an amplifier with additional facilities for carrying out discontinuous single-electrode current- and voltage-clamp recordings (Axoclamp-2A).

Prior to impalement of cells, electrode resistance and tip liquid junction potentials were nulled to allow estimation of input resistance and membrane potential to be made during recording. These were checked at the end of the experiment by withdrawing the electrode and passing currents of similar magnitudes to those used during the impalement.

In current-clamp experiments, and experiments using simple voltage recording techniques, measurement of input resistance was made by passing brief constant current pulses (50-100 ms / 50-100 pA) through the electrode and measuring the amplitude of the evoked voltage changes. In voltage-clamp experiments, conductance changes were monitored by imposing small negative voltage commands (5-10 mV) and measuring the amplitudes of the evoked currents. The fractional increase in membrane conductance was calculated as $(R/R^1)-1$, where R was the input resistance under control conditions and R^1 was that at any given time during an evoked response. The predicted amplitudes for observed responses (v) were calculated using the equation: $v=(1-R^1/R)(E-E_m)$ where E was the equilibrium potential for the observed response. In the case of the spike after-hyperpolarization, E was equal to the observed equilibrium potential for the underlying calcium-activated potassium

current ($E_{K,Ca}$; see Chapter 3); whilst for the muscarine induced inhibitory response E was equal to the reversal potential for this response ($E_{K,i}$; see Chapter 4). E_m was the membrane potential of the cell. Under voltage-clamp, predicted equilibrium potentials were calculated from the observed current and conductance changes using a modified version of this equation: $V_h-E_r=1/(G^1-G) \times I$, where V_h was the membrane potential at which the cell was held, E_r was the equilibrium potential for the response, G was the resting membrane conductance, G^1 was the membrane conductance at any given time (t) during the response and I was the amplitude of the current at time (t).

Data from recordings were either stored for future analysis on an fm tape recorder (Racal store 4DS) or displayed using a Tektronix storage oscilloscope (model D13) and a Gould pressure ink recorder (model 2200S). All numerical data is given as the mean ± S.E.M.

Discontinuous single-electrode current- and voltage-clamp recording

When recording using discontinuous single-electrode current- and voltage-clamp modes, settling of the voltage waveform was monitored on a second oscilloscope to ensure that all transients had decayed to baseline before the next sample was taken. In order to obtain the highest sampling rates and therefore the best frequency response in discontinuous modes, the fluid level in the recording chamber was kept as low as possible and electrodes were coated with Sylgard to reduce the transmural capacitance (see below). Fine adjustment of the phase controls and anti-alias filter were used to improve the step response of the system and also reduce the overall level of current noise. When optimally set, sampling frequencies of between 3 and 5 KHz were usually obtained, with the final output being filtered to

between 0.3 and 1 KHz.

When constructing current-voltage relationships, the values for the instantaneous currents could not be measured directly due to the presence of transient currents at the start of the voltage command. Estimation of the instantaneous current flow was made by extrapolating the current measured after all transients had decayed back to time zero.

"Hybrid" clamp recording

The limited frequency response obtainable when combining the discontinuous voltage-clamp technique with the use of high resistance microelectrodes, prevented adequate clamping of rapid currents such as those underlying the action potential. In order to overcome this problem, when studying the current underlying the slow after-hyperpolarization, a "hybrid" type of voltage-clamp technique was utilised. This entailed briefly switching the recording amplifier from voltage-clamp to "current-clamp" mode. In "current clamp" mode, trains of action potentials were generated by passing brief intrasomal current pulses (5-15 ms) of sufficient intensity to elicit action potential discharge. At the end of the period of stimulation, the amplifier was then switched back into voltage-clamp mode to permit measurement of the evoked slow post-spike currents. Action potential discharge was elicited using a brief series, rather than prolonged current pulses, as this minimised the activation of slow time-dependent currents such as the M-current. In addition, this method was also found to be better for evoking a consistent action potential discharge when the cells were superfused with solutions of widely differing ionic compositions.

Electrodes

Electrodes were pulled using a Brown and Flaming model P77 electrode puller (Sutter Instruments). Impalements were made using electrodes with d.c. resistances of between 90 and 130 MΩ filled with 2 M potassium citrate solution (pH adjusted to 7.2 with citric acid). Attempts were also made to use potassium chloride and potassium acetate as filling solutions. Potassium chloride and to a lesser extent potassium acetate tended to cause vacuoles to form in the cytoplasm and deterioration in the condition of the cell.

To improve the frequency response of electrodes, which was particularly important when using discontinuous sampling modes of recording, electrodes were coated to within 100 μm of their tips with with Sylgard (Dow Corning) to improve their capacity characteristics. A minor modification was made to the electrodes used when recording from tracheal ganglia. In order to aid the placement of electrodes and impalement of neurones, the final 3-6 mm of the electrode was bent through an angle of 60 degrees prior to filling.

Microelectrodes were connected to the headstage of the pre-amplifier using a Perspex electrode holder with an integral sintered silver-silver chloride half-cell (Clarke Electromedical) filled with the same electrolyte as the microelectrode. A small (0.5 mm) hole was drilled in the side of the holder to relieve any pressure build-up when inserting the electrode into the holder, thereby minimising pressure-related changes in the tip liquid junction potential. Earthing of the recording chamber was by way of a similar silver-silver chloride half-cell. To avoid the problem of contaminating the preparation with toxic silver ions, the earth electrode was connected to a small reservoir containing the same electrolyte used to fill

electrodes. This reservoir was then coupled to the recording chamber using a plastic encapsulated agar bridge (see Fig. 2.3).

Whole-cell patch-clamp recording

The whole-cell patch-clamp recording technique (Hamill, Marty, Neher, Sakmann & Sigworth, 1981) was used to make recordings from a small sample of M type intracardiac neurones (see Chapter 3 for the definition of the different cell types), which due to their small size, were otherwise difficult to record from using conventional intracellular microelectrodes. A few AH type cells were also studied using this technique, but the presence of glial cells over these neurones (see ultrastructural study by Kobayashi et al. 1986a, b) prevented the use of this technique to study the majority of cells. Patch-clamp recordings were made using an Axoclamp-2A amplifier and electrodes with resistances between 3 and 7 MΩ. Prior to filling, electrodes were fire polished using a glass-coated platinum heating element and coated to within 100-200 μm of their tip with Sylgard to reduce transmural capacitance. The electrode filling solution had the following composition (mM): KCL 110; HEPES 40; $MgCl_2$ 3 and EGTA 3 (pH 7.2).

SECTION 5: Drugs used and their suppliers

Acetylcholine chloride	ACh	Sigma
See below for full name	AF-DX 116	Karl Thomae GmBh
Adenosine 5'-triphosphate	ATP	Sigma
4-Aminopyridine	4-AP	Sigma
γ-Aminobutyric acid	GABA	Sigma
Atropine sulphate	-	Sigma
Baclofen	-	CIBA
Bicuculline methiodide	-	Sigma
Barium chloride	$BaCl_2$	Sigma
Cadmium chloride	$CdCl_2$	Fisons
Caesium Chloride	CsCl	Sigma
Caffeine	-	Sigma
Cobaltous chloride	$CoCl_2$	Sigma
See below for full name	4-DAMP	A gift from Dr. R.B. Barlow
Gallamine triethiodide	-	Sigma
Manganese sulphate	$MnSO_4$	Sigma
2-Methylthio ATP	2-me.S.ATP	Sigma
α,β-Methylene ATP	α,β-me-ATP	Sigma
D-L muscarine chloride	-	Sigma
Muscimol	-	Sigma
Ouabain	-	Sigma
Phaclofen	-	Tocris Neuramin
8-Phenyltheophylline	8-PT	Calbiochem
Picrotoxin	PTX	Sigma
Pirenzepine dihydrochloride	-	Boots

Reactive Blue 2	RB 2	Sigma
Sodium cyanide	-	Sigma
Tetraethylammonium	TEA	Sigma
Tetrodotoxin	TTX	Sigma

AF-DX 116 11-[[2-[(diethylamino)methyl]-1-piperidinyl]acetyl]-5,11-dihydro-6H-pyrido[2,3-b][1,4]benzodiazepine-6-one.

4-DAMP 4-Diphenylacetoxy-N-methyl-piperidine methiodide

Chapter 3

INTRACELLULAR STUDIES OF THE ELECTROPHYSIOLOGICAL PROPERTIES OF CULTURED INTRACARDIAC NEURONES OF THE GUINEA-PIG

SUMMARY

1. The electrophysiological properties of intracardiac neurones cultured from ganglia within the atria and interatrial septum of the newborn guinea-pig heart were studied using intracellular microelectrodes.

2. Three types of neurones with resting membrane potentials in the range -45 to -76 mV were detected. The first, AH_s cells, had high (15-28 mV) firing thresholds, pronounced slow spike after-hyperpolarizations and fired only once to prolonged intrasomal current injection. The second type AH_m cells, were similar to AH_s cells, except that they could fire short bursts of spikes (100-400 ms) at the onset of current injection. The third type, M cells, had low firing thresholds (10-15 mV), no prolonged after-hyperpolarization and produced non-adapting trains of action potentials in response to depolarizing current injection.

3. The generation of action potentials in M cells was prevented by tetrodotoxin (TTX; 0.3 μM), whereas in AH_s and AH_m cells action potentials displayed a calcium-dependent, TTX-insensitive component which was abolished by calcium channel blockade using solutions containing the divalent cations cadmium, cobalt or manganese (0.02-1 mM).

4. The after-hyperpolarization in AH_s and AH_m cells was abolished by the removal of extracellular calcium, shortened in solutions containing the calcium entry blockers $CdCl_2$, $MnSO_4$ and $CoCl_2$ (0.02-1 mM) and prolonged by the addition of calcium (5.0 mM), tetraethylammonium (1-3 mM) 4-aminopyridine (1-3 mM), cyanide (10 μM) or caffeine (100 μM) to the perfusate.

5. The reversal potential of the after-hyperpolarization was -89.1 mV. This value changed by 62.9 mV for a 10-fold increase in extracellular potassium concentration.

6. The peak conductance change during the after-hyperpolarization ($g_{K,Ca}$), was largely independent of membrane potential between -50 and -110 mV. The peak increase in $g_{K,Ca}$ and the duration of the after-hyperpolarization increased with the number of spikes preceding it.

7. It is concluded that calcium entry during the action potential is responsible for the activation of an outward potassium current in the two types of AH cells; the roles played by intracellular calcium extrusion as well as sequestration mechanisms in the generation of the response are discussed.

INTRODUCTION

Over the past 20 years, studies of isolated sympathetic, parasympathetic and enteric ganglia have provided considerable insight into the functional roles and interactions occurring within peripheral autonomic ganglia (Elfvin, 1983). These investigations have demonstrated that in many instances peripheral ganglia do not act purely as passive relay stations for the transfer of information from higher centres. Instead they may form independent integrative networks that are modulated, rather than directly controlled, by extrinsic nerves.

Direct studies of many intramural ganglia has been impeded by their inaccessibility and diffuse distribution within a tissue. These problems have been no more striking than in the study of mammalian intracardiac ganglia. In mammals, the ganglia are mainly concentrated within the interatrial septum and subepicardially in the left atrium around the vena cava (King & Coakley, 1958). Ultrastructural studies of mammalian intracardiac ganglia in situ have visualised synapses on intrinsic nerve cell bodies (Ellison & Hibbs, 1976), whilst immunocytochemical studies have localised VIP-, NPY- and SP-immunoreactive cell bodies, together with VIP-, NPY-, SP-, neurotensin-, CGRP-, and enkephalin-immunoreactive nerve fibres in the heart in situ (Weihe, McKnight, Corbett, Hartschuh, Reinecke & Kosterlitz, 1983; Weihe, Reinecke & Forssmann, 1984; Gibbins, Furness, Costa, MacIntyre, Hillyard & Girgis, 1985; Dalsgaard, Franco-Cereceda, Saria, Lundberg, Theodorsson-Norheim & Hökfelt, 1986; Baluk & Gabella, 1989b)). However, most of these studies were unable to determine whether any immunoreactive nerves or synapses were of intrinsic origin.

With the exception of amphibian intracardiac ganglia (McMahan & Purves, 1976; Roper, 1976; Hartzell et al. 1977), few direct electrophysiological studies of

intramural heart neurones have been reported. In an extracellular study of cat intracardiac ganglia a number of different patterns of neuronal firing in response to mechanical stimulation were observed (Nozdrachev & Pogorelov, 1982), while in a brief abstract it was reported that a subpopulation of neurones responding to SP and SOM were detected with intracellular micro-electrodes within a large ganglion exposed by dissection of the guinea-pig heart (Konishi et al. 1984).

Recently, a dissociated cell culture preparation has been developed in our laboratory in order to overcome many of the problems inherent in the study of intramural heart neurones in situ (Hassall & Burnstock, 1986). The ultrastructural integrity of the neurones and their interactions with many of their associated cells are maintained under the conditions of culture (Kobayashi et al. 1986a, b), whilst immunocytochemical studies indicate that the neurones also retain a high degree of neurochemical specialisation (Hassall & Burnstock, 1984, 1986).

In the present study, it is reported that single identified intracardiac neurones also show differentiation of electrophysiological properties when maintained in tissue culture.

RESULTS

The results reported here were based upon intracellular recordings from more than 230 intracardiac neurones maintained in dissociated cell culture for 5-14 days. In culture these neurones ranged in diameter from 8 to 40 μm. The majority of recordings were obtained from larger diameter (>12 μm) neurones. Some data has been gathered from the small neurones; however, due to difficulties in recording from such cells they must be considered an under-sampled population, within which there may be classes of neurones not yet studied.

In all cases, impaled neurones were only considered suitable for study if they had a stable membrane potential of at least -45 mV (range -45 to -76 mV), and were capable of generating an action potential in response to the injection of depolarizing current pulses. Most impalements were made with electrodes containing 2 M potassium citrate as this gave the most successful long-term recordings. Potassium chloride and, to a lesser extent, potassium acetate generally caused vacuoles to form in the cytoplasm which resulted in a marked deterioration in the condition of the cell. Following the initial impalement, neurones frequently hyperpolarized by a further 5-10 mV before a stable membrane potential was established. Input resistances measured after this initial settling period ranged from 46 to 280 MΩ (mean 123.4 ± 8.83 MΩ, n=57).

Active membrane properties

On the basis of their responses to depolarizing current injection, three different classes of neurone could be distinguished. In the first group, consisting of 65-75% of the neurones studied, only one, or occasionally two, action potentials

could be elicited, regardless of the stimulus intensity or duration. The excitability of these cells was quite low, and they required a 15-28 mV depolarization of the membrane in order to elicit an action potential. These action potentials were invariably followed by a marked after-hyperpolarization ranging in amplitude from 8 to 22 mV which persisted for up to 3 s (Fig. 3.1A). Of these neurones, 25-30% also exhibited anodal-break firing. In the present study these neurones have been termed AH_s cells, the AH to denote the presence of a prolonged spike after-hyperpolarization and the s to signify single firing to prolonged depolarizing current injection (see Fig. 3.1B).

A second group of cells, consisting of 10-15% of the neurones studied, exhibited similar firing thresholds and prolonged spike after-hyperpolarizations; however, these neurones were capable of short bursts of multiple firing. Typically, injection of 100-150 pA of current elicited only a single action potential. If, however, the current was then increased by a few hundred picoamperes, a greater number of spikes could be generated. In this manner, short bursts of firing at rates as high as 90 Hz could be evoked. These trains were followed by prolonged after-hyperpolarizations (Fig. 3.1C), the duration of which was dependent upon the preceding number of spikes. This second group of neurones have been termed AH_m cells, the m denoting multiple firing to prolonged current injection.

The third type of neuronal properties that were observed, arose primarily amongst small rounded mononucleate neurones. These cells had low firing thresholds (10-15 mV) and generated trains of action potentials for prolonged periods (up to 3 min) in response to sustained depolarizing current injection and on this basis these have been termed M cells. Action potentials in these neurones never exhibited prolonged (>100 ms) after-hyperpolarizations (Fig. 3.1D). Unlike either of the other

neuronal types, these cells occasionally displayed spontaneous tonic firing, which could be inhibited by passing hyperpolarizing current through the electrode.

Sodium- and calcium-dependence of spikes

The relative contributions played by sodium and calcium ions in the generation of action potentials in different cell types were studied using solutions containing sodium and/or calcium channel blocking agents (Fig. 3.2). In AH_s and AH_m type cells, TTX (0.3 μM) failed to abolish either the current-induced action potential or the post-spike hyperpolarization. The magnitude of the remaining spike was often small. However, by raising the stimulating current and/or adding extra calcium (5 mM) or TEA (1mM) to the perfusate, a larger TTX-insensitive action potential could be generated. Characteristically this spike had a lower rate of rise and was smaller than the pre-TTX action potential (Fig. 3.2B). When TTX (0.3 μM) and $CdCl_2$ (20 μM) were applied together, both the spike and the slow after-hyperpolarization were abolished in all cells (n=15; Fig. 3.2C). Action potentials in multiple firing (M) cells were unaffected by $CdCl_2$ (20 μM), whereas TTX (0.3 μM) prevented all spike generation (n=8; Fig. 3.2F).

Slow after-hyperpolarization

To study the slow after-hyperpolarization following one or more action potentials in AH_s and AH_m neurones, different periods and rates of firing were induced using trains of brief (5-15 ms) depolarizing current pulses.

Peak amplitude

The amplitude of the after-hyperpolarization increased with the preceding number of action potentials (Fig. 3.3A & B). The mean amplitude following a single spike was 14.4 ± 0.96 mV (n=13) and rose rapidly following two to three spikes (delivered at 20 Hz). Subsequent action potentials produced only a gradual increase in the amplitude of the response, with a maximum response of 19.2 ± 1.02 mV (n=11) being reached after thirty action potentials (Fig. 3.3A).

By assuming the after-hyperpolarization was due entirely to an increase in potassium conductance, peak amplitude was calculated from the observed conductance change (see methods section for details). The observed peak amplitudes agreed well with these predicted values (see Fig. 3.3A).

Duration of the after-hyperpolarization

The duration of the after-hyperpolarization in AH_s and AH_m cells following either single or multiple action potentials varied considerably. Following a single spike, the duration of the slow after-hyperpolarization was in the range 200-3000 ms (mean 927.9 ± 64.7 ms, n=92) whereas following thirty spikes the range was 1.2-8.0 s (mean 3.63 ± 0.194 s, n=71). The decay of the response following the first few spikes was exponential. Following greater numbers of spikes, however, the decay could no longer be fitted by either one or the sum of two exponential functions. Total after-hyperpolarization duration showed little prolongation beyond the first five to ten action potentials. However, the time during which the maximum after-hyperpolarization amplitude was maintained and the duration of the underlying peak conductance phase of the response continued to increase. The decline time to half-

peak amplitude was used as a measure of this phenomenon and it can be seen that although the peak amplitude and conductance were reached following the first few spikes (Fig. 3.3A) the decline time to half-peak amplitude rose more slowly and continued to rise up to and beyond thirty action potentials (Fig. 3.4).

Voltage-dependence of the after-hyperpolarization

The effects of membrane potential upon the amplitude and conductance change of the slow after-hyperpolarization were studied. Amplitude was linearly related to membrane potential between -50 and -110 mV (Fig. 3.5B). Membrane hyperpolarization reduced the amplitude of the response with reversal occurring at -89.1 ± 0.71 mV (n=9). The voltage-dependence of the underlying conductance change was studied taking advantage of the lack of membrane rectification in many cells between -50 and -110 mV. Over this range the time course and peak conductance change of the slow after-hyperpolarization was largely independent of membrane potential (see Fig. 3.5A).

Ionic-dependence of the after-hyperpolarization

The ionic-dependence of the slow after-hyperpolarization following thirty action potentials (20 Hz/1.5 s) was examined.

Potassium. The after-hyperpolarization at a given membrane potential depended upon the external potassium concentration. For any particular membrane potential, raising the concentration of potassium reduced the amplitude of the slow after-hyperpolarization, whilst reduced concentrations had the reverse effect (Fig. 3.6). The reversal potential of the slow after-hyperpolarization was examined at two

elevated potassium concentrations (10 and 20 mM). The mean reversal potentials in these solutions were -68.4 ± 1.32 mV (n=5) and -49.6 ± 0.33 mV (n=3) respectively. The reversal potential of the slow after-hyperpolarization was related to the external potassium concentration by the relationship: $62.9 \log_{10} [\text{potassium}]_o/[\text{potassium}]_i$. This compares well with the value of 61 predicted from the Nernst equation for a response brought about exclusively by an increase in potassium conductance. However, in order to maintain Donnan equilibrium between potassium and chloride ions in these solutions, chloride concentration had by necessity also to be altered. Therefore, the reversal potential in low chloride (9 mM) was examined. Altering chloride concentration did not significantly alter the reversal potential from the control value (control -87.7 ± 0.88 mV; low chloride -87.3 ± 0.62 mV, n=3).

Calcium. The calcium-dependence of the potassium conductance underlying the slow after-hyperpolarization was examined. Complete removal of extracellular calcium caused a 5-15 mV depolarization of the cell membrane, and often led to the generation of spontaneous firing. By substituting magnesium for calcium ions, the depolarization as well as the spontaneous firing could largely be prevented. In all cases, whether extra magnesium ions had been added or not, the slow after-hyperpolarization and underlying conductance change were completely abolished in the absence of calcium ions (Fig. 3.7). The removal of calcium also reduced the strength of the depolarizing current needed to elicit trains of action potentials, and in some cases enabled a neurone previously only capable of firing one action potential to fire multiply to prolonged current injection. Raising the calcium concentration (from 2.5 to 5.0 mM) caused an increase in the duration of the slow after-hyperpolarization and underlying conductance change (mean 121.6 ± 24.1%, n=8) whilst it had little effect upon the peak amplitude of the response (mean 102.9 ±

4.2% of control, n=8).

Drug-induced alterations in the slow after-hyperpolarization

Calcium entry blockers $CoCl_2$ and $MnSO_4$ (1-3 mM) generally caused only partial blockade of the slow after-hyperpolarization; on the other hand, $CdCl_2$ significantly reduced the early component of the slow after-hyperpolarization at concentrations as low as 20 μM (Fig. 3.8C). Higher concentrations completely abolished the slow after-hyperpolarization; however, these effects were rarely fully reversible.

TEA(1 mM) and 4-AP (1 mM) both caused a marked prolongation of the repolarization phase of the action potential and an increase in the duration of the slow after-hyperpolarization (Fig. 3.8A and B). The mean increase in the duration of the slow after-hyperpolarization for TEA was 97 ± 10.5% (n=4), and in 4-AP it was 124.2 ± 21.9% (n=4). 4-AP was generally more potent than TEA, and at the concentrations used was never seen to have a direct blocking effect upon $I_{K,Ca}$.

Caffeine (10 μM), which is believed to promote calcium release from intracellular stores (Kuba, 1980), also prolonged the duration of the slow after-hyperpolarization (mean 124 ± 20.5%, n=4), but had no effect upon the spike (Fig. 3.9A).

Blockade of mitochondrial calcium sequestration by cyanide also prolonged the slow after-hyperpolarization (mean 63.3 ± 9.1%, n=3) suggesting that uptake at this site may play an important role in the control of slow after-hyperpolarization duration (Fig. 3.9C).

The contribution played by electrogenic sodium pumping in the generation of the after-hyperpolarization was examined using ouabain (100-300 nM). At these concentrations there was no alteration in either the amplitude or the duration of the response (Fig. 3.9B).

DISCUSSION

The results of the present study indicate that the electrophysiological properties of guinea-pig intracardiac neurones are maintained in dissociated cell culture. From these results, it is evident that the intracardiac neurones are a heterogeneous population, possessing a number of features in common with neurones from other autonomic ganglia. On the basis of the spike-generating properties of the soma, three electrophysiologically distinct types of neurones were distinguished. One type, termed M cells, consisted mainly of small mononucleate neurones that exhibited firing properties similar to A type sympathetic (Blackman & Purves, 1969; Gallego & Eyzaguirre, 1978) and S/type 1 enteric neurones (Nishi & North, 1973; Hirst, Holman & Spence, 1974). They were highly excitable, occasionally exhibiting spontaneous firing and discharged in a non-adapting manner to direct stimulation. Action potentials in these neurones were of the typical TTX-sensitive sodium type as seen for example in S/type 1 enteric neurones (Hirst et al. 1974). However, due to the small size of most type M neurones, stable recordings were difficult to achieve using conventional microelectrodes. Therefore in the present study, no accurate estimate of the true numbers of intracardiac neurones exhibiting these properties could be made. To overcome these problems, it may be possible to study these cells further using the whole-cell patch-clamp technique (Hamill et al. 1981).

In the remaining two groups of neurones, the underlying spike generating mechanism was different to that encountered in M cells. In these cells, action potentials all exhibited a TTX-insensitive component, which was abolished by the removal of calcium or the addition of cadmium to the perfusate. Similar mixed sodium and calcium spikes have been reported in populations of neurones in many invertebrate and vertebrate ganglia (e.g. Hirst & Spence, 1973; Meech & Standen,

1975; McAfee & Yarowsky, 1979; Ito, 1982) as in this study of intracardiac neurones, they are often associated with the presence of non-synaptic prolonged spike after-hyperpolarizations. During the slow after-hyperpolarization, the excitability of AH_s and AH_m intracardiac neurones was strongly attenuated, with much larger stimulating currents required to generate firing. Whilst it was apparent that the slow after-hyperpolarization produced a powerful inhibitory effect upon these neurones, it was not clear why only AH_m and not AH_s cells were capable of short bursts of firing to prolonged current injection. The magnitude of the slow after-hyperpolarization was similar in both types of neurone and therefore the strength of this inhibition does not appear to be a factor. From measurements of input resistance and the general responsiveness of AH_s cells, it also seems unlikely that this neuronal type were injured AH_m cells.

In both AH_s and AH_m neurones the slow after-hyperpolarization resulted from calcium entry during the action potential producing a subsequent increase in membrane potassium conductance ($g_{K,Ca}$). Two lines of evidence support the view that potassium was the only ion involved in the after-hyperpolarization in these neurones. Firstly, the response reversed symmetrically about the potassium equilibrium potential, with changes in extracellular potassium concentration shifting the reversal potential in a manner predicted by the Nernst equation; on the other hand, altering chloride concentration had no effect. Secondly, the observed conductance changes during the slow after-hyperpolarization were in good agreement with theoretical values calculated assuming the response was entirely due to an increase in potassium conductance.

The generation of the slow after-hyperpolarization relied upon calcium influx, and could be abolished by removal of extracellular calcium or the addition of

specific calcium-channel blockers which prevent entry. Conversely, TEA and 4-AP which indirectly enhance the period of calcium entry by blocking the potassium currents involved in the repolarization of the spike (Yeh, Oxford, Wu & Narahashi, 1976a, b; Ahmed & Connor, 1979), both prolonged the response. Neither TEA nor 4-AP appeared to have a direct blocking effect upon $I_{K,Ca}$ in intracardiac neurones over the range of concentrations used. TEA is known to inhibit $I_{K,Ca}$ in a number of other preparations (for review see Brown, Constanti & Adams, 1983), whereas it acts upon enteric and nodose ganglion cells to promote the slow after-hyperpolarization in a similar way to that observed in intracardiac neurones (Morita, North & Tokimasa, 1982a; Fowler, Greene & Weinreich, 1985). On the other hand, it is interesting that 4-AP has a direct and potent blocking effect upon $I_{K,Ca}$ in AH/type 2 enteric neurones (Hirst, Johnson & Van Helden, 1985), whereas in intramural heart neurones its actions seemed to be confined to voltage-sensitive potassium channels, where it produced effects similar to, although more potent than, those of TEA.

Whether it is the calcium that enters during the spike or a secondary release of calcium from intracellular stores that is responsible for the direct activation of the potassium conductance in this and other preparations is a matter for debate. Caffeine, which releases calcium from intracellular stores (Kuba, 1980) prolonged the slow after-hyperpolarization in intracardiac neurones. A similar phenomenon has been observed in bull-frog and rat sympathetic neurones (Fujimoto, Yamamoto, Kuba, Morita & Kato, 1980; Higashi, Morita & North, 1984) as well as in AH/type 2 enteric cells (Morita et al. 1982a).

From studies of single calcium channels, it seems unlikely that the kinetics of these channels are responsible for the prolonged duration of the slow after-

hyperpolarization (Marty, 1981; Barrett, Magleby & Pallota, 1982). Rather, it would appear from the present study and those of other ganglia (see Meech, 1978 for review), that the time course of $I_{K,Ca}$ activation is governed by the period of elevated intracellular calcium, which in turn is regulated by the rates of sequestration and extrusion of intracellular calcium. The main site for calcium uptake in Helix neurones is believed to be the mitochondria (Meech, 1980), whilst in the bull-frog sympathetic ganglion, as in skeletal muscle fibres, it is thought to occur in the endoplasmic reticulum (Fujimoto et al. 1980). It is possible therefore, that in intracardiac neurones, rates of release from the endoplasmic reticulum and uptake by the mitochondria are both implicated in the regulation of slow after-hyperpolarization duration since both caffeine and cyanide prolong it. Even though caffeine could promote the slow after-hyperpolarization in these neurones by elevating or prolonging the period of raised intracellular calcium, there is still no clear-cut evidence to suggest that release from this site plays any role in the normal generation of the slow after-hyperpolarization. It has been suggested that a rise in intracellular calcium may not cause direct activation of a calcium-sensitive potassium current; instead, the transient rise in intracellular calcium may alter some aspect of cellular metabolism which leads to the activation of a non-calcium-sensitive potassium current (Higashi et al. 1984).

In intracardiac neurones, ouabain, which blocks electrogenic sodium pumping, had no effect upon either the amplitude or the duration of the slow after-hyperpolarization. The apparent lack of any contribution played by electrogenic sodium pumping could possibly explain the relatively short duration of the slow after-hyperpolarization in these neurones compared to the enteric nervous system, where blockade by ouabain significantly reduces the duration of its late component (Morita et al. 1982a). In leech neurones (Jansen & Nicholls, 1973), as well as in

rabbit non-myelinated vagal fibres (Rang & Ritchie, 1968), electrogenic pumping is the major regulator of the post-tetanic after-hyperpolarization.

The role played by calcium-activated potassium currents in the control of neuronal excitability has been stressed by a number of workers. The presence of such a powerful regulatory system amongst neurones of the guinea-pig intracardiac ganglia raises many important questions as to the role played by these ganglia in the normal regulation of the heart. Preganglionic input to these neurones is predominantly from the left and right vagal nerves, and as such they are ideally placed to have a powerful effect upon coronary vagal tone. At present, there is no direct evidence to suggest that these ganglia are involved in local reflex control of the heart, although a population of mechanosensitive intracardiac neurones has been reported in the cat (Nozdrachev & Pogorelov, 1982). Many neurotransmitters and neuromodulators influence the excitability and transfer of information in other autonomic ganglia by acting to inhibit or promote the slow after-hyperpolarization. Additional studies, (see following two chapters) indicate that a similar system of regulation exists amongst intracardiac neurones. Thus, the integration of neural input at the intracardiac ganglion level may alter the inotropic and chronotropic state of the heart, or play a role in the regulation of coronary vascular tone. In the enteric nervous system the slow after-hyperpolarization has been suggested to act as a gating mechanism for the spread of excitation across the soma from one neurite to another (Wood, 1984). If a similar situation occurs in the heart, then drugs which act to modulate the slow after-hyperpolarization may control the spread of information from one area of the heart to another.

It is evident from the present study that intramural ganglia of the mammalian heart possess considerable neuronal specialisation and may be involved in complex integrative and regulatory functions within the heart. In the following two chapters some of the neurochemical properties of these neurones are reported. In particular, the actions of exogenously applied muscarinic and purinergic agonists and antagonists.

Fig. 3.1. Responses to direct intrasomal current injection in cultured intracardiac neurones (bars indicate period of stimulation). A, a typical after-hyperpolarization following a single spike in AH_s and AH_m cells (resting membrane potential -52 mV). B, an AH_s cell firing a single action potential to prolonged current injection which was followed by a large after-hyperpolarization (resting membrane potential -53 mV). C, response from an AH_m type neurone to prolonged current injection; the after-hyperpolarization was preceded by a short burst (approx. 300 ms) of action potentials (resting membrane potential -56 mV). D, an M cell capable of prolonged multiple firing (not shown here) exhibiting no slow after-hyperpolarization (resting membrane potential -56 mV). Note: spike amplitudes attenuated due to the frequency response of the pen recorder.

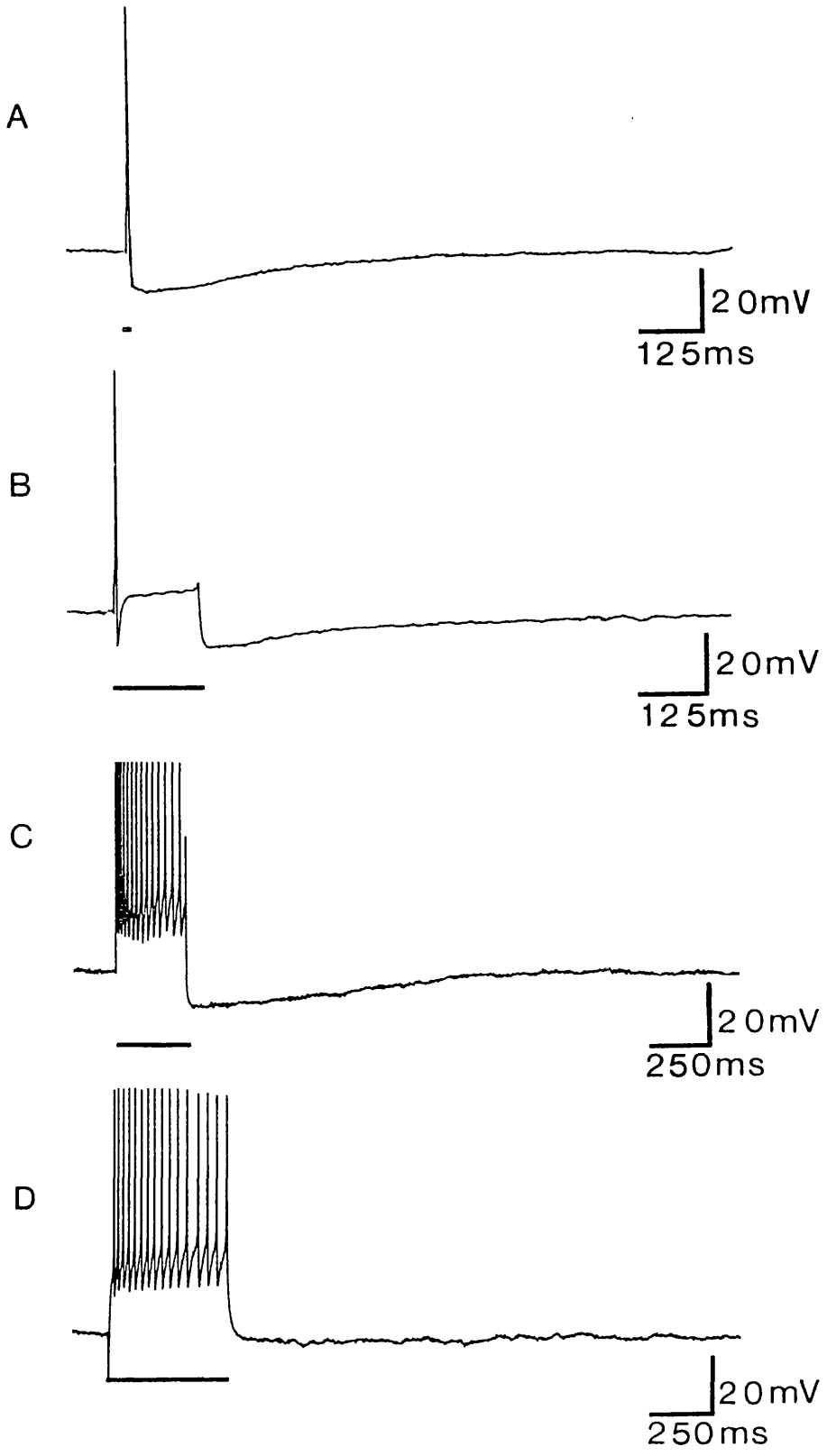
A
20mV
125ms
B
20mV
125ms
C
20mV
250ms
D
20mV
250ms

Fig. 3.2. Spike-generating properties: records A-D were obtained from an AH_s cell and indicate the presence of mixed sodium- and calcium-dependent action potentials. The spike persisted in the presence of 0.3 μM-tetrodotoxin (TTX) and 1 mM-tetraethylammonium (TEA; B), whilst the addition of TTX (0.3 μM) and cadmium (20 μM) abolished all firing (C). Records E-G were obtained from an M cell. Multiple firing to current in this cell was completely abolished by 0.3 μM TTX (F). Bars indicate period of current stimulation.

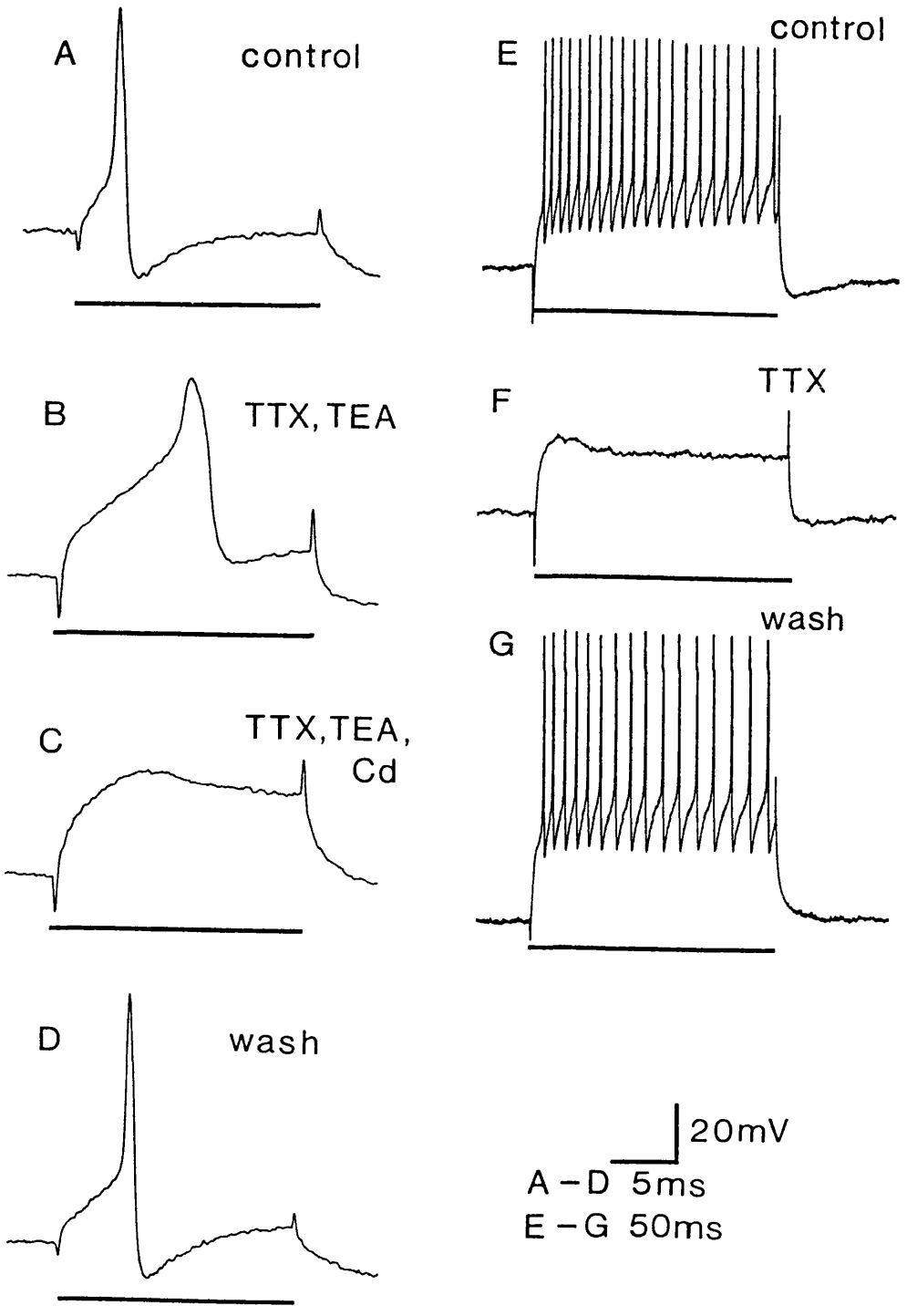
A
control
B
TTX, TEA
C
TTX, TEA,
Cd
D
wash
E
control
F
TTX
G
wash
20mV
A – D 5ms
E – G 50ms

Fig. 3.3. A, peak after-hyperpolarization amplitude with preceding spike number (●); ▲ , observed increase in peak conductance with spike number, expressed as the fractional conductance increment (see Methods). □ (dashed line), predicted after-hyperpolarization amplitude calculated from the observed conductance change (see methods, $E_{K,Ca}$ = -89.1 mV, E_m = -53.2 mV). All points are means (± S.E. of mean) of eleven to thirteen observations. Note: $E_{K,Ca}$ and E_m were experimentally determined values from experiments similar to those shown in Figs. 3.5 and 3.6. B, increase in after-hyperpolarization amplitude, duration and conductance with the preceding number of action potentials (firing frequency 20 Hz). Note: action potentials are attenuated by pen recorder (resting membrane potential -55 mV).

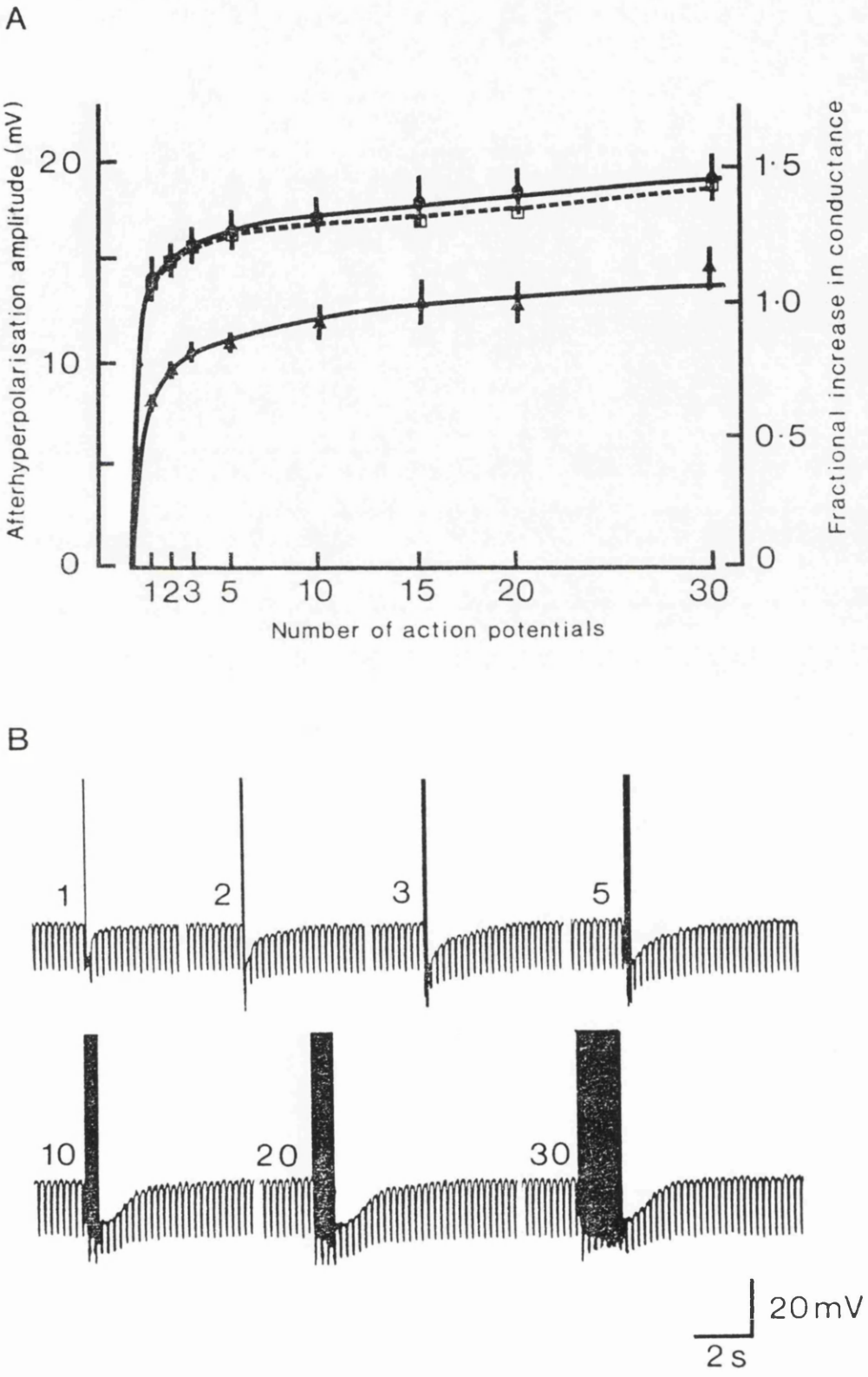
A
Afterhyperpolarisation amplitude (mV)
20
10
0
1·5
1·0
0·5
0
Fractional increase in conductance
1 2 3 5 10 15 20 30
Number of action potentials
B
1
2
3
5
10
20
30
20mV
2s

Fig. 3.4. Decay time to half-peak after-hyperpolarization amplitude was dependent upon the number of action potentials used to evoke the response (stimulus firing rate 20 Hz). Unlike the amplitude or peak conductance changes (Fig. 3.3), the decay time to half peak amplitude continued to increase significantly as the number of preceding action potentials was raised from 1 to 30. Points are means (± S.E. of the mean) of eleven to thirteen observations.

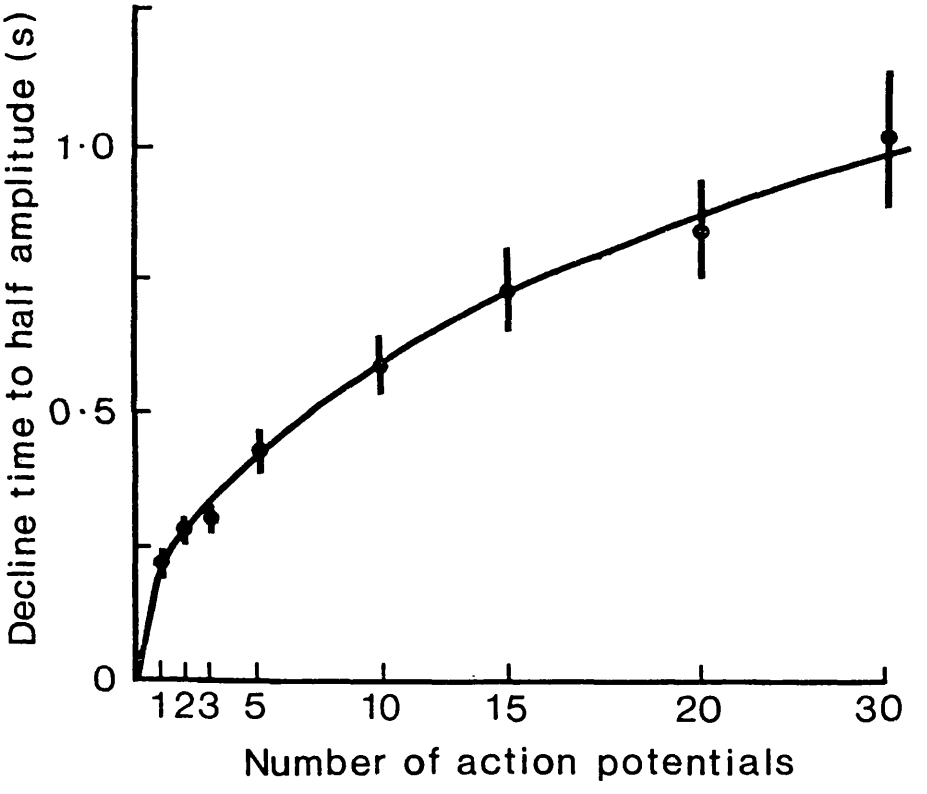
Decline time to half amplitude (s)
1·0
0·5
0
1 2 3 5 10 15 20 30
Number of action potentials

Fig. 3.5. After-hyperpolarization amplitude as a function of membrane potential. A, the voltage-dependence of the prolonged after-hyperpolarization following thirty action potentials (20 Hz/1.5 s) Note the relative insensitivity of the peak conductance increase to changes in membrane potential. B, after-hyperpolarization amplitude is linearly related to membrane potential (coefficient of correlation r=0.997) in the range -50 to -115 mV.

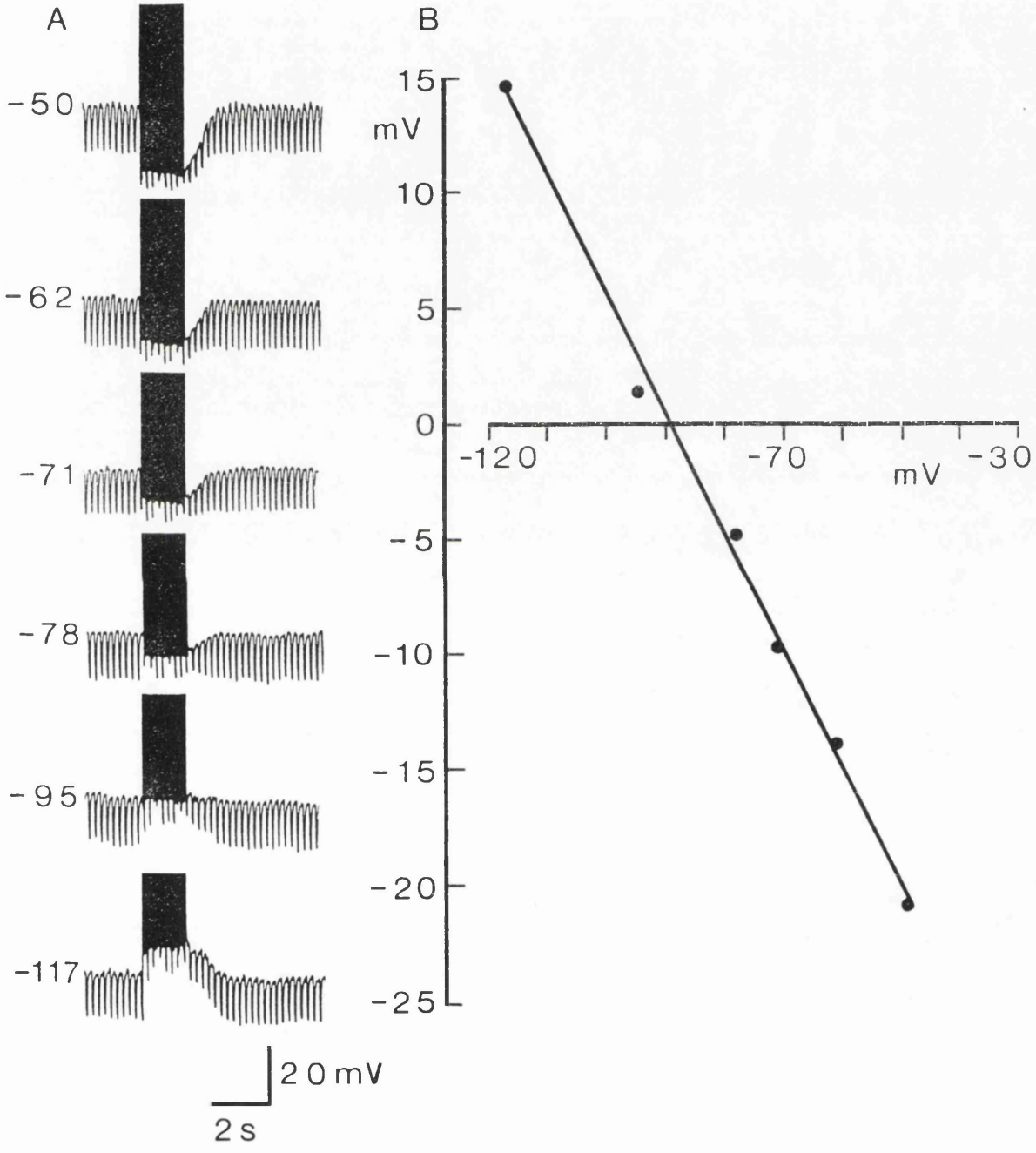
A
B
-50
-62
-71
-78
-95
-117
15
mV
10
5
0
-5
-10
-15
-20
-25
-120
-70
mV
-30
20 mV
2 s

Fig. 3.6. A, ionic- and voltage-dependence of the slow after-hyperpolarization following 30 spikes (20 Hz/1.5 s). Records from a single neurone in two elevated potassium- and one reduced chloride-containing solutions. It can be seen that for similar membrane potentials the amplitude of the slow after-hyperpolarization was reduced in solutions containing elevated potassium concentrations. B, the reversal potential for the slow after-hyperpolarization was related to the external potassium but not the chloride concentration of the perfusing Krebs solution. Line is least squares fit to the raw data from experiments similar to those shown in A. Slope of the line is -62.9 mV $\log_{10} [K^+]_o/[K^+]_i$ (coefficient of correlation r=0.993, n=17). All points are means (± S.E. of the mean) of the number of observations indicated.

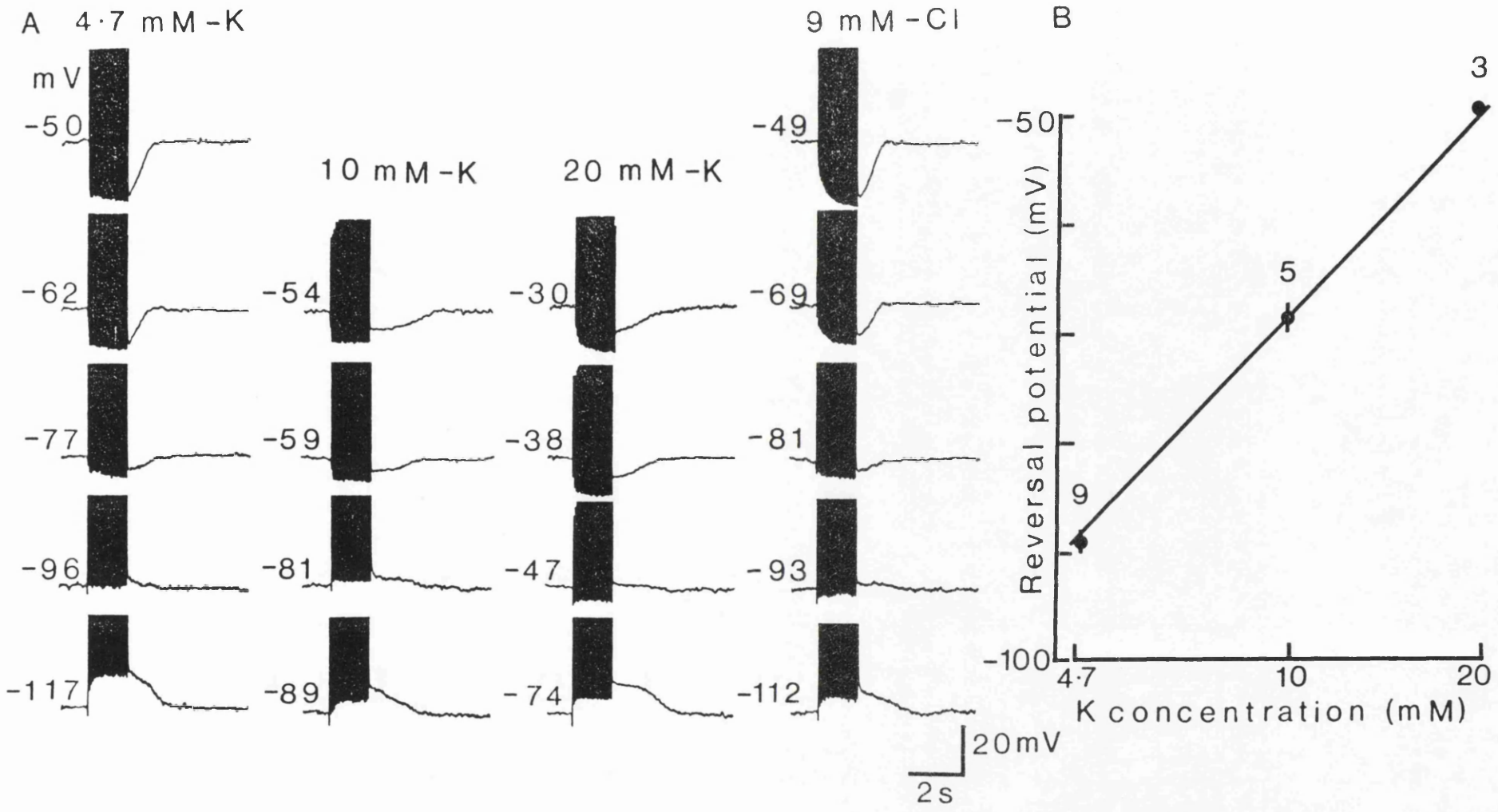
A
4·7 mM-K
mV
-50
-62
-77
-96
-117
10 mM-K
-54
-59
-81
-89
20 mM-K
-30
-38
-47
-74
9 mM-Cl
-49
-69
-81
-93
-112
20mV
2s
B
Reversal potential (mV)
-50
-100
3
5
9
4·7
10
20
K concentration (mM)

Fig. 3.7. Calcium-dependence of the slow after-hyperpolarization following thirty spikes (20 Hz/1.5 s).The numbers refer to the calcium concentration (mM). A, complete removal of extracellular calcium abolished the response (membrane depolarization prevented by replacement of calcium by magnesium ions). B, low extracellular calcium (0.5 mM) reduced the amplitude and duration of the response. C, raised extracellular calcium concentration (5 mM) prolonged the duration but had no significant effect upon the amplitude of the slow after-hyperpolarization (see text; resting membrane potential -62 mV).

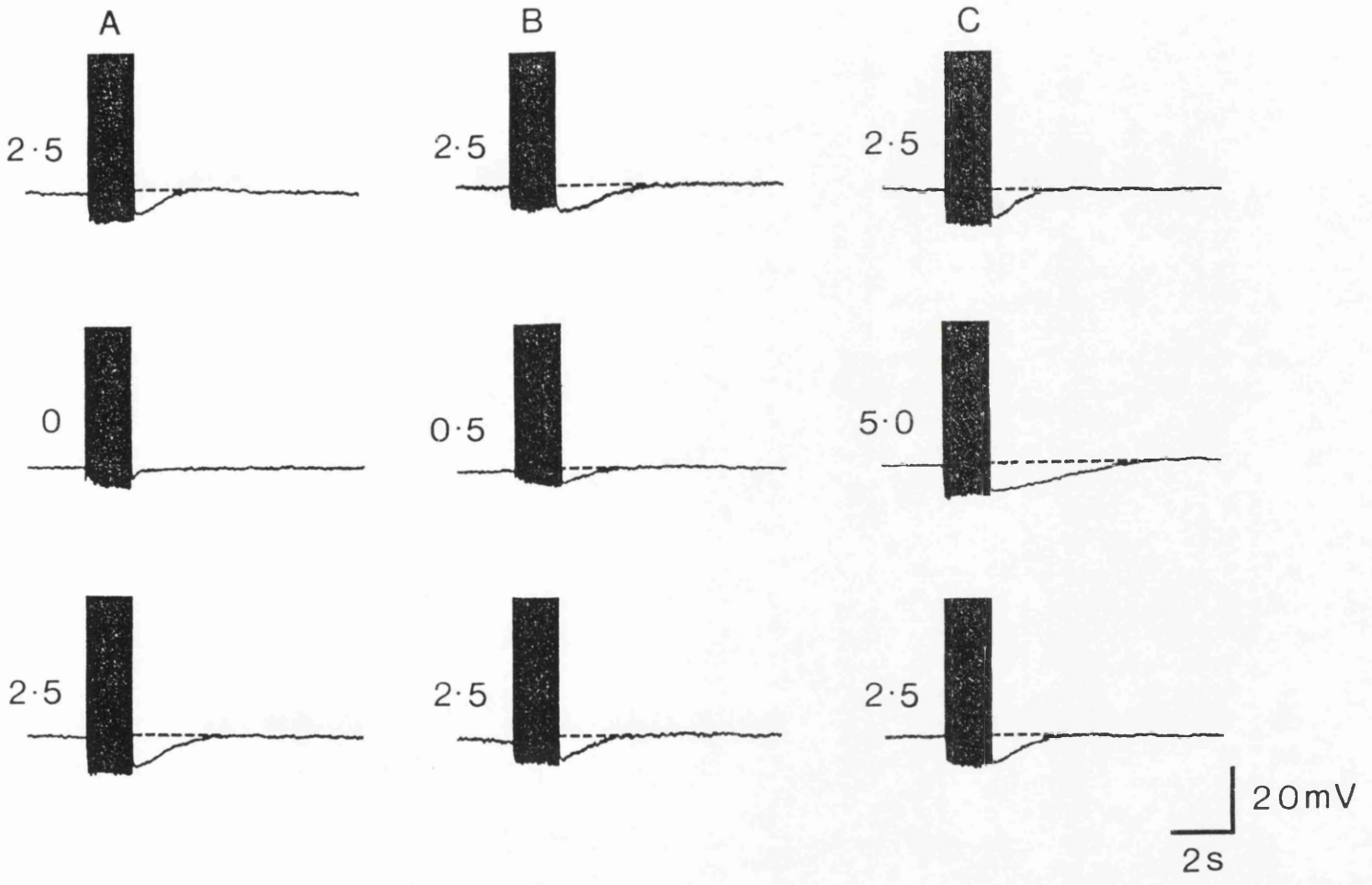
A
B
C
2·5
2·5
2·5
0
0·5
5·0
2·5
2·5
2·5
20mV
2s

Fig. 3.8. Drug-induced alterations in the slow after-hyperpolarization following thirty spikes (20 Hz/1.5 s). A, tetraethylammonium (TEA; 1 mM) reversibly prolonged the duration and the period of elevated potassium conductance in an AH_s cell. (Effect is thought to be mediated by raised calcium influx during the spike due to prolongation of the repolarization phase of the action potential; see text). B, 4-aminopyridine (4-AP; 1 mM) on the same cell produced a similar effect to TEA. 4-AP was generally more potent on intracardiac neurones than TEA. C, reduction of the slow after-hyperpolarization produced by calcium channel blockade using $CdCl_2$ (20 μM). The fast component of the slow after-hyperpolarization was most sensitive to cadmium (Cd), and greater concentrations of this drug (up to 200 μM) totally abolished the response; however, wash-out to pre-drug values was rarely possible.

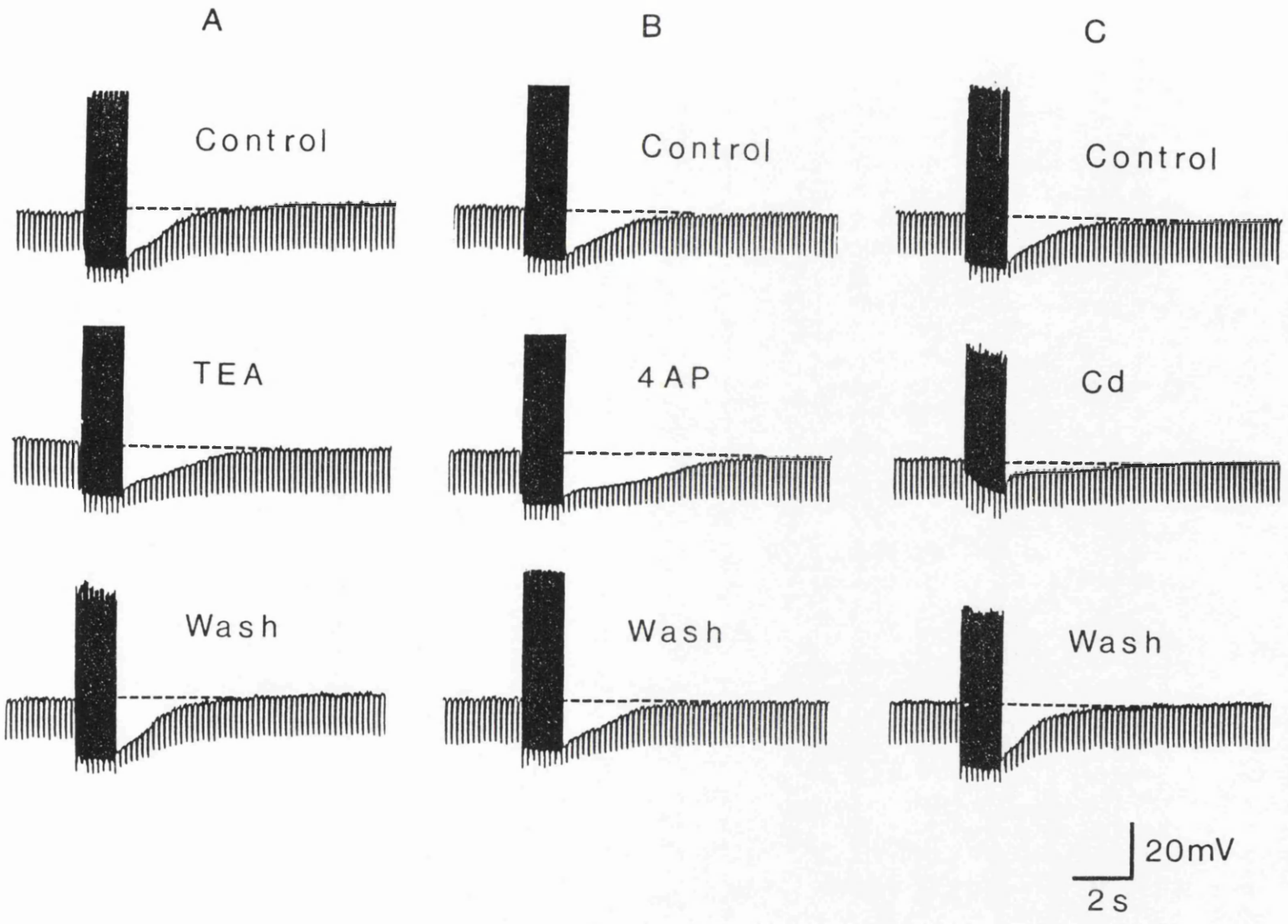
A
B
C
Control
Control
Control
TEA
4AP
Cd
Wash
Wash
Wash
20mV
2s

Fig. 3.9. Effects of caffeine, ouabain and cyanide upon the slow after-hyperpolarization following thirty spikes (20 Hz/1.5 s). A, caffeine (10 μM) causes release of intracellular calcium and prolonged the slow after-hyperpolarization. B, ouabain (100 nM), a blocker of electrogenic sodium pumping, had no effect upon either the amplitude or duration of the slow after-hyperpolarization. C, cyanide (10 μM) which was used to block calcium uptake by mitochondria caused a prolongation of the response.

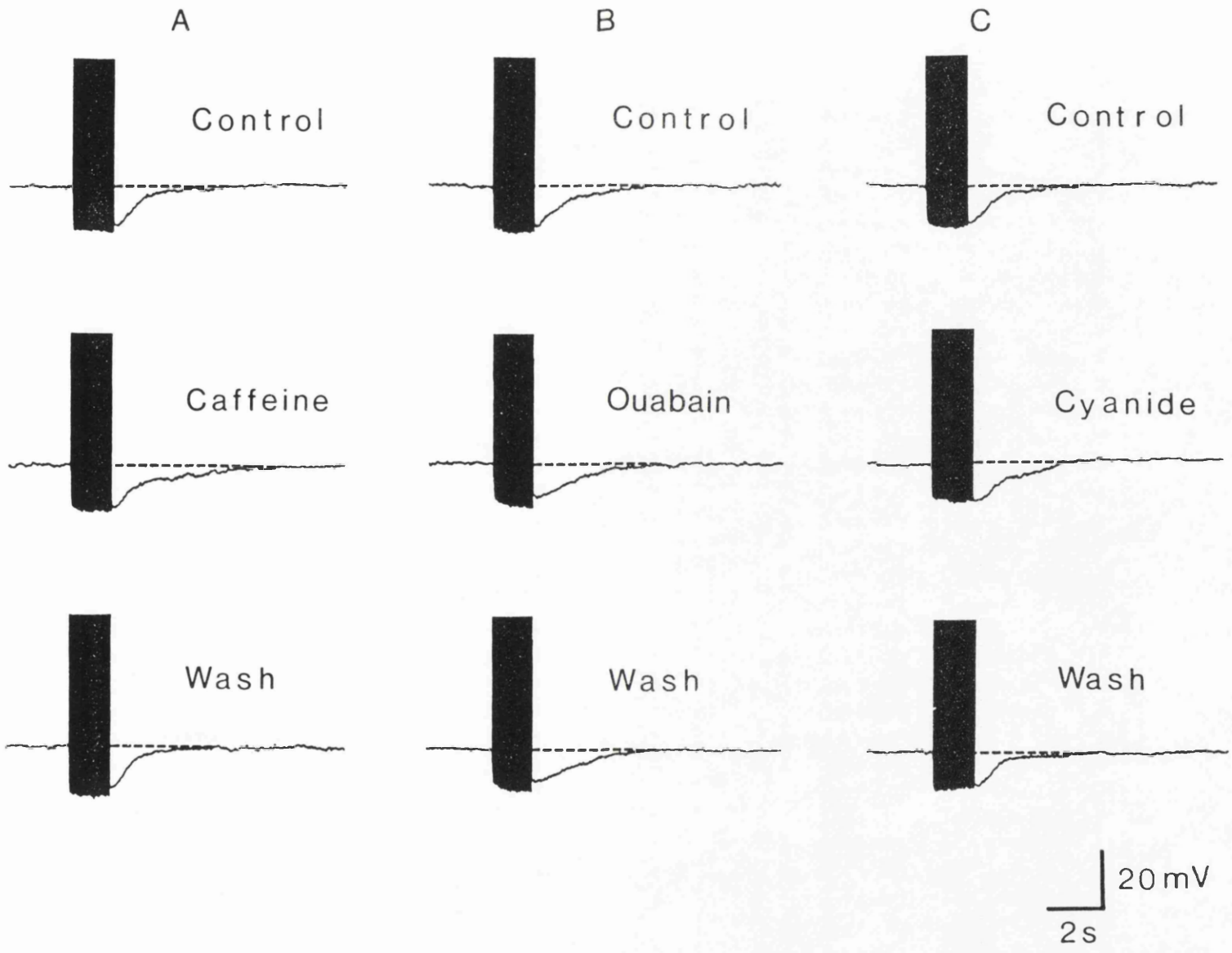
A
B
C
Control
Control
Control
Caffeine
Ouabain
Cyanide
Wash
Wash
Wash
20mV
2s

Chapter 4

M_1 AND M_2 MUSCARINIC RECEPTORS MEDIATE EXCITATION AND INHIBITION OF GUINEA-PIG INTRACARDIAC NEURONES IN CULTURE

SUMMARY

1. The effects of muscarine upon intracardiac neurones cultured from ganglia within the atria and interatrial septum of the newborn guinea-pig heart are reported. The mechanisms underlying the different conductance changes and the effects of muscarinic antagonists upon these responses have been investigated.

2. Muscarine typically produced a biphasic change in membrane potential which consisted of a small inhibitory potential followed by a slow depolarization when applied to the neuronal soma. In addition, muscarine (0.01-10 μM) inhibited the calcium-dependent, post-spike hyperpolarization in a concentration-dependent manner and greatly increased the cells' capacity to fire tonically to prolonged intrasomal current injection.

3. The inhibitory response resulted from an increase in membrane conductance and reversed close to E_K, at a potential of -86.5 mV. This response was antagonized by 4-diphenylacetoxy-N-methyl-piperidine (4-DAMP; 100 nM) and AF-DX 116 (500 nM), but was unaffected by pirenzepine (0.1-5 μM).

4. Two types of slow depolarization were observed in the presence of muscarine, one associated with a fall in membrane conductance, the other with an increase. The latter response was rarely observed (5% of cells) and therefore was not studied in detail. The slow depolarization associated with a fall in membrane conductance resulted from inhibition of a time- and voltage-dependent current which activated with membrane depolarization from potentials around -70 to -65 mV. Pirenzepine (100 nM) selectively antagonized this response, 4-DAMP (100 nM) similarly antagonized the response, but was non-selective. AF-DX 116 (0.5-5 μM) showed no antagonist effect.

5. Muscarine reduced the duration of the action potential and inhibited the spike after-hyperpolarization. Calcium channel blockade by $CdCl_2$ (100 μM) mimicked these actions of muscarine. Enhancement of the delayed rectifier current ($I_{K,V}$) did not appear to underlie the reduction in calcium entry as inhibition of $I_{K,V}$ by 4-aminopyridine (1 mM) in the presence of either $CdCl_2$ (100 μM) or muscarine (10 μM) did not prolong the slow after-hyperpolarization. Application of muscarine immediately following a train of action potentials did not inhibit the slow after-hyperpolarization, suggesting that muscarine did not directly inhibit the calcium-activated potassium current ($I_{K,Ca}$). Muscarine-induced depression of the slow after-hyperpolarization was potently, but non-selectively antagonized by 4-DAMP (100 nM) but was not antagonized by either pirenzepine (0.1-0.5 μM) or AF-DX 116 (0.5-5 μM).

6. It is concluded that inhibition of the time- and voltage-dependent current underlying the slow depolarization was mediated via M_1 muscarinic receptors, whilst the inhibitory response and inhibition of the slow after-hyperpolarization were mediated via M_2 muscarinic receptors which may belong to the M_2-cardiac and M_2-glandular subtypes respectively.

INTRODUCTION

Extensive studies of neurones from autonomic ganglia have demonstrated a wide range of actions directly attributable to muscarinic receptor activation. Within these ganglia, muscarinic receptors have been shown to be involved in the mediation of slow excitatory postsynaptic potentials (sEPSPs; Libet, Chichibu & Tosaka, 1968; Nishi & Koketsu, 1968; Koketsu, 1969; Neild, 1978; North & Tokimasa, 1982), as well as slow inhibitory postsynaptic potentials (sIPSPs; Tosaka, Chichibu & Libet, 1968; Hartzell et al. 1977; Horn & Dodd, 1981; Gallagher, Griffith & Shinnick-Gallagher, 1982). In addition to these postsynaptic effects, presynaptic inhibition of acetylcholine release involving muscarinic autoreceptors has also been reported, (Koketsu & Yamada, 1982; North & Tokimasa, 1982).

Electrophysiological studies of several different types of neurone have shown that muscarinic receptor activation can result in the opening and/or closing of ion channels selective for calcium, potassium, sodium or chloride ions (Kuba & Koketsu, 1976a, b; Grafe, Mayer & Wood, 1980; Horn & Dodd, 1981; Adams & Brown, 1982; Morita, North & Tokimasa, 1982b; Belluzzi, Sacchi & Wanke, 1985; Brown & Selyanko, 1985a, b; Egan & North, 1986). In many instances the muscarinic responses evoked from a single neurone are the result of a modification in the conductance state of two or more of such channels (Mochida & Kobayashi, 1986a, b; Cassell & McLachlan, 1987; Galligan, North & Tokimasa, 1989).

Considerable progress in our understanding of how acetylcholine could produce these multiple actions on a single cell came from the discovery that muscarinic receptors were a heterogeneous population that could be distinguished by using the selective antagonist pirenzepine (Hammer, Berrie, Birdsall, Burgen & Hulme, 1980). Receptors exhibiting a high affinity for pirenzepine have been classified as M_1,

whilst those with a low affinity are termed M_2. The subsequent development of other selective agonists and antagonists has shown clear subdivisions in the M_2 receptor subtype, with M_2 cardiac muscle receptors being distinct from those on smooth muscle and glandular tissue (for review see Birdsall & Hulme, 1987).

Selective muscarinic agents have been used to demonstrate the presence of both M_1 and M_2 receptor subtypes on neurones in a number of autonomic ganglia. For example, in the guinea-pig myenteric plexus, different muscarinic receptor subtypes have been shown to be responsible for mediating the pre- and postsynaptic muscarinic actions of acetylcholine (North, Slack & Surprennant, 1985). To date however, there have been no reports of the direct actions of muscarinic agonists on the intramural neurones of the mammalian heart. Using autoradiographic techniques, it has been shown that in the mixed cell culture preparation of guinea-pig atria, muscarinic receptors are present on all intracardiac neurones and atrial myocytes (Hassall, Buckley & Burnstock, 1987). In addition, muscarinic receptors have been localised over intramural cardiac ganglia in situ in the rat atria (Hancock, Hoover & Houghland, 1987). Studies of the receptors present on mammalian cardiac muscle have shown that they are of a predominantly M_2 subtype, characterised as having a low affinity for pirenzepine and a high affinity for the antagonist 11-[[2-[(diethylamino)methyl]-1-piperidinyl]acetyl]-5,11-dihydro-6H-pyrido[2,3-b][1,4]benzodiazepine-6-one (AF-DX 116) and himbacine (Anwar-UL, Gilani & Gobbin, 1986; Giraldo, Hammer & Ladinsky, 1986). However, a small percentage of the muscarinic receptors in the heart were found to be of the M_1 subtype, a type commonly found within autonomic ganglia (Watson, Yamamura & Roeske, 1983). It is possible therefore that these M_1 receptors may be associated with the intramural neurones of the heart, rather than the cardiac muscle, and that the neuronal muscarinic receptors may be a heterogeneous population consisting of M_1 and M_2 receptor subtypes.

In a previous investigation of the electrophysiological properties of guinea-pig intracardiac neurones in culture, three distinct cell types were distinguished and termed M, AH_s and AH_m cells respectively (see Chapter 3 and Allen & Burnstock, 1987). M cells displayed non-accommodating tonic firing characteristics when stimulated by intrasomal current injection. The AH_s and AH_m type intracardiac neurones which accounted for more than 80% of the cells studied, where highly refractory and displayed pronounced calcium-dependent post-spike hyperpolarizations. In the present study, the actions of muscarine have been examined and a variety of muscarinic receptor antagonists have also been utilised to determine the receptor subtypes involved in mediating these actions in AH_s and AH_m type guinea-pig intracardiac neurones.

RESULTS

The actions of muscarinic agonists and antagonists were studied on more than 200 AH_s and AH_m guinea-pig intracardiac neurones (Allen & Burnstock, 1987) maintained in dissociated cell culture for 5-14 days. Cells were only considered to be suitable for study if, after an initial settling period, they had a stable membrane potential of at least -45 mV and could produce an action potential with a minimum amplitude of 70 mV. Typically, spike amplitudes were between 85 and 100 mV. Every cell tested in these experiments responded to muscarine, the preferred muscarinic agonist used in these experiments.

Brief application of muscarine (10-50 μM) through a blunt micropipette placed close to the neuronal soma evoked a variety of different responses as shown in Fig. 4.1. All these actions could be abolished by atropine (10 nM) but, with the exception of the evoked firing, were resistant to tetrodotoxin (330 nM). In every case different combinations of between one and four separate conductance changes were found to underlie the observed actions of muscarine. The relative contributions played by the individual conductance changes to the overall response of a given cell were dependent upon its resting membrane potential and also whether the neurone was actively firing or was quiescent.

Actions of muscarine on resting membrane potential and conductance

The most commonly observed action of muscarine on the resting membrane potential of a cell consisted of an inhibitory component followed by a slower rising, more prolonged excitatory response (see Fig. 4.1A). The inhibitory response had a short latency (150-500 ms) and was associated with a decrease in input resistance. The excitatory response, on the other hand, was generally associated

with an increase in input resistance which reached a peak 5-10 s after the application of muscarine. During this depolarization, cells would either fire spontaneously or display a greater tendency for anodal-break firing at the end of hyperpolarizing current pulses (see Fig. 4.1A). A third type of response, again involving membrane depolarization, was observed in less than 5% of the cells studied. This response appeared to result from an increase, rather than a decrease, in membrane conductance (see later), during which cells occasionally fired spontaneously or following anodal-break stimulation (see Fig. 4.1B). Various different combinations of these three conductance changes were seen in other cells. For example, in Fig. 4.1C, the different time courses and conductance changes underlying the two muscarine-induced depolarizations can clearly be seen in a neurone displaying both of these components. Finally, cells that initially responded to muscarine in the manner shown in Fig. 4.1A, could frequently be seen to exhibit a much larger inhibitory response if the cell was first hyperpolarized slightly to inactivate the voltage-dependent excitatory component (Fig. 4.1D).

Effects of muscarine on current-evoked firing

The normal current firing characteristics of AH_s and AH_m guinea-pig intracardiac neurones have previously been described (see Chapter 3 and Allen & Burnstock, 1987). Both cell types display pronounced post-spike hyperpolarizations and this causes them to be strongly refractory. However, in the presence of muscarine (1-10 μM), both of these cell types could be induced to fire tonically for prolonged periods (5-30 s) in response to low stimulus currents (50-200 pA; see Fig. 4.2A). The frequency of this firing varied between cells and could be raised by increasing the stimulating current. Over prolonged periods of stimulation, average firing rates ranged between 2 and 12 Hz. However, short bursts of firing for up to 250 ms, at frequencies as high as 80-90 Hz, could be elicited at the onset of

current stimulation. This raised excitability was facilitated by an increase in the rate of spike repolarization, a decrease in the amplitude and duration of the post-spike hyperpolarization (see following sections; Fig. 4.3) and a reduction in the level of outward rectification (see following sections).

Mechanisms underlying the different responses

Inhibitory potential

The amplitude and conductance increase associated with the muscarine-induced hyperpolarization varied considerably from one cell to another. In 57 cells with an average membrane potential of -57.5 ± 0.13 mV the amplitude of the inhibitory response ranged between -2 and -17 mV (mean -7.3 ± 0.55 mV, n=57), with an apparent mean fractional increase in peak conductance (see methods) of 0.36 ± 0.04 (n=31). One source of this variability in the amplitude of the response was that in cells with a membrane potential less than -60 mV, it was often masked by the opposing action of other muscarine-induced conductance changes. In such cells, the inhibitory response could frequently be separated from these other components by either hyperpolarizing the cell to a membrane potential where these responses were largely suppressed, or by the use of selective antagonists (see later). As with all other muscarine-induced conductance changes, the inhibitory response was resistant to TTX (330 nM), indicating that it resulted from the direct action of muscarine and did not involve any synaptic interactions.

In all cells tested, the inhibitory response was nulled at, or near to, the potassium equilibrium potential. In many cells, hyperpolarization revealed pronounced inward rectification which resulted in a fall in input resistance. In such cases, the amplitude of the inhibitory response was not linearly related to the

membrane potential at which it was elicited. However, in cells where this anomalous rectification was absent, the inhibitory response was linearly related to membrane potential and reversed symmetrically near the potassium equilibrium potential. The mean value for the reversal of the inhibitory response in these cells was -86.5 ± 1.01 mV (n=7; see Fig. 4.4) which is very close to E_K (see Chapter 3 and Allen & Burnstock, 1987).

Further indirect evidence to suggest that the inhibitory response resulted from an increase in potassium conductance, was derived by comparing the observed mean amplitude for the response with the value calculated from the mean observed increase in conductance. The predicted values for the peak amplitude of the inhibitory response were calculated using the equation $v=(1-R^1/R)(E_{Ki}-Em)$ (see methods), which assumes the response is due to a specific increase in potassium conductance. The predicted peak amplitude of -7.7 mV compares well with the observed value of -7.3 mV (see above).

It is worth noting that the incidence of inward rectification in the voltage-current relationship of AH_s and AH_m cells was much higher than that observed in the previous study of these cells (see Chapter 3 and Allen & Burnstock, 1987). In the current study, inward rectification was observed in approximately 70-75% of AH cells in contrast to only about 15-20% of the cells in the previous study, a finding which cannot at present be explained.

The time course and the observed decrease in input resistance during the inhibitory response were found to be very similar to that associated with the slow after-hyperpolarization following a train of action potentials. The slow after-hyperpolarization in these cells results from the activation of a calcium-dependent potassium conductance ($I_{K,Ca}$) and the calcium entry responsible for its activation

is inhibited by Cd^{2+} ions (see Chapter 3 and Allen & Burnstock, 1987). However, $CdCl_2$ (100 μM) failed to reduce the current underlying the inhibitory response (n=4), indicating that raised calcium entry was not responsible for its activation. Whether or not an increase in $I_{K,Ca}$ could underlie this response through a rise in intracellular calcium brought about by release from intracellular stores cannot be excluded.

Depolarization associated with a fall in membrane conductance

At the normal resting membrane potential for intracardiac neurones (-55 to -65 mV) the amplitude of the muscarine-induced depolarization was usually small and rarely exceeded 4-6 mV in amplitude. It was also common for this response to be partially shunted by the opposing action of the preceding inhibitory potential. The size of the depolarization and the associated increase in input resistance were also strongly voltage dependent. At membrane potentials greater than -60 to -65 mV, the response was almost totally abolished, whilst membrane depolarization increased its amplitude and frequently led to spontaneous and anodal-break action potential discharge during the response (see Fig. 4.5C). The voltage-current relationships of all AH_s and some AH_m type neurones displayed strong outward rectification which first became evident at about -70 to -65 mV and which increased with depolarization (see Fig. 4.5B). In addition, during the first 100-150 ms, a time-dependent sag occurred in the voltage response to constant depolarizing current. Likewise at the offset of the current injection, there was a slow relaxation from an initial hyperpolarized potential back to the resting level (see Fig. 4.5A). This behaviour was strongly suggestive of the presence of an outward current in these neurones similar to the M-current (I_M) first described in bull-frog sympathetic neurones (Brown & Adams 1980). Application of muscarine (1-10 μM) greatly reduced, although never fully abolished, the slow sag in the voltage records (see

Figs. 4.2B & 4.5A) and also markedly reduced outward rectification in the voltage-current relationship at depolarized potentials (see Fig. 4.5B).

To determine whether the increase in input resistance that underlies the slow depolarization could arise through inhibition of a tonically operated calcium-activated potassium conductance, we performed a number of experiments where either magnesium was substituted for calcium, or cadmium (100 μM) was added to the superfusing solution of cells previously shown to be depolarized by muscarine. In none of the cells tested (n=7) was there any observed increase in input resistance resulting in depolarization of the cell.

A further consequence of muscarinic inhibition of the M-conductance in conjunction with inhibition of the after-hyperpolarization (see below), was a marked increase in the ability of AH_m and, in particular, AH_s type neurones to fire tonically to prolonged intrasomal current injection (see Fig. 4.2A).

Depolarization associated with a rise in membrane conductance

Studies of this response were severely restricted due to the infrequency of its occurrence. Out of more than 200 neurones tested, only 7 cells were found to respond in this way. From the limited data obtained, this response was seen to have a long latency (3 to 7 s) which did not appear to be the result of synaptic interaction with an interneurone as it was unaffected by TTX (n=2). The amplitude of the response increased with membrane hyperpolarization, indicating that it may result from an increase in sodium, or possibly chloride conductance. In all cases the response was associated with a large increase in membrane conductance. However, from the recordings made, the possibility that a proportion of the apparent increase in membrane conductance was the result of membrane rectification could not be excluded.

Effects on the post-spike after-hyperpolarization

An after-hyperpolarization lasting up to 3 s follows a single action potential in AH_s and AH_m intracardiac neurones. Both the amplitude and the duration of this response were reduced by muscarine in a concentration-dependent manner (see Fig. 4.6). The mean reduction in AH amplitude in the presence of 0.01, 0.1, 1 and 10 μM muscarine were 23 ± 12.2%, 47 ± 10%, 59 ± 9.2% and 73 ± 11.8% (n=6) respectively. Whilst AH duration (measured as decline time to half peak amplitude) recorded under the same conditions was reduced by 7.1 ± 4.2%, 18 ± 19.7%, 26 ± 21.9% and 46 ± 18.2% (n=6) respectively. Concomitant with the decrease in after-hyperpolarization amplitude and duration was a reduction in the width of the preceding action potential, an effect which became marked at higher concentrations (1-10 μM; see Fig. 4.3). The after-hyperpolarization in intracardiac neurones results from an outward calcium-activated potassium current (see Chapter 3 and Allen & Burnstock, 1987). Possible mechanisms for the inhibition of this current are firstly, that muscarine in some way acted to directly inhibit $I_{K,Ca}$ and secondly, that the level of its activation may have been diminished due to a reduction in the amount of calcium entering during the action potential. To test the first of these possibilities, a brief pulse of muscarine (100-500 ms) was applied at different times before, during and after a train of action potentials evoked by intrasomal current injection (20 Hz/1.5 s). Muscarine was found to be most effective when applied immediately prior to the train of action potentials. If applied during the train its effect decreased, becoming less effective the later the delay in its application. When applied immediately following the train of action potentials, it became totally ineffective in inhibiting the after-hyperpolarization (see Fig. 4.7A-D). This decrease in the efficacy of muscarine was not due to the latency of its action, as a decrease in the after-hyperpolarization following a single spike could be observed within 50-100 ms of the start of the application of muscarine.

At concentrations of muscarine equal to or greater than 0.1 μM, the observed decrease in the after-hyperpolarization was always associated with a concomitant decrease in the duration of the action potential preceding it. Under control conditions the mean spike duration (measured at half peak amplitude) was 1.44 ± 0.9 ms (n=11), whilst in the presence of muscarine (0.1, 1.0 and 10 μM), the duration was reduced to 1.35 ± 0.1 ms, 1.21 ± 0.09 ms and 1.09 ± 0.08 ms (n=6) respectively. This strongly suggests that muscarine did not directly inhibit $I_{K,Ca}$ rather it may have reduced the level of its activation by decreasing the level of calcium entry into the cell during the action potential. This could have been achieved by one of two processes: firstly, muscarine may have increased the level of activation of the delayed rectifier current ($I_{K,V}$) which caused a secondary reduction in the period and therefore the amount of calcium entering the cell; secondly, muscarine could have acted directly to inhibit calcium entry through voltage-sensitive calcium channels.

In the presence of TTX (330 nM), muscarine abolished the calcium action potential in these cells, however this again could result from enhancement of $I_{K,V}$ resulting in a shunting of the calcium spike. Cadmium is a potent blocker of calcium channels in intracardiac neurones and it mimicked the action of muscarine in reducing spike width as well as the after-hyperpolarization amplitude and duration (see Fig. 4.7 F/f and G/g). In the presence of cadmium, at a concentration (100 μM) which maximally blocks calcium channels in these neurones, muscarine was found to produce no further decrease in either the spike width or the duration of the after-hyperpolarization (see Fig. 4.7 H/h). In order to determine whether muscarine was capable of enhancing the delayed rectifier current, its actions were investigated in the presence of 4-aminopyridine (4-AP; see Fig. 4.7 I/i, J/j and K/k) a potent blocker of $I_{K,V}$ but not $I_{K,Ca}$ in these cells (Chapter 3 and Allen & Burnstock, 1987). In the presence of 4-AP (1 mM), muscarine abolished the hump in

the falling phase of the action potential and reduced the after-hyperpolarization. These actions were again mimicked by cadmium, however subsequent addition of muscarine in the presence of cadmium (100 μM) did not act to antagonize the actions of 4-AP on $I_{K,V}$ or further reduce the after-hyperpolarization (see Fig. 4.7 J/j and K/k).

Antagonist studies

The receptor subtypes underlying the different muscarinic responses were examined using a variety of different antagonists. Due to the strong interactions between the different component responses on a given cell, it was not possible to calculate specific antagonist dissociation constants. Therefore, in this study the relative potency and selectivity of various antagonists has been assessed in terms of the concentrations required to inhibit the different muscarinic responses by greater than 90%.

Pirenzepine (M_1 receptor antagonist)

The muscarine-induced depolarization and reduction in the membrane conductance (agonist concentration 0.5-10 μM) were potently antagonized by pirenzepine at concentrations between 50 and 150 nM (n=37; see Figs. 4.8 and 4.10). At these concentrations, pirenzepine did not antagonize any of the other muscarinic responses, indicating that the I_M-like current inhibition was mediated through M_1 receptors. Antagonism of the inhibitory potential and the muscarine-induced inhibition of the after-hyperpolarization did not occur until pirenzepine concentrations reached 5-10 μM. The low affinity of pirenzepine for these receptors suggests that these responses result from the activation of M_2 muscarinic receptors. Note: the particularly high concentrations of pirenzepine required to

antagonize this response may partly be explained by the method by which the responses were elicited. In order to obtain large reproducible inhibitory responses, it was necessary to apply muscarine using a puffer pipette containing high concentrations of muscarine (up to 50 μM) placed close to the cell soma. Using the same means of stimulation, high concentrations of pirenzepine were also required to antagonize the muscarine-induced inhibition of the after-hyperpolarization. Unlike the inhibitory response however, muscarinic inhibition of the after-hyperpolarization could reliably be achieved by superfusing muscarine. When superfused at known concentrations (0.1-1 μM), much lower concentrations of pirenzepine (0.5-1 μM) were required to antagonize muscarinic inhibition of the after-hyperpolarization. Therefore the high concentrations of pirenzepine required to antagonize the inhibitory response when using a puffer pipette to deliver the muscarine may simply be due to the high concentrations of agonist applied.

Gallamine, 4-DAMP & AF-DX 116 (M_2 receptor antagonists)

Gallamine (10μM) selectively antagonized the inhibitory response in all cells tested (n=9). A further 2-3-fold increase in gallamine concentration was required to antagonize the muscarinic I_M-like depolarization. However, problems were encountered when gallamine was used to antagonize the muscarinic inhibition of the after-hyperpolarization. Initially, gallamine appeared to be ineffective in inhibiting this response, but at raised concentrations (≥ 10μM) it was seen to directly inhibit the potassium current responsible for the after-hyperpolarization. This occurred in the absence of muscarine. This finding makes interpretation of the actions of gallamine difficult, because the inhibitory potential may result from activation of the same potassium channels as those responsible for the after-hyperpolarization. If this was the case, then gallamine may be inhibiting the opening of the potassium channels rather than antagonizing the muscarinic receptors

mediating the inhibitory response.

4-DAMP is an antagonist previously found to display some selectivity towards M_2 smooth muscle/glandular type muscarinic receptors. In the present study it potently antagonized all the different muscarine-induced conductance changes seen in these neurones (see Figs. 4.8, 4.9, 4.10 and 4.11). 4-DAMP displayed almost no selectivity for any particular response on any of the cells tested (n=43), inhibiting them equipotently at a concentration of approximately 100 nM.

AF-DX 116, a selective M_2 cardiac receptor antagonist, showed much lower potency than either pirenzepine or 4-DAMP in inhibiting any of the muscarinic responses. Concentrations in excess of 500 nM were generally required before any antagonism was observed. AF-DX 116 showed a limited degree of selectivity towards the muscarinic inhibitory component, antagonizing this response at concentrations between 0.5 and 1 μM (n=10; see Fig. 4.11). Antagonism of the other muscarinic responses occurred at slightly higher concentrations in the range 2-5 μM.

DISCUSSION

The wide variety of muscarinic responses displayed by guinea-pig intracardiac neurones suggests that they may play an important role in integrating and/or modulating the action of extrinsic nerves upon the heart. Furthermore, the intracardiac ganglia are well placed in the heart to perform this function as many of these ganglia are concentrated in the nodal regions and at the points of insertion of the great veins (King & Coakley, 1958). The muscarinic receptor-mediated actions on intracardiac neurones reported in the present study have a number of similarities to those previously described in other peripheral ganglia and some central neurones.

Cholinergic membrane hyperpolarizations and sIPSPs that result from an increase in potassium conductance have been described in mudpuppy cardiac ganglion cells (Hartzell et al. 1977), bull-frog C cells (Dodd & Horn, 1983), rat superior cervical neurones (Brown, Fatherazi, Garthwaite & White, 1980) and also centrally in rat thalamic reticular and nucleus parabrachialis neurones (Egan & North, 1986; McCormick & Prince, 1986). The latency, duration and receptor subtype (M_2) responsible for mediating the inhibitory response observed in intracardiac neurones were similar to those of the cholinergic sIPSPs described in these other preparations. This raises the possibility that intracardiac ganglion cells in situ may also display sIPSPs and that the increase in membrane conductance underlying the inhibitory potential seen in the cultured neurones could form the basis of such a response. At present there is no direct way of testing this hypothesis as no synaptically intact intracardiac ganglia preparation has been developed.

The result of the inhibitory potential on cultured intracardiac neurones was

to move the cell away from firing threshold and to raise the stimulus intensity required to elicit an action potential. As the basic properties of AH_s and, to a lesser extent, AH_m type intracardiac neurones were highly refractory, it is difficult to see the value of further inhibition, unless one considers the effects of excitatory muscarinic stimulation at the same time. Together, the excitatory responses led to a depolarization and a change from highly phasic to sustained tonic firing behaviour. A possible role for the inhibitory potential could therefore be to punctuate or terminate a period of tonic firing by hyperpolarizing the cell away from firing threshold. A comparable role has been proposed in bull-frog C cells, where the IPSP induced persistent patterned burst firing by interacting with the sEPSP (Dodd & Horn, 1983). In intracardiac neurones, the inhibitory potential may be generated by specific inhibitory nerves. On the other hand, it may be some form of automatic regulatory mechanism activated during periods of intense excitatory stimulation. In the present study, it was noted that the concentrations of muscarinic agonists required to promote multiple firing were generally much lower than those needed to evoke the slow inhibitory potential. If, as has been reported in rabbit superior cervical neurones (Mochida & Kobayashi, 1986a), activation of the different conductances were to take place at different agonist concentrations, then the inhibitory potential could act to control excitability without the need for specific inhibitory input.

A slow depolarization and a fall in membrane conductance frequently followed the inhibitory response seen in both AH types of intracardiac neurone and the voltage dependence of the response indicated that it resulted from inhibition of resting potassium conductance. Cholinergic sEPSPs and muscarine-induced depolarizations that result from a decrease in membrane potassium conductance have been described in a number of other neurones (Weight & Votava, 1970; Krnjević, Pumain & Renaud, 1971; Halliwell & Adams, 1982; North & Tokimasa, 1983).

Examination of the ionic mechanisms underlying these responses have shown that they result from the inhibition of up to three different types of potassium currents, I_M, $I_{K,Ca}$ and a background/leak current (Dodd, Dingledine & Kelly, 1981; North & Tokimasa, 1983; Tokimasa, 1984, 1985; Brown, 1988). In the present study, muscarinic inhibition of $I_{K,Ca}$ and of a time- and voltage-dependent conductance similar to I_M was observed. In intracardiac neurones, inhibition of this I_M-like conductance was largely responsible for the generation of the slow depolarization. Many AH_s and some AH_m type intracardiac neurones were seen to display a marked outward rectification in their voltage-current relationships. This rectification was the result of an outward current which activated with membrane depolarization from potentials around -65 mV. In addition to voltage-dependent activation, the current also displayed time-dependent activation. This could be seen as a sag in the voltage record during prolonged depolarizing current injection, and a subsequent overshoot and relaxation back to resting potential at the end of the period of current injection. M-currents, which display very similar characteristics, were first described in B cells of the frog lumbar sympathetic ganglion (Brown & Adams, 1980), and have since been demonstrated in a variety of other neurones (for review, see Brown, 1988). During a prolonged depolarization, the M-current shows no inactivation, therefore the contribution played by the M-current to the overall resting membrane conductance of a cell will depend upon the membrane potential of that cell. In neurones with high membrane potentials (greater than -70 mV), its level of activation would be small and as a consequence it would play little or no role in setting resting membrane potential. Intracardiac neurones have somewhat lower membrane potentials that usually lie between -55 and -65 mV. If the time- and voltage-dependent current described in these neurones displays the same characteristics as the M-current, then this current should show significant activation at resting potential. Furthermore, any agents causing it to be suppressed would therefore be predicted to precipitate membrane depolarization. In intracardiac

neurones, the observed depolarization was usually quite small and was only occasionally seen to evoke spontaneous firing. This may indicate that in intracardiac neurones the time- and voltage-dependent current has a low conductance, or as has been seen in a number of intracardiac neurones, muscarine only partially inhibited this current at the concentrations used.

Possibly a more striking feature of this time- and voltage-dependent current was its ability to oppose membrane depolarization. Increased intensities of depolarizing current led to increased activation of this current and inhibition by muscarine produced a large reduction in the resulting outward rectification. Together with muscarinic inhibition of $I_{K,Ca}$ (see later), this permitted greater tonic firing and reduced the current intensity required to elicit trains of action potentials. In other ganglia, similar M-current inhibition occurs during the sEPSP and this has been shown to facilitate synaptic transmission, increase the amplitude of the fast EPSP and promote multiple firing (Schulman & Weight, 1976; Adams, Brown & Constanti, 1982b; Brown & Selyanko, 1985b). In intracardiac neurones, as in other cells, part of the action of muscarine in promoting multiple firing can be attributed to the inhibition of the slow after-hyperpolarization and in intracardiac neurones, inhibition of $I_{K,Ca}$ appeared to be the predominant factor in determining the degree of tonic firing behaviour. Two pieces of evidence support this suggestion: firstly, significant inhibition of $I_{K,Ca}$ took place at muscarine concentrations as low as 50 nM, whilst inhibition of the M-like current (measured as a muscarine-induced depolarization) did not occur until considerably higher concentrations were used (greater than 1 μM); secondly, prevention of calcium entry, and therefore activation of $I_{K,Ca,}$ using Cd^{2+} ions mimicked to a large extent the action that muscarine had upon multiple firing. However, subsequent addition of muscarine in the presence of Cd^{2+} further facilitated tonic firing in most cells. Therefore, it would appear that these two currents act together to produce the normal refractory firing

characteristics of AH type intracardiac neurones and are both modulated by muscarinic agonists. The apparently dominant role played by $I_{K,Ca}$ over I_M in facilitating sustained multiple spike discharge was similar to that seen in hippocampal neurones (Madison & Nicoll, 1984), where Cd^{2+} ions also mimicked muscarinic agonists in their ability to promote multiple firing. Interestingly, this differs from what has been found in some other peripheral ganglia, where inhibition of I_M was found to exert a more predominant role in the regulation of tonic firing behaviour (see review by Brown, 1988).

Muscarinic inhibition of the calcium-dependent after-hyperpolarization in intracardiac neurones appeared to result from decreased calcium entry during the action potential and not from direct inhibition of $I_{K,Ca}$. The main evidence for this was the observation that no reduction in $I_{K,Ca}$ activation occurred if muscarine was applied immediately after a train of action potentials, whereas reduction in the after-hyperpolarization was observed if muscarine was applied at any point during the spike train: the earlier its application the greater the inhibition. This is in contrast to AH/type 2 enteric neurones, where inhibition of $I_{K,Ca}$ by muscarinic agonists is effective even when applied after the action potential (North & Tokimasa, 1983). Unlike intracardiac neurones, inhibition of this current in enteric neurones was not associated with a concomitant reduction in spike width, on the contrary, spike duration was often seen to increase following the application of muscarinic agonists (North & Tokimasa, 1983). In intracardiac neurones, inhibition of calcium entry through specific cadmium-sensitive calcium channels and not accelerated spike repolarization resulting from increased activation of $I_{K,V}$ appeared to be responsible for the fall in calcium entry. Similar inhibition of calcium currents by muscarinic agonists has been suggested to underlie the inhibition of the slow after-hyperpolarization observed in a number of other neurones (Belluzi et al. 1985; Mochida & Kobayashi, 1986b, c). In each case a reduction in the calcium-

dependent action potential was also seen (see also Wanke, Ferroni, Margaroli, Ambrosini, Pozzan & Meldolesi, 1987).

A slow depolarization with a long latency resulting from an increase in membrane conductance was evoked from a small number of intracardiac neurones. In the present report, no detailed analysis of this phenomenon was possible but slow depolarizations associated with an increase in conductance have been described in a number of other ganglia, and have been suggested to arise as the result of an increase in either a mixed cation conductance (Kuba & Koketsu, 1976a; Akasu, Gallagher, Koketsu & Shinnick-Gallagher, 1984), or from an increase in chloride conductance (Mochida & Kobayashi, 1986a). Whether the response described in the present study was generated by a similar mechanism will require further studies.

The antagonist experiments performed here indicate that there were both M_1 and M_2 muscarinic receptor subtypes present upon guinea-pig intracardiac neurones. M_1 receptors with a high affinity for pirenzepine were responsible for mediating inhibition of the I_M-like time- and voltage-dependent current. Muscarinic inhibition of M-currents in other neurones is also predominantly through the mediation of M_1 receptors (Brown, Forward & Marsh, 1980; Brown & Selyanko, 1985a; Brown, Gähwiler, Marsh & Selyanko, 1986), however this is not exclusively the case as M_2 receptor-mediated inhibition of the M-current has recently been described in guinea-pig olfactory neurones (Constanti & Sim, 1987) and rat hippocampal neurones (Dutar & Nicoll, 1988).

Both the slow inhibitory potential and the inhibition of the slow after-hyperpolarization showed a low affinity for pirenzepine, indicating that these responses were mediated through M_2 muscarinic receptors. M_2 receptors appear to

be a heterogeneous population and new selective agonists and antagonists are being developed to help discriminate between the different M_2 receptor subtypes. In particular, the muscarinic receptors on cardiac muscle appear to differ so extensively from those on smooth muscles and gland cells that they are currently thought to be distinct subtypes of M_2 receptor (Mutschler & Lambrecht, 1984; Barlow & Shepherd, 1985, 1986; Hammer, Giraldo, Schiavi, Montiferini & Ladinsky, 1986). Two antagonists frequently used to discriminate between these subtypes are AF-DX 116 and 4-DAMP. AF-DX 116 shows a high affinity for cardiac muscarinic receptors and a low affinity for those on smooth muscle/gland cells (Giraldo et al. 1986; Hammer et al. 1986), whilst 4-DAMP shows the reverse selectivity (Barlow, Berry, Glenton, Nikolaou & Soh, 1976). On intracardiac neurones, 4-DAMP was found to show almost no selectivity, inhibiting all M_1 and M_2 receptor-mediated actions at concentrations around 100 nM. AF-DX 116 had a much lower affinity than 4-DAMP, but did show a small degree of selectivity (2-5 fold) in antagonizing the inhibitory response. This suggests that the M_2 receptor subtype responsible for the inhibitory response may have been of the cardiac M_2 type, whilst those responsible for inhibiting the after-hyperpolarization may have been of a smooth muscle/glandular type. However, the very low selectivity showed by these compounds could also indicate that these receptors may belong to yet another subclass of muscarinic receptor for which selective antagonists have yet to be developed. Recent molecular cloning experiments suggest that this might be the case as there is now evidence for at least five different muscarinic receptor subtypes (for review see, Bonner, 1989).

In conclusion, guinea-pig AH type intracardiac neurones in culture exhibit at least four different membrane conductances that can be modulated by muscarinic agonists. In the intact ganglia these currents may well underlie both sIPSPs and sEPSPs, whilst the reduction of calcium entry during the action potential might lead

to presynaptic inhibition of transmitter release onto the target tissue. If this is so, then far from being simple relay stations for extrinsic nerves, the intracardiac ganglia may play a very important role in modulating their extrinsic inputs with respect to the local requirements of the heart.

Fig. 4.1. Examples of the different actions of muscarine upon resting membrane potential and conductance in cultured guinea-pig intracardiac neurones. In all cases muscarine was applied as indicated by the arrows, using a brief pressure pulse (100-500 ms, 0.5-1 bar) applied to a micropipette containing muscarine (10 μM) made up in Krebs, positioned 10-20 μm from the soma of the impaled cell. A, muscarine elicited a small inhibitory response associated with a decrease in input resistance that was followed by a slow depolarization and an increase in input resistance (resting potential -49 mV). B, less frequently observed, muscarine evoked, after a longer latency, a second slower type of depolarization associated with a decrease in input resistance (resting potential -58 mV). C, in this cell muscarinic receptor stimulation elicited both types of slow depolarization. The different time courses of the two conductance changes can be clearly seen (resting potential -55mV). D, by first hyperpolarizing a cell with DC current injection to a membrane potential in excess of -60 mV, a large pure inhibitory response to muscarine could often be elicited. In the cell shown, membrane potential was hyperpolarized to -67 mV. Note: under control conditions, resting membrane potential -53 mV, this cell responded to muscarine in a similar way to the cell shown in A.

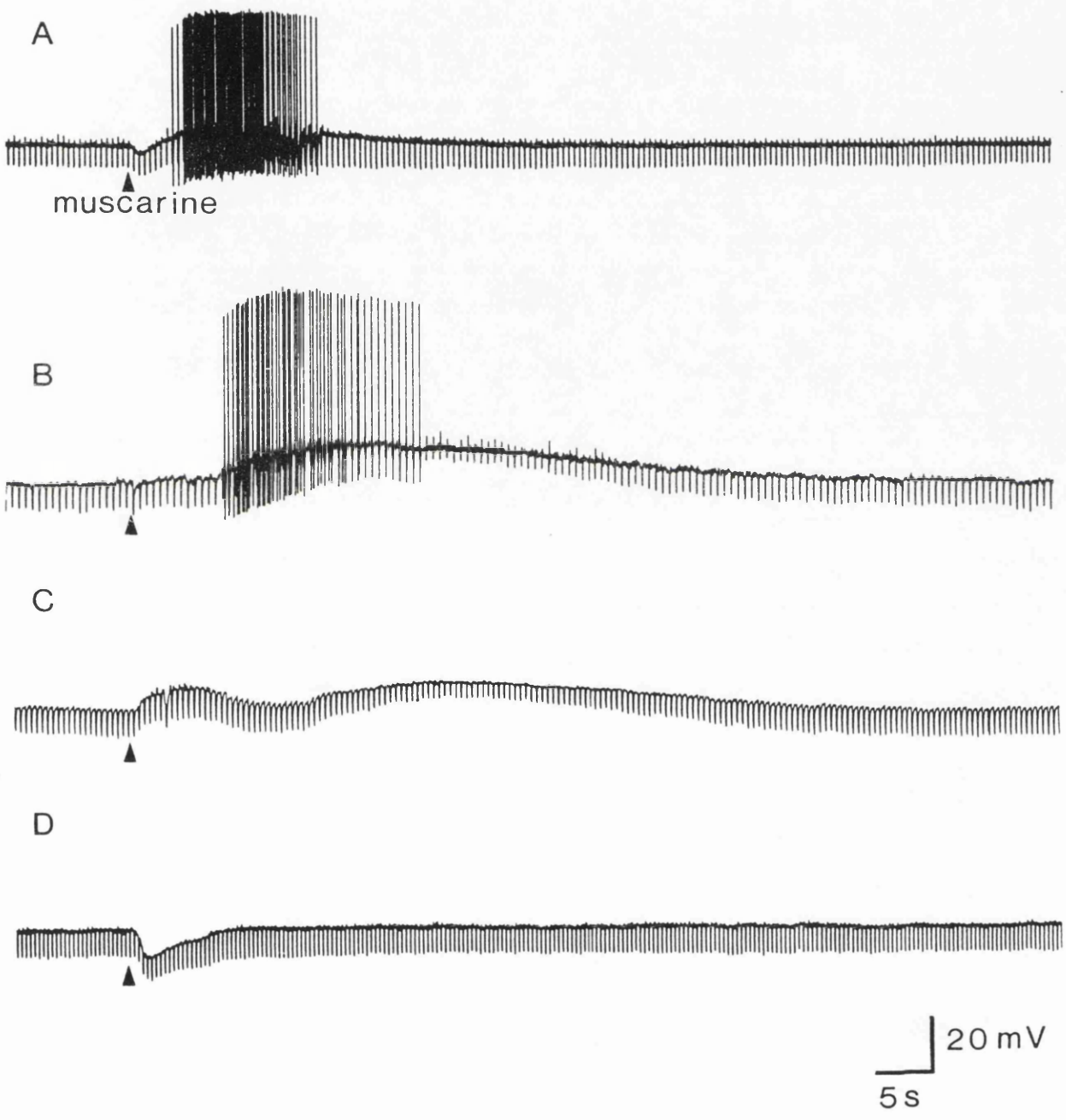
A
muscarine
B
C
D
20 mV
5 s

Fig. 4.2. The action of muscarine (10 μM) on the current firing characteristics of AH_s and AH_m types of guinea-pig intracardiac neurone. A, prolonged intrasomal current injection (200 pA for the period indicated by the bars) in the absence of muscarine only elicited firing at the onset of current injection. In the presence of muscarine this refractory behaviour was converted to one of sustained tonic firing for the duration of the current stimulus (resting potential -58 mV). B, the slow conductance change underlying the refractory behaviour in a cell similar to the one shown in A. The cell (membrane potential -58 mV) was stimulated using hyperpolarizing and depolarizing current of known amplitude (± 250 pA) in the presence of TTX (330 nM). Under control conditions (upper panel), the cell displays pronounced outward rectification resulting in a sag in the voltage records to depolarizing current. In the presence of muscarine (10 μM; depolarization offset by passing constant hyperpolarizing current) both the rectification and the voltage sags were reduced. Lower panel shows washout in presence of TTX.

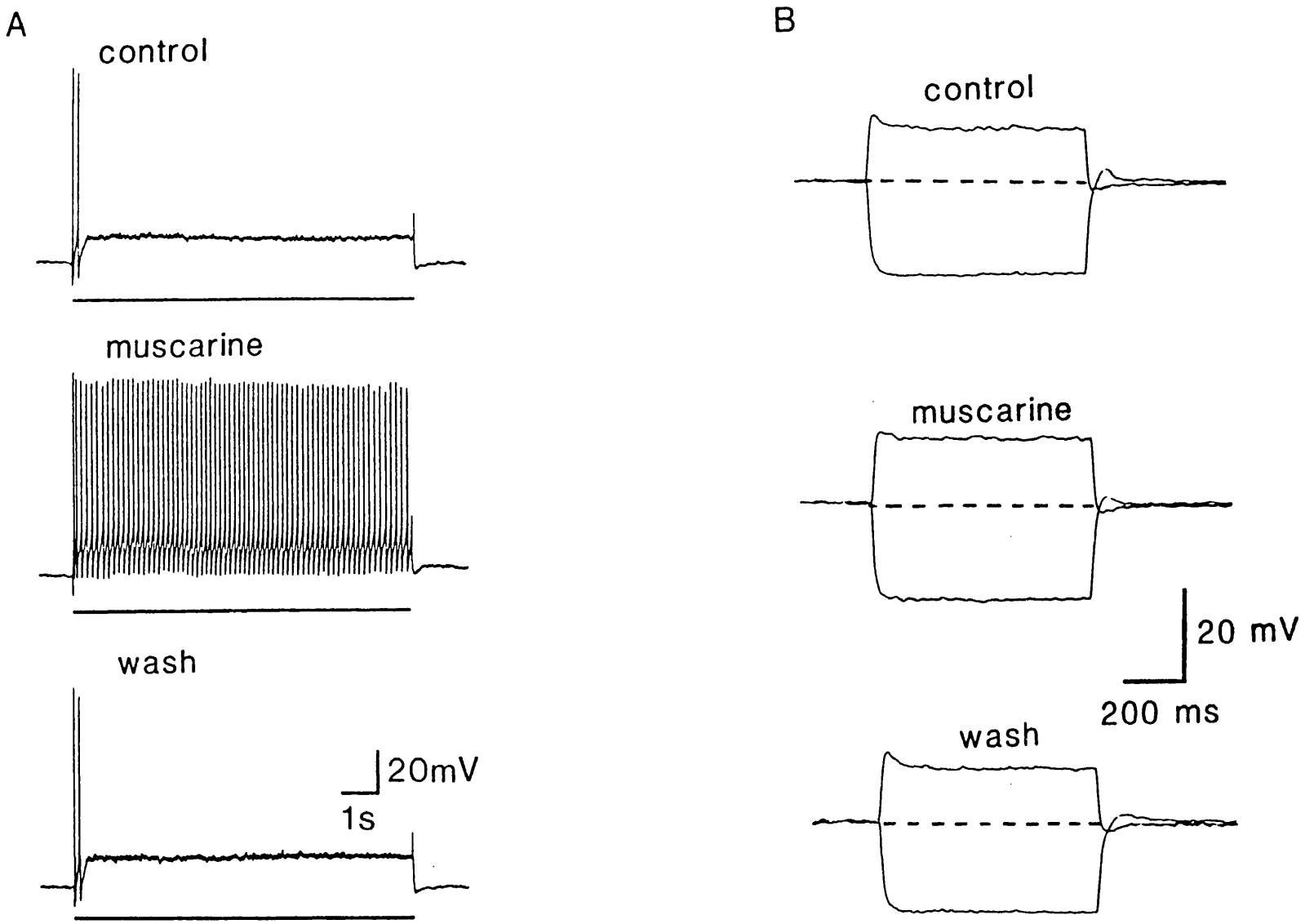
A
control
muscarine
wash
20mV
1s
B
control
muscarine
20 mV
200 ms
wash

Fig. 4.3. Muscarine-induced inhibition of the post-spike hyperpolarization and action potential duration in a guinea-pig intracardiac neurone. A, control after-hyperpolarization following a single spike and C, in the presence of muscarine (1 μM). B and D, fast records from the same cell (25 ms current stimulation) before and during the application of muscarine (1 μM) respectively. Muscarine reduced the characteristic hump on the falling phase of the action potential, which is associated with calcium entry (see text), but had little effect upon spike amplitude (resting membrane potential -57 mV). E, muscarine (10 μM) reversibly reduced the slow after-hyperpolarization and associated increase in membrane conductance following a train of 30 action potentials. Action potentials were evoked by a train of intrasomal current pulses delivered at 20 Hz for 1.5 s (resting membrane potential -56 mV). Note: in E, action potential amplitudes were attenuated due to the limited frequency response of the pen recorder.

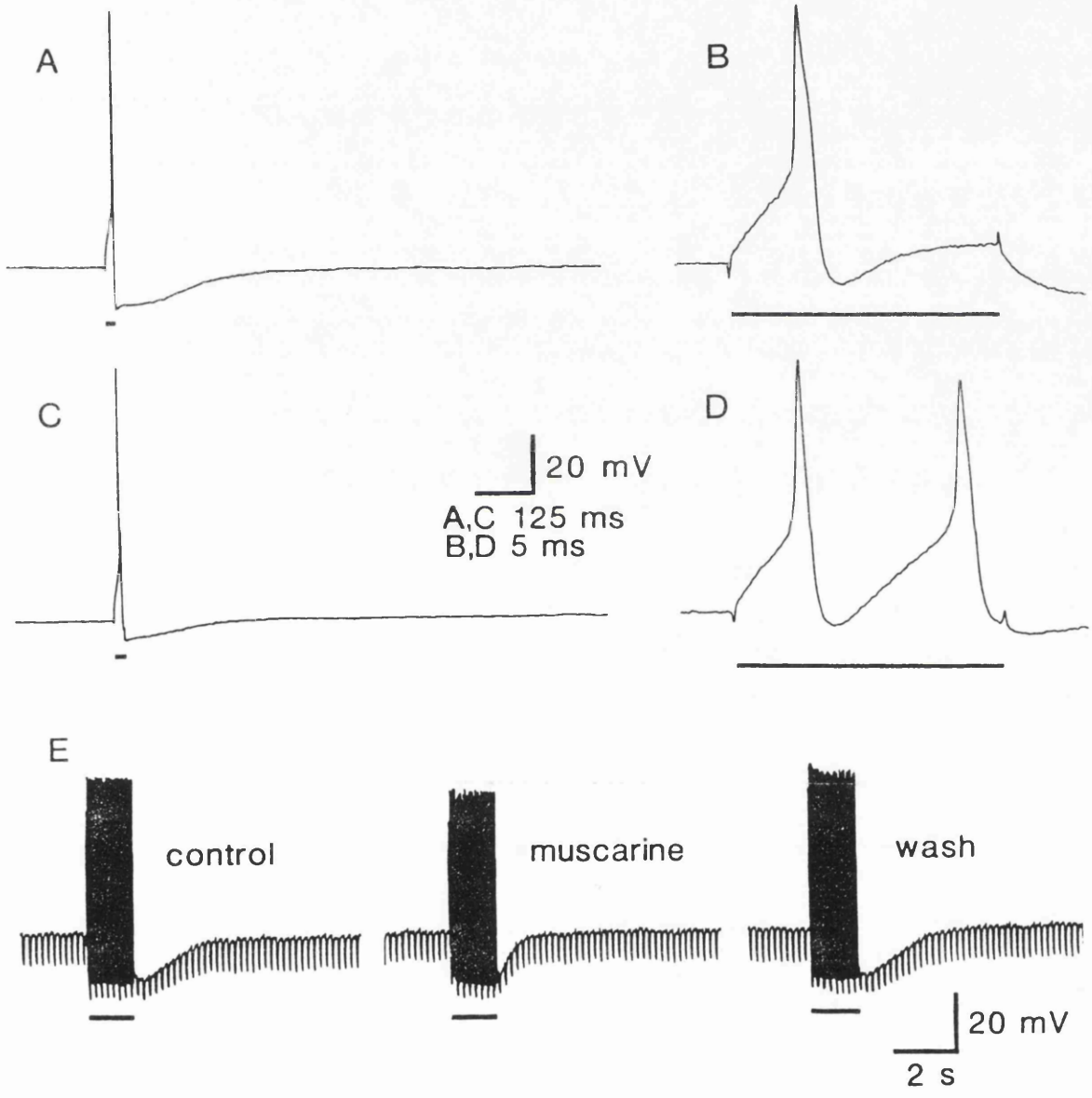
A
B
C
D
20 mV
A,C 125 ms
B,D 5 ms
E
control
muscarine
wash
20 mV
2 s

Fig. 4.4. Voltage-dependence of the inhibitory response to muscarine in guinea-pig intracardiac neurones. In all cells tested, the inhibitory response nulled or reversed near the potassium equilibrium potential. A, the amplitude of the inhibitory response in an AH_m cell at different membrane potentials. Muscarine (10 μM) was applied by local pressure ejection for the period indicated by the bars. Downward deflections are the result of passing brief 50 ms duration constant hyperpolarizing current pulses (100 pA) in order to monitor changes in membrane input resistance. B, a plot of amplitude against membrane potential for the cell shown in A. The amplitude was linearly related to membrane potential over the range -51 to -110 mV (coefficient of correlation r=0.993) and reversed at a membrane potential of -87.4 mV. Note: in a number of cells which displayed pronounced inward rectification, the amplitude of the inhibitory response was not linearly related to the membrane potential, however, it was always seen to reverse at around -90 mV.

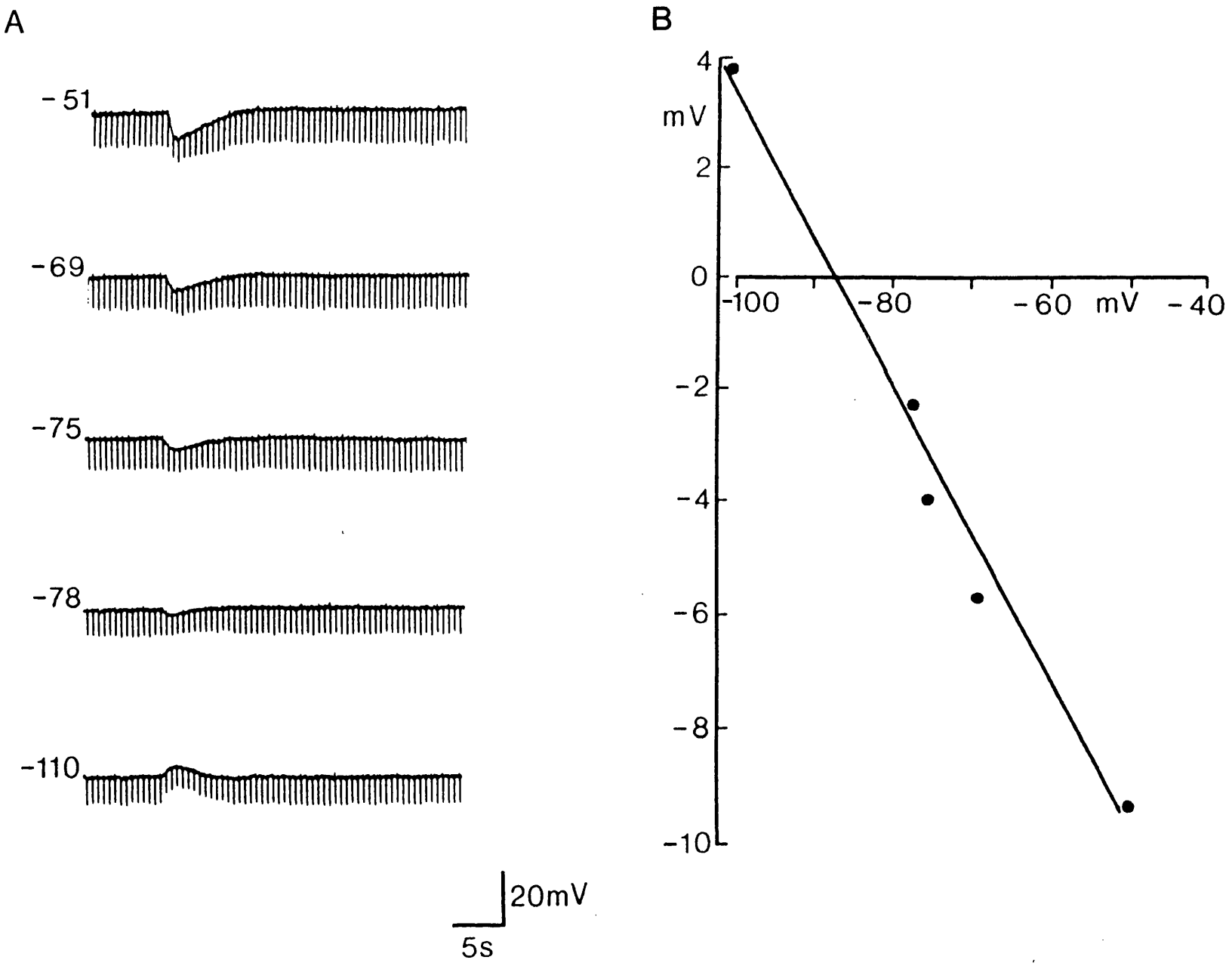
A
-51
-69
-75
-78
-110
20mV
5s
B
4
mV
2
0
-2
-4
-6
-8
-10
-100
-80
-60 mV
-40

Fig. 4.5. A, the membrane voltage responses of a guinea-pig intracardiac neurone to 500 ms current pulses of varying intensity in the presence and absence of muscarine 10 μM (all records obtained in the presence of TTX, 330 nM). Under control conditions the cell showed a pronounced sag in the voltage response to depolarizing current, whilst in the presence of muscarine this was largely abolished. (Note: in the cell shown, muscarine also reduced the fast calcium-dependent depolarizing voltage transient that occurred at the onset of depolarizing current injection and also appeared to promote inward rectification at strongly hyperpolarized potentials). B, the steady-state current-voltage relationship for the responses shown in A. Under control conditions, marked outward rectification was observed at membrane potentials of less than -65 mV (resting potential -59 mV). Muscarine (10 μM) reduced this rectification and depolarized the cell by approximately 2 mV. C, a second cell exhibiting similar voltage-current characteristics to those shown in A and B. The effect of varying membrane potential on the size of the muscarine-evoked slow depolarization associated with a fall in membrane conductance. At membrane potentials greater than -70 mV no depolarization or conductance change could be elicited. Progressive depolarization led to larger slow depolarizations being evoked. At sufficiently depolarized levels the muscarine-induced depolarization produced spontaneous spike discharge and a greater tendency for anodal-break current firing.

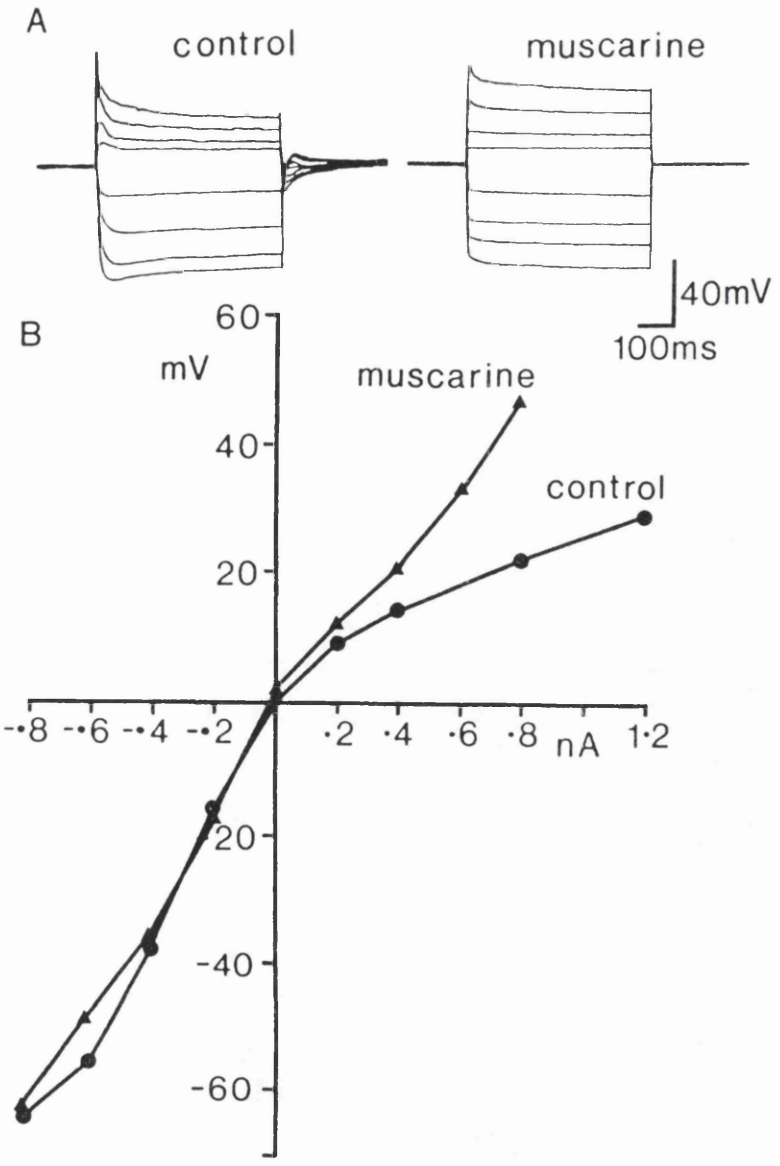
A
control
muscarine
40mV
100ms
B
60
mV
muscarine
40
control
20
-·8 -·6 -·4 -·2
·2 ·4 ·6 ·8 nA 1·2
-20
-40
-60

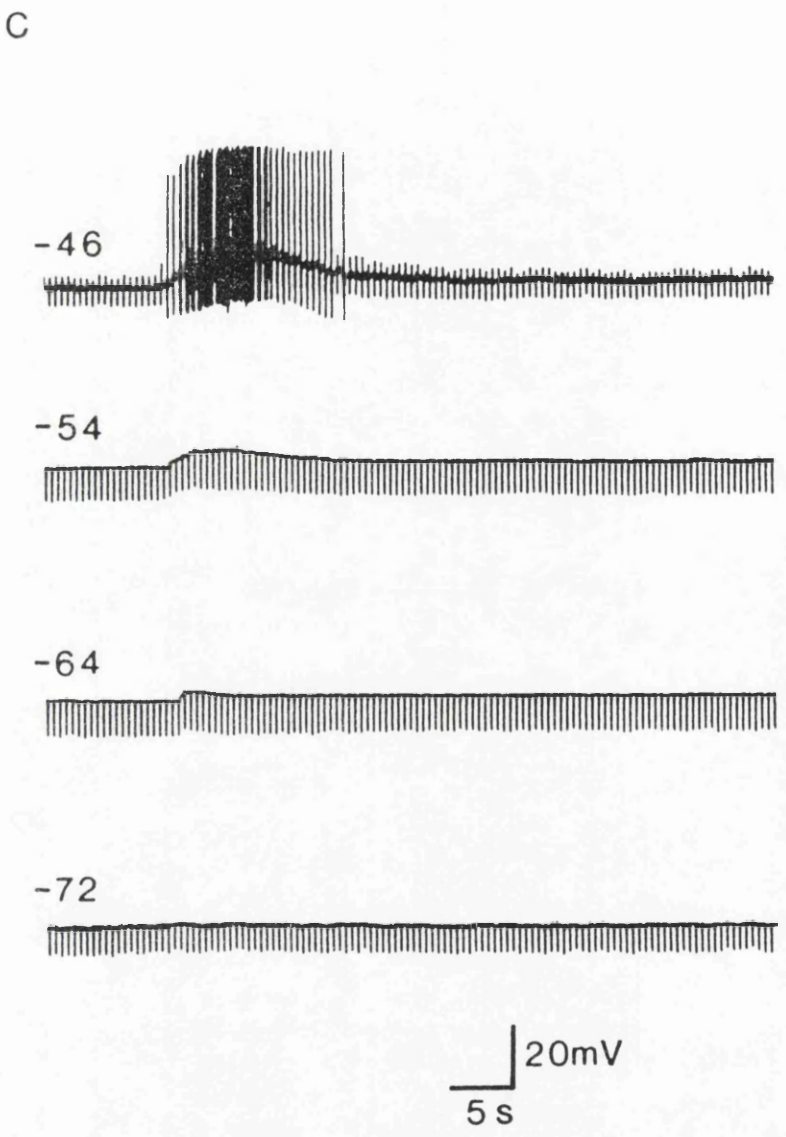
C
-46
-54
-64
-72
20mV
5 s

Fig. 4.6. The amplitude and duration of the slow after-hyperpolarization following a single action potential in the presence of increasing concentrations of muscarine. Top panel, control after-hyperpolarization. Subsequent panels show the effect of superfusion with muscarine at 0.01-10 μM respectively. Note: in each case any depolarization produced by muscarine was offset by passing hyperpolarizing DC current. Resting membrane potential -58 mV.

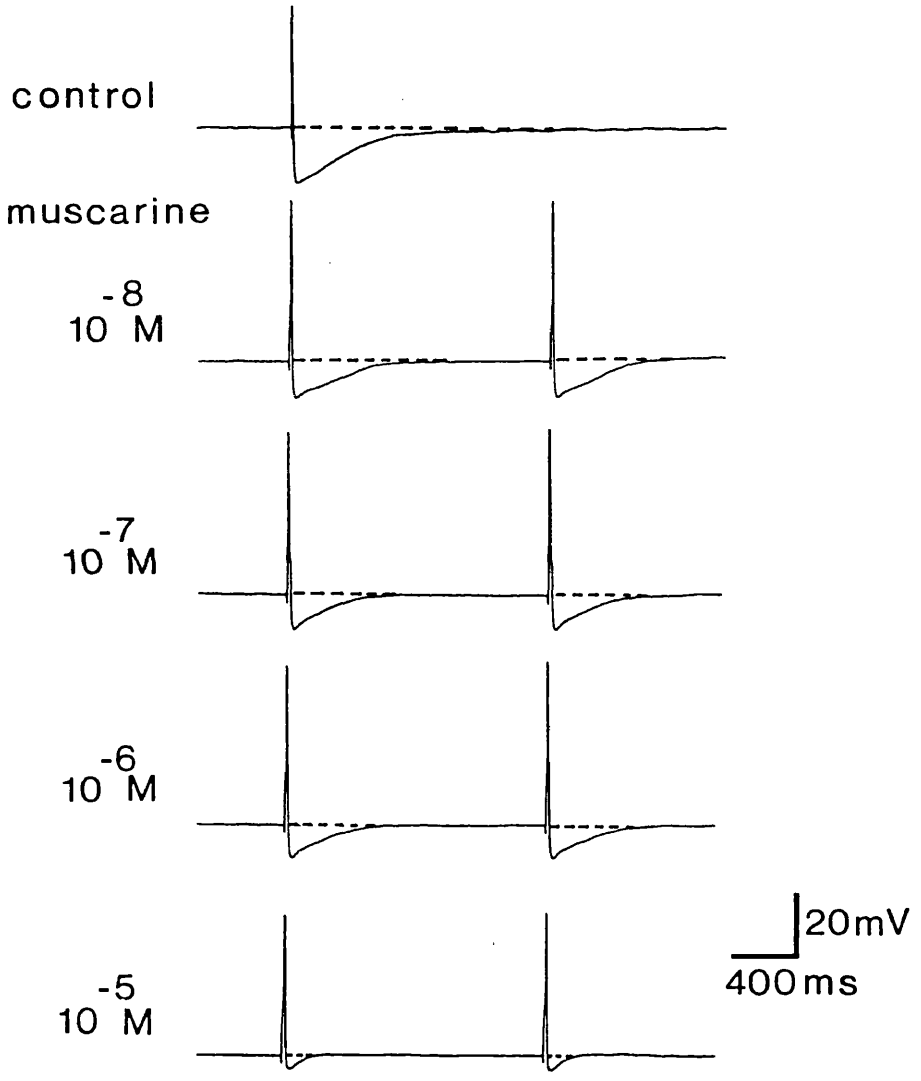
control
muscarine
-8
10 M
-7
10 M
-6
10 M
-5
10 M
20mV
400ms

Fig. 4.7. A, control slow after-hyperpolarization and underlying conductance increase in guinea-pig intracardiac neurones following a train of action potentials produced by intrasomal current injection (20 Hz/1.5 s). B to D show the relative effectiveness of muscarine (10 μM) in inhibiting the slow after-hyperpolarization when applied before, during and after the spike train for the periods indicated by the bars. Resting membrane potential -62 mV. Note: spikes were attenuated by the pen recorder. E to K and insets e to k show that the muscarine-induced reduction of spike width and slow after-hyperpolarization could be mimicked by calcium channel blockade with cadmium chloride ($CdCl_2$). E/e, control; F/f, muscarine (10 μM); G/g, $CdCl_2$ (100 μM), H/h, $CdCl_2$ (100 μM) and muscarine (10 μM). Note: no further shortening of the spike or the slow after-hyperpolarization occurred when muscarine was added following calcium channel blockade by $CdCl_2$. I/i, the spike and slow after-hyperpolarization in the presence of 4-aminopyridine (1 mM). J/j, in the presence of 4-aminopyridine, $CdCl_2$ abolished the calcium-dependent hump in the falling phase of the spike and also reduced the after-hyperpolarization. K/k, no further reduction of either component occurred following subsequent addition of muscarine (10 μM), indicating that muscarine did not act to antagonize the action of 4-aminopyridine on the delayed rectifier current (resting membrane potential -57 mV).

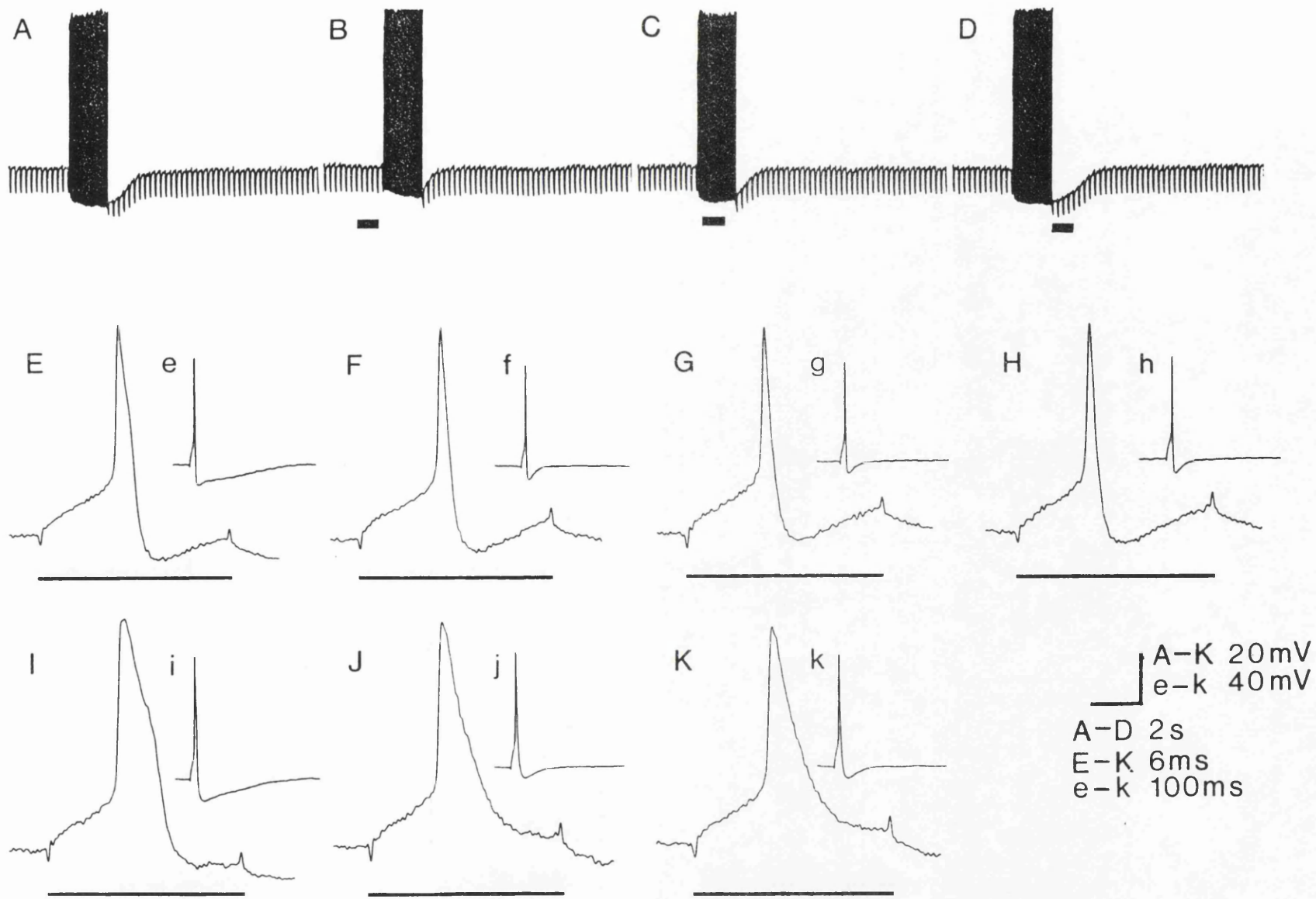
A
B
C
D
E
e
F
f
G
g
H
h
I
i
J
j
K
k
A–K 20mV
e–k 40mV
A–D 2s
E–K 6ms
e–k 100ms

Fig. 4.8. Antagonism of the muscarine-induced slow depolarization with associated fall in membrane conductance in guinea-pig intracardiac neurones. In order to raise the level of activation of this current, the cell was depolarized slightly using intrasomal current injection. Muscarine (10 μM) was applied by pressure ejection (250 ms pulses) from a blunt micropipette placed close to the neuronal soma. This produced a slow depolarization, a fall in resting membrane conductance and induced spontaneous action potential discharge (see A). B, pirenzepine (100 nM) reversibly antagonized the depolarization and fall in membrane conductance without inhibiting any of the other muscarinic receptor-mediated effects. D, AF-DX 116 at a concentration which antagonized the inhibitory response (500 nM) had no effect upon the depolarization. E, 4-DAMP (100 nM) inhibited the depolarization, but unlike pirenzepine, it also antagonized all the other muscarine-induced responses with no selectivity.

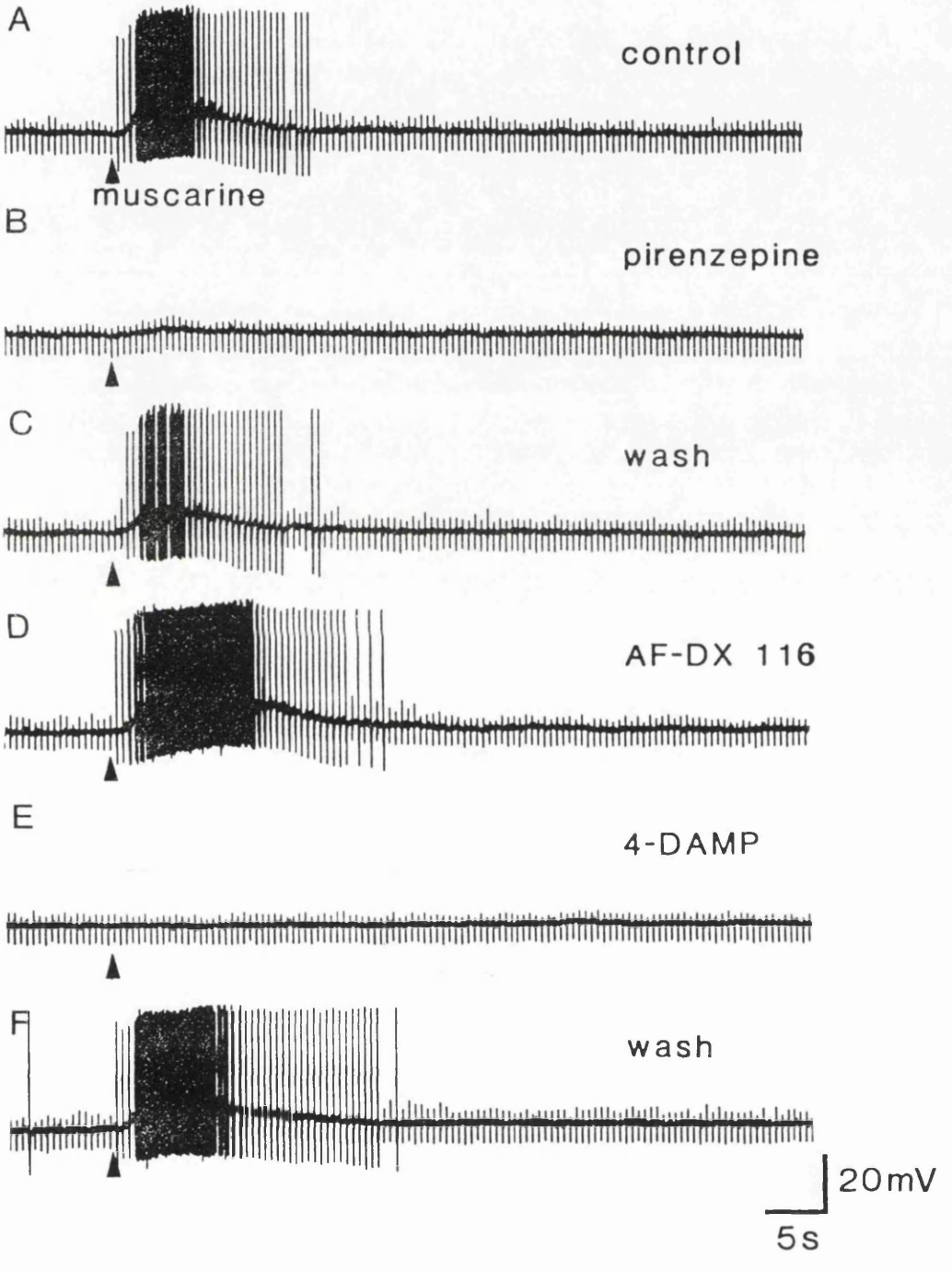
A
control
muscarine
B
pirenzepine
C
wash
D
AF-DX 116
E
4-DAMP
F
wash
20mV
5s

Fig. 4.9. Antagonism of the muscarine-induced depression of spike width and post-spike after-hyperpolarization in guinea-pig intracardiac neurones. A and D, control spike and after-hyperpolarization; B and E, in the presence of muscarine (10 μM). Note: any depolarization was nulled by passing hyperpolarizing current through the electrode. C and F, 4-DAMP (100 nM) totally antagonized the effect of muscarine (10 μM) in inhibiting the after-hyperpolarization and in reducing spike width. Bars beneath traces indicate periods of current stimulation. Resting membrane potential -57 mV.

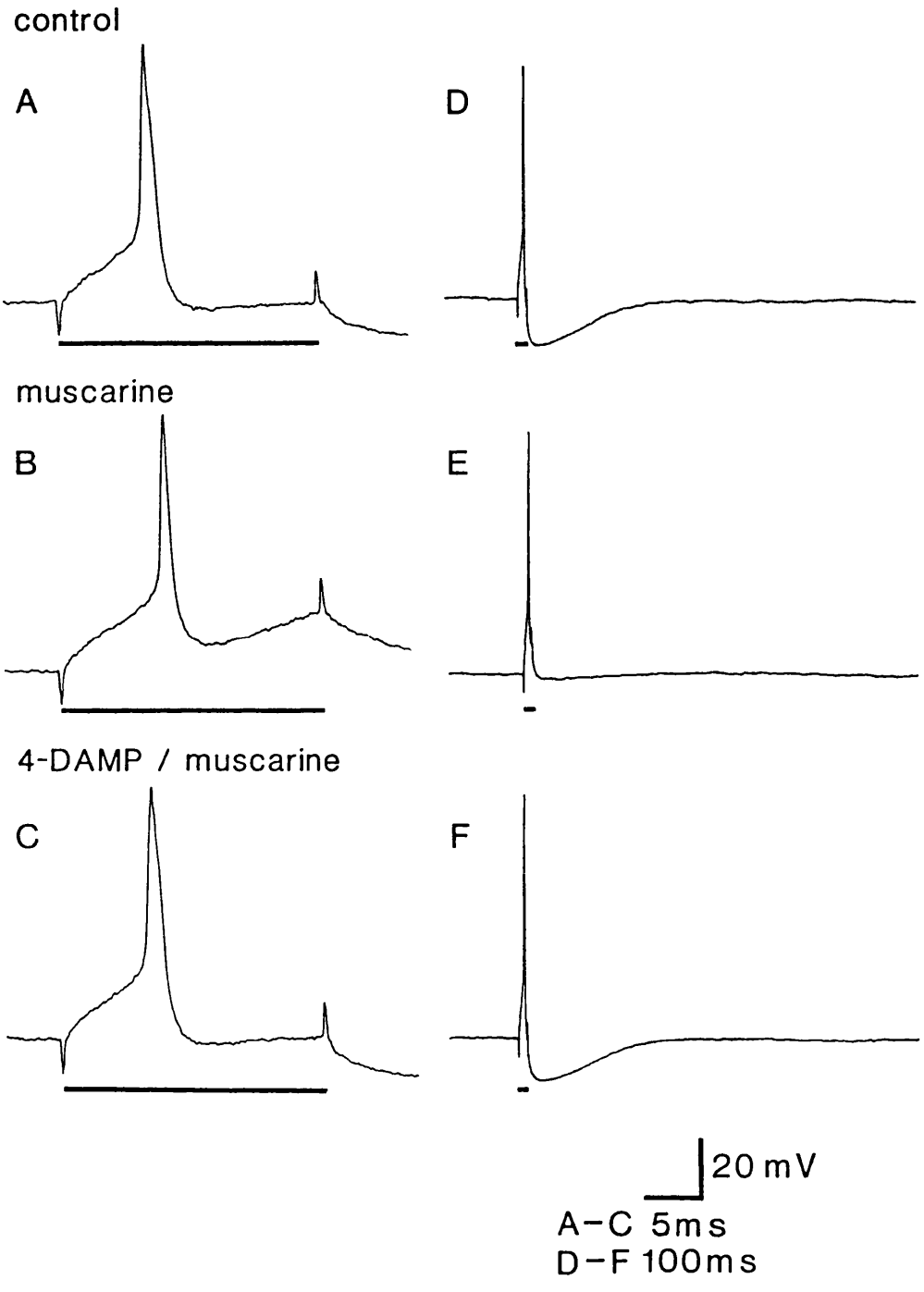
control
A
D
muscarine
B
E
4-DAMP / muscarine
C
F
20 mV
A–C 5ms
D–F 100ms

Fig. 4.10. Antagonism by pirenzepine and 4-DAMP of the muscarine-induced depolarization and inhibition of the post-spike after-hyperpolarization in guinea-pig intracardiac neurones. Muscarine (10 μM) was applied by local pressure ejection for 150 ms at the points indicated by the arrows. A, control; the cell depolarized and there was a concomitant decrease in the amplitude and duration of the after-hyperpolarization. B, pirenzepine (100 nM) antagonized the depolarization induced by muscarine, but had no effect on the muscarine-induced decrease in the after-hyperpolarization. C, washout. D, 4-DAMP (100 nM) antagonized both the actions of muscarine but displayed no notable selectivity for any one component. Resting membrane potential -50 mV. Note: spikes were attenuated in the pen recording.

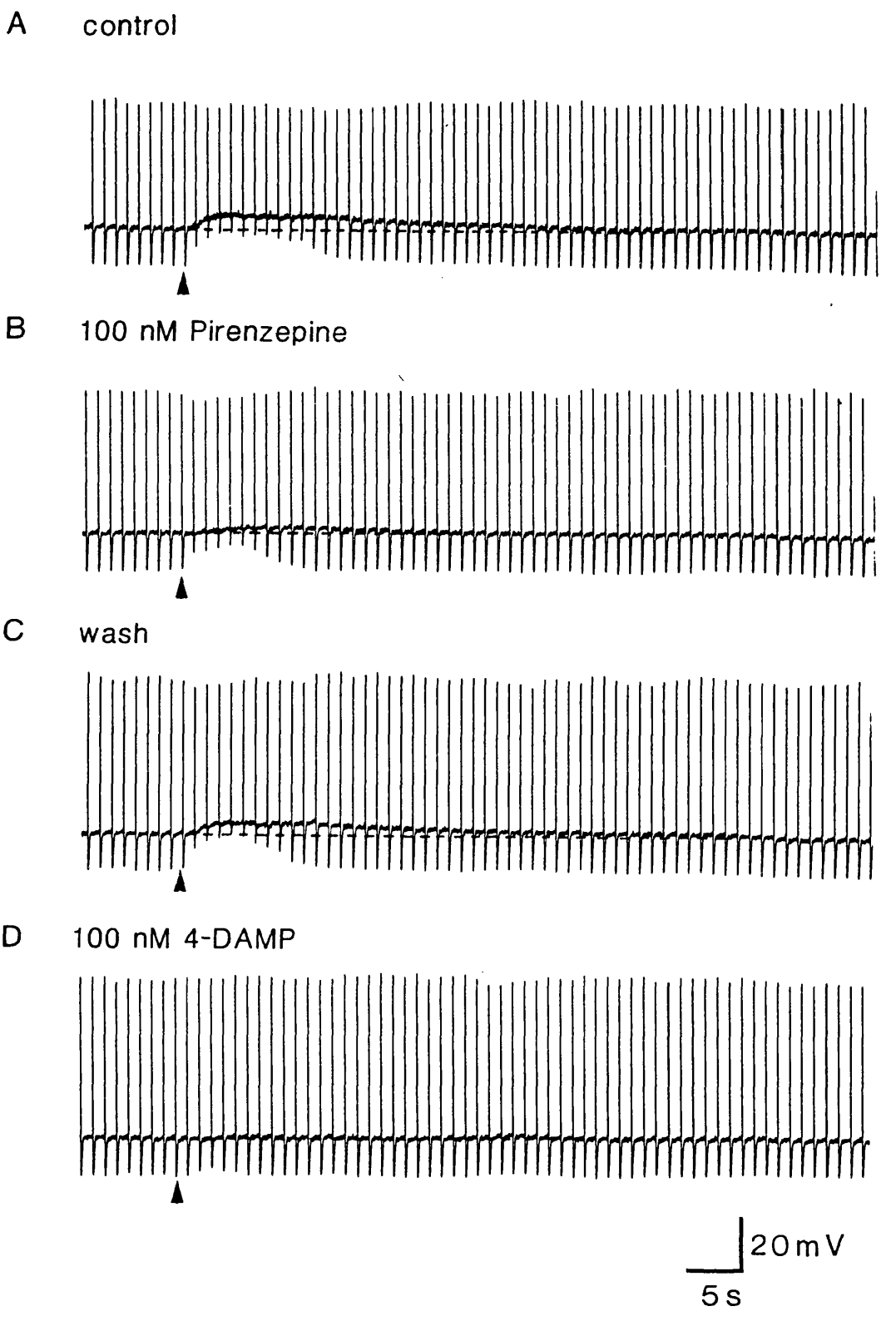
A
control
B
100 nM Pirenzepine
C
wash
D
100 nM 4-DAMP
20 mV
5 s

Fig. 4.11. Antagonism of the muscarine-induced inhibitory potential in guinea-pig intracardiac neurones. A, control response to muscarine. B, the inhibitory response was completely antagonized by AF-DX 116 (500 nM). At this concentration, AF-DX 116 showed a limited degree of selectivity for the inhibitory response and generally required a 2- to 5-fold increase in concentration before it antagonized any of the other muscarinic responses. C, washout to control conditions. D, as with all the other muscarinic responses, 4-DAMP (100 nM) potently, but non-selectively, antagonized the inhibitory response. E, washout to control conditions. F, pirenzepine, at a concentration (100 nM) that inhibited the slow depolarization had no effect upon the inhibitory potential. Resting membrane potential -64 mV.

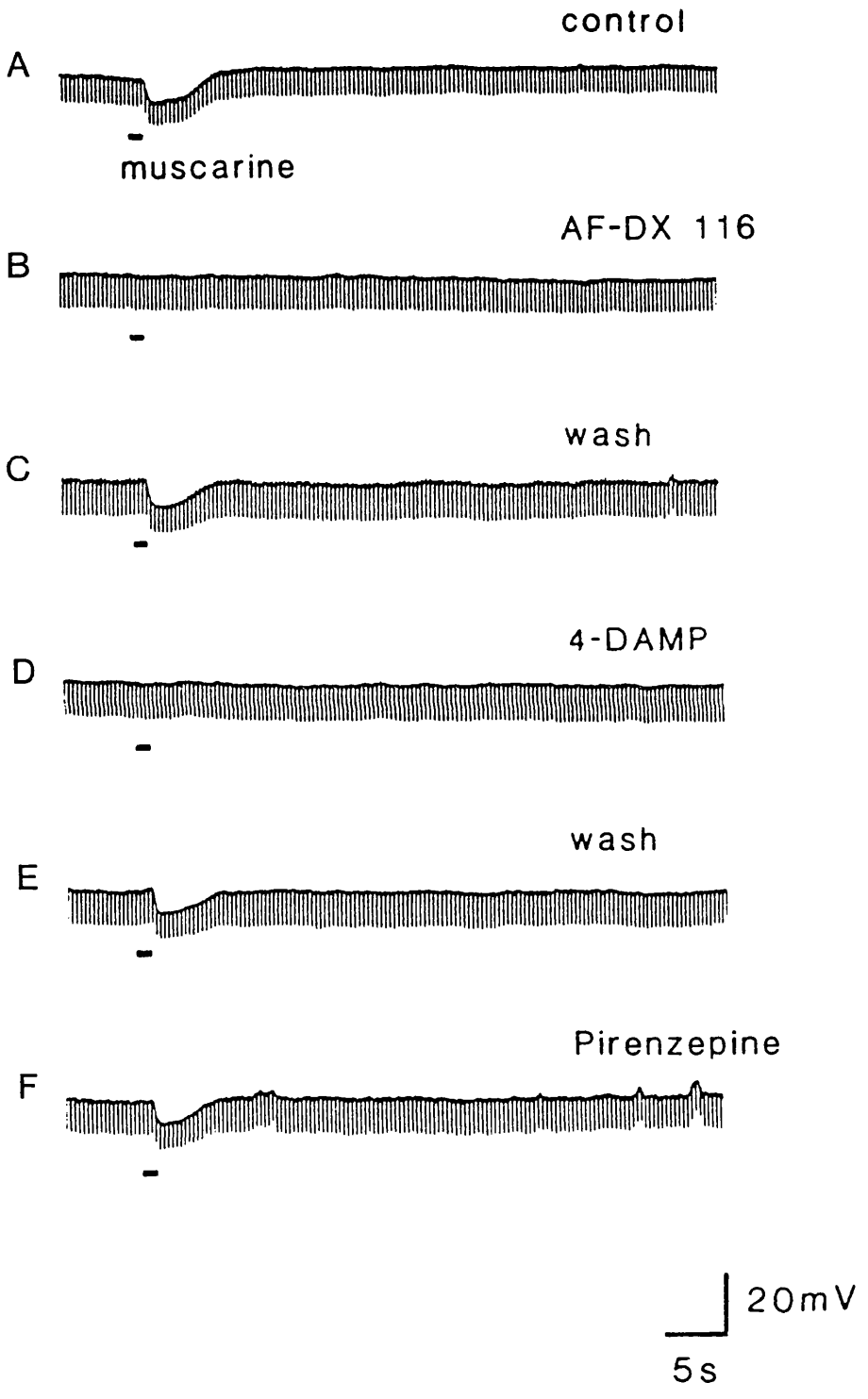
control
A
muscarine
AF-DX 116
B
wash
C
4-DAMP
D
wash
E
Pirenzepine
F
20mV
5s

Chapter 5

THE ACTIONS OF ADENOSINE 5'-TRIPHOSPHATE ON GUINEA-PIG INTRACARDIAC NEURONES IN CULTURE

SUMMARY

1. The actions of adenosine 5'-triphosphate and related nucleotides and nucleosides on the membrane ion conductances of M and AH type intracardiac neurones cultured from ganglia within the atria and interatrial septum of newborn guinea-pig heart were studied using intracellular current- and voltage-clamp techniques.

2. Approximately 74% (120 out of 161) of AH type cells and 41% (5 out of 12) M cells responded to direct application of ATP (500 μM) on to their soma.

3. In 41% of M and 43% of AH type cells, focal application of ATP (500 μM) evoked a rapid depolarization and an increase in conductance which frequently elicited action potential discharge. The underlying inward current had a null potential of -11.2 mV and was reduced in solutions containing low extracellular sodium and calcium but was unaffected by reduced chloride-containing solutions.

4. In a further 31% of AH type cells, ATP evoked a multi-component response consisting of an initial depolarization followed by a hyperpolarization and a slow prolonged depolarization. The current underlying the initial depolarization resulted from an increase in conductance and had null potential of -19.1 mV. The current was increased in low chloride- and was only slightly reduced in low sodium- and calcium-containing solutions. The subsequent hyperpolarization and outward current resulted from an increase in membrane conductance and had a null potential of -88.5 mV, which was close to the potassium equilibrium potential in these cells. The slow depolarization and inward current was not associated with any change in membrane conductance.

5. In less than 2% of AH cells, ATP evoked a second type of slow depolarization. This was associated with a fall in conductance and had a null

potential of -90.7 mV.

6. In 40% of AH cells, adenosine (10-100 μM) inhibited the calcium-sensitive potassium current responsible for the after-hyperpolarization. The action of adenosine was antagonized by the P_1-purinoceptor antagonist 8-phenyltheophylline (1-10 μM).

7. The potency order of agonists for all of the ATP-evoked responses, except the slow depolarization associated with a fall in conductance, was ATP > ADP with AMP and adenosine being ineffective.

8. Responses to ATP were only weakly desensitized by α,β-methylene ATP (3×10^{-6}M) and the potency order of analogues was 2-methylthio ATP ≥ ATP > α,β-methylene ATP, indicating the involvement receptors similar to P_{2y}-purinoceptors.

INTRODUCTION

There is now considerable evidence to suggest that purine nucleotides and nucleosides act as neurotransmitters and neuromodulators in a variety of different tissues (Burnstock, 1972, 1985, 1986b; Phillis & Wu, 1981; Stone 1981; Su, 1983; Gordon, 1986). In addition, exogenously applied purines have also been shown to act directly on a number of peripheral and central neurones (for example see Jahr & Jessell, 1983; Krishtal, Marchenko & Pidoplichko, 1983; Salt & Hill, 1983; Fyffe & Perl, 1984; Akasu & Koketsu, 1985; Dolphin, Forda & Scott, 1986; Palmer, Wood & Zafirov, 1987; Williams, 1987; Katayama & Morita, 1989).

The division of purinoceptors into two subtypes was first proposed by Burnstock (1978). According to this classification, P_1-purinoceptors, which are most sensitive to adenosine, produce changes in the levels of cyclic adenosine 3' 5'-monophosphate (cyclic AMP) and are competitively inhibited by methylxanthines; whereas P_2-purinoceptors recognise ATP, are not associated with changes in intracellular levels of cyclic AMP and are not antagonized by methylxanthines. Subdivisions of both these receptor subtypes have subsequently been proposed. P_1-purinoceptors consist of two subtypes: $A1/R_1$ and $A2/R_2$ (Van Calker, Müller & Hamprecht, 1979; Londos, Cooper & Woolf, 1980); while P_2-purinoceptors have been subdivided into P_{2t}, P_{2x}, P_{2y} and P_{2z} receptors (Burnstock & Kennedy, 1985; Gordon, 1986).

For many years it has been known that exogenous ATP and adenosine exert a powerful influence upon the mammalian heart (Drury & Szent-Györgyi, 1929). Their effects include negative chronotropic and dromotropic actions upon the sino-atrial

and atrio-ventricular nodes, as well as potent vasodilatation of coronary blood vessels (for review see Burnstock, 1980). The possibility that there might be purinergic innervation of the heart is supported by the observation of nerve fibres and intramural neurones in guinea-pig and rabbit atria showing positive reactions to quinacrine, a fluorescent compound that binds strongly to ATP (Irvin & Irvin 1954; Da Prada et al. 1978; Crowe & Burnstock, 1982). At present, the projections of the intramural ganglia are largely unknown; however, many of the ganglia are concentrated around the sino-atrial node and in the interatrial septum and, as such, are ideally placed to influence both nodal and conducting tissues (King & Coakley, 1958).

A dissociated mixed cell culture preparation of newborn guinea-pig atria and interatrial septum (Hassall & Burnstock, 1986) has been utilized to study the electrophysiological and neurochemical properties of intracardiac neurones (see Chapters 3 and 4 and Allen & Burnstock, 1987, 1990a). In a previous electrophysiological study of the properties of guinea-pig intracardiac neurones in culture, two main cell types which were termed AH and M cells were distinguished (see Chapter 3 and Allen & Burnstock, 1987). M cells displayed non-accommodating tonic firing characteristics when stimulated by intrasomal current injection, whilst AH type neurones were highly refractory and displayed pronounced calcium-dependent after-hyperpolarizations. In the present study the actions of exogenously applied ATP and related nucleotides and nucleosides on these neurones have been investigated using single electrode current- and voltage-clamp techniques.

RESULTS

The actions of exogenously applied ATP, adenosine and related purine nucleotides upon guinea-pig intracardiac neurones in culture were studied using single-electrode current- and voltage-clamp techniques. The majority of recordings were made from the larger AH type cells, with a few additional studies being made of M type cells using the whole-cell patch-clamp technique.

With the exception of the evoked firing, all of the observed actions of ATP were unaffected by superfusion with tetrodotoxin (0.3 μM). Approximately 74% (120 out of 161) of AH type and 41% of M type cells (5 out of 12) responded to direct application of ATP on to their soma. Three different responses were observed. In 43% of AH type cells and all ATP responsive M cells, ATP elicited a short latency (18-55 ms) monophasic depolarization (amplitude 5-30 mV) which was associated with an increase in membrane conductance that frequently resulted in action potential discharge (see Fig. 5.1A). In a further 31% of AH cells, ATP evoked a multi-component response. This second type of response consisted of an initial transient depolarization, followed by a small hyperpolarization and a slow prolonged depolarization (see Fig. 5.1B). In a number of cells, the hyperpolarizing outward current phase of the response was observed to be very small or absent. The initial inward current in all cells resulted from an increase in membrane conductance (see Fig. 5.1Bii). The subsequent hyperpolarization and outward current also resulted from a small increase in membrane conductance (see Fig. 5.1Bii). However, the slow membrane depolarization/inward current following these initial components was never seen to be associated with any measurable change in input resistance. The third type of response to ATP, seen in only two of the cells studied (both AH type),

consisted of a slow depolarization lasting for up to 2 min which was associated with a fall in resting membrane conductance (see Fig. 5.1C).

The rapid depolarization and inward current evoked by ATP in neurones displaying only a monophasic response differed in a number of respects from the initial depolarization seen in cells exhibiting multi-phase responses. Although both these events resulted in an increase in membrane conductance, the latency and rate of rise of the rapid monophasic depolarization, observed in the majority of cells, was considerably shorter than the initial depolarization seen in cells displaying multi-component responses. The latency of this response in "monophasic" cells was between 18 and 55 ms (mean 39.4 ± 2.2 ms, n=20) and the mean time to peak was 304 ± 22.4 ms (n=17), compared with a latency of 90 to 210 ms (mean 155.4 ± 15.3 ms, n=11) and a mean time to peak of 662 ± 35 ms (n=18) for the response in cells displaying multi-component responses.

Ionic- and voltage-dependence

ATP-induced transient depolarizations

The amplitude of the ATP-induced transient depolarization in monophasically responsive M and AH type cells when held at resting membrane potential, ranged between 5 and 30 mV (mean 16.6 ± 1.27 mV, n=22). Under voltage-clamp, the underlying increase in conductance calculated as a fractional increase (see methods) was 2.45 ± 0.28 (n=12) and resulted in a large inward flow of current, mean 788.8 ± 86.2 pA (n=21). The inward current was linearly related to membrane potential and increased with hyperpolarization (see Fig. 5.2A & B). Extrapolation of the plot of

ATP-induced current against membrane potential, indicated a mean null/equilibrium potential for this current of -11.2 ± 1.45 mV (n=10). The amplitude of the ATP-induced inward current was reduced when the cell was superfused with low sodium- (26.2 mM) and/or calcium- (0.25 mM) containing solutions, whereas reducing extracellular chloride concentration (9 mM) had no effect on either the evoked current or the underlying conductance change (n=3; see Fig. 5.3).

The longer latency, initial transient depolarization in AH cells displaying multi-component responses to ATP was generally smaller than that seen in mono-phasically responsive M and AH cells and never elicited action potential discharge. The average amplitude of the response was 11.2 ± 1.15 mV (n=18), whilst the underlying fractional increase in conductance and evoked currents were also smaller, having mean values of 0.46 ± 0.08 (n=15) and 203.7 ± 22.4 pA (n=30) respectively. The inward current increased with membrane hyperpolarization and was linearly related to membrane potential between -75 and -45 mV (see Fig. 5.4A). The predicted null/equilibrium potential of this response, determined by extrapolation was -19.1 ± 1.1 mV (n=2), which was slightly more negative than the value for the fast inward current in other M and AH cells (see Fig. 5.4B). Low extracellular chloride-containing solutions (9 mM) increased the current (mean increase 58 ± 8.1%, n=3), whilst superfusion with low sodium- or low calcium-containing solutions only slightly reduced the current, mean reduction 15.7 ± 1.45% and 9.3 ± 3.71% (n=3) respectively (see Fig. 5.5).

Slow outward current/hyperpolarization

This response was generally small, range -1 to -3.5 mV (mean-2.0 ± 0.27 mV,

n=10) and resulted from a small increase in membrane conductance, mean fractional increase 0.11 ± 0.025 (n=6). Under voltage-clamp, the ATP-induced outward current at resting membrane potential was 41.1 ± 5.6 pA (n=13). In all cells studied, the current decreased with membrane hyperpolarization (see Fig. 5.4A & C). The current was linearly related to membrane potential and extrapolation of the plot of evoked current against membrane potential gave a predicted mean null/equilibrium potential of -88.5 mV (n=2), indicating that the current may have resulted from an efflux of potassium ions.

Slow inward current with no associated change in conductance

This current was the most commonly observed slow inward current seen in AH cells displaying multi-component responses. The response had a slow rate of rise and reached a peak (10.8 ± 0.37 s, n=23) following focal application of ATP (500 μM). The mean inward current associated with this ATP-induced current was 107.1 ± 13 pA (n=28), and the average observed depolarization was 4.5 ± 0.64 mV (n=9). However, no significant change in membrane conductance was observed in any of the cells studied. Furthermore, it was not possible to determine ionic- or voltage-dependence of this current because of difficulties encountered in reproducibly eliciting the response. However, it was generally observed to increase with membrane hyperpolarization (see Fig. 5.4A).

Slow inward current associated with a fall in conductance

This ATP-induced slow inward current was only observed in two cells. It was distinct from the more commonly observed slow inward current that was seen in

cells displaying multi-phase responses, in that it resulted from a clear decrease in membrane conductance. The outward current was reduced by membrane hyperpolarization (Fig. 5.6A), and was linearly related to membrane potential between -40 and -70 mV (see Fig. 5.6B). Extrapolation of the least squares fit of the raw data gave an equilibrium potential for the response of -90.7 mV (n=1).

Other purine compounds

2-Methylthio ATP, which potently stimulates P_{2y}-purinoceptors, mimicked all the observed actions of ATP and was generally found to be slightly more potent than ATP (see Fig. 5.7A & B). In general, α,β-methylene ATP, which has been shown to potently stimulate P_{2x}-purinoceptors, only poorly mimicked the ATP-evoked rapid transient depolarization (see Fig. 5.7A). In most cells, α,β-methylene ATP evoked only a very small depolarization/current. In a few cells however (n=4), it was seen to elicit a depolarization of similar amplitude to that produced by ATP. In these cells, the peak increase in conductance and current examined under voltage-clamp was always smaller than that evoked by ATP and the rate of rise of the depolarization produced was notably slower. When applied to cells that produced a multi-component response to ATP, α,β-methylene ATP weakly mimicked the initial transient inward current, but was never observed to evoke the subsequent slow outward and inward currents (see Fig. 5.7B).

ADP only very weakly mimicked the actions of ATP, whilst AMP and adenosine were ineffective in mimicking any of the actions of ATP. However, adenosine (10-100 μM) was found to reduce the calcium-dependent after-hyperpolarization that followed a train of action potentials (see Fig. 5.8). Both the amplitude and duration

of the potassium current and the underlying conductance increase recorded using a "hybrid" voltage-clamp technique (see methods) were reduced by adenosine in a concentration-dependent manner. This effect was antagonized by 8-phenyltheophylline (10 μM; see Fig. 5.8).

Antagonism of the actions of ATP

Superfusion with the putative P_{2y} receptor antagonist, reactive blue 2, at concentrations up to 3×10^{-5} M initially enhanced the fast transient inward current evoked by ATP by up to 100% (mean 40.4 ± 15.1%, n=5). With continuous application (> 3 min) the duration of responses became considerably prolonged. The mean increase in duration was 203 ± 23% (n=7). In addition, there was generally a fall in input resistance and an increase in the overall level of current noise, which reflected a general reactive blue 2-induced deterioration in the cell (see Fig. 5.9C and D). With longer periods of application (up to 25 min) responses to ATP slowly declined in all cells studied (n=14). Complete washout of the effects of reactive blue 2 was never achieved even after prolonged periods (up to 45 min). Reactive blue 2 also strongly depressed $GABA_A$ receptor-mediated chloride currents (mean reduction 78.7 ± 7.2%, n=3) and reduced, though to a lesser extent, the amplitude of the acetylcholine-induced nicotinic responses (mean reduction 26 ± 2.6%, n=3).

Superfusion with α,β-methylene ATP (3×10^{-6} M) only partially reduced the amplitude of the ATP-induced brief latency inward current observed in M and AH type cells (see Fig. 5.9A). The maximum observed reduction in this inward current ranged between 24 and 60% (mean 44.8 ± 6.3%, n=6). When applied to neurones exhibiting multi-component responses to ATP, a similar 19-59% reduction in the

initial transient current (mean 35.6 ± 7.2%, n=5) was observed (see Fig. 5.9B).

Inhibition of prostaglandin synthesis with indomethacin (5×10^{-5} M) had no effect upon any of the ATP-induced currents (n=7). Similarly the P_1-purinoceptor antagonist 8-phenyltheophylline (10 μM) was also without effect (n=11).

DISCUSSION

The present study shows that a large population of guinea-pig intracardiac neurones in culture were responsive to exogenous application of ATP. Three different responses to ATP were observed. The first was a rapid transient depolarization, exhibited by all ATP-responsive M cells (41%) and approximately 43% of AH type neurones. This response displayed a similar agonist potency (ATP> ADP with AMP and adenosine ineffective) and brief latency to the ATP-induced responses seen in mammalian dorsal horn and sensory ganglion neurones (Jahr & Jessell, 1983; Krishtal et al. 1983). In all these cell types, ATP produced a transient increase in membrane conductance resulting in a large inward current. In rat dorsal horn and cat vesical parasympathetic ganglia (Jahr & Jessell, 1983; Akasu, Shinnick-Gallagher & Gallagher, 1984) as in the present study, application of ATP frequently evoked action potential discharge. The underlying ionic conductance changes observed were similar, in that a large proportion of the current was carried by sodium ions. In dorsal horn and dorsal root ganglion cells, sodium appears to be the sole charge carrier, whilst in sensory, vesical parasympathetic and intracardiac neurones the response to ATP appeared to be mediated via non-selective cationic channels (Krishtal et al. 1983; Akasu et al. 1984). Interestingly, the inward current in AH and M cells that gave single component responses to exogenous application of ATP, differed from the initial inward current displayed by AH cells exhibiting multi-component responses. In the latter type of cell, the latency of the response was approximately 100 ms slower and was never observed to evoke action potential discharge. In addition, the ionic- and voltage-dependence of the underlying current was different. The null/equilibrium potential was 7-8 mV more negative and the current was only

slightly reduced in low extracellular calcium- and sodium-containing solutions, but was greatly enhanced when the chloride concentration was reduced, indicating that this response may have resulted primarily from an increase in chloride conductance.

The inhibitory response which was frequently observed following the initial inward current in AH type cells displaying multi-component responses to ATP, resulted from an increase in membrane conductance and had a null potential close to the potassium equilibrium potential (E_K) in these cells (see Chapter 3 and Allen & Burnstock, 1987), suggesting that it may result from an increase in potassium conductance. Similar biphasic responses to ATP, consisting of an initial depolarization followed by a hyperpolarization have also been reported in cat vesical parasympathetic neurones and in chick skeletal muscle cells (Akasu et al. 1984; Hume & Thomas, 1988). As in intracardiac neurones, the inhibitory response in these cells also appeared to be the result of an increase in potassium conductance. In vesical parasympathetic neurones, this response was mimicked by adenosine, indicating that it was mediated via P_1-purinoceptors. Adenosine-induced hyperpolarizations resulting from an increase in potassium conductance have also been reported in rat hippocampal, mouse striatal and guinea-pig myenteric plexus neurones (Segal, 1982; Haas & Greene, 1984; Trussell & Jackson, 1985; Palmer et al. 1987). In the current study of intracardiac neurones however, adenosine was never observed to mimic the ATP-induced hyperpolarization, indicating that this response was not mediated by P_1-purinoceptors.

Two different types of ATP-induced slow depolarization were observed in AH type cells but were never observed in M type cells. In the majority of cells, the ATP-evoked depolarization and inward current was not associated with any

measurable change in membrane conductance. Furthermore, it was not antagonized by indomethacin or the P_1-purinoceptor antagonist 8-phenyltheophylline, suggesting that it did not arise as a result of increased prostaglandin synthesis or from the breakdown of ATP to adenosine. Unlike the most commonly observed slow depolarization, the second type of ATP-induced slow depolarization was associated with a distinct decrease in membrane conductance and was not preceded by a transient depolarization or hyperpolarization. This current most probably resulted from inhibition of a tonically active potassium conductance since it displayed a null potential close to E_K (see Chapter 3 and Allen & Burnstock, 1987). ATP and adenosine have similar actions on a variety of different neurones (Akasu, Hirai, & Koketsu, 1983; Morita, Katayama, Koketsu & Akasu, 1984; Katayama & Morita, 1989). Possible mechanisms for this action include M-current inhibition, or inhibition of tonically operating calcium-sensitive and calcium-insensitive potassium conductances. Although AH type intracardiac neurones exhibit an M-like current (see Chapter 4 and Allen & Burnstock, 1990a) it would appear that M-current inhibition is unlikely to be a significant factor because a fall in membrane conductance and prolonged inward current could still be evoked at membrane potentials where M-channels are largely inactivated.

Both P_1- and P_2-purinoceptor subtypes were expressed by guinea-pig intracardiac neurones. All of the observed actions of ATP appeared to result from the direct action of ATP on P_2-purinoceptors rather than as a consequence of its breakdown to ADP, AMP or adenosine. Exogenous application of adenosine was never observed to mimic any of the actions of ATP. However, although the actions of adenosine were not studied in detail here, adenosine, acting on P_1-purinoceptors, was observed to inhibit the outward post-spike calcium-sensitive potassium current

in a significant population of AH type cells.

In a number of tissues, α,β-methylene ATP, a slowly degraded analogue of ATP has been shown to potently (> ATP) and selectively act on P_{2x}-purinoceptors, whilst 2-methylthio ATP acts most potently (>> ATP) upon P_{2y}-purinoceptors (for review see Burnstock & Kennedy, 1985). In the current study, α,β-methylene ATP only weakly mimicked the initial transient inward currents evoked by ATP and was never seen to mimic the slow outward or inward currents. On the other hand, 2-methylthio ATP mimicked all the observed actions of ATP, but was only slightly more potent than ATP. Thus the order of potency for these purines on intracardiac neurones was 2-methylthio ATP ≥ ATP > α,β-methylene ATP. According to the original classification proposed by Burnstock & Kennedy (1985), α,β-methylene ATP also selectively desensitizes P_{2x}-receptors. Prolonged exposure to α,β-methylene ATP generally reduced, but never abolished the response to ATP, indicating that these responses to ATP were not mediated via P_{2x}-purinoceptors. Reactive blue 2, an anthraquinone sulphoric acid derivative, has been shown to display a degree of selectivity in antagonizing P_{2y}-purinoceptors in a variety of tissues (Kerr & Krantis, 1979; Manzini, Hoyle & Burnstock, 1986; Burnstock & Warland, 1987; Hopwood & Burnstock, 1987; Houston, Burnstock & Vanhoutte, 1987). In the current study, reactive blue 2 initially increased and promoted the duration of the observed actions of ATP, whilst prolonged exposure generally reduced the amplitude of the ATP-induced responses and also caused a slow deterioration in the input resistance of all cells studied. Furthermore, at concentrations as low as 10 μM, it also reduced responses to exogenously applied GABA and acetylcholine, indicating that reactive blue 2 was non-selective in its actions.

The expression of receptors for ATP and adenosine raises the possibility that in the heart they may act pre- or post-junctionally to modulate transmitter release from the intramural neurones and thereby regulate the activity of the effector tissue. In addition, the presence of quinacrine-positive intramural neurones and nerve fibres in guinea-pig atria suggests that some intracardiac neurones may be purinergic (Crowe & Burnstock, 1982). ATP and adenosine are known to produce potent vasodilation of coronary vessels and also to have pronounced effects upon heart muscle, particularly in the atrium and the sino-atrial node (Drury & Szent-Györgyi, 1929; Yatani, Goto & Tsuda, 1978; Berne, 1980; West & Bellardinelli, 1985). Therefore, it is possible that release of ATP from intracardiac neurones may be responsible, at least in part, for mediating some of these actions. Furthermore, the present finding that a considerable proportion of the intracardiac neurones were responsive to ATP and adenosine, raises the possibility that ATP may be released from one population of intracardiac neurones to modulate the excitability of other intracardiac neurones through local reflex pathways.

Fig. 5.1. The actions of exogenously applied ATP on AH type intracardiac neurones cultured from guinea-pig heart. A, responses from an AH type cell to focally applied ATP (500 μM) for the period indicated by the arrows (membrane potential -64 mV). Upper records were obtained under current-clamp and the lower records were voltage-clamp. Downward deflections on current- and voltage-clamp records were responses to 110 pA/-10 mV pulses of 50 ms duration which were used to monitor changes in input resistance. B, multi-component responses to ATP evoked from AH type cells. Upper trace (i), a current-clamp recording showing a three component response to ATP consisting of an initial transient depolarization followed by a small hyperpolarization and a prolonged depolarization. Membrane potential -64 mV, downward deflections were membrane voltage changes to 150 pA/50 ms intrasomal current pulses. Traces (ii) and (iii), voltage-clamp records from two cells displaying multi-component responses to ATP (membrane potentials were -60 and -52 mV respectively). Downward deflections in (ii) were membrane currents evoked by passing -10 mV/100 ms duration voltage steps. C, ATP-induced membrane depolarization and fall in membrane conductance in an AH type cell evoked by application of ATP (500 μM) for 100 ms at point indicated by arrows. Membrane potential was -53 mV, downward deflections were the result of 100 pA/50 ms and -9 mV/50 ms duration current/voltage steps used to monitor changes in input resistance.

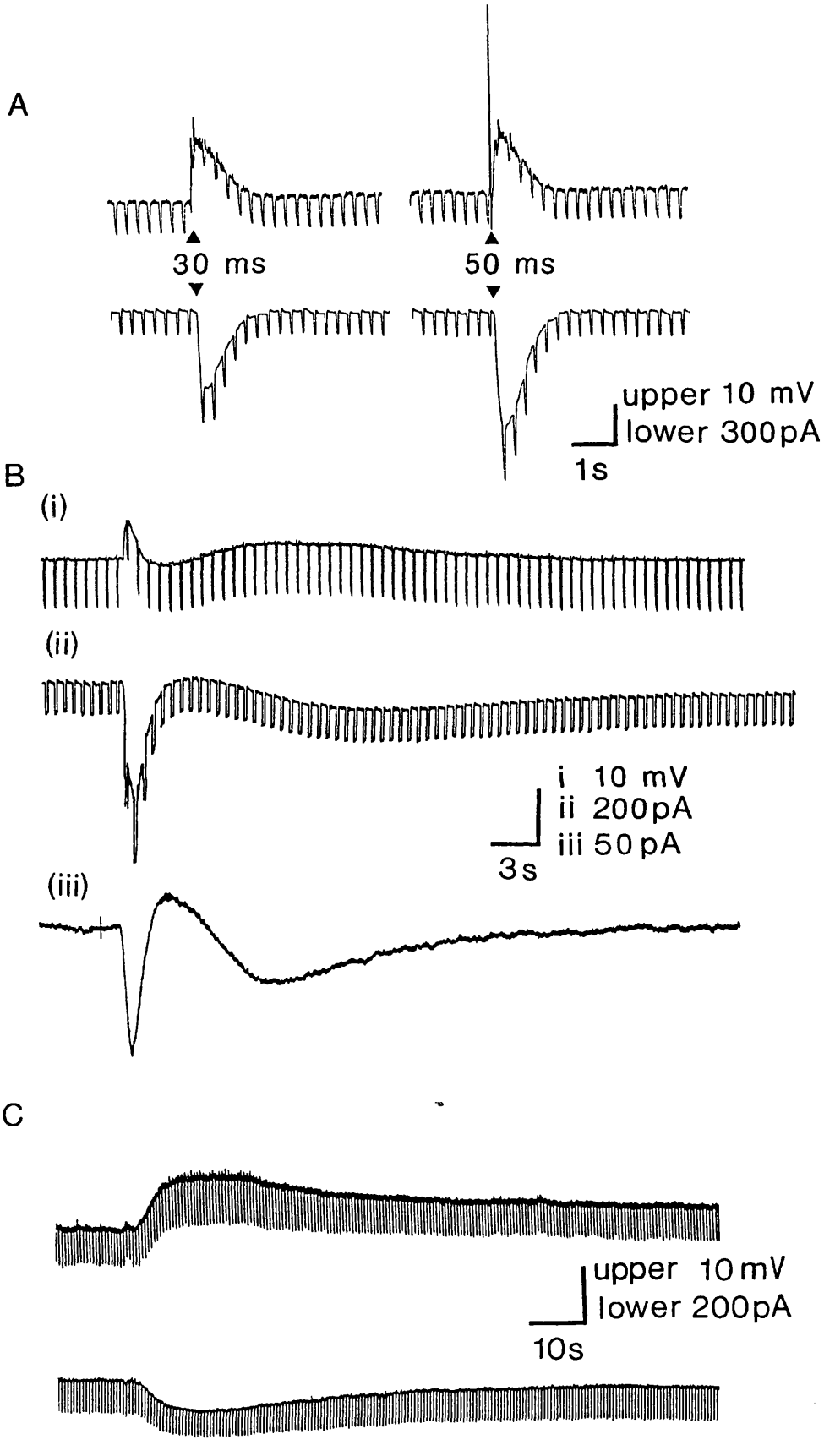
A
30 ms
50 ms
upper 10 mV
lower 300pA
1s
B
(i)
(ii)
i 10 mV
ii 200pA
iii 50 pA
3s
(iii)
C
upper 10 mV
lower 200pA
10s

Fig. 5.2. The voltage-dependence of the ATP-induced rapid transient inward current and increase in conductance in an AH type intracardiac neurone. A, the inward current evoked by focal application of ATP (500 μM/50 ms; as indicated by the arrows) at different holding potentials. Downward deflections were the currents evoked by -10 mV/50 ms duration voltage steps used to monitor changes in membrane conductance. B, a plot of evoked current against membrane potential for the cell shown in A. The amplitude of the ATP-induced current was linearly related to membrane potential (correlation coefficient r=0.998) and had a null/equilibrium potential of -9.8 mV.

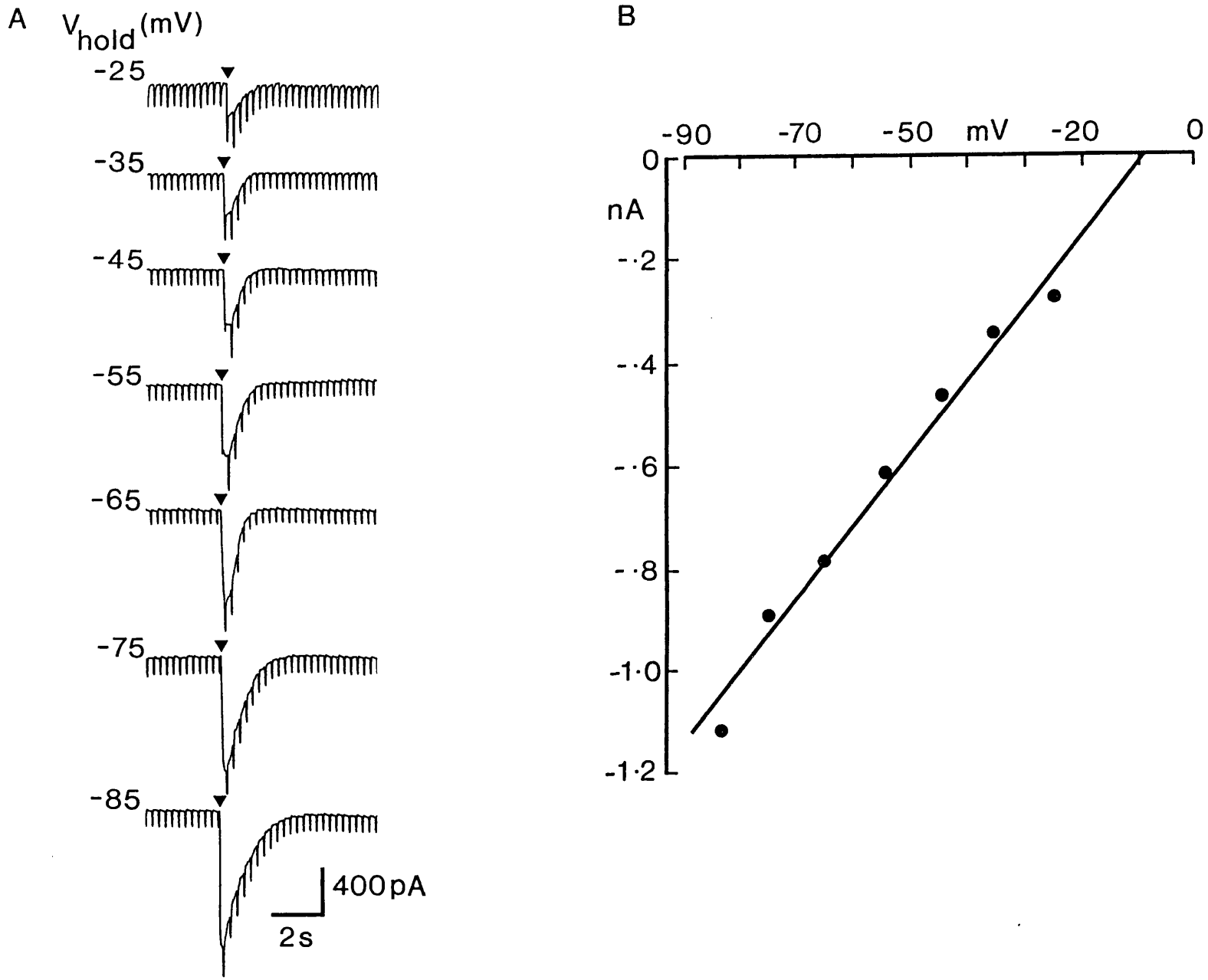
A
V_{hold} (mV)
-25
-35
-45
-55
-65
-75
-85
400pA
2s
B
-90
-70
-50
mV
-20
0
0
nA
-·2
-·4
-·6
-·8
-1·0
-1·2

Fig. 5.3. The ionic-dependence of the ATP-induced transient inward current in an AH type intracardiac neurone. ATP (500 μM) was applied by focal pressure ejection for the period indicated by the bar above each trace. Left panel, superfusion with low (9 mM) chloride-containing solution had no effect on the ATP-induced inward current or conductance change. Middle panel, superfusion with low (26.2 mM) sodium-containing solutions reduced the amplitude of the ATP-induced inward current by approximately 34%, but had little effect upon the time course of the underlying conductance change. Right panel, superfusion with low (0.25 mM) calcium-containing solutions increased resting membrane conductance and greatly reduced (approximately 68%) the amplitude of the inward current. Subsequent superfusion with a low calcium- and low sodium-containing solution (0.25 and 26.2 mM respectively) produced a further reduction in the amplitude of the inward current (approximately 82%). Holding potential throughout the recording was -70 mV.

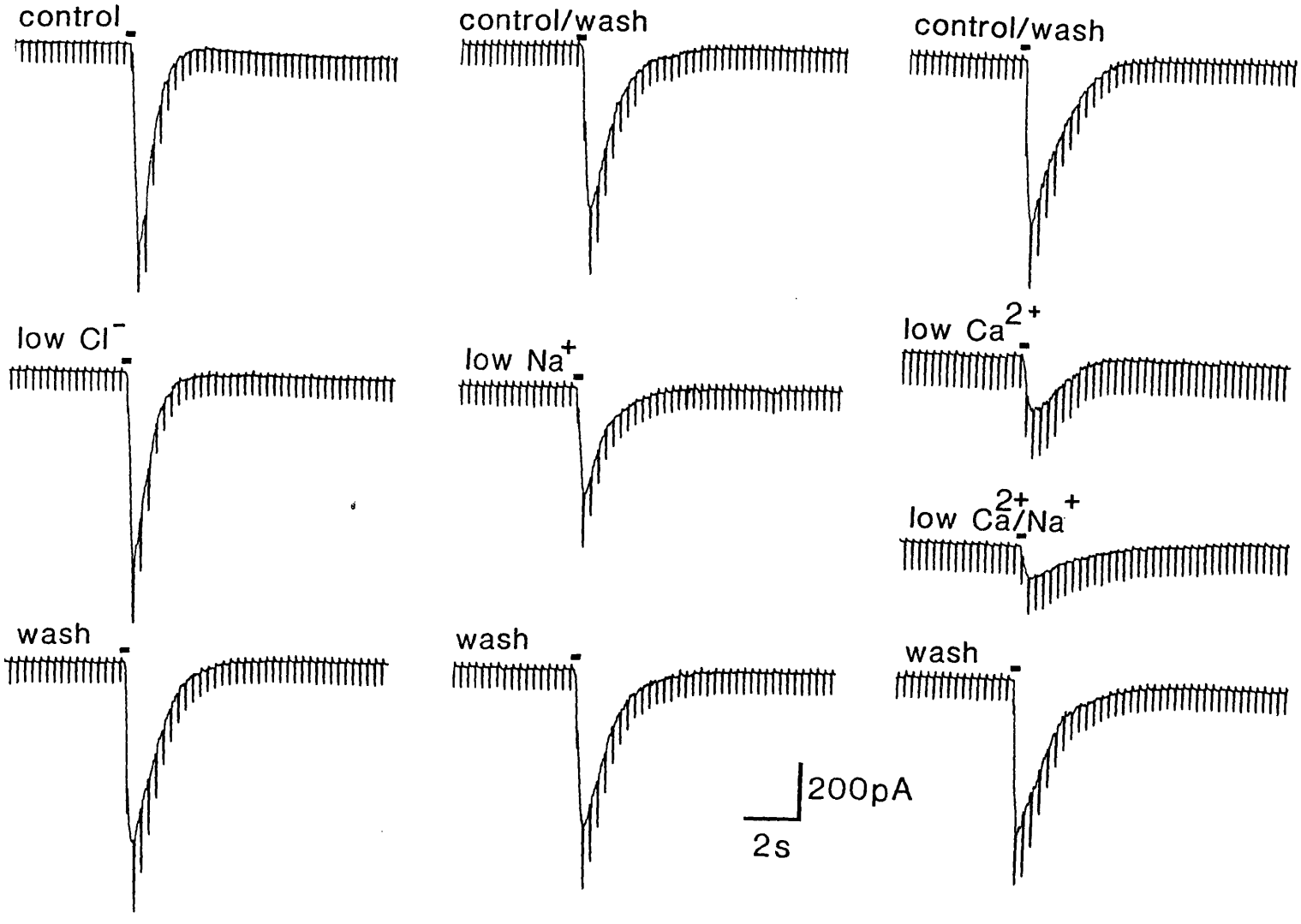
control
control/wash
control/wash
low Cl^-
low Na^+
low Ca^{2+}
low Ca^{2+}/Na^+
wash
wash
wash
200pA
2s

Fig. 5.4. The voltage-dependence of the initial transient inward and slow outward current in AH type neurones cultured from the guinea-pig heart. A, the voltage-dependence of a typical three-component response to brief (50 ms) focal application of ATP (500 μM) on to the soma of the cell. B & C, plots of the amplitude of the initial inward (I_i) and subsequent outward currents (I_o) as a function of membrane potential. In both cases the evoked currents were linearly related to membrane potential between -45 and -75 mV (correlation coefficients, 0.987 and 0.978 respectively). Extrapolation from the obtained data gave a predicted null/equilibrium potential for the inward current of -18 mV and a value of -90.8 mV for the outward current.

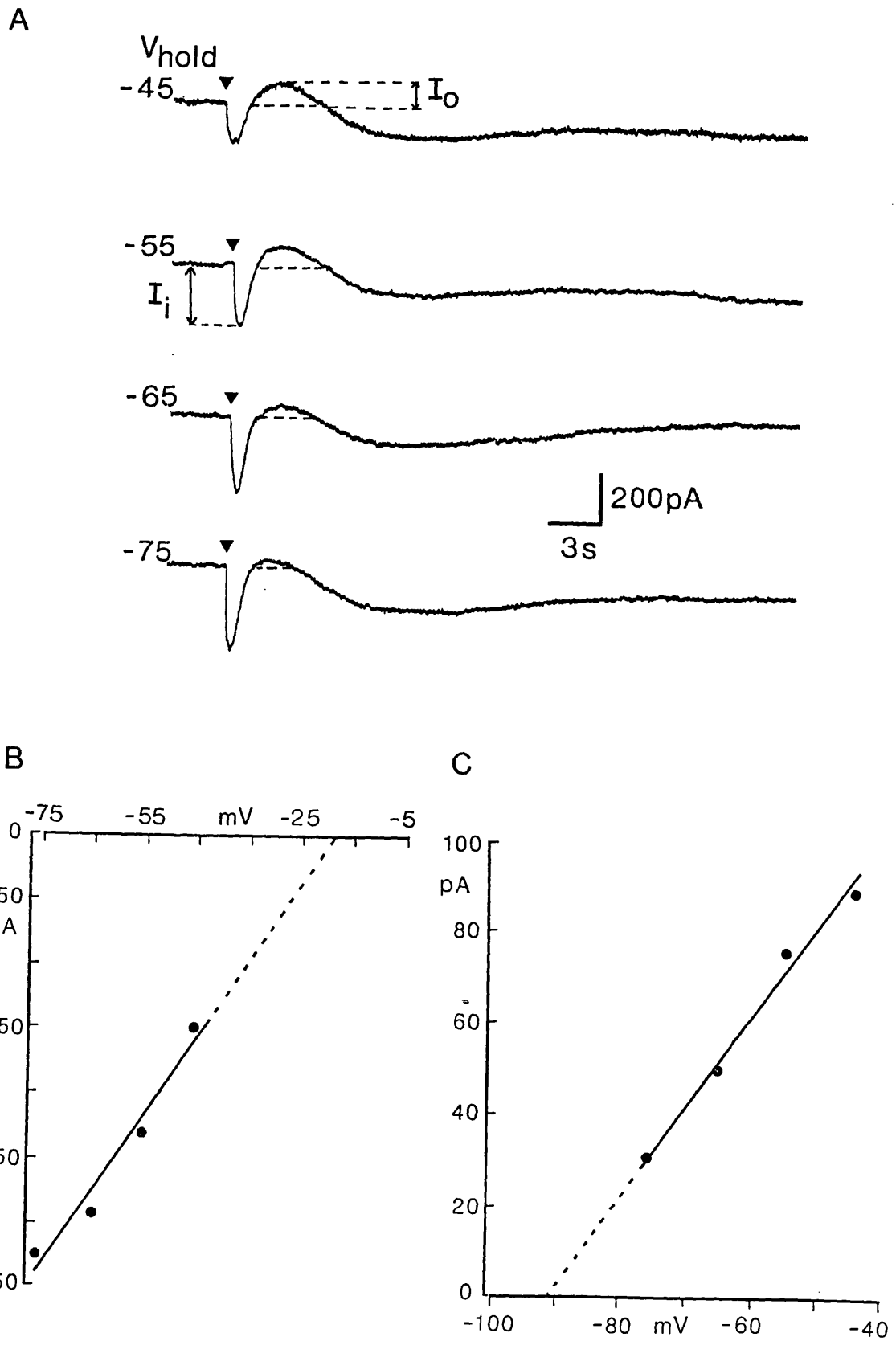
A
Vhold
-45
Io
-55
Ii
-65
200pA
3s
-75
B
-75
-55
mV
-25
-5
0
-50
pA
-150
-250
-350
C
100
pA
80
60
40
20
0
-100
-80
mV
-60
-40

Fig. 5.5. The ionic-dependence of the transient inward current in an AH type cell displaying a multi-component response to ATP. In low extracellular chloride- (9 mM) containing solutions the current was enhanced by approximately 88%. Superfusion with low sodium- (26.2 mM) or low calcium- (0.25 mM) containing solutions produced only a small reduction in the amplitude of the evoked current. Holding potential -57 mV.

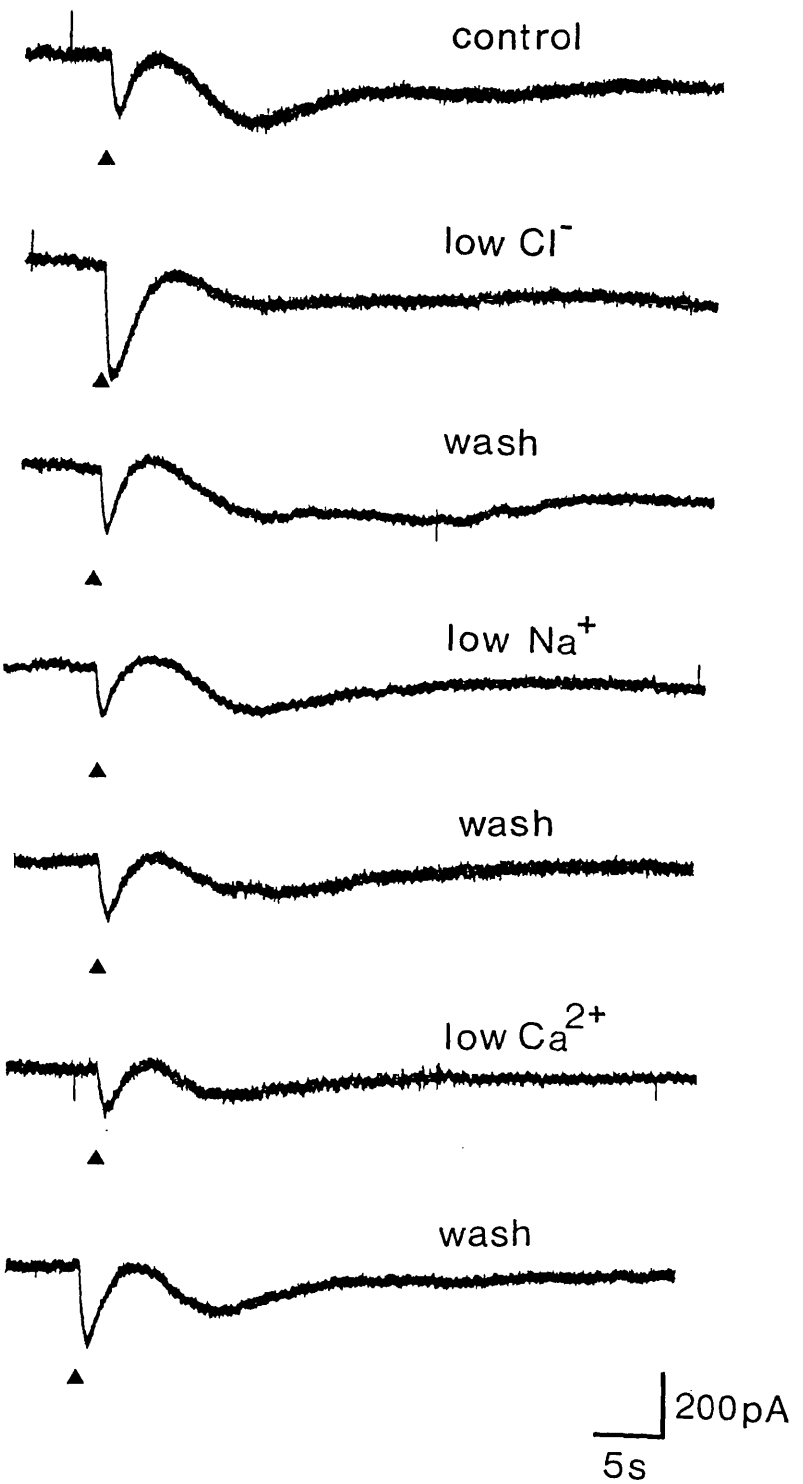
control
low Cl^-
wash
low Na^+
wash
low Ca^{2+}
wash
200pA
5s

Fig. 5.6. The voltage-dependence of the slow ATP-induced inward current in an AH type intracardiac neurone. A, the inward current and underlying fall in conductance evoked by focal pressure application of ATP (500 μM/100 ms) at different holding potentials. Application of ATP (see arrows) in this cell evoked a very small transient inward current followed by a slowly developing inward current. This current increased with membrane depolarization. The underlying conductance decrease was monitored by using a series of 10 mV/50 ms duration voltage steps and measuring the evoked current. B, a plot of evoked current versus membrane potential for the cell shown in A. The evoked current was linearly related to membrane potential between -70 and -40 mV (correlation coefficient r=0.989). Extrapolation of the least squares fitted line gave a predicted equilibrium/null potential for the ATP-induced current of -90.7 mV.

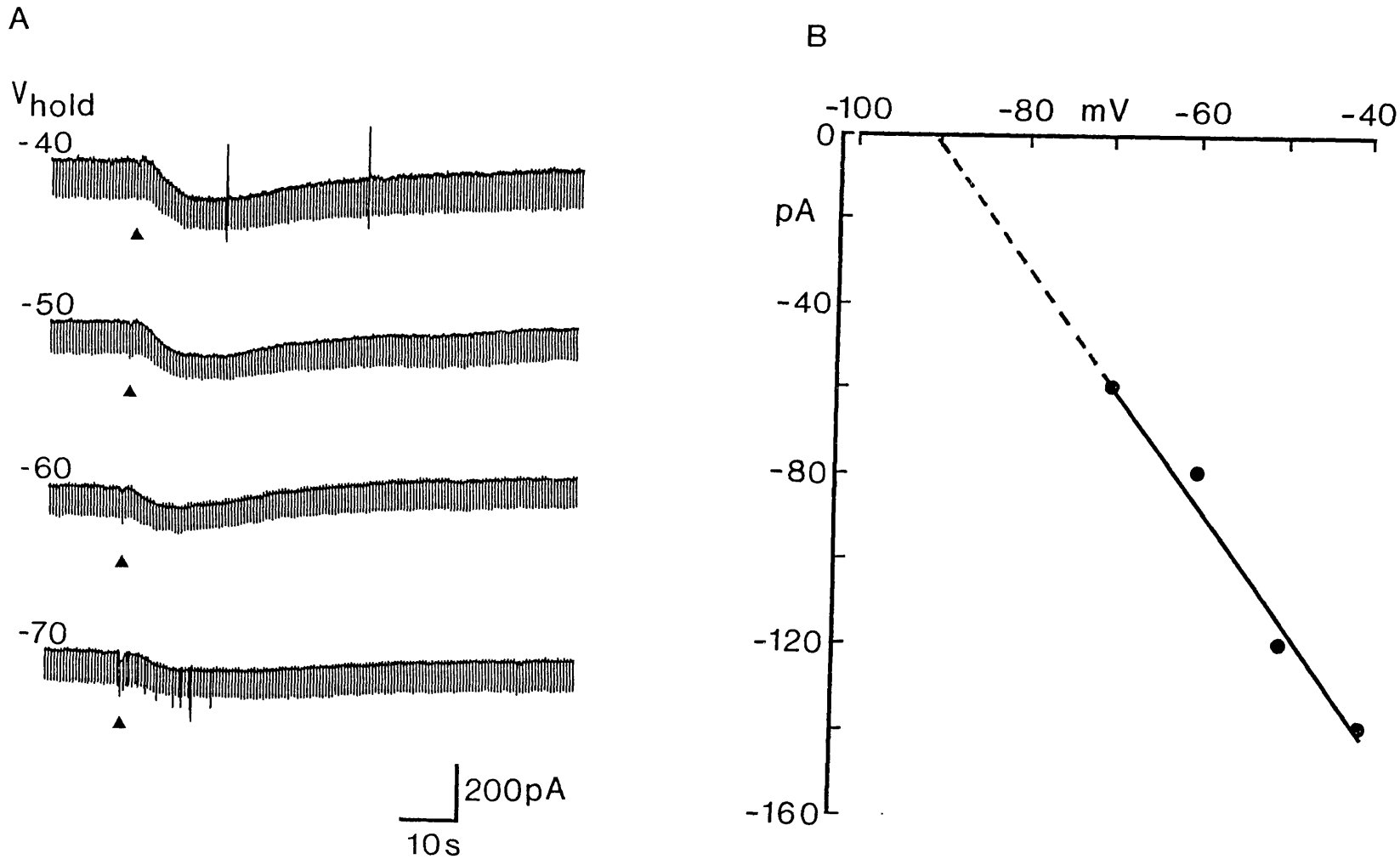
A
V_{hold}
-40
-50
-60
-70
200pA
10s
B
-100
-80
mV
-60
-40
0
pA
-40
-80
-120
-160

Fig. 5.7. The actions of ATP, α,β-methylene ATP (α,β-me-ATP) and 2-methylthio ATP (2-me.S.ATP) on intracardiac neurones cultured from the guinea-pig heart. A, the rapid monophasic inward current evoked by focal pressure application of ATP (500 μM/50 ms). α,β-Me-ATP (500 μM/50 ms) only weakly mimicked this response, whereas 2-me.S.ATP (500 μM/50 ms), potently mimicked this action of ATP. Downward deflections were evoked by -10 mV hyperpolarizing voltage steps of 50 ms duration used to monitor changes in input resistance. Holding potential -60 mV. B, an AH type cell exhibiting a three-component response to exogenous application of ATP. α,β-me-ATP weakly mimicked the initial transient inward current but did not evoke the subsequent slow outward and inward components of the response. 2-Me.S.ATP mimicked ATP and evoked a similar three-component response which was slightly larger than that produced by ATP. Holding potential -58 mV.

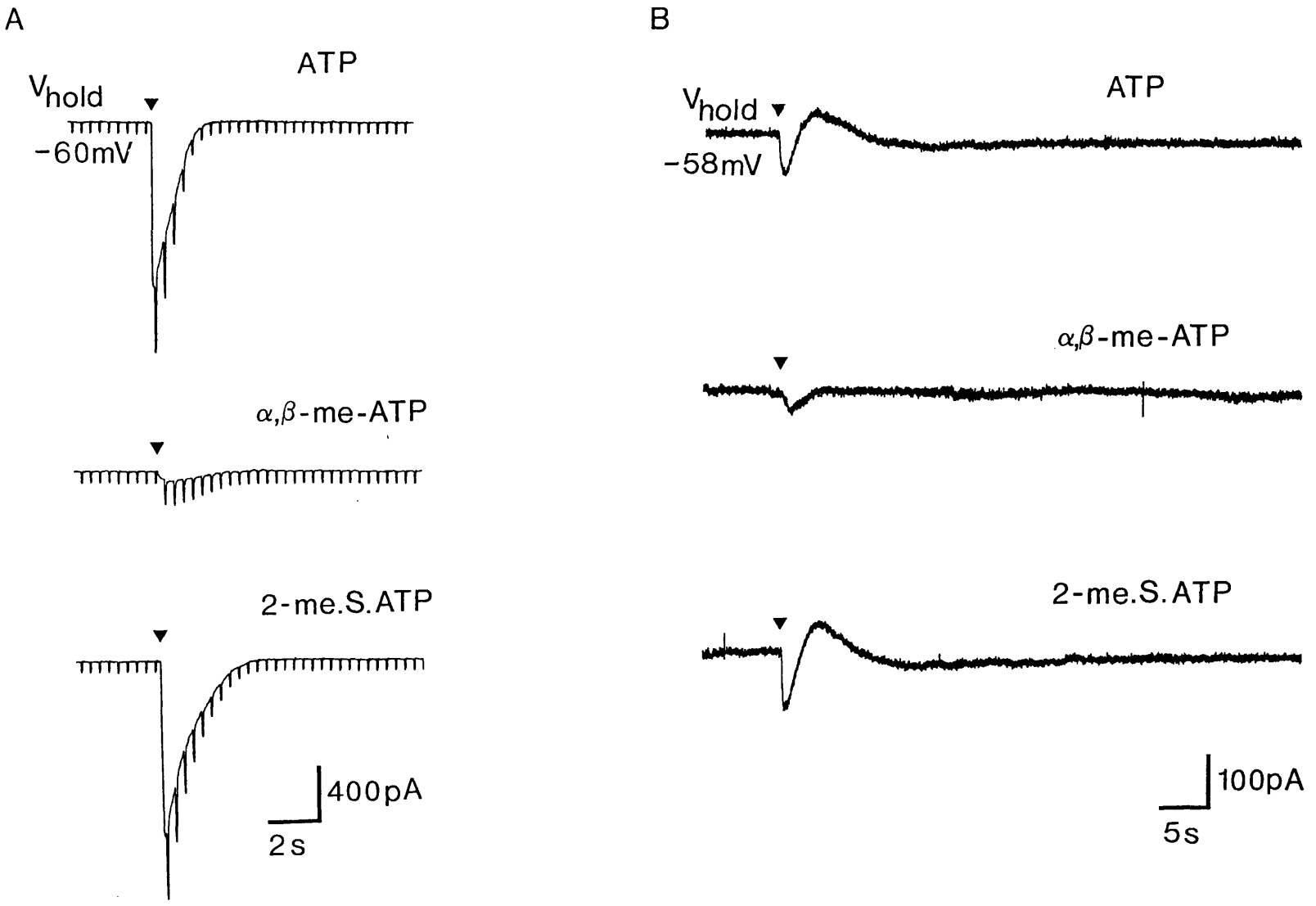
A
ATP
Vhold
-60mV
α,β-me-ATP
2-me.S.ATP
400pA
2s
B
ATP
Vhold
-58mV
α,β-me-ATP
2-me.S.ATP
100pA
5s

Fig. 5.8. Inhibition of the post-spike calcium-activated potassium current in an AH type intracardiac neurone cultured from guinea-pig heart. The recording was carried out using a "hybrid" voltage-clamp technique (see methods). Under voltage-clamp at a membrane potential of -58 mV, the cell was briefly switched into current-clamp and a train of action potentials was evoked by passing a train of intrasomal current pulses (30 Hz/1.5 s). At the end of this train, the cell was then switched back to voltage-clamp and the evoked outward current and conductance change monitored. Downward deflections were elicited by -10 mV negative command pulses of 50 ms duration used to monitor changes in membrane conductance. Adenosine (50 μM) reduced the outward current and conductance that underlies the after-hyperpolarization. In the presence of 8-phenyltheophylline (8-PT; 10 μM) this inhibitory action of adenosine was inhibited.

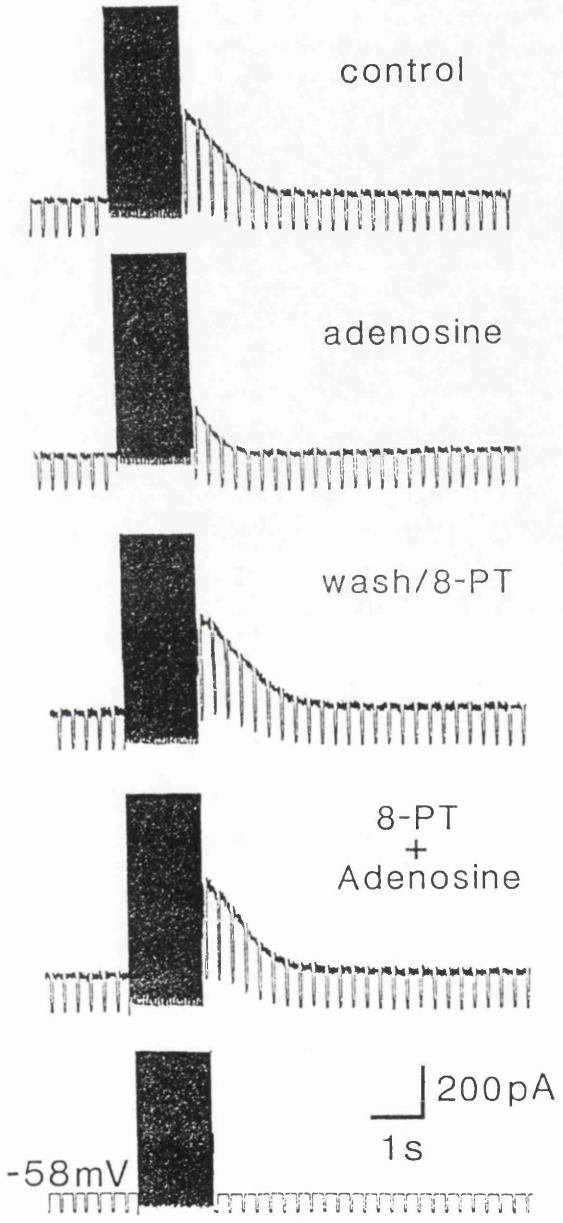
control
adenosine
wash/8-PT
8-PT
+
Adenosine
200pA
1s
-58mV

Fig. 5.9. The actions of α,β-methylene ATP (α,β-me-ATP) and reactive blue 2 (RB 2) on AH and M type intracardiac neurones. A, prolonged superfusion with α,β-me-ATP (3×10^{-6} M) reduced the amplitude of the fast transient inward current evoked by focal application of ATP (500 μM/70 ms) in an M type cell. The ATP-evoked current was maximally inhibited after 9 min superfusion, at which point the current was reduced by approximately 50%. Holding potential -68 mV. A similar reduction in the ATP-induced currents was also seen in cells (all AH type) displaying multi-component responses to ATP (see panel B; holding potential -58 mV). Panels C and D show the effect of prolonged superfusion with RB 2 (3×10^{-5} M). In cells displaying only a single transient inward current in response to ATP, RB 2 produced an initial increase in the evoked current and a slight increase in resting membrane conductance. During prolonged application input resistance continued to decline and the duration of the response was increased. Continued superfusion (up to 30 min) subsequently led to a slow decline in the amplitude of the current and further reduction in input resistance. Washout of RB 2 back to control values was never obtained in any of the cells studied. Holding potential -62 mV. D, superfusion with RB 2 on to cells displaying multi-component responses produced a similar prolongation of the initial transient inward current and fall in resting membrane conductance. With prolonged exposure to RB 2 all of the different component currents were substantially reduced and input resistance continued to decline. Holding potential -61 mV.

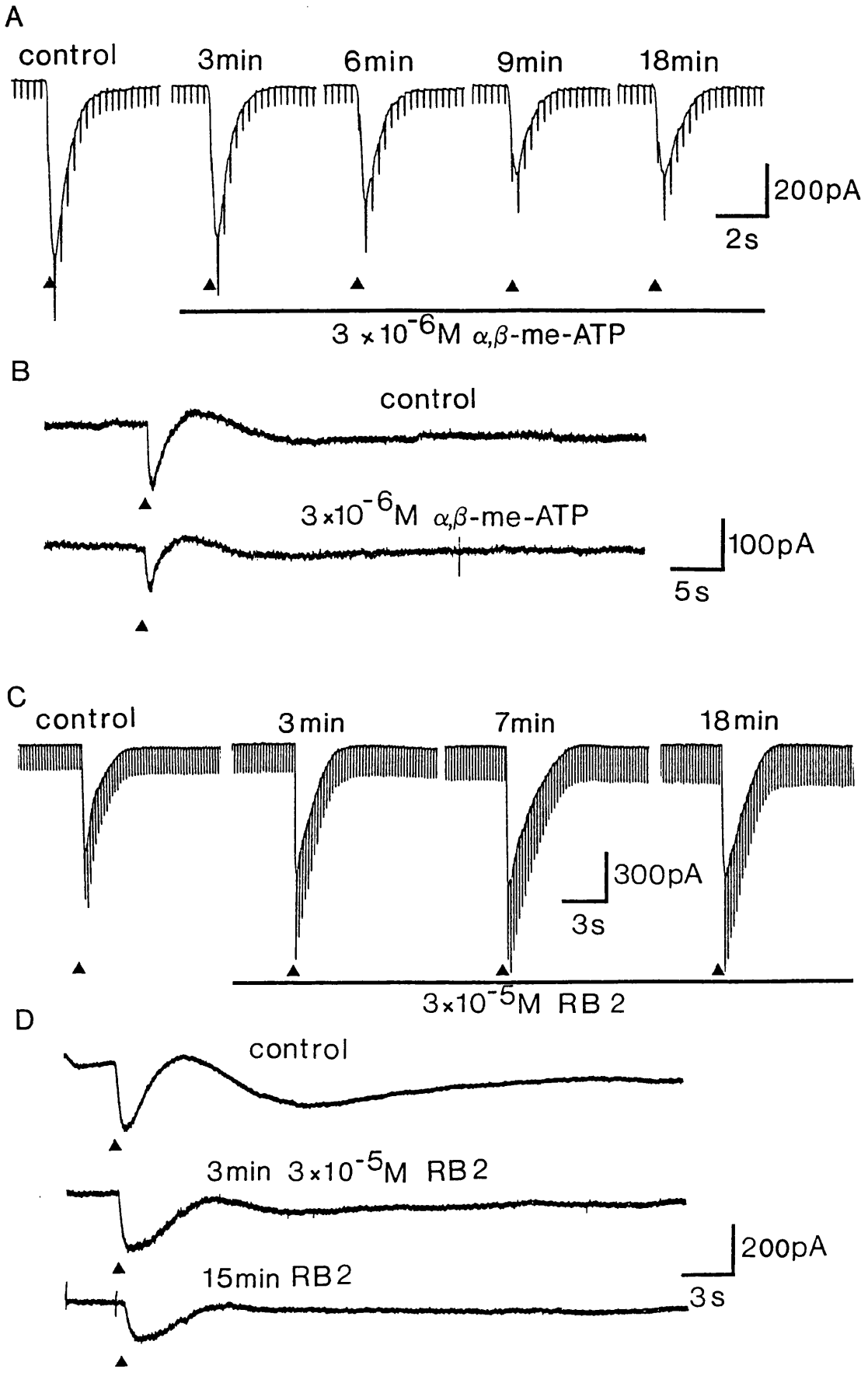
A
control
3min
6min
9min
18min
200pA
2s
3 ×10-6M α,β-me-ATP
B
control
3×10-6M α,β-me-ATP
100pA
5s
C
control
3min
7min
18min
300pA
3s
3×10-5M RB 2
D
control
3min 3×10-5M RB2
15min RB2
200pA
3s

Chapter 6

A VOLTAGE-CLAMP STUDY OF THE ELECTROPHYSIOLOGICAL CHARACTERISTICS OF THE INTRAMURAL NEURONES OF THE RAT TRACHEA

SUMMARY

1. The electrophysiological characteristics of intramural neurones from the paratracheal ganglia of 14-18 day old rats were studied in vitro using intracellular, single-electrode current- and voltage-clamp techniques.

2. Resting membrane potentials ranged between -50 and -73 mV. In 50-60% of all neurones, random and occasionally patterned bursts of spontaneous, fast synaptic potentials were observed. In all cases, superfusion with either hexamethonium (100 μM), or Ca^{2+}-free high magnesium-containing solutions abolished all synaptic activity.

3. Two distinct patterns of spike discharge were observed in response to prolonged intrasomal current injection. 65-75% of cells fired rhythmic, high-frequency (50-90 Hz) bursts of action potentials, with inter-burst intervals of between 300 and 500 ms, throughout the period of current stimulation. A further 10-15% of cells fired tonically at low frequencies (10-15 Hz) for the duration of the applied stimulus. In both cell types, trains of action potentials were followed by a pronounced calcium-dependent after-hyperpolarization which persisted for up to 3 s. The magnitude of the after-hyperpolarization following a single spike in tonic firing cells was considerably larger than in burst firing cells. Both the action potential and the after-hyperpolarization in all cells displayed a calcium-dependent, tetrodotoxin (TTX; 0.3 μM) -resistant component which was abolished by the removal of extracellular calcium.

4. The after-hyperpolarization resulted from activation of an outward calcium-dependent potassium current which reversed at -86.5 mV. This value was shifted by 63.6 mV for a 10-fold increase in extracellular potassium concentration.

5. All of the cells studied exhibited marked outward rectification when depolarized. This resulted from activation of a time- and voltage-dependent M-

current. The slow inward current relaxations associated with the M-current became faster at more negative potentials and reversed at around -85 mV. Raising the extracellular potassium concentration shifted the reversal potential for the current relaxations to more depolarized potentials in a manner predicted by the Nernst equation for a current carried by potassium ions. Both the outward current at depolarized potentials and the slow current relaxations were potently inhibited by extracellular $BaCl_2$ (1 mM) but were unaffected by CsCl (1-3 mM).

6. Inward rectification at hyperpolarized potentials was a characteristic of all cells. Membrane hyperpolarization revealed inward rectification in the "instantaneous" current-voltage (I/V) relationship at membrane potentials greater than -80 mV. In addition, cells also exhibited slow inward current relaxations (which did not show reversal at -85 mV) that became faster at hyperpolarized potentials, and resulted in inward rectification in the steady-state I/V relationship between -60 and -120 mV. The current underlying the observed relaxations showed voltage-dependent activation which became maximal at around -100 mV. The fast "instantaneously" rectifying current was potently inhibited by extracellular CsCl (1 mM) and $BaCl_2$ (1 mM). In contrast, the slowly developing inwardly relaxing current was potently inhibited by CsCl (1 mM), but was largely resistant to $BaCl_2$ (1 mM). In the presence of CsCl (1 mM) and $BaCl_2$ (1 mM), the input resistance of paratracheal neurones was greatly increased and the I/V relationship became almost linear between -45 and -120 mV.

7. The roles played by the different membrane currents in the control of excitability of paratracheal neurones and the possible role of intrinsic synapses between ganglion cells are discussed.

INTRODUCTION

The existence of an extensive network of nerve fibres and large numbers of small ganglia in the walls of the trachea was first described by Landois (1885). Although there have subsequently been many studies of the extrinsic innervation of the trachea (e.g. Elfman, 1943; Honjin, 1954, 1956; Fisher, 1964; Pack, Al-Ugaily & Widdicombe, 1984), little direct evidence has been gathered to determine the role played by the intramural tracheal ganglia. The ganglia are concentrated along the posterior wall of the trachea, opposite the intervals between the cartilage rings and make up part of an extensive plexus of nerve fibres. Branches from this network send fibres to the tracheal mucous glands, into the trachealis muscle, and also contribute to the fine plexuses accompanying the tracheal vessels (Larsell, 1922; Smith & Taylor, 1971).

Ultrastructural studies of ganglia from both the mouse and guinea-pig trachea have revealed that there are large differences in the sizes of tracheal neurones from the same animal, and it has been suggested that this may indicate the presence of more than one neuronal population (Baluk et al. 1985; Chiang & Gabella, 1986). In addition, direct visualisation of ferret and rat paratracheal ganglia, using acetylcholinesterase histochemistry, has revealed that there are also regional variations in the numbers and size of neurones making up these ganglia (Baker et al. 1986; Baluk & Gabella, 1989a).

Neural control of tracheobronchial function involves not only the classical cholinergic and adrenergic systems, but it also incorporates pathways which are neither adrenergic nor cholinergic (NANC; Coburn & Tomita, 1973; Coleman & Levy, 1974; Richardson & Bouchard, 1975; Richardson & Beland, 1976; Diamond &

O'Donnell, 1980). Evidence for the involvement of intramural neurones in NANC innervation have come from studies of the cat and guinea-pig trachea, where the NANC component of bronchodilation evoked by stimulation of the preganglionic vagal nerves is blocked by hexamethonium, but is unaffected by either adrenergic or muscarinic receptor blockade (Diamond & O'Donnell, 1980; Yip, Palombini & Coburn, 1981). A prime candidate for the mediation of part, if not all of the NANC response is vasoactive intestinal polypeptide, which has been localised in intrinsic tracheal ganglion cells (Uddman, Alumets, Densert, Håkanson & Sundler, 1978; Dey et al. 1981). Other peptides present within and around intrinsic ganglia have also been shown to alter a number of aspects of tracheal function (for review see Lundberg & Saria, 1987). In general, however, the mechanisms by which these actions are mediated remain largely unknown.

To date, there have been relatively few direct electrophysiological studies of the neurones from the intrinsic paratracheal ganglia. The majority of these have been carried out on ferret ganglia, where 30-40% of the neurones reside within two superficial ganglionated chains, which run along the posterior wall of the trachealis muscle. In the first intracellular studies of these neurones, two cell types were reported. One type, termed AH cells, displayed prolonged spike after-hyperpolarizations, whereas a second cell type, B cells, exhibited no somal spikes, but displayed slow inhibitory and excitatory post-synaptic potentials (EPSPs) in response to preganglionic stimulation (Cameron & Coburn, 1984). Subsequent studies of ferret ganglia in general concur with these early findings (Baker, 1986; Baker et al. 1986; Coburn & Kalia, 1986). However, Baker and his colleagues have reported an additional type of cell capable of firing damped trains of action potentials in response to prolonged intrasomal current injection (Baker et al. 1986). In an <u>in vivo</u> study of the cat, spike discharge in paratracheal neurones has been shown to

parallel activity in the phrenic nerve (Mitchell et al. 1987), with different populations of cells being distinguished by whether they fired with either an inspiratory or expiratory rhythm.

A preparation that permits the direct visualisation and recording from intact intramural paratracheal neurones present in the trachealis muscle of the rat has been developed as part of this thesis. In the present study, the firing characteristics and the currents responsible for the control of excitability in these cells have been investigated. The possible implications of these findings to our understanding of the role of the intrinsic ganglia in the control of airway function are discussed.

RESULTS

Recordings were made from more than 150 paratracheal neurones from Sprague-Dawley rat pups aged between 14 and 18 days. Resting membrane potentials recorded after an initial settling period were between -50 and -73 mV (mean= -57.1 ± 0.73 mV, n=68).

Spontaneous synaptic activity

A common feature seen in approximately 50-60% of all neurones studied was the presence of spontaneous fast synaptic potentials (see Fig. 6.1A). In general, these potentials were small, ranging in amplitude from 3 to 10 mV, but occasionally large potentials leading to spike discharge were also observed. The amount of spontaneous synaptic activity varied considerably from one cell to another and in general, appeared to be random in nature. However, a distinct pattern to the synaptic activity was occasionally seen, with a small burst of synaptic potentials being observed at regular intervals (see Fig. 6.1B). In all cases, perfusion with hexamethonium (100 μM) or 0 Ca^{2+}, 3.2 mM Mg^{2+}-containing solutions, abolished all spontaneous synaptic activity. Superfusion with TTX (0.3-1 μM) reduced, though never totally abolished, the observed spontaneous synaptic activity. However, TTX displayed a greater potency in inhibiting the larger synaptic potentials. This indicates that at least some of the observed synaptic activity may be due to action potential-induced, rather than purely spontaneous, release of acetylcholine from presynaptic nerve terminals.

Current firing characteristics

On the basis of their responses to intrasomal current injection, two patterns of neuronal firing were observed. These did not represent clearly distinct neuronal subpopulations, rather they were the two extreme types of behaviour observed in the present study. At one extreme, and the most frequently observed characteristic (65-75% of cells), was burst firing activity in response to prolonged intrasomal current injection. Typically, when stimulated at low current intensities (50-100 pA), these cells would only fire at the onset of current injection (see Fig. 6.2A). When the stimulating current was increased (100-300 pA), the cell would start to fire short, high-frequency bursts of action potentials for the period of stimulation (see Fig. 6.2B). Firing frequencies within these bursts were generally high (50-90 Hz) with an inter-burst interval of between 300 and 500 ms. Further increasing the stimulating current acted to prolong the duration of these bursts and also decreased the inter-burst interval (see Fig. 6.2C). At high current intensities (500-800 pA) the bursts would merge and the cell would fire tonically, at high frequencies, for the duration of current stimulation (see Fig. 6.2D). The long trains of action potentials generated in this way were invariably followed by a pronounced after-hyperpolarization, with an amplitude of between 10 and 20 mV, which persisted for up to 3 s (see Fig. 6.2D). In general, neurones exhibiting long spike after-hyperpolarizations required higher current intensities in order to induce tonic firing than cells with shorter after-hyperpolarizations.

The other type/extreme firing characteristic seen in paratracheal neurones, occurred in about 10-15% of the cells studied. These cells characteristically displayed longer spike after-hyperpolarizations than the burst firing cells (see later). In response to prolonged intrasomal current injection (50-100 pA), these cells again

only fired at the start of current injection (see Fig. 6.2E). However, slightly raising the current intensity evoked tonic firing that was of a low frequency (1-5 Hz) and was not preceded by burst firing behaviour (see Fig. 6.2F). Higher stimulating currents (500-1000 pA) increased firing rate to a maximum of between 10 and 15 Hz (see Fig. 6.2G & H). Following a period of prolonged firing in these cells, there was similar slow spike after-hyperpolarization. However, due to the much lower frequency of the preceding spike train, this was usually considerably shorter than that observed following periods of firing in cells displaying bursting characteristics (see Fig. 6.2H). Between these two extreme types of behaviour a number of cells responded with weak burst firing behaviour, had intermediate firing rates and slow spike after-hyperpolarization durations.

Sodium- and calcium-dependence of action potentials

The action potential and spike after-hyperpolarization of both burst and tonic firing paratracheal neurones exhibited strong TTX resistance. In the presence of TTX (0.3-1 μM) the action potential amplitude was reduced, revealing a smaller, slower rising, TTX-resistant spike (see Fig. 6.3A). The spike after-hyperpolarization was largely unaffected by TTX (see Fig. 6.3B).

Superfusion with a mixture of TTX and 0 Ca^{2+}-high Mg^{2+}-containing solutions reversibly abolished both the remaining action potential and also the subsequent spike after-hyperpolarization (see Fig. 6.3A & B).

Current-voltage relationships

All of the paratracheal neurones studied displayed a characteristic sigmoidal current-voltage relationship. This resulted from the presence of an outward M-current activated upon depolarization and of inward rectifier currents activated when the cell was hyperpolarized from resting potential.

M-current characteristics

In all paratracheal neurones, marked outward rectification in the steady-state current-voltage relationship was observed at membrane potentials less than -60 mV. This resulted from the progressive activation of an outward current with increased levels of depolarization. The current underlying this response was non-inactivating and displayed slow time- and voltage-dependent activation. This resulted in a sag in the voltage response to depolarizing current injection followed by an overshoot and slow relaxation back to resting potential at the end of current injection. In order to study this current in more detail, neurones were voltage-clamped at a depolarized membrane potential of between -25 and -30 mV. Under such conditions a significant number of M-channels were in an open state, resulting in a large outward current flow. From this holding potential, cells were then subjected to a series of hyperpolarizing commands of sufficient duration (0.5-1 s) and amplitude to allow the channels previously opened by depolarization to close (see Fig. 6.4). Note: ideally, steps to potential of at least -60 mV would have been used to more fully inhibit the M-conductance; however, in the cell shown in Fig. 6.4 this would have caused significant activation of the slow inward rectifier current (see later), therefore -55 mV was chosen as a compromise.

Two clearly separate components to the inward current were observed during the hyperpolarizing voltage steps. At the start of the voltage step, there was a near "instantaneous" current step due to current flow through both "leak" and open M-channels. This was then followed by a much slower inward current relaxation which resulted from a fall in steady outward current flowing through M-channels as they closed in response to membrane hyperpolarization.

Upon repolarization to -25 mV at the end of the voltage step, a similar sequence of "instantaneous" and slow **outward** currents was observed. However, the relative magnitudes of these two phases of current flow differed from those seen at the start of the step command. As a result of M-channel closure during the hyperpolarizing command, the "instantaneous" outward current seen at the end of the voltage step was smaller than the "instantaneous" inward current seen at the start. The recorded current now resulted almost exclusively from flow through leak channels only. The subsequent slow outward current relaxation was the result of re-opening of the M-channels previously closed by membrane hyperpolarization. The size of this slow outward relaxation was larger than the initial inward relaxation as a result of the difference in the electrochemical driving force on the M-current at -25 mV compared to that at -55 mV (reversal potential for the M-current was approximately -85 mV, see below).

The slow inward current relaxations initiated by hyperpolarizing steps were found to fit a single exponential (see Fig. 6.5A). In addition, the rate of relaxation increased markedly at more hyperpolarized potentials (see Fig. 6.5A). The mean time constant for the relaxations (from a holding potential of -30 mV) at -40, -50 and -60 mV calculated from four separate cells was 86.5 ± 4.3 ms, 67.2 ± 3.8 ms and 49.7 ± 2.8 ms respectively.

Ionic- and voltage-dependence of the M-current

The ionic basis and voltage-dependence of the M-current was investigated by examining the slow current relaxations evoked during hyperpolarizing command steps in the presence of 4.7 and 20 mM extracellular potassium-containing solutions. From a holding potential of between -25 and -30 mV, cells were subjected to a series of 500 ms duration hyperpolarizing command pulses of increasing amplitude (10 mV increments). As the cell was stepped to successively more hyperpolarized potentials, the slow inward current relaxation first decreased, then nulled, and at sufficiently hyperpolarized potentials reversed to become a slow outward current relaxation (see Fig. 6.6A). Reversal of the current relaxation was most clearly observed in neurones where there was little slow inward rectification or where inward rectification had been inhibited by extracellular caesium ions. In cells where this was not so, reversal could still be detected as a small outward relaxation at the start of the current response. In cells with little time-dependent inward rectification, plotting the "instantaneous" and steady-state current-voltage relationships allowed the reversal potential for the M-current relaxation to be estimated from the point of intersection of the two curves (see Fig. 6.6B). Under control conditions with an extracellular potassium concentration of 4.7 mM, the mean null/reversal potential measured in this way was -85.1 $\pm$ 0.69 mV (n=9). Raising extracellular potassium concentration to 20 mM shifted the reversal potential for the M-current relaxation to -44.7 $\pm$ 1.16 mV (n=5). This shift of approximately 40 mV in the equilibrium potential for the M-current agrees well with that predicted from the Nernst equation for a current carried exclusively by potassium ions.

Inhibition of the M-current

The effects of extracellular caesium and barium ions on the outward rectification and current relaxations which resulted from M-current activation were studied. As in the previous section, neurones were voltage-clamped at a depolarized potential between -25 and -30 mV in order to open a substantial proportion of the M-channels. The cells were subjected to a series of 0.5-1 s duration hyperpolarizing voltage commands of increasing amplitude (see Fig. 6.7A). From these experiments, steady-state current-voltage curves were constructed under control conditions and in the presence of caesium and barium ions. Figure 6.7 shows the results of a typical experiment performed on a burst firing paratracheal neurone. Under control conditions, the cell displayed a sigmoidal current-voltage relationship with strong inward and outward rectification characteristic of paratracheal neurones. In the presence of CsCl (1-3 mM), inward rectification at hyperpolarized potentials (> -65 mV) was greatly reduced (see below), whilst the outward rectification and current relaxations due to the M-current remained almost totally unaffected (see Fig. 6.7A & B). Subsequent addition of $BaCl_2$ (1 mM) either in the presence or absence of caesium, produced a large reduction in the steady outward current flow at -30 mV and reduced the amplitude, but not the time course, of the slow current relaxations associated with M-current (see Fig. 6.4 & 6.7A). Barium was also seen to reduce inward rectification (see later). Together, the presence of extracellular caesium and barium ions produced a marked increase in the input resistance of cells and linearized the current-voltage relationship between -45 and -120 mV (see Fig. 6.7B).

Inward rectifier current

Membrane hyperpolarization revealed marked inward rectification in all paratracheal neurones. In almost all cells, activation of this inward current occurred close to resting membrane potential between -55 and -70 mV. The exact potential at which inward rectification commenced was difficult to assess, as in most cases it overlapped with the activation range of the M-channels.

In order to examine the inward rectification under conditions where current flow through M-channels was minimal, cells were voltage-clamped at a potential of -60 mV. From this holding potential, they were then subjected to a series of negative voltage steps of sufficient duration (0.5-1 s) to facilitate activation of the inward rectifier current. Stepping membrane potential in this way elicited an "instantaneous" current flow, followed by a slow inward current relaxation during the first 300-800 ms (time constant of relaxation τ=80-160 ms). At the end of the voltage commands, repolarization to -60 mV elicited a similar "instantaneous" current flow and a slow outward tail current as the inward rectifier current declined (see Fig. 6.5B & 6.8A). The amplitude of the inward relaxation and the tail current increased as the command potential was made more negative (see Fig. 6.8A). The rate of current relaxation also increased with hyperpolarization: at -80 mV the mean time constant for the relaxation was 142.2 ± 4.7 ms (n=4), whilst at -90 and -100 mV this value was reduced to 126.7 ± 5.4 ms (n=4) and 87.2 ± 4.2 ms (n=4) respectively.

In some cells, where the slow inward current relaxation and tail currents were small (it was never observed to be totally absent), inward rectification was still observed, but did not become pronounced until considerably more hyperpolarized

potentials (> -80 mV).

By plotting the initial "instantaneous" (see methods) and final steady-state currents flowing during the individual voltage steps, "instantaneous" and steady-state current-voltage curves could be constructed (see Fig. 6.8B). From such curves it was apparent that the observed inward rectification consisted of two components. The first displayed near instantaneous activation, and resulted in inward rectification at potentials greater than -75 to -85 mV (see Fig. 6.8B). The second component showed much slower activation and produced rectification at all potentials from approximately -60 to -120 mV (see Fig. 6.8B). In the group of cells where the amplitude of the slow time-dependent inward rectifier current was small, inward rectification resulted almost exclusively from activation of the "instantaneous" rectifier current.

The level of activation of the slow inward rectifier was examined by plotting "instantaneous" minus steady-state current values as a function of membrane potential (see Fig. 6.8C). Activation of the slow inward rectifier current increased with membrane hyperpolarization from -60 mV, before reaching a peak at around -100 mV. With further hyperpolarization up to -120 mV, the amplitude of the inward current relaxation declined slightly, but was never observed to null or reverse (see Fig. 6.8A & C).

Inhibition of the inward rectifier by Cs^+ and Ba^{2+} ions

Extracellular caesium (1 mM) potently inhibited both the "instantaneous" and slow time- and voltage-dependent inward rectifier currents (see Fig. 6.9A). This produced a marked linearization of the "instantaneous" (see Fig. 6.9B) and steady-

state (see Fig. 6.9C) current-voltage relationships in all cells for potentials between -60 and -120 mV.

Superfusion with barium (1 mM) also reduced inward rectification. Like caesium, barium potently inhibited the fast inward rectifier current (see Fig. 6.10A) and linearized the "instantaneous" current-voltage relationship (see Fig. 6.10B). However, at concentrations up to 1 mM, barium only slightly reduced the slow time-dependent inward rectifier current (see Fig. 6.10A & C).

The spike after-hyperpolarization

The slow after-hyperpolarization following a single action potential in paratracheal neurones typically persisted for between 90 and 500 ms and ranged in amplitude between 5 and 15 mV. In general, the spike after-hyperpolarization in tonic firing neurones was more prolonged than that seen in the burst firing cells. Mean duration for burst firing cells was 114 ± 4.7 ms (n=42) whilst that for tonic firing cells was 315 ± 17.5 ms (n=19). In all cells, the amplitude and duration of the after-hyperpolarization increased markedly as the number and frequency of the preceding action potentials increased.

Voltage-dependence of the slow after-hyperpolarization

The attainable cycling frequencies (3-5 kHz) of the discontinuous single-electrode voltage-clamp used in the present study were insufficient to permit clamping of the currents activated during an action potential. Therefore, the outward current underlying the slow after-hyperpolarization was examined by using a "hybrid" voltage-clamp technique (see methods). Using this technique, the voltage-

and ionic-dependence of the outward current underlying the slow spike after-hyperpolarization (I_{AHP}) were investigated. I_{AHP} was activated by stimulating action potential discharge using a short train (200-300 ms) of brief intrasomal current pulses (10-15 ms/30-40 Hz). The amplitude of the I_{AHP} was found to be voltage-dependent and linearly related to the membrane potential at which it was elicited. With membrane hyperpolarization from rest, the outward current decreased and finally nulled at between -83 and -91 mV (mean -86.5 ± 0.8 mV, n=14). Further hyperpolarization reversed the current leading to inward current flow (see Fig. 6.11A).

Ionic-dependence of the slow after-hyperpolarization

The ionic-dependence of I_{AHP} was examined in two elevated potassium-containing solutions (12.5 and 20 mM; see Fig. 6.11A & B). The mean null/reversal potentials recorded in these solutions were -59.3 ± 1.11 mV (n=3) and -46.4 ± 1.15 mV (n=3) respectively. These values agree well with those predicted by the Nernst equation for a current carried exclusively by potassium ions, with the reversal potential shifted by 63.6 mV for a 10-fold increase in extracellular potassium concentration.

Calcium-dependence of the slow after-hyperpolarization

Removal of extracellular calcium abolished the after-hyperpolarization following both single or trains of action potentials. Superfusion with low (0.25 mM) calcium-containing solutions markedly reduced the magnitude and duration of the outward current underlying the after-hyperpolarization (see Fig. 6.12). The mean reduction in the duration of the outward current flow was 62 ± 5.15% (n=4) and the reduction in

peak current was 52.7 ± 4.64% (n=4).

Raising extracellular calcium produced an increase in I_{AHP}. In the presence of Ca^{2+} (5 mM) the mean increase in duration of I_{AHP} was 135 ± 6.1% (n=4), whilst the increase in peak current flow was 105.6 ± 0.92% (n=5).

DISCUSSION

The findings of the present study demonstrate that the parasympathetic intramural neurones of the rat trachea contain neurones which display a high degree of electrophysiological specialisation, and as such, may act as sites of integration and/or modulation of the input from extrinsic nerves. Furthermore, where the plexus of intrinsic ganglia remained largely intact, spontaneous synaptic activity was frequently observed. Spontaneous activity consisted largely of subthreshold, and occasionally suprathreshold, fast cholinergic potentials. It is likely that the majority of the small synaptic potentials arose as a result of spontaneous transmitter release from extrinsic nerve terminals. However, the presence of rhythmic bursts of TTX-sensitive synaptic potentials in a number of cells, under conditions where the extrinsic nerves had been separated from their cell bodies, suggests that at least a proportion of the synaptic activity was the result of intrinsic synaptic interactions between paratracheal neurones within these ganglia. Such synapses would permit a degree of local, as well as extrinsic, control of airway function; this type of activity has also been demonstrated in the enteric nervous system of the gut (see Costa & Furness, 1982).

The presence of high levels of subthreshold fast synaptic activity has also been observed in an in vivo study of cat paratracheal ganglia (Mitchell et al. 1987). In this report on cat ganglia, two cell types were distinguished which fired in a phasic/bursting manner, similar to the majority of rat paratracheal neurones in the present investigation. The bursts of firing in the two types of cat ganglion cells were synchronised with either inspiration or expiration. Generation of this discharge was attributed to synchronisation of the multiple subthreshold synaptic inputs from preganglionic nerves. In the present study, it was not possible to determine

whether rat paratracheal neurones fired with a similar respiratory rhythm. However, from the present study of the basic properties of these neurones, it would appear that the burst/phasic behaviour may be an inherent feature of these cells, which results from the complex underlying intrinsic membrane currents. Therefore, the intrinsic neurones may generate their own burst firing pattern which is activated or synchronised to inspiration or to expiration by either extrinsic nerves or through local reflex mechanisms.

In order to better understand the potential of these neurones to autoregulate their excitability, the mechanisms underlying the different membrane currents present in these cells were examined. All of the paratracheal neurones studied exhibited an M-current that resulted in outward rectification in the current-voltage relationship at depolarized potentials. This current was similar to the M-current first identified in large (B) cells of frog lumbar sympathetic ganglia (Brown & Adams, 1980) and subsequently in other sympathetic and central neurones (for review see Brown, 1988). The M-current in paratracheal neurones was a non-inactivating, time- and voltage-dependent potassium current, which, as in other cells, was potently inhibited by low concentrations of extracellular barium, but not caesium ions (Constanti, Adams & Brown, 1981; Adams, Brown & Constanti, 1982a, b). M-channel closure resulting in depolarization and a fall in membrane conductance has been found to underlie the cholinergic slow EPSP in a number of different cells (Adams & Brown, 1982; Brown & Selyanko, 1985b; Gähwiler & Brown, 1985b). At present, it is not known whether paratracheal neurones display slow EPSPs, however, in future studies it should be possible to focally stimulate the interganglionic nerve trunks in an attempt to elicit slow synaptic responses. Direct application of muscarinic agonists to determine the effects on the M-current were not carried out in the present investigation, primarily because of difficulties

encountered in immobilizing the underlying muscle. However, autoradiographic studies of rat paratracheal neurones in culture have localised muscarinic receptors on the vast majority of these cells (James, Bailey & Burnstock, 1990). Furthermore, in rabbit ganglia, M1 muscarinic receptors, which are thought to reside on intramural neurones, have been shown to modulate vagally induced bronchoconstriction (Bloom, Yamamura, Baumgartener & Halonen, 1987). It is possible, therefore, that inhibition of the M-current may result from activation of these receptors and lead to the generation of a slow EPSP in these cells. However, further work will be required to elucidate the role of these receptors.

In addition to its possible role in the generation of a slow EPSP, the M-current also exerts a powerful clamping action upon membrane potential by acting to oppose prolonged membrane depolarization. This, together with the presence in the majority of paratracheal neurones of an additional slow inward rectifier current which opposes membrane hyperpolarization, raises the possibility that these two currents may act in concert and be responsible for setting the resting membrane potential of these cells. In the present study, the activation points for the two currents were very similar and in some cells appeared to slightly overlap. Therefore, the membrane potential may be effectively squeezed into the narrow potential range where the effects of these two currents are minimal or cancel each other out. Indeed, the resting membrane potentials observed in the majority of rat paratracheal neurones were found to lie within this range (-55 to -65 mV). Small changes in the level of activation of either of these currents would, therefore, produce a sensitive mechanism for adjusting resting membrane potential and hence, the medium and long-term excitability of these cells with minimal expenditure of metabolic energy, since one current would be activating as the other was de-activating.

Both the "instantaneous" and slow inward rectifier currents in paratracheal neurones, like all other inward rectifiers studied so far, were potently inhibited by low concentrations of caesium ions. The "instantaneous" component of inward rectification in paratracheal neurones, unlike the slow component, was potently inhibited by both caesium and barium ions. It seems unlikely that this rectification resulted from current flow through slow inward rectifier channels open at rest, as the current only displays significant activation at potentials greater than -80 mV. The behaviour of the "instantaneous" component of rectification and its sensitivity to barium ions was similar to that of the classical anomalous rectifier currents seen in, for example, marine eggs and skeletal muscle (Hagiwara, Miyazaki, Moody & Patlak, 1978; Standen & Stanfield, 1978). The anomalous rectifier in these cells results from a specific increase in potassium conductance, with the magnitude of the current being dependent upon the difference between membrane and the potassium equilibrium potentials, the so-called $V-V_K$ relationship (Hagiwara, Miyazaki & Rosenthal, 1976). Although the potassium-dependence of the fast inward rectifier was not specifically studied in the present series of experiments, during superfusion with high potassium-containing solutions whilst investigating the M-current, a shift in the activation point of the fast inward rectifier current to considerably more depolarized potentials was observed, thus indicating a possible role for potassium in the generation of this response.

The slow inward rectifier current was clearly distinguishable from the "instantaneous" rectifier and also the anomalous rectifiers in striated muscle, marine eggs and mammalian olfactory cortical neurones (Hagiwara et al. 1976; Gay & Stanfield, 1977; Constanti & Galvan, 1983) in that it was largely insensitive to barium ions. This insensitivity to barium and also the finding that the current did not reverse near the potassium equilibrium potential, indicates that the slow inward

rectifier in paratracheal neurones may be similar to I_Q, I_h and I_h-I_f-I_{k2} (Brown & DiFrancesco, 1980; DiFrancesco & Ojeda, 1980; Halliwell & Adams, 1982; Mayer & Westbrook, 1983; Crepel & Penit-Soria, 1986). In the present study, the ionic nature of the inward rectifier current was not determined. However, it may be like I_Q and I_h, which are known to result from a change in potassium and sodium conductance, in contrast to the relatively specific potassium conductance which underlies inward rectification in marine eggs, muscle and olfactory cortical neurones (Hagiwara & Takahashi, 1974; Standen & Stanfield, 1980; Constanti & Galvan, 1983). The slow inward rectifier currents I_f and I_{k2} in atrial tissue and Purkinje fibres are thought to be involved in the pacemaker activity in cardiac tissue (Brown & DiFrancesco, 1980; DiFrancesco & Ojeda, 1980). This has led to the suggestion that the slow inward rectifier currents in guinea-pig hippocampal and cat motoneurones may in some way contribute to some form of pacemaker activity in these cells. If this were true for rat paratracheal neurones, then under certain conditions, this current may act to help regulate the interval between bursts of firing.

Another current which may act to regulate excitability in rat paratracheal neurones is the spike calcium-activated potassium current ($I_{K,Ca}$). This outward current, like that described in many other neurones (for example see Nishi & North, 1973; Fowler et al. 1985; Allen & Burnstock, 1987 and Chapter 3), was activated by calcium entry during the action potential and was responsible for the slow after-hyperpolarization seen in these cells. Similar slow after-hyperpolarizations have been described in neurones from ferret, rabbit and cat paratracheal ganglia (Cameron & Coburn, 1984; Fowler & Weinreich, 1986; Mitchell et al. 1987), but have only been demonstrated to be calcium-dependent in the ferret (Cameron & Coburn, 1982). The size and duration of the slow after-hyperpolarization following a single action potential was found to be significantly smaller in burst firing than in tonic firing

rat paratracheal neurones. However, even in the tonic firing cells, the magnitude of the slow after-hyperpolarization was considerably shorter than that observed in some of the highly refractory AH type cells found in, for example, mammalian enteric and intracardiac ganglia (Morita et al. 1982a; Allen & Burnstock, 1987 and Chapter 3). The after-hyperpolarization in rat paratracheal neurones increased dramatically following a train of action potentials. This was most marked in the burst firing cells and may act to terminate prolonged spike discharge and so determine the duration of each burst of firing. The inhibitory action of the larger after-hyperpolarization in non-bursting cells may prevent high rates of firing being initiated and thus account for their slow tonic firing behaviour. In addition to the outward $I_{K,Ca}$ seen in paratracheal neurones, a rapid transient outward current similar to the A current was also observed (Allen, unpublished observation; for review see Rogawski, 1985). This rapid outward current was generally more pronounced in tonic than in burst firing cells and would, like $I_{K,Ca}$, be expected to control the rate of firing in these cells.

In conclusion, the present study of the electrophysiological properties of rat paratracheal neurones shows that these cells have considerable intrinsic electrophysiological complexity. This may allow subtle modulation of the effects of extrinsic nervous input by paratracheal neurones, or may even permit some local control of aspects of airway function by local reflex mechanisms.

Fig. 6.1. Spontaneous synaptic potentials recorded from paratracheal neurones. A (upper panel), random spontaneous fast EPSPs in a tonic firing neurone. Synaptic activity was greatly reduced in the presence of TTX (330 nM; middle panel) and totally abolished in the presence of hexamethonium (100 μM; lower panel). Resting membrane potential -57 mV. B, another cell where the spontaneous synaptic activity consisted of small bursts of six fast synaptic potentials which repeated every 3-5 s. At resting membrane potential (-52 mV; i) the cell was only stimulated to fire in response to the largest of the synaptic potentials. When the cell was depolarized using intrasomal current injection, an increase in the frequency of discharge could be elicited (ii). Hyperpolarization of the cell away from spike threshold led to inhibition of spike discharge and an increase in the amplitudes of the synaptic potentials (iii). Note: action potentials were attenuated by the pen recorder.

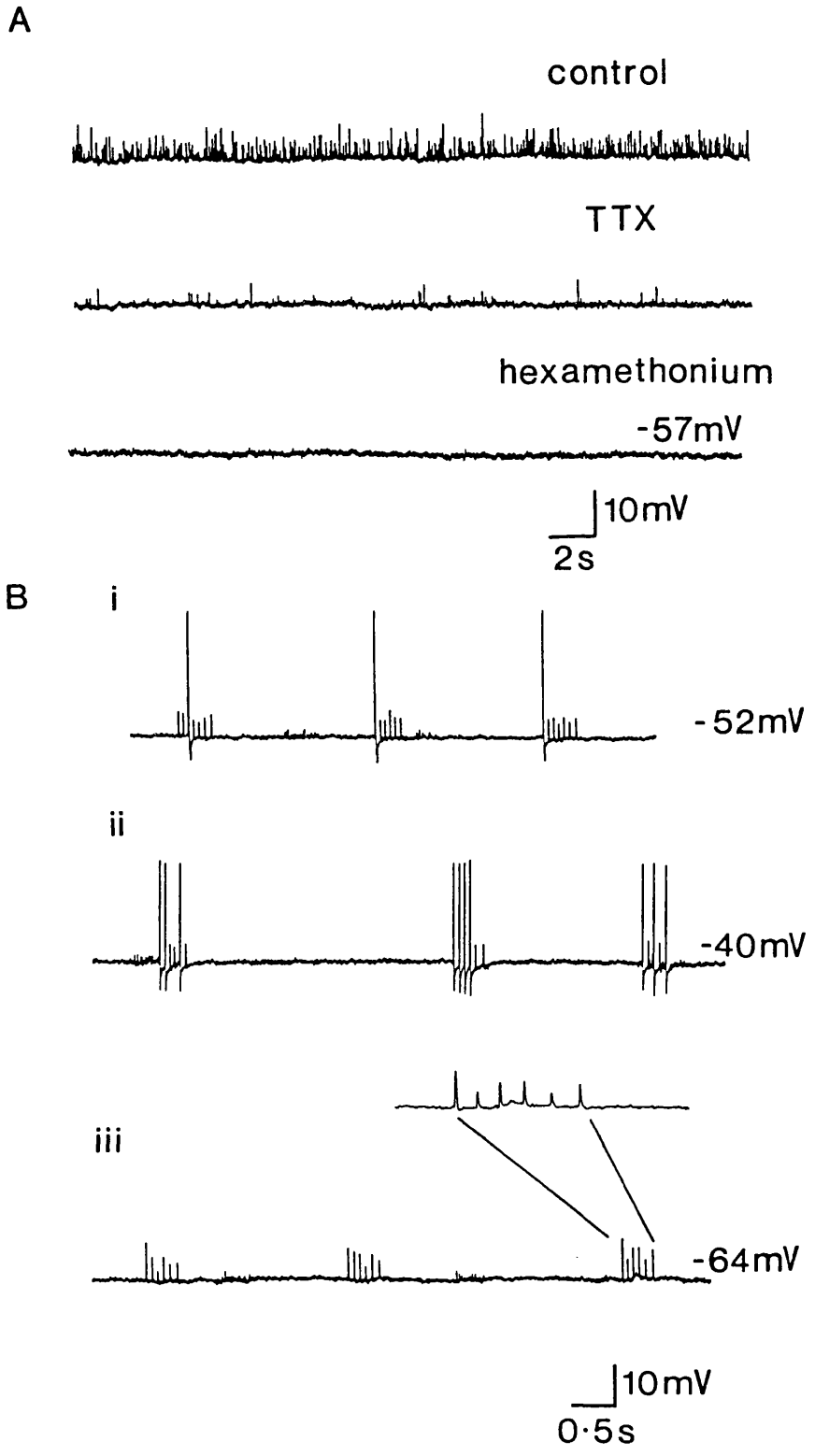
A
control
TTX
hexamethonium
-57mV
10mV
2s
B
i
-52mV
ii
-40mV
iii
-64mV
10mV
0·5s

Fig. 6.2. The firing characteristics of paratracheal neurones stimulated by prolonged intrasomal current injection of increasing intensities. The left hand column, A-D, were recorded from a burst firing neurone. A, stimulation with low current intensities (150 pA/5 s) only elicited firing at the onset of current injection. B, increasing the current intensity to 300 pA induced the cell to fire short high-frequency bursts of action potentials for the duration of current stimulation. C, further increasing the stimulating current to 500 pA increased the duration of these bursts and slightly decreased inter-burst interval. D, at high current intensities (800 pA) the bursts of firing fused and the cell started to fire tonically at high frequencies for the duration of the stimulus. Trains of action potentials generated in this way were invariably followed by a slow after-hyperpolarization which persisted for up to 3 s and ranged in amplitude between 10 and 20 mV. Records E-H were obtained under similar conditions from a non-burst firing cell. E, at low current intensities the cell again only fired at the start of the stimulus. Note the long spike after-hyperpolarization as compared to the cell in A. F, increasing the stimulus current induced low-frequency multiple firing. Further increases in stimulus intensity, records G and H, produced an increase in this discharge but never to the levels seen in the burst firing neurones.

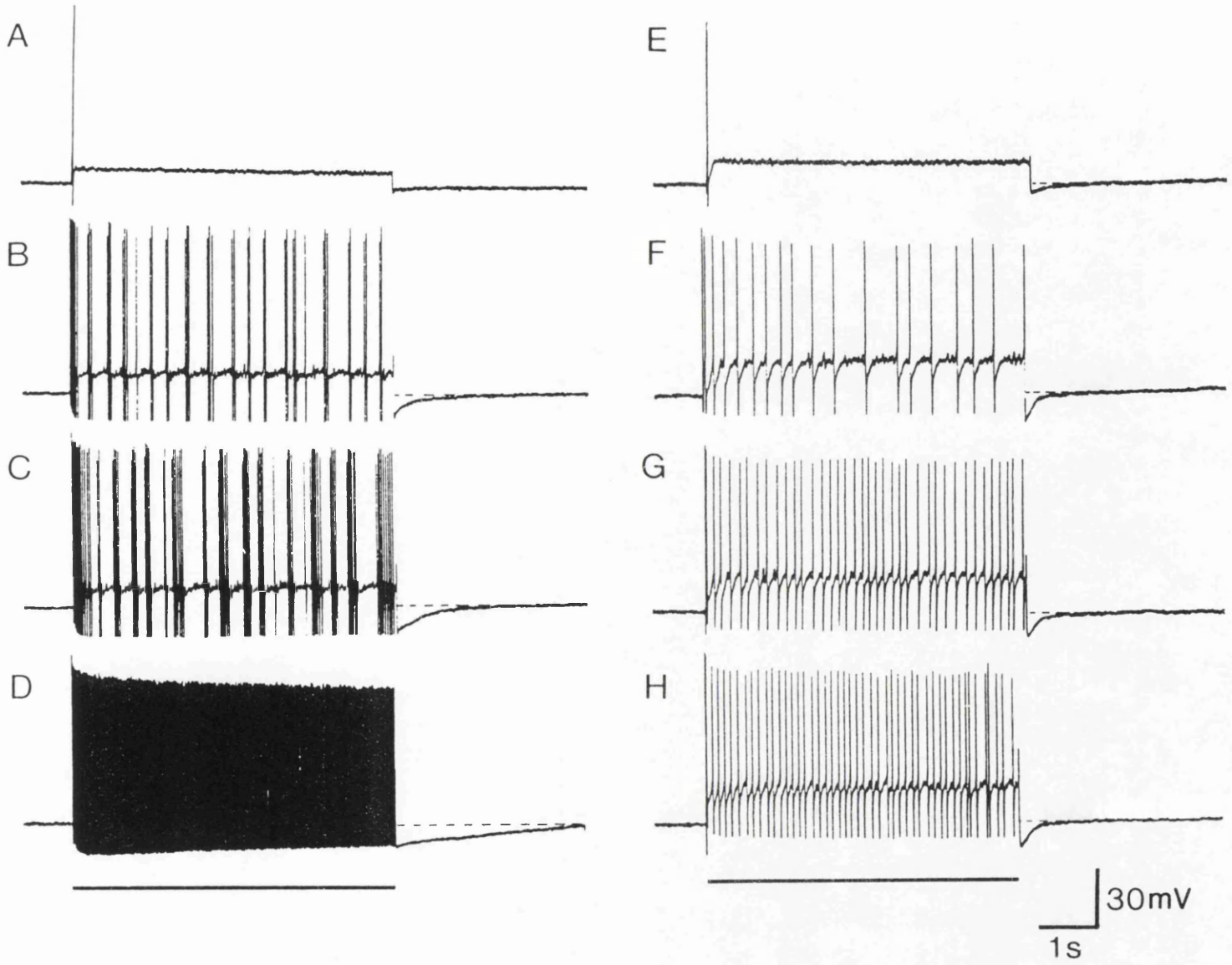
A
B
C
D
E
F
G
H
30mV
1s

Fig. 6.3. Sodium- and calcium-dependence of the action potential (column A) and spike after-hyperpolarization (column B) in paratracheal neurones. A (i) and B (i), control spike and after-hyperpolarization. In the presence of TTX (0.3-1 μM) the amplitude of the action potential was reduced but not abolished. By slightly raising the intensity of the stimulating current an improvement in the amplitude of the TTX-resistant spike could frequently be achieved (see A ii). Under these conditions the spike after-hyperpolarization was observed to be largely unaffected by TTX (see B ii). A (iii) and B (iii), superfusion with Ca^{2+}-free and 0.3-1 μM TTX-containing solutions abolished both the TTX-resistant action potential and the spike after-hyperpolarization. A (iv) and B (iv), wash.

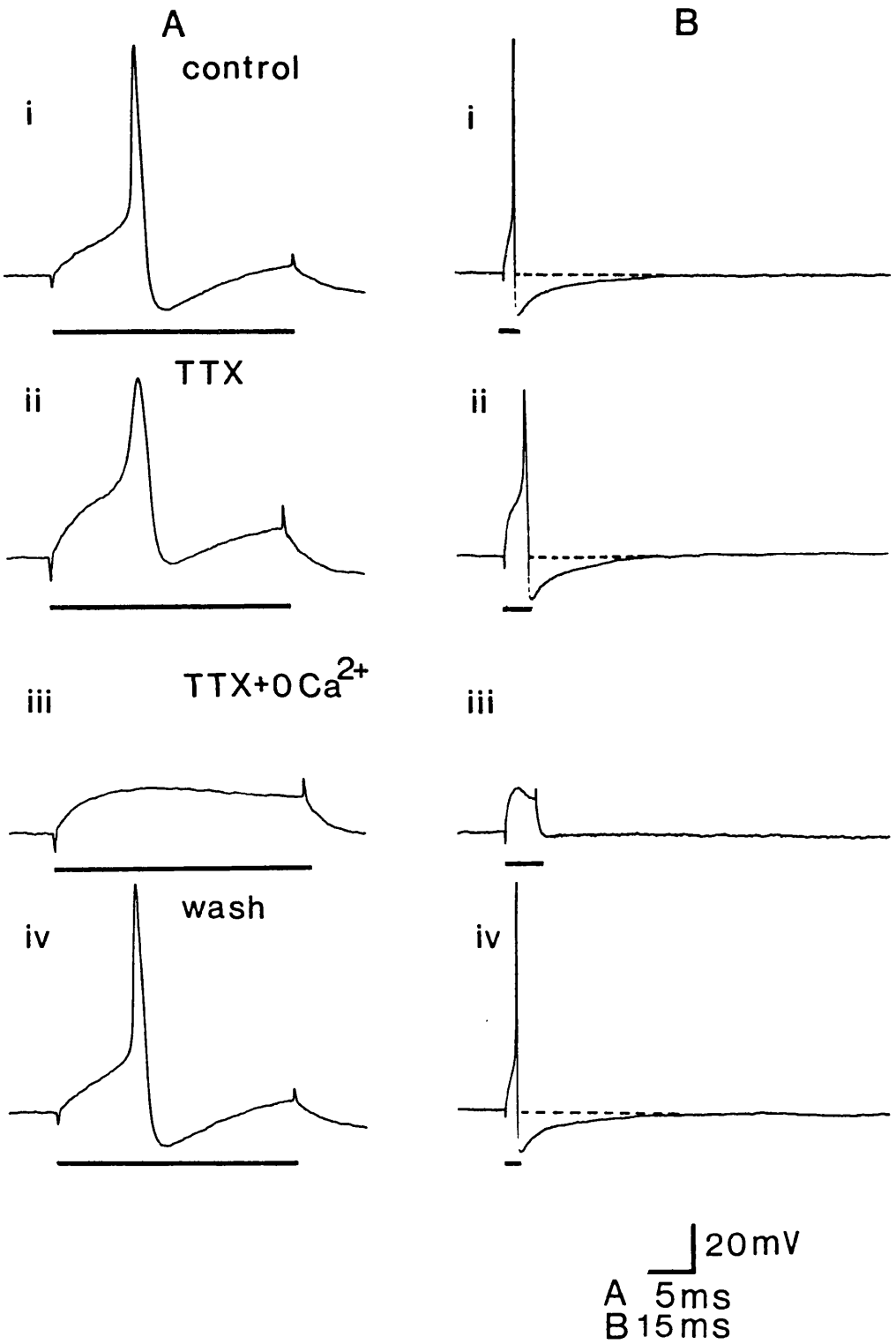
A
B
control
i
i
TTX
ii
ii
iii
TTX+0 Ca2+
iii
wash
iv
iv
20mV
A 5ms
B 15ms

Fig. 6.4. The M-current in a burst firing paratracheal neurone examined under voltage-clamp. From a holding potential of -25 mV a voltage step to -55 mV was imposed for 500 ms. This produced a near-instantaneous flow of current through both "leak" and M-channels open at -25 mV. This was followed by a slow inward current relaxation (1) as the M-channels closed in response to membrane hyperpolarization. At the end of the command step, a similar pattern of "instantaneous" and slow current relaxations was observed. The "instantaneous" current step was smaller due to an increase in input resistance following M-channel closure. The subsequent outward relaxation (2), which resulted from the re-opening of M-channels at -25 mV, was larger than the initial inward relaxation at -55 mV, due to a larger electrochemical gradient (equilibrium potential for current flow through M-channels was approximately -85 mV). Superfusion with $BaCl_2$ (1 mM) produced marked inhibition of the M-current. This was seen as a large reduction in the outward current flowing at -25 mV and also a reduction in the amplitude of the slow inward and outward current relaxations.

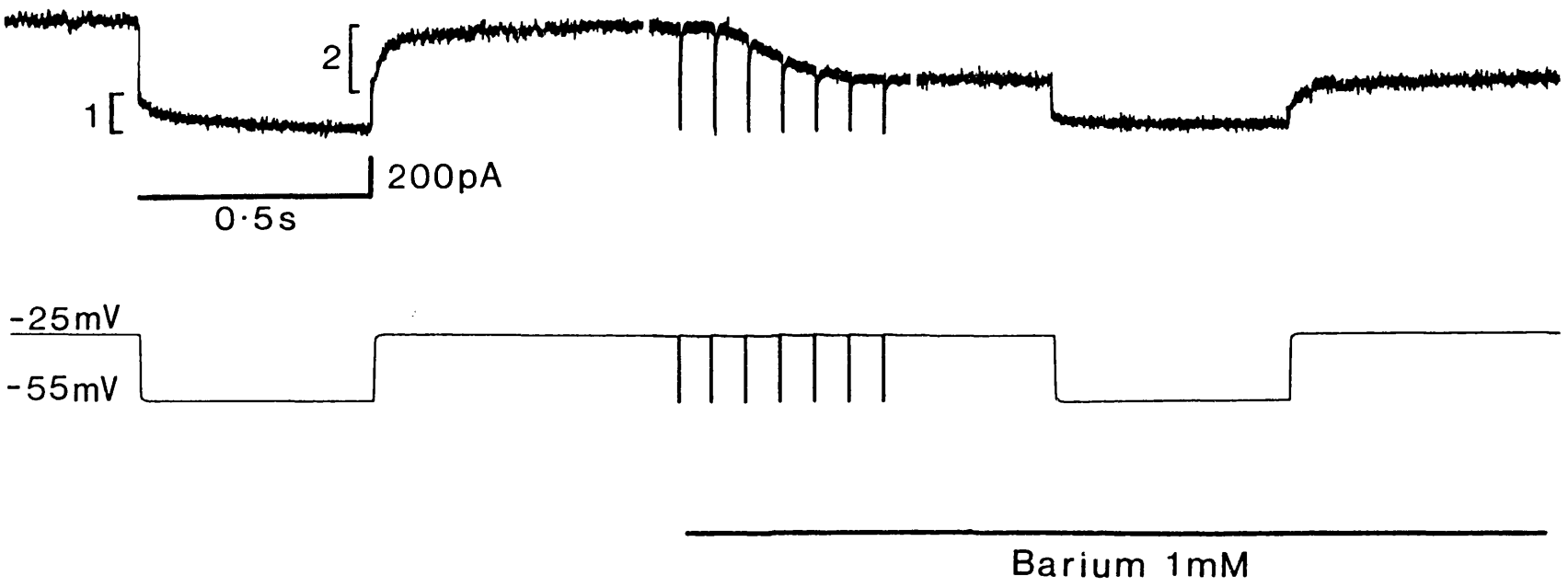
2
1
200pA
0·5s
-25mV
-55mV
Barium 1mM

Fig. 6.5. Kinetics of the current relaxations underlying A, the M-current and B, the slow inward rectifier. Graphs are semi-log plots of current relaxations against time. Lines are least squares fit to data from traces on left of figure. The zero time intercept (Io) was calculated as the difference between the "instantaneous" and steady-state current values. The different values of Io were used to normalise data in each case, relaxation currents being plotted as, $\log_{10}$ % of Io vs time.
A, traces on left show slow inward M-current relaxations initiated by stepping the cell from a holding potential of -30 mV to -40 and -60 mV respectively. M-current relaxations were best fitted by a single exponential (correlation coefficient r=0.998 at -40 mV and 0.990 at -60 mV), with relaxation time constants of 86 ms at -40 mV and 51 ms at -60 mV. B, traces show inward current relaxations initiated by hyperpolarization to -80 and -100 mV from a holding potential of -60 mV. Current relaxations were best fitted by a single exponential with correlation coefficients of 0.978 and 0.994 at -80 and -100 mV respectively. Time constants for the current relaxations were 146 ms at -80 mV and 94.5 ms at -100 mV.

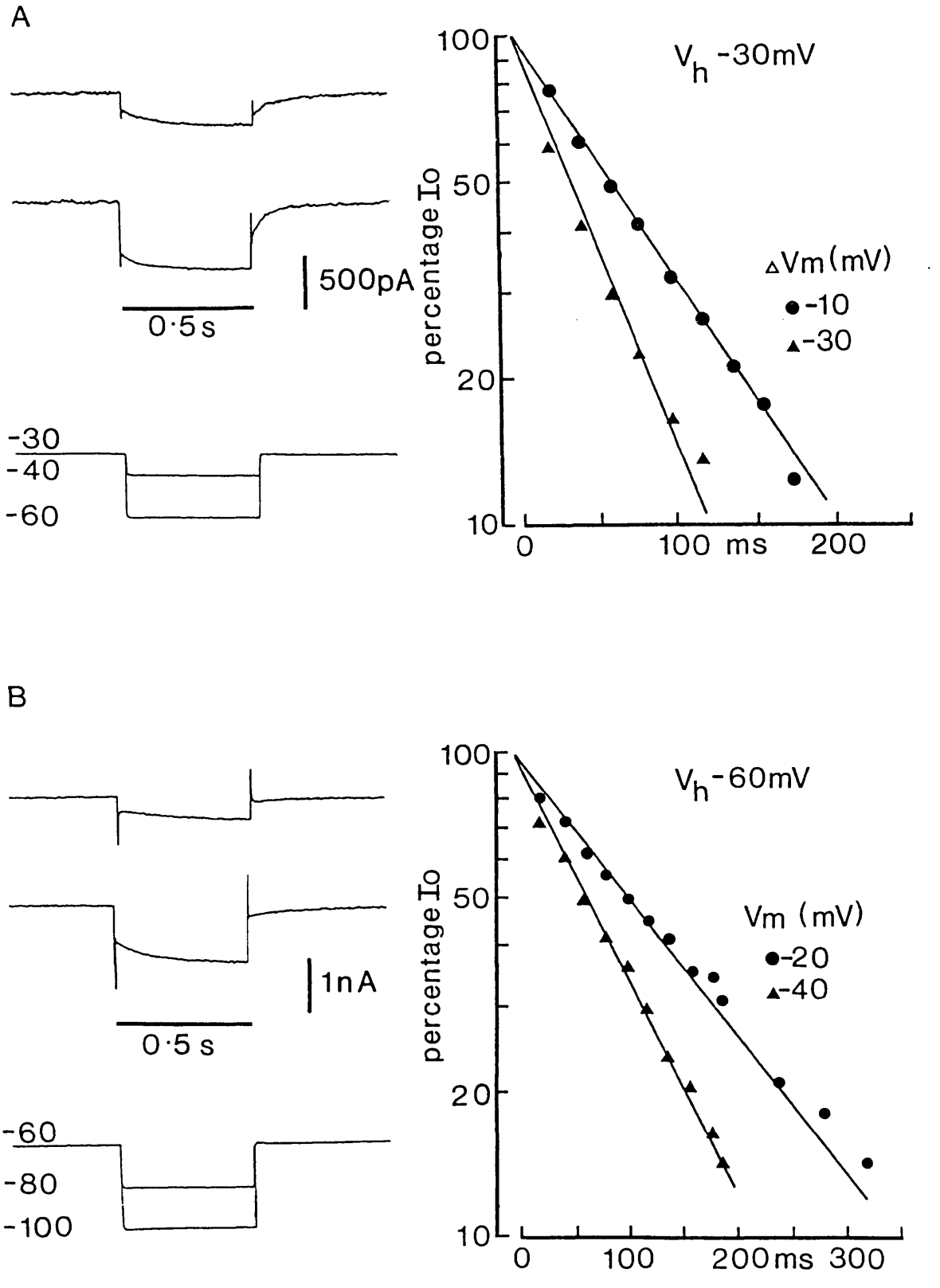
A
500pA
0·5 s
-30
-40
-60
100
50
20
10
percentage Io
V_h -30mV
ΔVm(mV)
-10
-30
0
100 ms
200
B
1nA
0·5 s
-60
-80
-100
100
50
20
10
percentage Io
V_h -60mV
Vm (mV)
-20
-40
0
100
200ms
300

Fig. 6.6. The ionic- and voltage-dependence of the M-current in a burst firing paratracheal neurone. A, M-current relaxations in 4.7 and 20 mM potassium-containing solutions. (i), the cell was voltage-clamped at -30 mV under control conditions (4.7 mM K^+) and then subjected to a series of 500 ms duration negative command pulses of increasing amplitude. With increasing hyperpolarization the slow inward current relaxation associated with M-channel closure first decreased, then nulled and finally reversed to become a slow outward relaxation at strongly hyperpolarized potentials. (ii), in 20 mM potassium (holding potential -25 mV) the reversal potential for the slow inward current relaxation was shifted to more depolarized potentials. B, by plotting the "instantaneous" (circles) and the steady-state currents (triangles) induced during the hyperpolarizing command steps for the cell shown in A, the equilibrium/reversal potential for the M-current could be determined. In 4.7 mM potassium the null potential was -84 mV, whilst in 20 mM potassium this value was shifted to -46 mV. The shift of 38 mV in the equilibrium potential agrees well with that predicted by the Nernst equation for a response generated exclusively by a flow of potassium ions (predicted shift at 37^{o}C equals -38.4 mV).

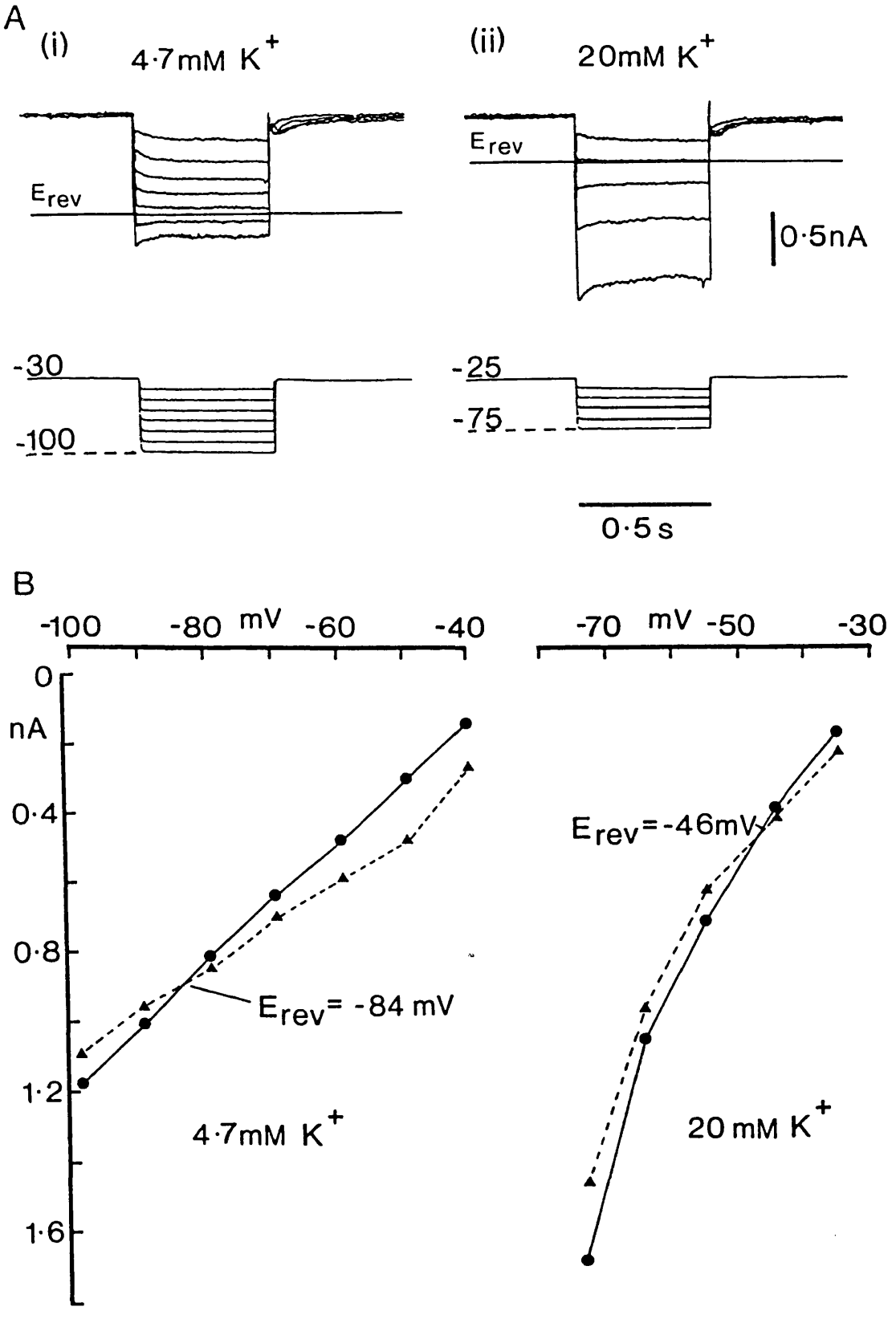
A
(i)
4·7mM K+
(ii)
20mM K+
Erev
Erev
0·5nA
-30
-100
-25
-75
0·5 s
B
-100
-80
mV
-60
-40
-70
mV
-50
-30
0
nA
0·4
0·8
1·2
1·6
Erev= -84 mV
4·7mM K+
Erev=-46mV
20 mM K+

Fig. 6.7. The inhibitory actions of Cs^+ and Ba^{2+} ions on the M-current in a paratracheal neurone. A, from a holding potential of -30 mV the cell was subjected to a series of 500 ms duration negative command pulses of increasing amplitude. With increasing hyperpolarization, the slow inward current relaxation associated with M-channel closure decreased, then reversed to become a slow outward relaxation. The null/reversal point for the M-current was approximately -85 mV. Superfusion with CsCl (2 mM) inhibited the inward rectifier current but had no effect upon the M-current. Superfusion with CsCl (2 mM) and $BaCl_2$ (1 mM) produced an inhibition of the M-current and a further decrease in inward rectification. B, the current-voltage (I/V) relationships for the cell shown in A. Under control conditions the cell displayed a characteristic sigmoidal steady-state I/V curve due to the presence of both outward and inwardly rectifying currents. In the presence of CsCl (2 mM) inward rectification in the I/V relationship at hyperpolarized potentials (>-60 mV) was reduced, but there was no observable reduction in the M-current. In the presence of both CsCl (2 mM) and $BaCl_2$ (1 mM) the M-current was inhibited and there was also a further reduction in inward rectification. This resulted in an increase in the input resistance of the cell and an almost linear I/V relationship between -45 and -120 mV.

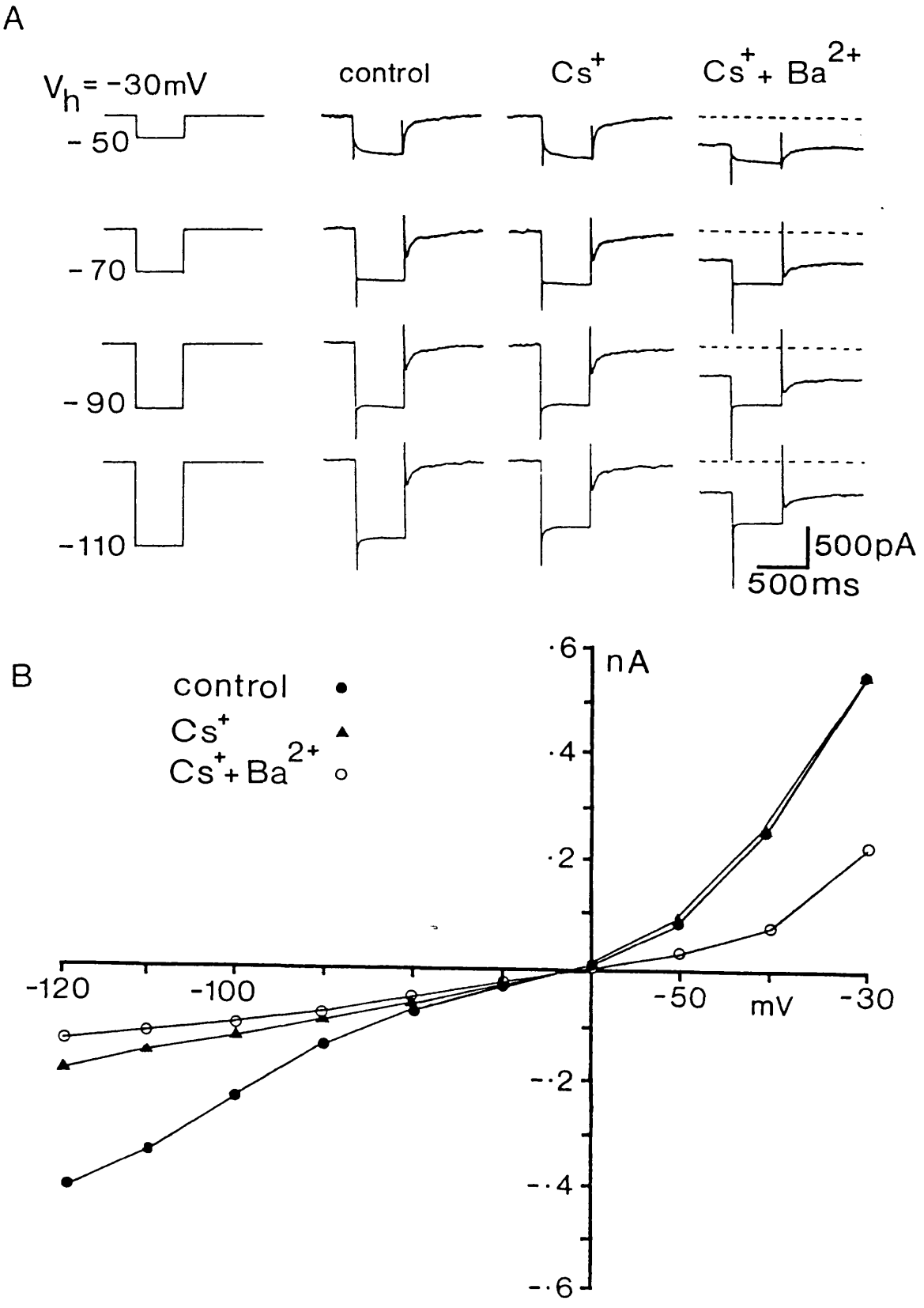
A
V_h = -30mV
control
Cs^+
$Cs^+ + Ba^{2+}$
-50
-70
-90
-110
500pA
500ms
B
control
Cs^+
$Cs^+ + Ba^{2+}$
·6
nA
·4
·2
-120
-100
-50
mV
-30
-·2
-·4
-·6

Fig. 6.8. Inward rectification in a typical paratracheal neurone. A, from a holding potential of -60 mV, negative voltage steps (10 mV increments) revealed inward rectification and a slow inward current relaxation in membrane current. At the end of the voltage steps the initial "instantaneous" current flow was followed by a slow outward current relaxation as the inward rectifier current inactivated.
B, the "instantaneous" (triangles) and steady-state (filled circles) current-voltage relationships for the cell shown in A. From these curves it was evident that the observed inward rectification consisted of two components. Examination of the "instantaneous" current-voltage relationship revealed the presence of an inwardly rectifying current activated at potentials greater than -80 mV. The steady-state current-voltage relationship on the other hand shows voltage-dependent inward rectification from all potentials negative to the holding potential (-60 mV). At potentials less than -80 mV the rectification resulted almost exclusively from activation of the slow time-dependent inward rectifier current which manifested itself as an inward relaxation in the current records shown in A. C, activation of the slow inward rectifier current. Current flow resulting from activation of the slow inward rectifier (steady-state minus "instantaneous" currents) represented as a fraction of peak current were plotted as a function of membrane potential. Values in each case are means ± S.E. of the mean for between 11 and 15 observations. From the curve it can be seen that peak activation of the slow inward rectifier current occurred around -100 mV then declined slightly with further hyperpolarization.

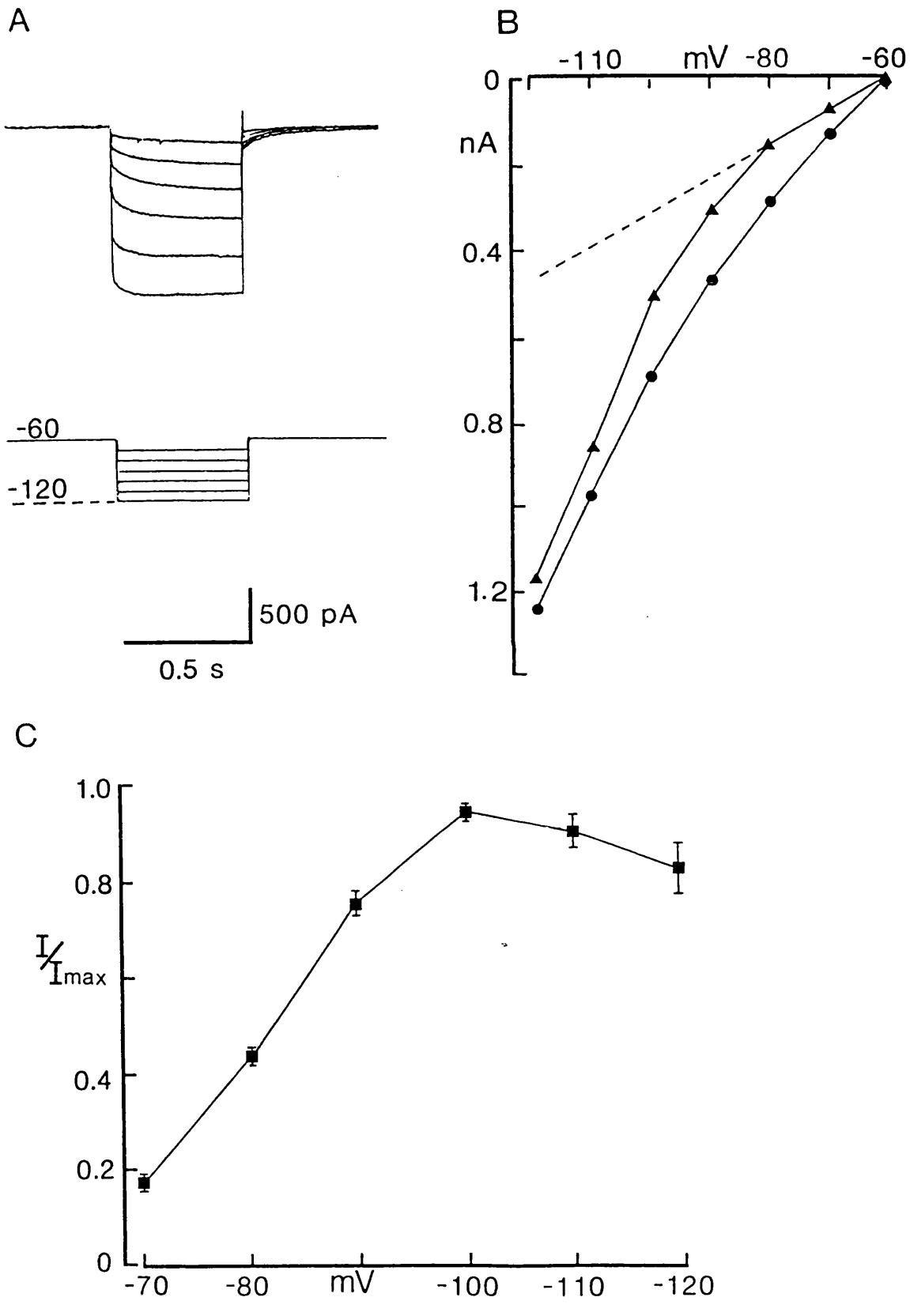
A
-60
-120
500 pA
0.5 s
B
-110
mV
-80
-60
0
nA
0.4
0.8
1.2
C
1.0
0.8
I/Imax
0.4
0.2
0
-70
-80
mV
-100
-110
-120

Fig. 6.9. The inhibitory actions of extracellular caesium upon the "instantaneous" and slow time-dependent inward rectifier currents in a paratracheal neurone. A, membrane currents recorded in response to negative voltage steps from a holding potential of -60 mV. In the presence of Cs^+ (1 mM) both the "instantaneous" current and slow inward rectifier current relaxation were strongly inhibited.
B, The "instantaneous" current-voltage relationship for the cell shown in A. In the presence of Cs^+ (1 mM) activation of the "instantaneous" inward rectifier between -75 and -80 mV was largely inhibited. C, The steady-state current-voltage relationship from the same cell. In this case caesium can be seen to reduce inward rectification at all potentials negative to the holding potential (-60 mV).

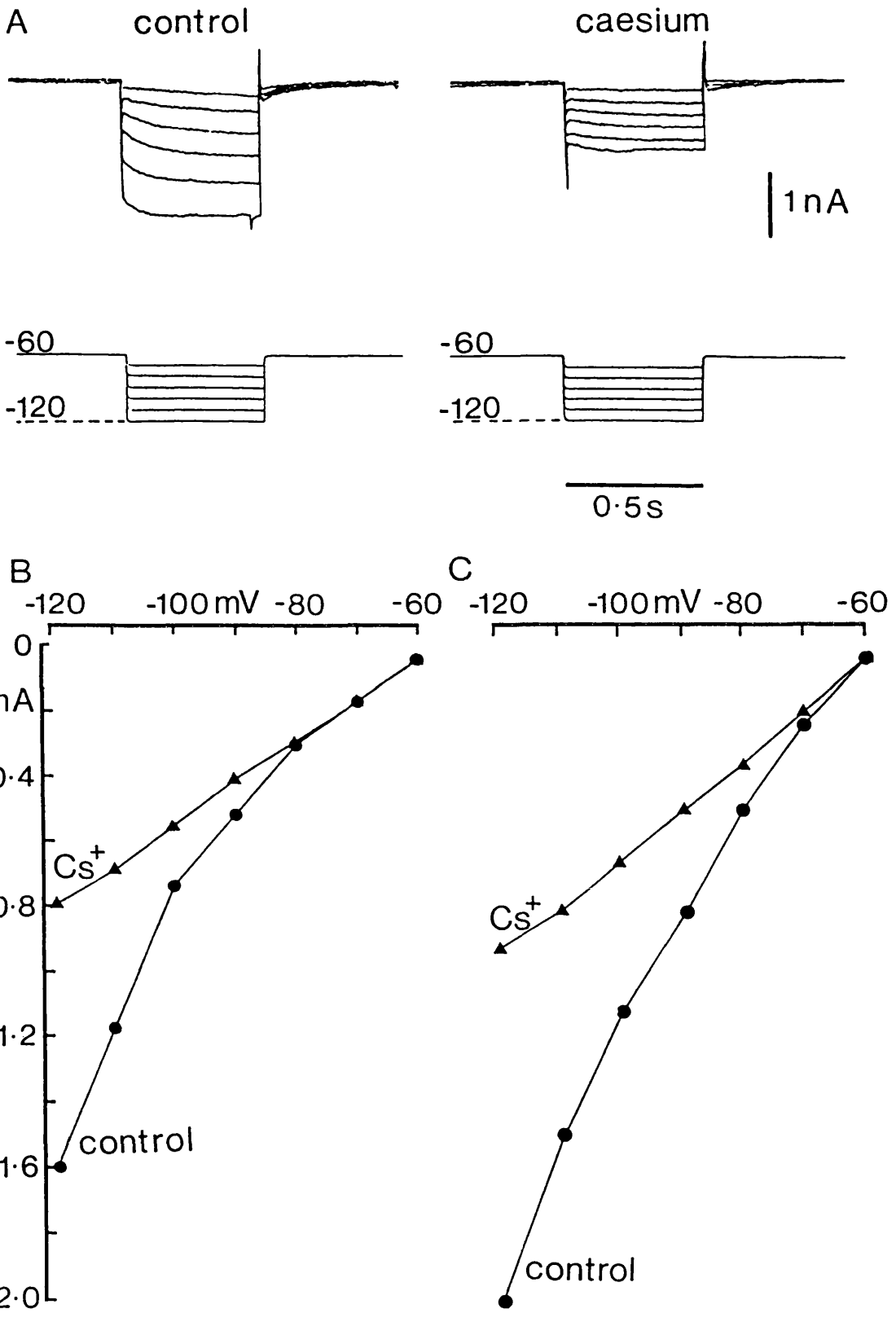
A
control
caesium
1nA
-60
-120
-60
-120
0·5s
B
-120
-100mV
-80
-60
0
nA
0·4
0·8
1·2
1·6
2·0
Cs+
control
C
-120
-100mV
-80
-60
Cs+
control

Fig. 6.10. The inhibitory actions of barium ions upon the instantaneous and slow time-dependent inward rectifier currents in the same cell as shown in Fig 6.8. A, membrane current in response to membrane hyperpolarization from -60 mV. In the presence of barium (1 mM) the "instantaneous" current flow at the start of each voltage step was strongly inhibited. In contrast however, the slow time-dependent inward rectifier current, though reduced, was less sensitive to inhibition by barium. B, The "instantaneous" current-voltage relationship for the cell shown in A. In the presence of barium (1 mM), inward rectification was strongly inhibited in a similar way to that observed in the presence of caesium (see Fig. 6.8B). Note: the slight increase in the steady inward current at rest most probably resulted from inhibition of either the M-current or the slow inward rectifier current activated at -60 mV. C, in the presence of barium (1 mM), inward rectification in the steady-state current-voltage relationship was reduced, but not to the same degree as seen in the presence of caesium (see Fig. 6.8C).

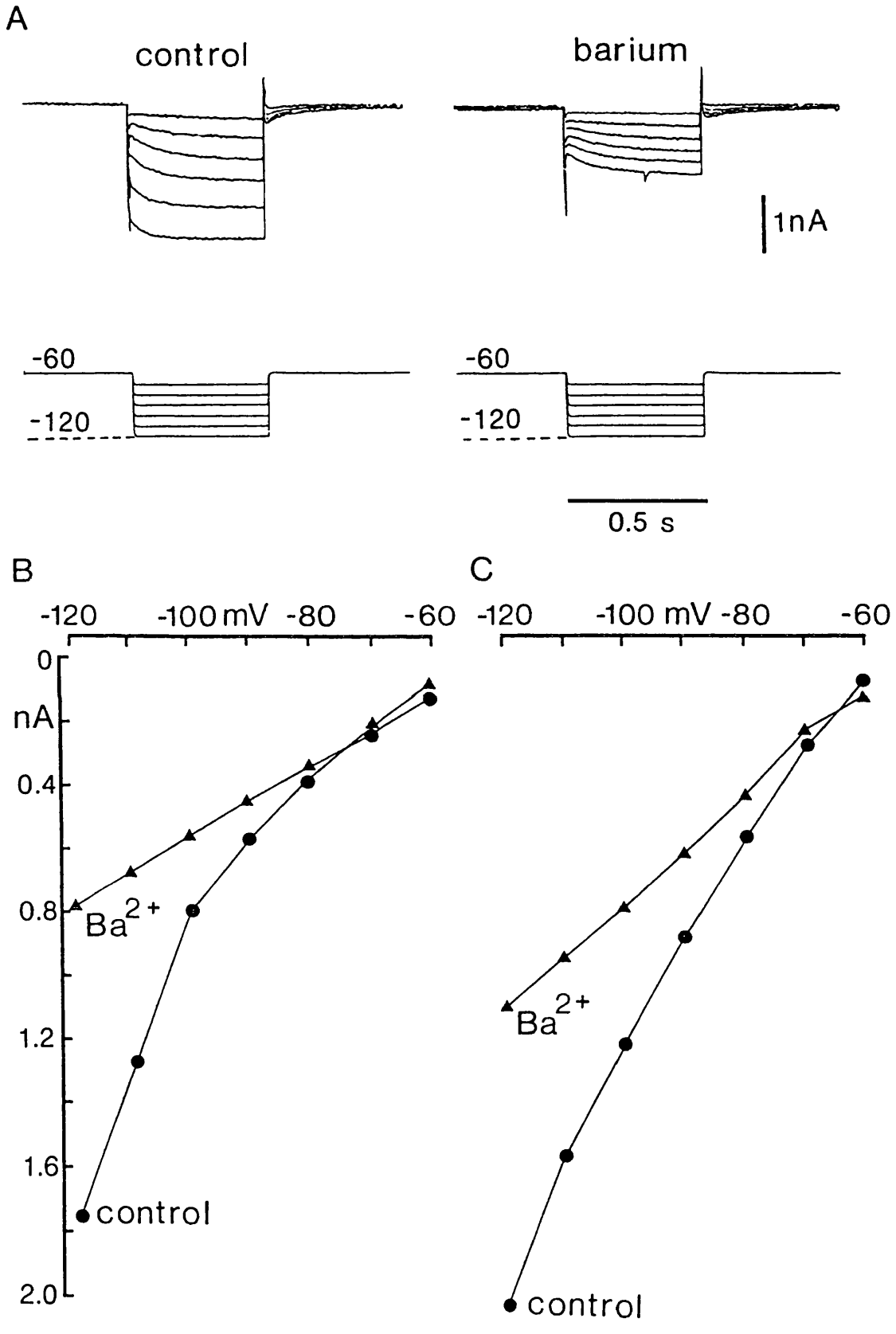
A
control
barium
1nA
-60
-120
-60
-120
0.5 s
B
-120
-100 mV
-80
-60
0
nA
0.4
0.8
1.2
1.6
2.0
Ba2+
control
C
-120
-100 mV
-80
-60
Ba2+
control

Fig. 6.11. The ionic- and voltage-dependence of the current underlying the slow spike after-hyperpolarization (I_{AHP}) in a tonic firing paratracheal neurone. A, recordings were made using a "hybrid" voltage-clamp technique (see methods). From a given holding potential the recording amplifier was switched from voltage-clamp into standard "current-clamp" recording mode and a train of action potentials was evoked by passing a series of intrasomal current pulses (10 ms/40 Hz) of sufficient intensity to elicit firing. At the end of the train of spikes the amplifier was then switched back to voltage-clamp mode to permit recording of the evoked current. Under control conditions (4.7 mM K^+) the amplitude of I_{AHP} was found to be linearly related to membrane potential and had a reversal potential of -85.5 mV (see B). In elevated potassium-containing solutions (12.5 and 20 mM) I_{AHP} was slightly prolonged and the reversal potential was shifted to more depolarized levels. B, the voltage-dependence of I_{AHP} for the cell shown in A was plotted for each different potassium-containing solution. In order to reduce the errors in measuring, the current measurements were made 100 ms after the train of action potentials. In all cases the amplitude of I_{AHP} was linearly related to the membrane potential at which it was elicited. In 4.7, 12.5 and 20 mM K^+-containing solutions, least squares fit of the raw data produced the regression coefficients of 0.996, 0.997 and 0.998 at reversal potentials of -85.5, -59.5 and -50.5 mV respectively. The values for the reversal potential show reasonable agreement with the values predicted by the Nernst equation for a current carried exclusively by potassium ions.

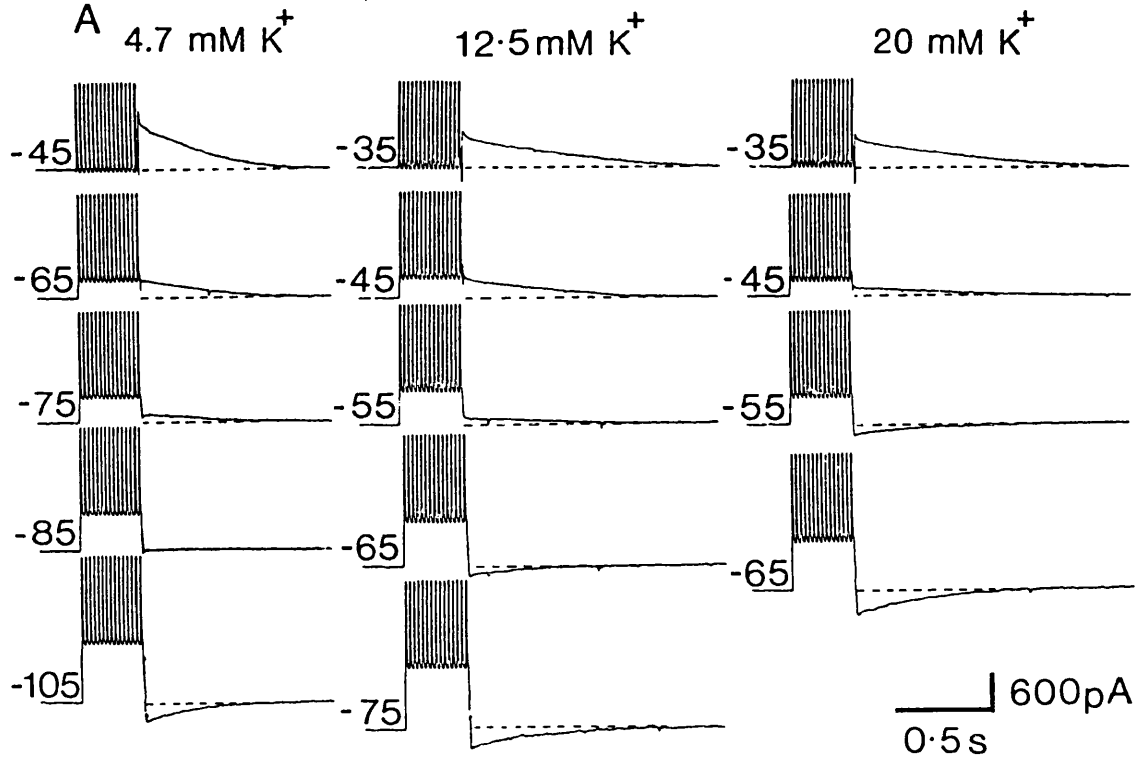
A
4.7 mM K+
12·5 mM K+
20 mM K+
-45
-35
-35
-65
-45
-45
-75
-55
-55
-85
-65
-65
-105
-75
600pA
0·5 s

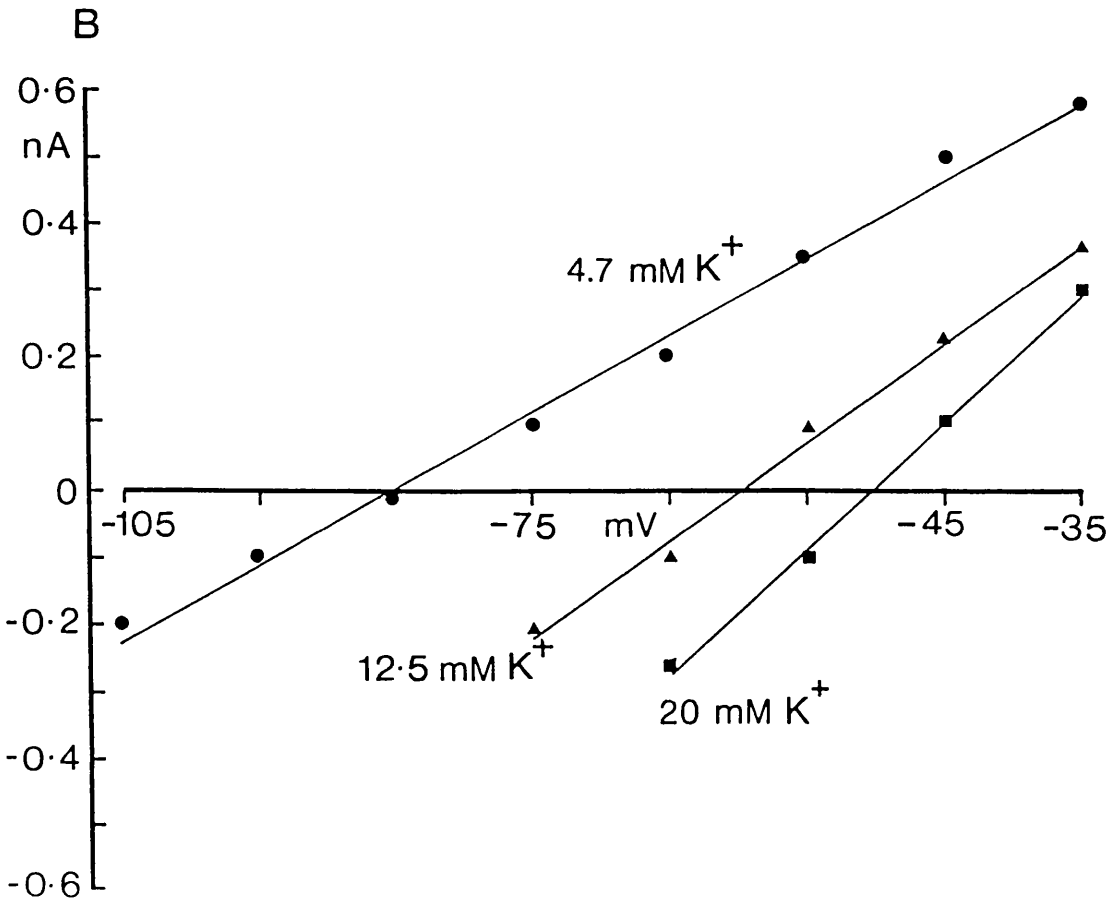
B
0·6
nA
0·4
0·2
0
-0·2
-0·4
-0·6
-105
-75
mV
-45
-35
4.7 mM K+
12·5 mM K+
20 mM K+

Fig. 6.12. Calcium-dependence of the current underlying the slow spike after-hyperpolarization (I_{AHP}) in a tonic firing paratracheal neurone. A, recordings were made using a "hybrid" voltage-clamp technique (see methods). From voltage-clamp recording at a holding potential of -53 mV the recording amplifier was briefly switched to standard "current-clamp" mode and a train of action potentials were generated by passing brief (10 ms/40 Hz) intrasomal current pulses. At the end of the train the amplifier was returned to voltage-clamp mode. B, in the presence of elevated calcium (5 mM) -containing solutions the duration of the current underlying the slow after-hyperpolarization was prolonged, whereas the amplitude of the current was almost unaffected. C, in low calcium (0.25 mM), elevated magnesium (3.45 mM) -containing solutions, both the amplitude and the duration of the I_{AHP} were greatly reduced. D, washout to control conditions. Lower trace shows the evoked train of action potentials recorded in "current-clamp" mode.

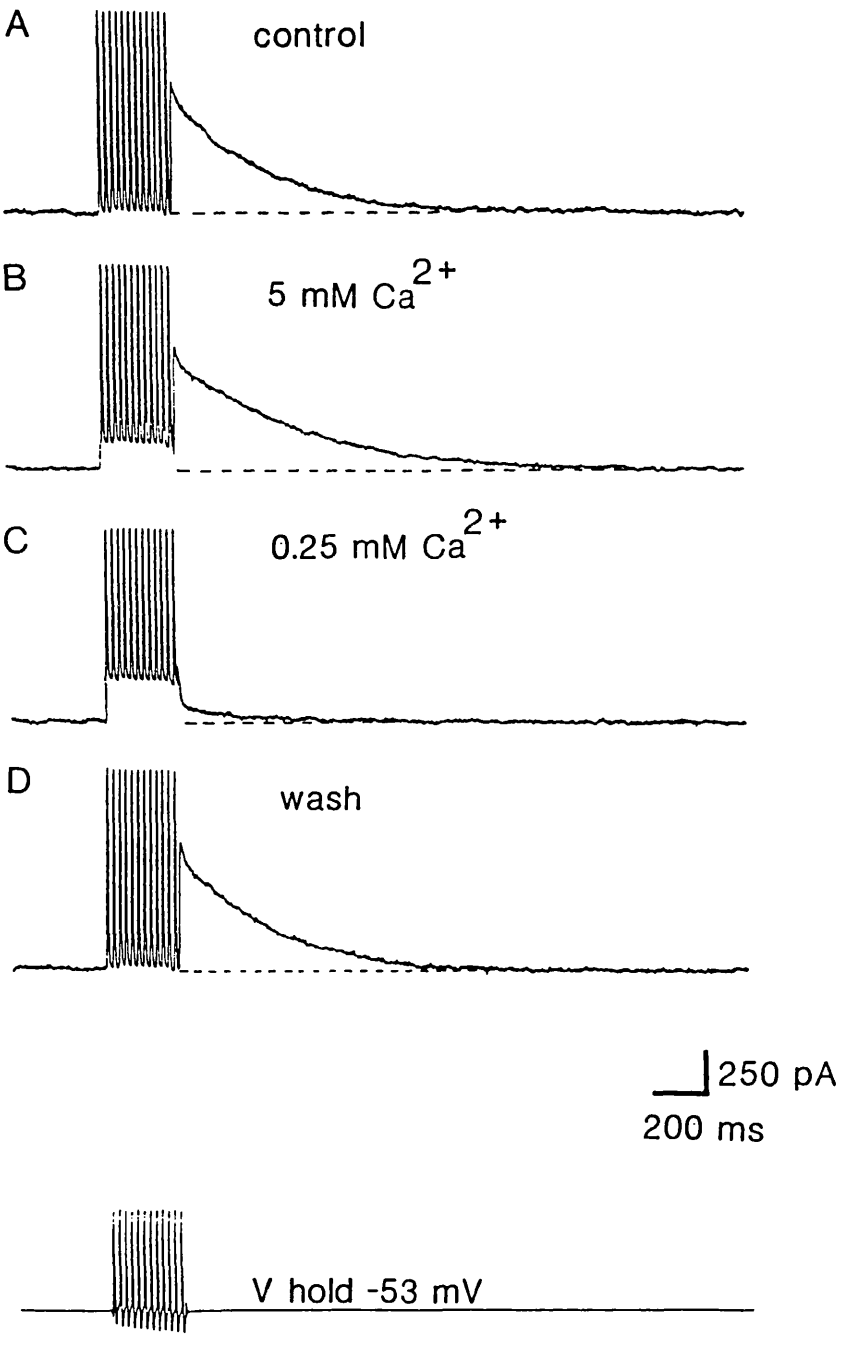
A
control
B
5 mM Ca2+
C
0.25 mM Ca2+
D
wash
250 pA
200 ms
V hold -53 mV

Chapter 7

$GABA_A$ RECEPTOR-MEDIATED INCREASE IN MEMBRANE CHLORIDE CONDUCTANCE IN RAT PARATRACHEAL NEURONES

SUMMARY

1. The actions of γ-aminobutyric acid (GABA) on the intramural neurones of 14-18 day old rats were studied in situ using intracellular current- and voltage-clamp techniques. The ionic conductance changes and the effects of various GABA-receptor agonists and antagonists on these neurones were also investigated.

2. Prolonged application of GABA, either by ionophoresis (10 pC-10 nC) or superfusion (10-100 μM), evoked a biphasic membrane depolarization in over 90% of all paratracheal neurones studied. Typically, the response consisted of an initial rapid depolarization (18-45 ms) that subsequently faded over a period of 15-25 s to reveal a second smaller depolarization which was maintained for the duration of GABA application. Both components of the evoked response resulted in an increase in membrane conductance and an inward flow of current.

3. The amplitude of the transient inward current, recorded during the initial phase of the response, was linearly related to the membrane potential at which it was elicited and reversed symmetrically at a membrane potential of -32.7 mV. The underlying increase in conductance was largely independent of membrane potential. The equilibrium potential for the sustained inward current was -38.7 mV. Replacement of extracellular chloride with gluconate ions initially enhanced the GABA-evoked inward current. With successive applications of GABA in low chloride, the evoked current and conductance changes declined markedly.

4. Muscimol superfusion (1-10 μM) or ionophoresis (10 pC-10 nC) mimicked both the initial and late phases of the GABA-induced conductance change and inward current. Baclofen (1-100 μM) had no effect upon either resting membrane potential or conductance in any of the cells tested.

5. The large transient initial phase of the GABA-evoked inward current and depolarization were potently inhibited by picrotoxin (1-50 μM), whereas the smaller

sustained inward current was largely resistant to picrotoxin.

6. All of the observed actions of GABA and muscimol were antagonized by bicuculline (0.1-10 μM) in an apparently competitive manner.

7. It is concluded that GABA acts via $GABA_A$ receptors present on the soma of paratracheal neurones to produce an increase in membrane chloride conductance. Prolonged application of GABA results in a decline in the observed current due to a combination of two processes: receptor desensitization and shifts in the chloride equilibrium potential. The possible roles for GABA in neural regulation of airway excitability are discussed.

INTRODUCTION

γ-Aminobutyric acid (GABA) is considered to be the principal inhibitory neurotransmitter in the mammalian central nervous system (CNS; Kelly & Beart, 1975). The first evidence to suggest that there were GABAergic neurones in the vertebrate peripheral nervous system was the discovery that a population of intrinsic neurones in the guinea-pig myenteric plexus possessed a high-affinity uptake system for GABA, and were able to synthesize GABA from glutamic acid (Jessen, Mirsky, Dennison & Burnstock, 1979). Subsequent investigations now indicate a possible neurotransmitter role for GABA in a number of peripheral tissues (for review see Erdo & Bowery, 1986). In the periphery, as in the CNS, both $GABA_A$ and $GABA_B$ receptor subtypes are present (Dunlap, 1981; Cherubini & North, 1984a, b). Peripheral $GABA_A$ receptors are similar to those in the CNS in that they have an integral chloride channel and are antagonized by bicuculline and/or picrotoxin (DeGroat, 1970; Adams & Brown, 1975; Bormann, Hamill & Sakmann, 1987). In contrast, peripheral $GABA_B$ receptors appear to differ from those found in the CNS, in that they are almost exclusively linked to calcium channels (Dunlap & Fischbach, 1981; Cherubini & North, 1984b; Deisz & Lux, 1985; Holz, Rane & Dunlap, 1986), whereas central $GABA_B$ receptor activation involves an increase in potassium conductance (Newberry & Nicoll, 1984; Gähwiler & Brown, 1985a). The main function of many of the GABA receptors, especially peripheral $GABA_B$ receptors, appears to be the modulation of release of other neurotransmitters such as acetylcholine, substance P and noradrenaline (Adams & Brown, 1975; Kato & Kuba, 1980; Cherubini & North, 1984b).

In the airways, GABA has been implicated in the regulation of tracheal smooth muscle tone through both central and peripheral mechanisms (Haxhui, Deal, Norcia,

Lunteren, Mitra & Cherniack, 1986; Tamaoki et al. 1987). Results suggest that GABA decreases the contractile response of airway smooth muscle to cholinergic nerve stimulation by inhibiting the release of acetylcholine from post-ganglionic parasympathetic nerves in the guinea-pig trachea. This effect is thought to be mediated by chloride-dependent, bicuculline-sensitive receptors present on the post-ganglionic neurones (Tamaoki et al. 1987). Furthermore, in an animal model of asthma, GABA and the $GABA_B$ agonist (-)-baclofen have been found to protect against anaphylactic bronchospasm as well as spasm induced by aerosols of histamine and prostaglandins (Luzzi, Franchi-Micheli, Folco, Rossoni, Ciuffi & Zilletti, 1987). More recently, GABA has also been shown to inhibit bronchoconstriction via the action of $GABA_B$ receptors that are thought to be present on sensory nerve terminals (Belvisi, Ichinose & Barnes, 1989).

A preparation of the rat trachea that permits visualisation and recording from intramural paratracheal neurones present in the trachealis muscle in situ has been developed and the basic electrophysiological characteristics of these cells have been examined (see Chapter 6). These cells constitute a population of neurones showing two extreme types of firing behaviour (see Chapter 6 and Allen & Burnstock, 1990b). The majority of cells (65-75%) discharged short high-frequency bursts of action potentials at regular intervals in response to prolonged stimulation; these bursts of firing were followed by a slow calcium-dependent after-hyperpolarization. A further 10-15% of cells showed no burst firing activity, but fired tonically at low frequencies for the duration of current stimulation; the remaining cells displayed characteristics in between these two extremes. In this chapter, the effects of GABA and related substances upon these cells are reported and the possible implications of these actions on airway function are discussed.

RESULTS

Application of GABA, either by superfusion (1-100 μM) or ionophoresis (0.5 M, pH 4.0, 2-100 nA) produced a membrane depolarization in 156 out of a total of 171 (approximately 90%) rat paratracheal neurones studied. Typically, GABA evoked a two-component response that consisted of a large initial depolarization which rapidly faded to reveal a second, smaller depolarization which was maintained for the duration of GABA application (see Fig. 7.1Ai, B & Ci). Both the initial transient and the slow sustained responses to GABA appeared to result from the direct action of GABA upon the impaled cell, since the responses were unaffected by superfusion with either calcium-free or tetrodotoxin-containing (0.3-1 μM) solutions.

The currents underlying the GABA-induced depolarizations were investigated under voltage-clamp. Brief ionophoretic application of GABA for a period of 1-100 ms (10 pC-10 nC) produced a large increase in membrane conductance that resulted in a transient inward flow of current (see Fig. 7.1Aii). Under optimal conditions, where there was no connective tissue between the ionophoretic electrode and the impaled cell, the latency of response was between 18 and 45 ms. The magnitude of the inward current was dependent upon the total amount of ionophoretic charge ejected (see Fig. 7.1Aii) and became larger at more negative potentials (see later). Prolonged application of GABA, either by superfusion or by ionophoresis (2-5 nA) for periods up to 2 min, induced a similar rapid, transient inward flow of current, which subsequently declined over a period of 15-25 seconds to reveal a second smaller, sustained component to the inward current. This sustained inward current was also associated with an increase in membrane conductance and showed little or no rundown during prolonged GABA application (see Fig. 7.1Cii). At the end of the period of stimulation, membrane conductance and current returned to control values within 10-20 s.

Conductance changes

Fast transient component

For any given cell studied under current-clamp, the greater the amplitude of the fast depolarization, the larger the underlying conductance increase. However, as the total ionophoretic charge ejected was increased, the amplitude of the response became maximal, whereas the peak conductance continued to rise (see Fig. 7.1Ai). When ionophoretic currents sufficient to evoke a maximal depolarization were applied, the absolute amplitude of the response was almost entirely dependent upon the membrane potential of the cell. At any given membrane potential, the maximum size of the evoked depolarization occurred when the amplitude of the response became large enough to cause the cell to depolarize to a potential of approximately -35 mV. This potential was found to correspond quite closely to the equilibrium/reversal potential for the response (see later).

Examination of the observed increase in conductance under voltage-clamp revealed that the magnitude of the GABA-evoked current was directly related to the observed increase in conductance. The peak fractional increase in conductance (see methods) varied considerably between cells, and ranged between 1.05 and 12.8 (mean 4.51 ± 0.336, n=83). For any given cell, the amplitude of the inward current was dependent upon membrane potential (see later), however, the fractional increase in conductance underlying the response was largely independent of the membrane potential at which it was evoked (see Fig. 7.2).

Slow sustained component

The conductance change and the resulting sustained inward current flow during prolonged application of GABA were considerably smaller than those seen during the initial transient response. The amplitude of the inward current became larger with increasing concentrations of GABA and was generally maximal in the presence of GABA at concentrations greater than 100 μM. Over the normal range of resting membrane potentials (-50 to -65 mV), the maximum amplitude of the sustained inward current rarely exceeded 150 pA (mean 107 ± 6.7 pA, n=19). When the response was evoked by prolonged ionophoretic application of GABA, the amplitude of the sustained inward current reached a maximum even using very low ejection currents (1-3 nA) and could rarely be increased by further raising the current. However, in the presence of agents which acted to inhibit the initial transient inward current, raising the ionophoretic ejection current increased the rate of rise to this plateau, maximum value of the sustained inward current. It is worth noting that care was needed when applying prolonged ionophoretic currents. If excessively high currents were applied (> 10 nA), then the prolonged ionophoretic current itself could induce a sustained inward current flow similar to the GABA-induced current. In order to remove this source of error, the ionophoretic current was adjusted to a level where all of the inward current was antagonized by superfusion with bicuculline (see later). The observed increase in conductance during the slow response varied between cells, with the mean fractional increase in conductance ranging between 0.15 and 1.78 (mean 0.846 ± 0.061, n=42).

Ionic- and voltage-dependence

Transient inward current

The voltage-dependence of the fast GABA-evoked inward current was investigated in the presence of tetrodotoxin (0.3-1 μM; see Fig. 7.2A). The amplitude of the inward current was linearly related to the membrane potential at which it was elicited (see Fig. 7.2B). When potassium citrate-filled electrodes were used in the recording, the mean null/reversal potential for the response was -32.7 ± 1.66 mV (n=8; see Fig. 7.2). Over the range of membrane potentials studied (-20 to -80 mV), both the time-course and the peak conductance change underlying the depolarization were largely independent of membrane potential (see Fig. 7.2A). Altering the extracellular chloride concentration from 124.1 to 12.1 mM transiently increased the amplitude of the fast GABA-evoked current by approximately 150-180%. However, multiple exposures to GABA, in the presence of low chloride-containing solutions, resulted in a pronounced decline in both the inward current and the observed conductance increase as a result of a fall in intracellular chloride concentration. On returning to normal chloride-containing solutions, both the inward current and the conductance increase slowly returned to their control values over a period of 5-10 min.

Slow sustained inward current

In order to determine the equilibrium potential for the sustained GABA-evoked response, current-voltage relationships were constructed before and during GABA ionophoresis (see Fig. 7.3A). The point of intersection of the curves gave a mean equilibrium/null potential for the response of -38.7 ± 1.56 mV (n=12; see Fig. 7.3B).

This value agrees well with the predicted equilibrium potential of -39.2 ± 1.1 mV (n=15) calculated from the observed increase in conductance (see methods).

GABA analogues

Muscimol, applied either by superfusion or ionophoretically, mimicked all the actions of GABA upon paratracheal neurones. When applied briefly by ionophoresis, it induced a similar rapid depolarization and an increase in conductance. Under voltage-clamp this could be seen to result from a transient inward flow of current (see Fig. 7.4A). When muscimol was applied for prolonged periods, the initial current subsided in a similar way to the GABA-induced response to reveal a non-inactivating component to the inward current (see Fig. 7.4B & C). The $GABA_B$ receptor agonist β-p-chlorophenyl-GABA (baclofen) at concentrations up to 100 μM had no effect upon either the resting membrane potential or conductance in any of the cells tested (n=11).

Antagonist studies

Both the fast transient depolarization evoked by brief application of GABA and the initial transient depolarization/inward current seen at the start of prolonged GABA ionophoresis were reversibly inhibited by picrotoxin (1-50 μM) in a dose-related manner (see Fig. 7.5A). However, picrotoxin at concentrations up to 500 μM was never observed to antagonize the sustained depolarization/inward current evoked by either superfusion or prolonged ionophoretic application of GABA or muscimol (see Fig. 7.5B).

Bicuculline (0.1-10 μM) reversibly inhibited the fast GABA-evoked depolarization. Approximate dose-response curves were constructed by briefly applying GABA using increasing ionophoretic currents (see Fig. 7.6A). Bicuculline produced a parallel shift to the right in the dose-response curve for GABA (see Fig. 7.6B). The GABA-induced sustained depolarization/inward current was also potently antagonized by bicuculline. However, the sensitivity of this response to inhibition by bicuculline was slightly lower than that observed for the transient component and required concentrations of bicuculline of between 10 and 50 μM to fully antagonize the actions of GABA (see Figure 7.7).

Phaclofen at concentrations up to 1 mM did not antagonize either of the GABA- or muscimol-induced inward currents in any of the cells tested (n=5).

Other agents

Superfusion with nipecotic acid (1-10 μM; n=5), a GABA uptake blocker, or inhibition of electrogenic pumping with ouabain (1-100 μM; n=4) were never observed to alter either the amplitude or the time-course of the two components of the GABA-induced inward currents. Superfusion with either calcium-free, high magnesium-containing solutions or blockade of calcium entry using $CdCl_2$ (100 μM) did not reduce the observed amplitude or the underlying increase in conductance during either phase of the GABA-induced response.

DISCUSSION

The findings of the present study showed that GABA exerted a powerful and direct effect upon a large proportion of the parasympathetic intramural neurones of the rat trachea. This effect was mediated via bicuculline-sensitive receptors and resulted in a large increase in resting chloride conductance. In a typical cell, held near its resting membrane potential, application of GABA produced a biphasic response consisting of an initial, transient depolarization, which rapidly declined to reveal a smaller, sustained depolarization. The maximum amplitude of the initial depolarization under these conditions was usually between 15 and 25 mV and reflected the level of the chloride equilibrium potential, which was approximately 20 mV positive to the resting membrane potential in these cells. Substituting extracellular chloride ions for a less permeant anion, such as gluconate, produced a transient increase in the amplitude of the GABA-induced depolarization and inward current. However, with repeated exposure to GABA in the presence of low extracellular chloride, both the current and the underlying increase in conductance declined markedly. This rundown of the GABA-evoked response in low chloride-containing solutions can best be explained by considering the underlying changes in the electrochemical gradient for chloride ions (see Adams & Brown, 1975). Initially, superfusion with low chloride-containing solutions would be expected to increase the net outward electrochemical driving force on chloride ions by shifting E_{Cl} to more positive potentials. This would result in a large increase in the outward flow of chloride ions from the cell during the GABA-evoked response, and account for the large increase in the observed depolarization. Repeated application of GABA would, however, reduce the intracellular concentration of chloride ions causing a large negative shift in E_{Cl}, which would lead to a decline in the amplitude of subsequent responses. This reduction in the concentration of intracellular chloride ions,

together with the low extracellular chloride concentration, would also explain the observed reduction in the underlying conductance that would be predicted to occur as a result of a deficiency in the total number of charge-carrying chloride ions.

In addition to the initial transient response, all paratracheal neurones displayed a second, sustained depolarization which persisted for the duration of GABA application. Biphasic responses to prolonged application of GABA have been described in a variety of different cells (Deschenes, Feltz & Lamour, 1976; Mayer, Higashi, Shinnick-Gallagher & Gallagher, 1981; Cherubini & North, 1984a; Yasui, Ishizuka, & Akaike, 1985). Superficially, the second depolarizing phase in many of these cells was similar to the sustained response seen in rat paratracheal neurones. However, in enteric AH type cells for example, the slow GABA response was mimicked by baclofen, had a low affinity for bicuculline and was attributed to activation of $GABA_B$ receptors (Cherubini & North, 1984a). In contrast, in rat paratracheal neurones, baclofen was never observed to produce membrane depolarization, whereas muscimol mimicked all the actions of exogenously applied GABA. This finding, together with the selective inhibition of all of the observed actions of GABA and muscimol by bicuculline, indicated that the sustained as well as the transient responses in rat paratracheal neurones, were mediated by $GABA_A$ receptors.

Multi-component, $GABA_A$ receptor-mediated chloride currents have been described in dorsal root ganglion neurones (Akaike, Inomata & Tokutomi, 1987). In these cells, the sustained inward current was similar to the one described here in rat paratracheal neurones, in that it was largely insensitive to picrotoxin (Yasui et al. 1985). The equilibrium potential for the sustained inward current in paratracheal neurones was close to that of the transient component, indicating that, as in the

dorsal root ganglion, it may also result from an increase in chloride conductance. The slightly more negative equilibrium potential of the sustained response probably reflected a small shift in E_{Cl} as a result of the large efflux of chloride ions that occurred during the initial, transient response. Similar shifts of the GABA reversal potential (E_{GABA}) between the initial and late phases of the GABA-evoked response have been described in rat and cat ganglion cells (Adams & Brown, 1975; Mayer, Higashi, Gallagher & Gallagher, 1983).

In paratracheal neurones, the time-dependent decline of the GABA-evoked current, which occurred during continuous application of GABA, was similar to that described in, for example, hippocampal and dorsal root ganglion neurones. In these cells, the initial and late phases of the GABA current have been shown to result from a combination of two processes; receptor desensitization and shifts in E_{GABA} (Yasui et al. 1985; Huguenard & Alger, 1986; Akaike et al. 1987). It seems likely that similar mechanisms underlie the biphasic inward current in rat paratracheal neurones.

Given the powerful effect that GABA exerted upon rat paratracheal neurones, it is obviously important to determine whether there is any endogenous GABA within the airways. GABA has been localised in a population of neurones in the enteric nervous system (Jessen, Hills & Saffrey, 1986) and it is possible, given the shared embryological origin of the gut and trachea, that there are also intrinsic GABAergic neurones in the airways. Alternatively, GABA may be released from extrinsic nerves to act upon the intramural ganglia. Another possible source of GABA could be the blood, since levels of circulating GABA, at concentrations near to those required to depress ganglionic transmission, have been reported in the bullfrog and cat (Crowcroft, Jessup & Ramwell, 1967; Kato, Morita, Kuba, Yamada, Kuhara, Shinka &

Matsumoto, 1980). In addition, it has been reported that glial cells in mammalian sympathetic ganglia are capable of taking up GABA from solutions containing concentrations of GABA as low as 1 μM (Bowery & Brown, 1972; Iversen & Kelly, 1975). Therefore, glial cells could regulate the extracellular GABA concentration and thereby modulate the excitability of neurones; it has been proposed that this type of mechanism may occur in sympathetic ganglia (Brown & Galvan, 1977).

If the excitability of paratracheal neurones were in some way modulated by either circulating or locally released GABA, then this could have wide-ranging consequences for airway function. It has previously been shown that rat paratracheal neurones display a high level of subthreshold, spontaneous synaptic activity (Allen & Burnstock, 1989b). High levels of subthreshold synaptic activity have also been observed in cat tracheal ganglia in vivo, and it has been suggested that synchronisation of multiple inputs are required to elicit action potential discharge in these cells (Mitchell et al. 1987). One of the observed actions of GABA in the present study was a large increase in resting membrane conductance. This would act as a shunt across the membrane and result in a decrease in the size of the depolarization produced by individual synaptic events. Under such conditions, the overall intensity of vagal input required to elicit action potential discharge would be greatly increased by GABA and may explain the observed GABA-evoked reduction in acetylcholine release from post-ganglionic parasympathetic nerves in the guinea-pig trachea (Tamaoki et al. 1987). Conversely, a fall in levels of GABA acting at the ganglion level or a reduction in the sensitivity of these cells to GABA could increase the excitability of the ganglion cells and partially explain the hyperreactivity of tracheobronchial smooth muscle observed in conditions such as asthma.

Fig. 7.1. The effects of brief and prolonged GABA application upon rat paratracheal neurones. A(i), rapid depolarizations induced by brief (100 ms) ionophoretic applications of GABA, the total charge ejected in each case is indicated in nC below the responses. Downward deflections are the membrane voltage responses to constant hyperpolarizing current pulses (100 pA/50 ms) used to monitor membrane resistance changes. A(ii), membrane currents for the same cell to similar GABA ionophoretic currents recorded under voltage-clamp. Downward deflections are membrane currents in response to -10 mV (50 ms duration) voltage steps. Membrane/holding potential in A(i) and A(ii) was -52 mV. B, the effect of prolonged superfusion of GABA (100 μM) for the period indicated by the bar. The recording was made under current-clamp (membrane potential -60 mV), downward deflections are membrane voltage responses to constant current pulses (100 pA/50 ms). C, the effects of prolonged ionophoretic application of GABA (8 nA) for the period indicated by the bar (1.5 min). At the onset of GABA ionophoresis there was a rapid depolarization, this response then subsided to reveal a sustained depolarization which persisted for the duration of GABA ionophoresis (see Ci). Downward deflections are the membrane voltage responses to passing brief (80 pA/50 ms) constant intrasomal current pulses to monitor input resistance. C(ii), the effects of prolonged GABA ionophoresis upon membrane current in the same cell as in C(i). Downward deflections are the membrane currents in response to -5 mV, 50 ms duration voltage commands. Resting/holding potential in C(i) and C(ii) was -50 mV.

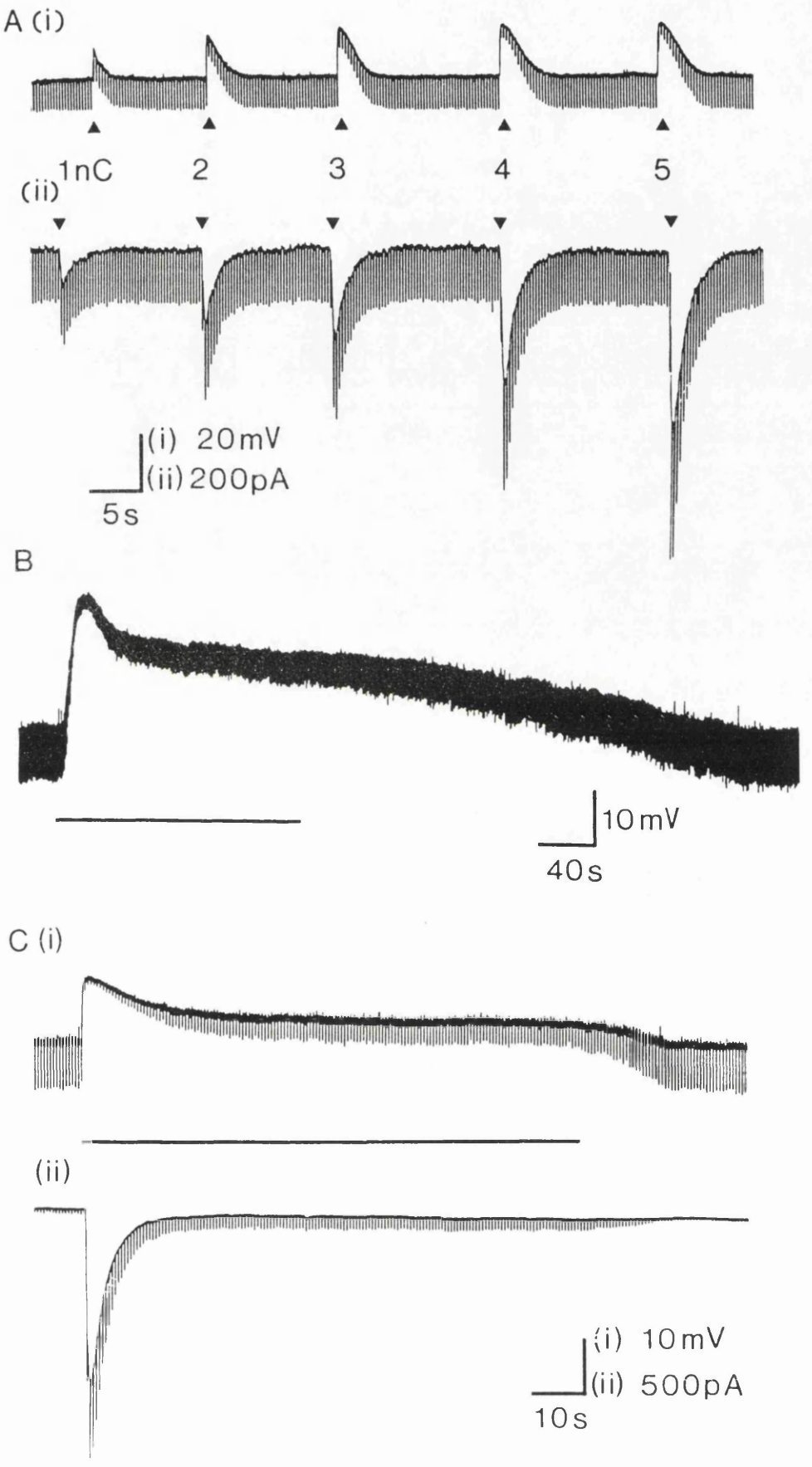
A (i)
1nC
2
3
4
5
(ii)
(i) 20mV
(ii) 200pA
5s
B
10mV
40s
C (i)
(ii)
(i) 10mV
(ii) 500pA
10s

Fig. 7.2. The voltage-dependence of the rapid transient GABA-induced inward current. A, records from a single paratracheal neurone held at different membrane potentials. Downward deflections are the membrane current responses to hyperpolarizing voltage commands (10 mV/50 ms) used to monitor changes in membrane conductance. Arrows beneath the records indicate the point at which GABA was applied (5 nA/100 ms). Note that the underlying fractional increase in membrane conductance was largely independent of the holding potential at which the response was elicited. B, the amplitude of the transient GABA-induced inward current as a function of holding potential. Line is least squares fit to raw data. The current was linearly related to membrane potential (correlation coefficient, r= 0.998) and reversed symmetrically at a membrane potential of -34.1 mV to become an outward current.

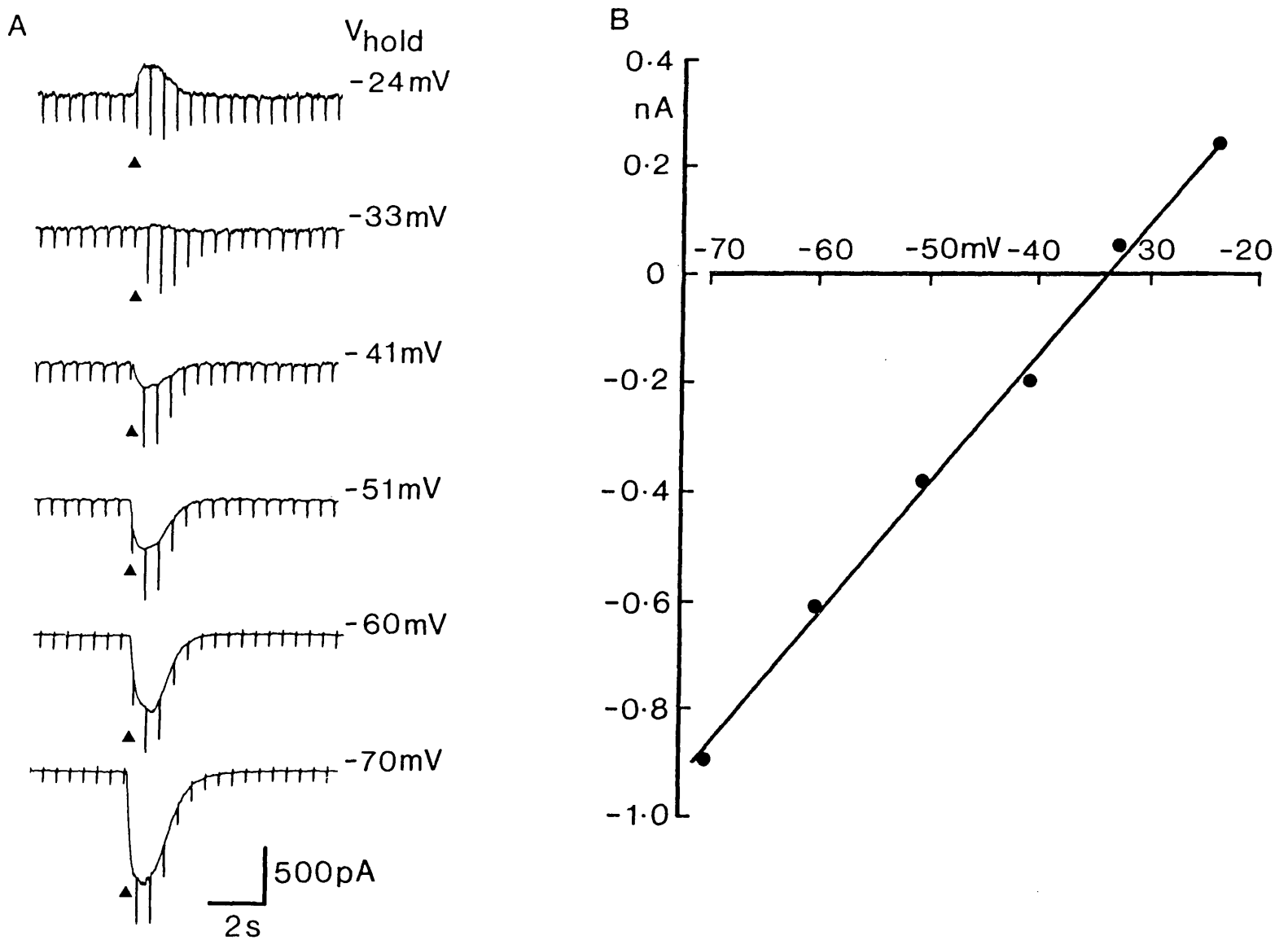
A
V_{hold}
-24mV
-33mV
-41mV
-51mV
-60mV
-70mV
500pA
2s
B
0·4
nA
0·2
0
-0·2
-0·4
-0·6
-0·8
-1·0
-70
-60
-50mV
-40
-30
-20

Fig. 7.3. The voltage-dependence of the sustained GABA-induced inward current in a paratracheal neurone examined under voltage-clamp. A, under control conditions with the cell held at a membrane potential of -50 mV (the resting membrane potential for this cell), the cell was subjected to a series of 500 ms duration positive and negative voltage commands of increasing amplitude (5 mV increments). GABA was then applied ionophoretically (ejection current 5 nA) for the period indicated by the bar. This evoked the characteristic transient inward current which subsequently declined to reveal the sustained inward current. During the plateau phase of the sustained current, the cell was subjected to a second series of voltage commands identical to those applied under control conditions. At the end of this procedure the ionophoretic ejection current was switched off and the current returned to control levels. B, the current-voltage relationships for the cell shown in A under control conditions and in the presence of GABA. The point of interception of the two curves gives a value for the equilibrium potential (E_S) for the sustained current response of approximately -38 mV.

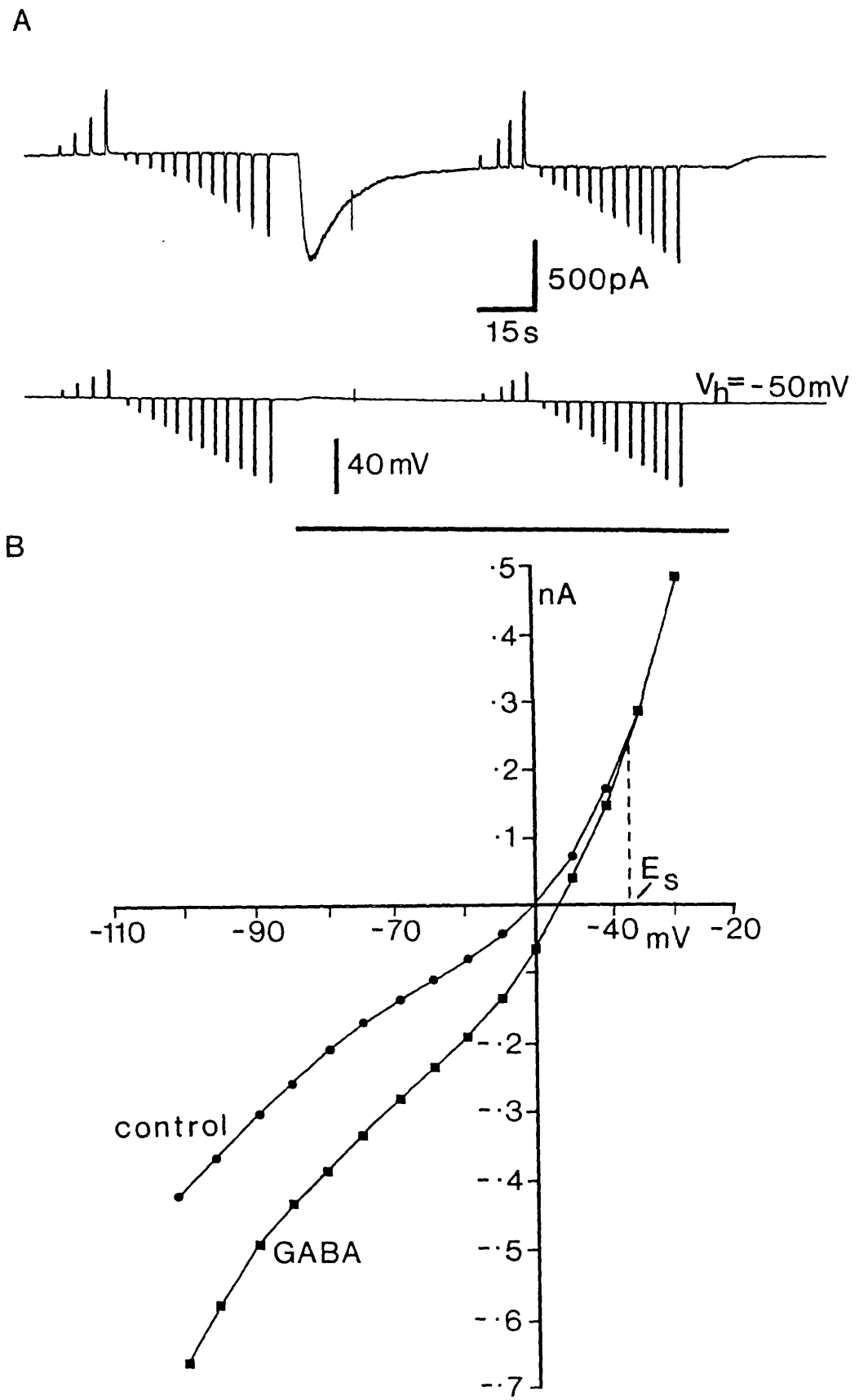
A
500pA
15s
V_h= -50mV
40 mV
B
·5
nA
·4
·3
·2
·1
E_s
-110
-90
-70
-40 mV
-20
control
GABA
-·2
-·3
-·4
-·5
-·6
-·7

Fig. 7.4. The actions of muscimol, a $GABA_A$ receptor agonist, upon rat paratracheal neurones. A, brief (100 ms) ionophoretic application of muscimol using increasing ejection currents (total ionophoretic charge ejected is given in nC below each record). Downward deflections are membrane current responses to -10 mV voltage steps used to monitor changes in membrane conductance. Holding potential for the cell shown in A was -62 mV. B, prolonged ionophoretic application of muscimol, for the period indicated by the bar (7 nA/1.5 min), produced a biphasic inward current similar to that produced by GABA (downward deflections are current responses to -10 mV voltage steps as in A). Holding potential -54 mV. C, superfusion with muscimol (10 μM) for the period indicated by the bar mimicked the effect of prolonged ionophoretic application, but the latency and rate of rise of the initial transient current were considerably slower. Downward deflections are current responses to 50 ms duration -10 mV voltage steps. Holding potential -53 mV.

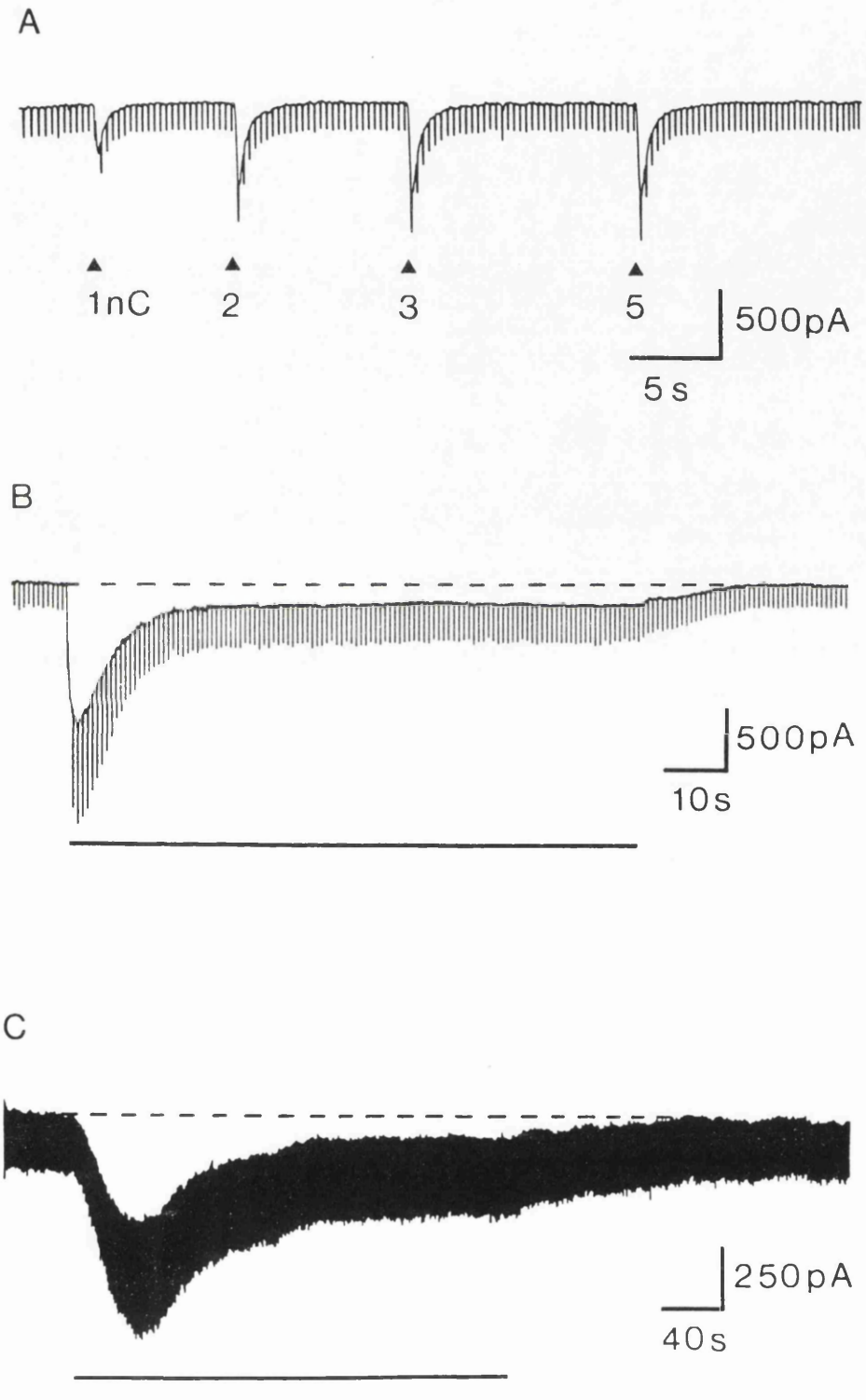
A
1nC
2
3
5
500pA
5 s
B
500pA
10s
C
250pA
40s

Fig. 7.5. Inhibitory action of picrotoxin (PTX) upon the GABA-evoked response in a rat paratracheal neurone. A, the fast GABA-evoked depolarization. Upper panel shows control depolarizations to GABA produced by increasing the total ionophoretic charge ejected (all pulses 50 ms duration; the amount of charge ejected in each case is indicated in nC below each response). In the presence of picrotoxin (10 and 50 μM; middle panels), the amplitude of the evoked depolarizations were reduced in a dose-related manner. Resting membrane potential -54 mV. B, the rapid transient and sustained inward currents evoked by prolonged ionophoretic application of GABA (8 nA/1.5 min). In the presence of picrotoxin (50 μM), the initial rapid transient component of the response was almost totally abolished, whilst the slow sustained current and associated increase in conductance remained largely unaffected. Downward deflections are membrane currents in response to 10 mV/50 ms voltage steps. Holding potential -68 mV.

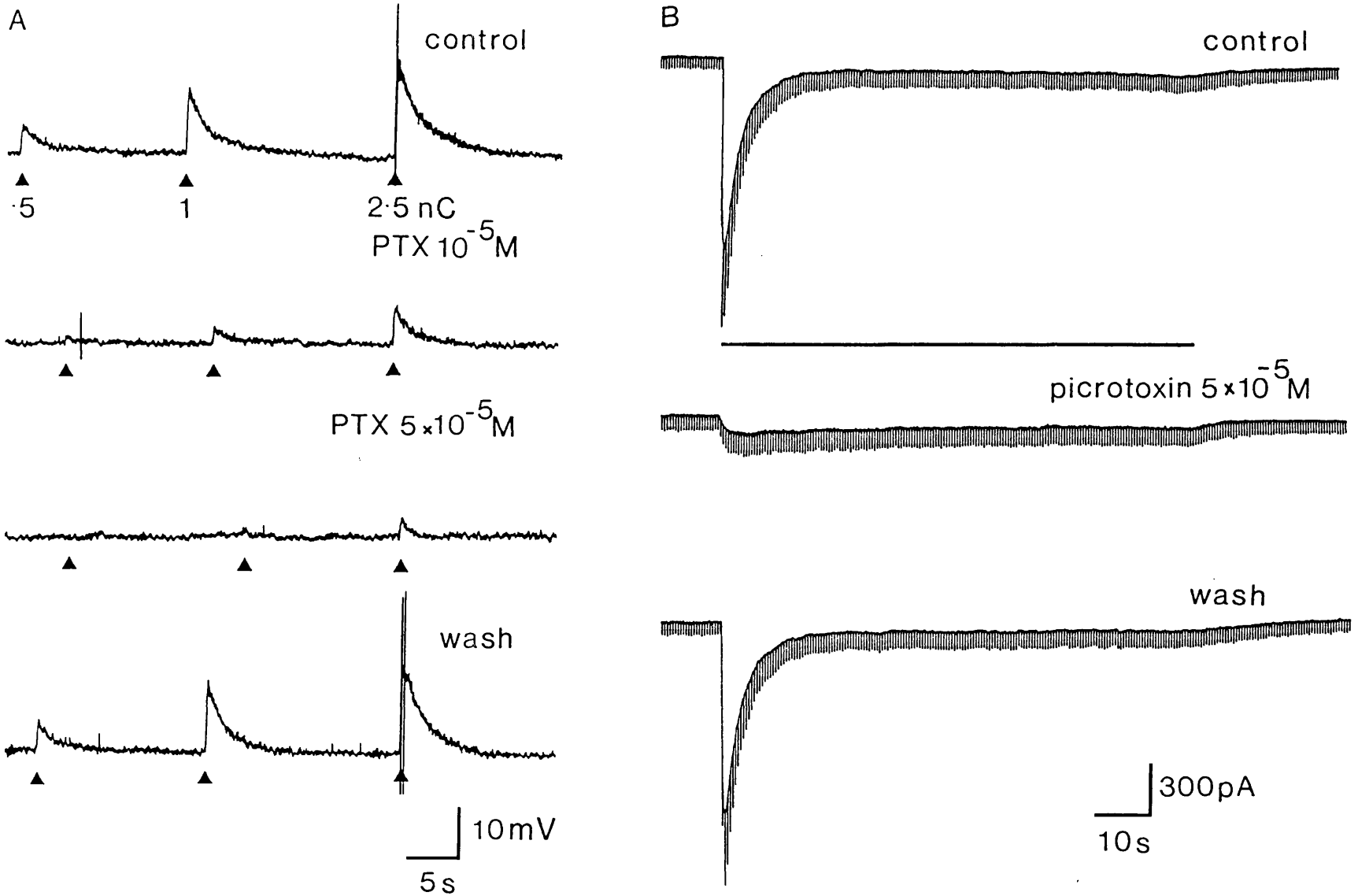
A
control
·5
1
2·5 nC
PTX 10^{-5}M
PTX 5×10^{-5}M
wash
10mV
5s
B
control
picrotoxin 5×10^{-5}M
wash
300pA
10s

Fig. 7.6. Antagonism by bicuculline of the transient depolarization in response to ionophoretic application of GABA. A, graded depolarizations were evoked by increasing the total ionophoretic charge ejected (all applications were for 100 ms, total charge ejected was increased from 1 to 10 nC as indicated). Upper panel, control depolarizations and associated increases in membrane conductance. Middle and lower panels show responses from the same cell to a similar series of ionophoretic applications of GABA in the presence of bicuculline (1 and 10 μM respectively). Resting membrane potential was -54 mV. B, dose-response curves constructed from an experiment similar to the one shown in A. Bicuculline at increasing concentrations produced a concentration-dependent shift in the dose-response curve to GABA.

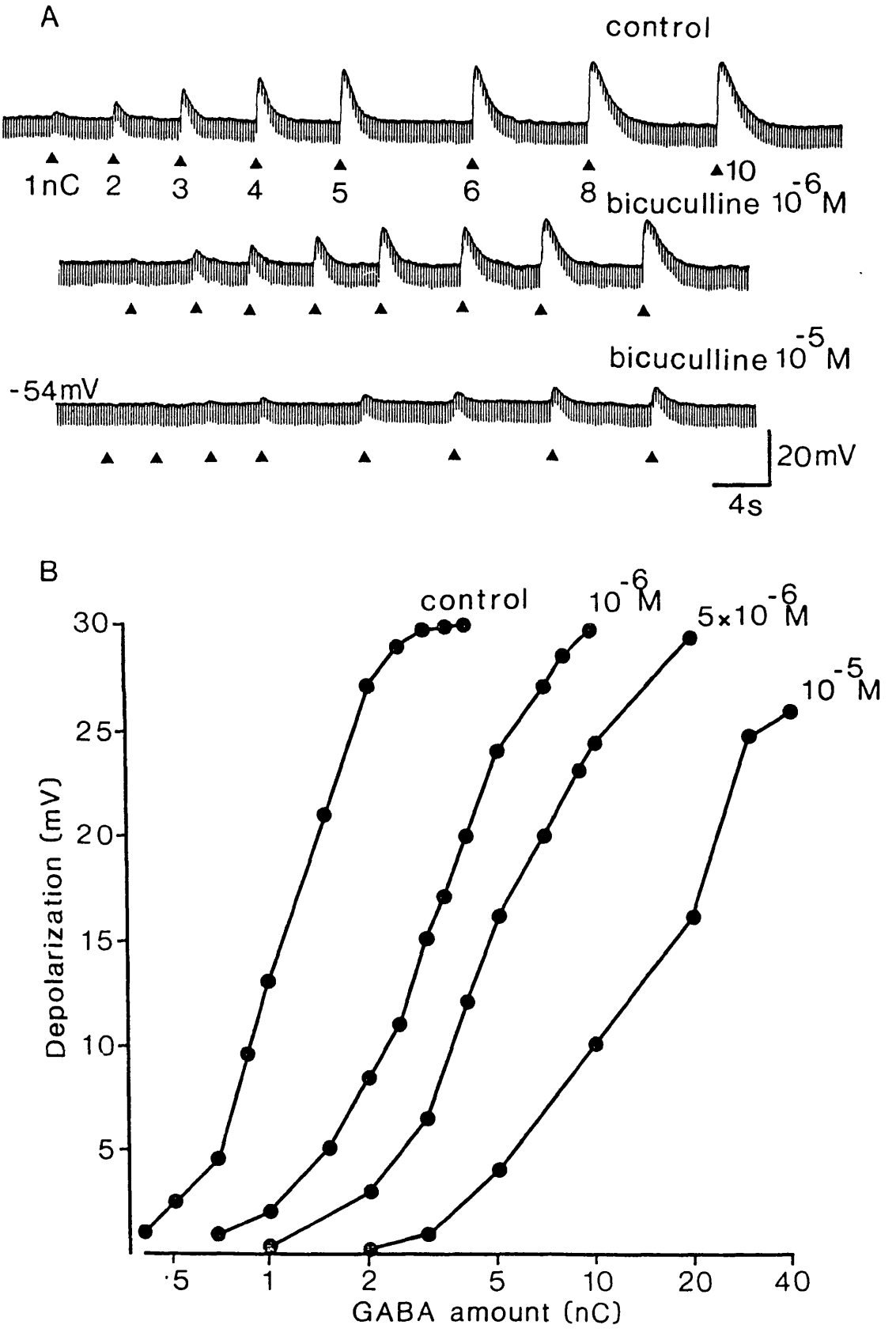
A
control
1nC
2
3
4
5
6
8
10
bicuculline 10^{-6}M
bicuculline 10^{-5}M
-54mV
20mV
4s
B
control
10^{-6} M
5×10^{-6} M
10^{-5} M
Depolarization (mV)
30
25
20
15
10
5
·5
1
2
5
10
20
40
GABA amount (nC)

Fig. 7.7. Antagonism of the transient and sustained inward currents by bicuculline in a rat paratracheal neurone voltage clamped at -54 mV. A, control response to prolonged GABA ionophoresis (8 nA/1.5 min). B, in the presence of 10 μM bicuculline, there was a pronounced decrease in the conductance change and inward current flowing at the start of GABA application and a smaller reduction in the size of the sustained inward current. C, in the presence of 50 μM bicuculline, both the initial transient and the slow sustained GABA-evoked currents were almost totally abolished. D, wash. Downward deflections are the induced membrane currents resulting from 10 mV negative commands (50 ms duration) used to monitor changes in membrane conductance.

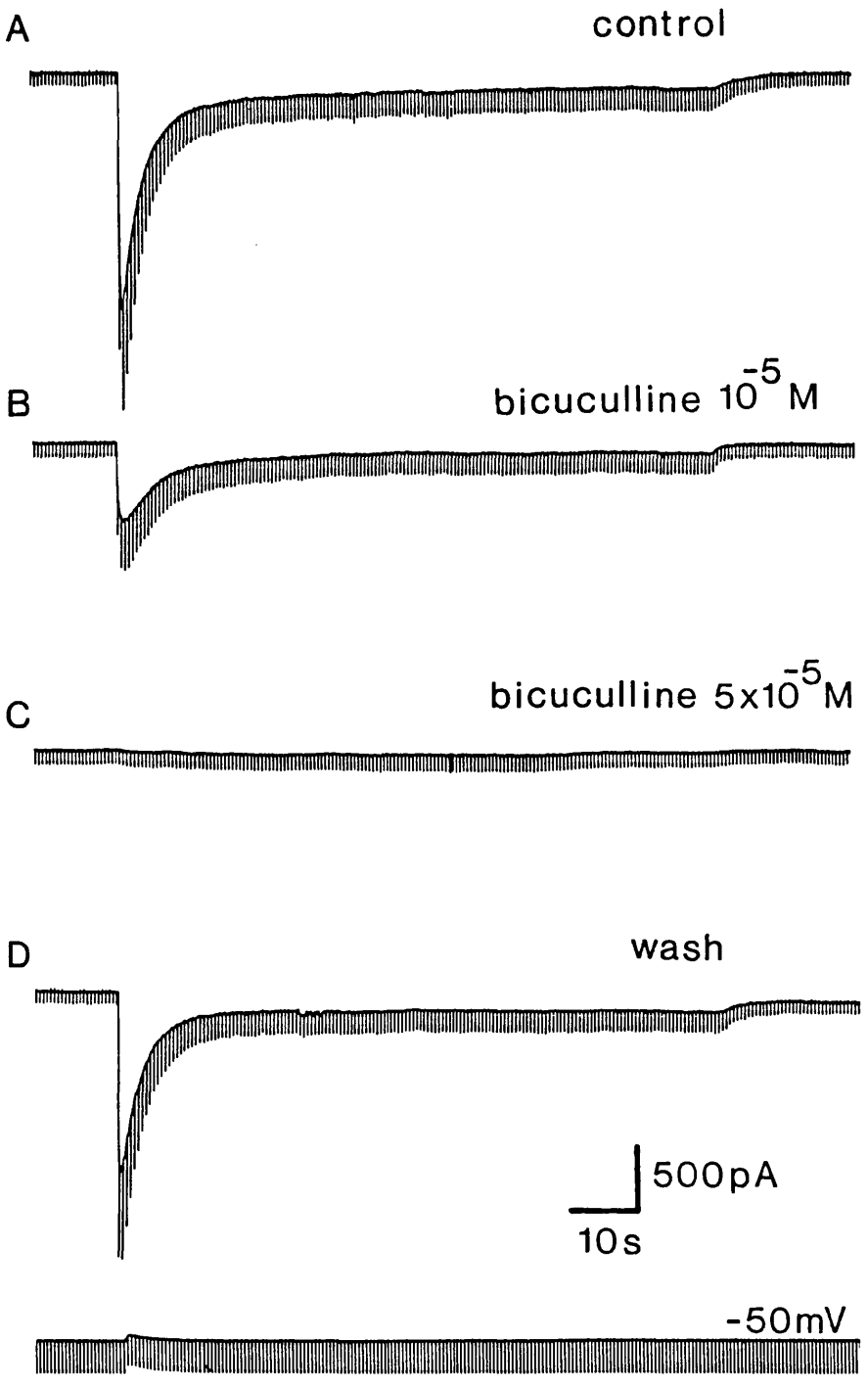
A
control
B
bicuculline 10^{-5} M
C
bicuculline $5x10^{-5}$M
D
wash
500pA
10s
-50mV

Chapter 8

GENERAL DISCUSSION

From the data presented in this thesis, it is clear that the degree of electrophysiological and neurochemical complexity displayed by neurones in the intramural ganglia of the heart and trachea is of a sufficiently high level for them to be capable of performing local modulatory roles in the neural control of these tissues. The findings of the current work, together with some additional data that has not been presented in the results section of this thesis, will now be discussed in the broader context of the properties and interactions occurring within these ganglia. This will then be followed by ideas and suggestions for future work designed to help to further clarify the possible functional roles of the intracardiac and paratracheal ganglia.

Intracardiac ganglia

The studies of intracardiac neurones that have been reported in this thesis have revealed three distinct types of neurone which could be distinguished on the basis of their current firing characteristics. In addition, a number of different membrane conductances have also been identified, including an M-conductance and a calcium-activated potassium conductance. The initial early studies of these neurones were performed without the facility to voltage-clamp the cells and therefore, analysis of the different currents was limited. Subsequent to these initial studies, additional membrane currents have also been detected, but have yet to be fully characterised. Preliminary investigations, using discontinuous single-electrode voltage-clamp techniques on AH type cells, have revealed the presence of inwardly rectifying currents, which display "instantaneous" and time-dependent activation. These currents are similar to those present in paratracheal neurones (as reported in Chapter 6) and are strongly inhibited by low extracellular concentrations of caesium

ions. In addition to inward rectifier currents, a large number of AH type intracardiac neurones exhibited a transient outward current, similar to the A-current first described in snail neurones (Connor & Stevens, 1971) and subsequently found in a variety of other neurones (for review see Rogawski, 1985). This "A type" current could be activated when a cell was rapidly depolarized after an initial period of hyperpolarization, and would be expected to delay the initiation of action potential discharge and thus help to control the rate of firing of AH type cells. At present, the relative contributions played by this current in controlling firing in AH_s and AH_m type neurones has not been determined, although preliminary data suggests that the current may be more pronounced in AH_s cells. If this current is larger in AH_s, than in AH_m cells, then it may explain the difference in their firing characteristics. For example, when stimulated by prolonged low intensity pulses of intrasomal current, both cell types fire only once, with action potentials being followed by a slow after-hyperpolarization. During the after-hyperpolarization, the cells require higher current intensities to evoke firing. In the absence of a significant A-current, raising the stimulating current would reduce the effective refractory period due to the after-hyperpolarization and, at sufficiently high current intensities, its inhibitory action could be overcome and the cell would then fire repetitively (as seen in AH_m cells). However, multiple spike discharge results in a significant increase in the size of the after-hyperpolarization (see Chapter 3) and this would therefore tend to terminate firing after a short period. Furthermore, the large depolarization produced by the increased current stimulation would, over a period of 100 to 150 ms, also result in activation of the M-current and this would again tend to inhibit prolonged firing. If AH_s cells have a larger A-current than AH_m cells, then in addition to the after-hyperpolarization, the stimulating current would also have to overcome the inhibitory effect of the A-current (which exceeds

1 nA at peak) and in the period of time it takes for the A-current to inactivate, the M-current would have activated. Thus, as observed, multiple discharge in AH_s cells would be difficult to elicit. Therefore, the A-current, together with the M-current and the calcium-activated potassium current which is responsible for the after-hyperpolarization, will all act to prevent sustained high frequency discharge of action potentials in AH type intracardiac neurones. This could be extremely important in the heart where excessive firing of these vagal post-ganglionic neurones could result in a fatal arrest of the heart.

In addition to the large population of highly refractory AH type cells, a small number of recordings have been from the more excitable cells M type cells. Cells of this type were generally observed to be small and this made them difficult to study using conventional microelectrodes. Recent studies employing the whole-cell patch-clamp recording technique have been far more successful. However, this technique could not be used to study the majority of intracardiac neurones in culture as most were covered by glial cells (Kobayashi et al. 1986a). Therefore, we still remain ignorant of the basic characteristics of what might be a significant subpopulation of intracardiac neurones.

Investigation of the muscarinic receptor subtypes expressed by AH type intracardiac neurones indicates that these cells have functional M_1 and M_2 receptors. Classification of the subtypes of muscarinic receptors was largely based on their affinity for pirenzepine. There is some evidence to suggest that the M_2 receptors on these cells (receptors exhibiting a low affinity for pirenzepine) may themselves be a heterogeneous population (see Chapter 4 and Allen & Burnstock, 1990a). AF-DX 116, which has a greater affinity for the muscarinic receptors on

cardiac muscle than for those on smooth muscle and glandular tissue (Giraldo et al. 1986), displayed a limited degree of selectivity, and antagonized the M_2 receptor-mediated muscarine-induced hyperpolarization at slightly lower concentrations than were required to antagonize the M_2 receptors that mediated the inhibition of the after-hyperpolarization. In contrast, however, the antagonist 4-DAMP which has a higher affinity for smooth muscle and glandular M_2 receptors than for those on cardiac muscle (Barlow et al. 1976), showed almost no selectivity for any one of the different muscarinic receptor subtypes present on intracardiac neurones. One possible explanation for the rather low selectivity of these M_2 receptor antagonists could be that the receptor subtypes on intracardiac neurones are different to those on cardiac and smooth muscle. Five separate genes that code for muscarinic receptors have been identified (Bonner, Buckley, Young & Brann, 1987; Bonner, Young, Brann & Buckley, 1988; Bonner 1989). Of these, at least four are expressed by rat intracardiac neurones in situ, but whether all intracardiac neurones express all of these genes, or whether different subpopulations of neurones express different combinations of genes has not yet been determined (N.J. Buckley, personal communication). Furthermore, there is evidence to suggest that the antagonists used in the current report (4-DAMP and AF-DX 116) do not show enough selectivity to unequivocally differentiate between the five cloned muscarinic receptors (N.J. Buckley, personal communication), which could explain the poor selectivity displayed by these agents in the current study.

As well as the complex muscarinic (Chapter 4 and Allen & Burnstock, 1990a) and purinergic (Chapter 5 and Allen & Burnstock, 1990d) receptor-mediated interactions that may take place within intracardiac ganglia, studies of the actions of other exogenously applied neurotransmitters have also been performed.

Noradrenaline (0.05-10 μM) acting via an α_2-receptor subtype reduces calcium entry through voltage-sensitive calcium channels. This results in an increase in the rate of spike repolarization and a decrease in the level of activation of the calcium-activated potassium conductance responsible for the prolonged after-hyperpolarization (Allen & Burnstock, in preparation). This effect is similar to the M_2 receptor-mediated action of muscarine and raises the excitability of these neurones causing them to fire multiply in response to prolonged intrasomal current injection. An additional effect of noradrenaline on AH type cells has also been observed. Focal or bath application of noradrenaline (1-10 μM) produces a slow depolarization and a fall in resting membrane conductance as a result of inactivation of a tonically operating current. At present, neither the receptor subtype, nor the ionic nature of this current have been fully analyzed, however, it does not appear to be mediated by the same α_2-receptor responsible for the inhibition of voltage-sensitive calcium channels. The finding that there are functional noradrenergic receptors present on the parasympathetic neurones of the heart is potentially very interesting. Several studies have reported the presence of adrenergic nerve fibres in and around intracardiac ganglia <u>in situ</u> (Yamauchi, 1973; Jacobowitz, 1974; Ellison & Hibbs, 1976; Papka, 1976; Shvalev & Sosunov, 1985) suggesting that there may be adrenergic innervation of these ganglia. Functional interactions between the sympathetic and parasympathetic nerves at the level of the intrinsic ganglia could be of considerable importance in the regulation of the heart. For example, adrenergic nerves acting at the ganglion level could inhibit vagal transmission and thereby augment the actions of sympathetic nerve stimulation. Alternatively, if the after-hyperpolarization acts as a gate to the transfer of information across the soma from one neural process to another, as has been suggested by Wood (1984), then inhibition of this response by noradrenaline could permit the rapid propagation

of nerve impulses from one area of the heart to another, which could be important in maintaining synchronous beating of the heart during high levels of sympathetic stimulation.

A large proportion of the intrinsic neurones present in the atria display NPY-immunoreactivity (Gu, Polak, Allen, Huang, Sheppard, Tatemoto & Bloom, 1984; Dalsgaard et al. 1986; Hassall & Burnstock, 1984), but no catecholamine-containing intracardiac neurones have been demonstrated using glyoxylic acid fluorescence histochemistry (Nielsen & Owman, 1968; Crowe & Burnstock, 1982; Hassall & Burnstock, 1984, 1986), even though some of these neurones are tyrosine hydroxylase and dopamine β-hydroxylase-immunoreactive in situ (Gu et al. 1984; Dalsgaard et al. 1986; Hassall & Burnstock, 1987b). Preliminary studies indicate that a subpopulation of intracardiac neurones are responsive to exogenous application of NPY (Allen, unpublished observation). When focally applied to the cell soma, NPY induced a small (5-9 mV) prolonged (15-20 s) membrane hyperpolarization associated with an fall in input resistance. This response had a null/reversal potential close to the potassium equilibrium potential of these cells (n=2), indicating that it may result from an increase in membrane potassium conductance. This raises the possibility that NPY, released from intracardiac neurones, may act as a local, intrinsic agent to modulate the activity of these ganglia. Furthermore, NPY has also been localised in extrinsic, sympathetic, catecholamine-containing nerve fibres within the heart (Lundberg, Terenius, Hökfelt & Goldstein, 1983; Uddman, Ekblad, Edvinsson, Håkanson & Sundler, 1985) indicating that NPY and noradrenaline may co-exist in these nerves and they may also act as cotransmitters, as in the nerves innervating the vas deferens (Stjärne, Lundberg & Åstrand, 1986). At present, it is not been determined whether the NPY-responsive intracardiac neurones coincide with those

responding to exogenous noradrenaline, or whether NPY and noradrenaline are co-released from extrinsic nerves on to intrinsic ganglion cells. However, there is evidence to suggest that NPY may be released from sympathetic nerves in the heart. In the dog, prolonged non-adrenergic inhibition of vagal responses have been reported following sympathetic nerve stimulation and this inhibitory response is mimicked by exogenous NPY (Potter, 1985) indicating that some sympathetic nerves in the heart may release both noradrenaline and NPY which could modulate neurotransmission in the intracardiac ganglia.

In addition to co-transmission at the level of the intracardiac ganglia involving NPY and noradrenaline, there may also be nerves in which noradrenaline is co-localised and released along with ATP, as for example in the vas deferens (Westfall, Stitzel & Rowe 1978; Sneddon, Westfall & Fedan, 1982; Sneddon & Burnstock, 1984). Experiments to determine whether ATP and noradrenaline are co-localised within the mammalian heart have yet to be carried out, however, the observation of large numbers of quinacrine-positive nerves, as well as catecholamine-containing nerve fibres within the atria (Jacobowitz, 1967; Ehinger et al. 1968; Crowe & Burnstock, 1982) could indicate some degree of overlap in their localisation. Furthermore, a large subpopulation of intracardiac neurones respond to exogenous ATP and adenosine (see Chapter 5 and Allen & Burnstock, 1990d), indicating that these neurones display functional purinergic, as well as adrenergic receptors. However, at present, it is not clear whether individual intracardiac neurones express both of these receptor subtypes.

As well as their possible roles in regulating vagal pathways, the presence of NPY- and ATP-containing intramural neurones (Crowe & Burnstock, 1982; Hassall &

Burnstock, 1984; Dalsgaard et al. 1986) may suggest a role for these neurotransmitters in the regulation of the sympathetic innervation of the heart. For example, in the atria, sympathetic and parasympathetic nerve fibres come into close contact, therefore NPY and/or ATP may be released from intracardiac neurones in response to vagal stimulation and act to modulate the release of noradrenaline from sympathetic nerves.

Studies of the guinea-pig intracardiac neurones in culture have also shown for the first time that GABA exerts a powerful effect on a significant population these neurones (Allen & Burnstock, in preparation). Exogenous application of GABA evokes a rapid depolarization in 40-60% of AH type neurones. This response, examined under voltage-clamp, was associated with a large increase in membrane conductance and had an equilibrium/reversal potential between -35 and -40 mV. The brief inward current and underlying increase in membrane conductance were inhibited by picrotoxin (10-50 μM) and by bicuculline (1-10 μM), indicating that the response resulted from a $GABA_A$ receptor-mediated increase in membrane chloride conductance, similar to that observed in paratracheal neurones (see Chapter 7 and Allen & Burnstock, 1990c). The finding that a large population of intracardiac neurones display functional $GABA_A$ receptors indicates that GABA may be utilised as a neurotransmitter in the mammalian heart. Evidence to support this suggestion has come from in situ studies of the neural innervation of the sinus node of the dog (Neely, Hageman & James, 1983). In this study, GABA acting on local nerves or ganglia has been found to attenuate sinus bradycardia induced by stimulation of the right vagosympathetic trunk. At present, GABA has yet to be localised within the heart, although a number of possible sources exist. Firstly, GABA may be derived from the circulation, as levels of GABA sufficient to produce activation of the

receptors on intracardiac neurones have been detected in the blood of the cat and bullfrog (Crowcroft et al. 1967; Kato et al. 1980). Secondly, there is evidence that the small intensely fluorescent (SIF) cells in some ganglia are GABA-immunoreactive (Kenny & Ariano, 1986; Karhula, Häppölä, Joh & Wu, 1988). This raises the possibility that SIF cells in the heart, which are in close association with intrinsic ganglia, may also contain GABA (Jacobowitz 1967; Ellison & Hibbs, 1976). Alternatively, GABA may be localised either within extrinsic nerves innervating the intracardiac ganglia or within intrinsic neurones as has been demonstrated in the gut (Jessen et al. 1986).

Finally, the possibility that there might be some intrinsic sensory neurones within the heart, which are involved in local reflexes, is supported by studies demonstrating that there is a small population of SP-containing intracardiac neurones (Baluk & Gabella, 1989b) and also the presence of intrinsic mechanosensitive neurones in the cat heart (Nozdrachev & Pogorelov, 1982). Furthermore, in the canine heart, spontaneous activity in intracardiac neurones was increased in 14% of cells as a result of mechanical stimulation of discrete areas of the heart (Gagliardi et al. 1988). In our studies of guinea-pig intracardiac neurones, gentle deformation resulted in spike discharge in a small population of neurones. In general, these cells were small and rounded in appearance and had firing characteristics similar to M cells. At present, we cannot exclude the possibilty that the evoked firing was some form of injury discharge however, the mechanical stimulation did not appear to cause any deterioration in the condition of the cells. Therefore, as in the cat and dog atria, there may also be a population of mechanosensitive neurones in the guinea-pig heart.

Paratracheal ganglia

Unlike the intrinsic neurones of the heart, the rat paratracheal neurones studied here could not be classified into distinct subtypes. Instead their firing characteristics ranged between two extremes. The most commonly observed type of behaviour, which represented one extreme, was the firing of short high frequency bursts of action potentials in response to prolonged intrasomal current injection. At the other extreme, and less commonly observed, were cells which fired tonically, at low frequencies in response current stimulation. Paratracheal neurones also displayed a variety of different membrane currents including an M-current, "instantaneous" and time-dependent inward rectifier currents and a calcium-activated potassium current (see Chapter 6). Analysis of these membrane currents indicates that one reason for the different firing characteristics of tonic and burst firing cells may be related to differences in the relative magnitudes of their post-spike calcium-activated potassium currents. This current was responsible for the generation of the slow after-hyperpolarization in these neurones and was activated by calcium entry into the cell during the action potential (see Chapter 6 and Allen & Burnstock, 1990b). In tonic firing cells, the duration of the after-hyperpolarization was, on average, almost three times as long as that displayed by burst firing cells and acted to inhibit rapid spike discharge. In burst firing cells, the after-hyperpolarization following a single action potential was quite small and would thus only have a limited inhibitory effect upon multiple spike discharge. However, following a rapid burst of firing, the size of the after-hyperpolarization in these cells increased dramatically and acted to prevent prolonged firing. Preliminary studies have also revealed an additional transient outward "A type" current in these cells (Allen, unpublished observation). This transient outward current was generally

smaller and shorter than that exhibited by intracardiac neurones (see earlier). The peak current (measured following a voltage step from -100 to -30 mV) rarely exceeded 500 pA and had a duration of approximately 50-70 ms (compared to currents of up to 1 nA and durations of 200-1000 ms seen in intracardiac neurones). In most paratracheal neurones, this current reached a peak within 6-10 ms, however, the time constant of inactivation varied considerably between cells (range 12-50 ms). From the limited data obtained about this current, it would appear that cells displaying larger and more slowly inactivating transient outward currents tended to fire at lower frequencies than cells exhibiting smaller, more rapidly inactivating currents. Therefore, this "A type" current, along with the after-hyperpolarization, may be involved in controlling the rate of action potential discharge in paratracheal neurones.

Studies of the paratracheal ganglia of other species have revealed the presence of a variety of different types of neurone. In the ferret trachea, a population of neurones have been reported to exhibit "profound" post-spike hyperpolarizations and, on the basis of the size of this after-hyperpolarization, they have been termed AH cells in order to emphasise their similarity to enteric AH/type 2 cells (Cameron & Coburn, 1984). However, the figures published to illustrate this "profound" after-hyperpolarization in ferret neurones do, in fact, only demonstrate after-hyperpolarizations of approximately 200 ms (Cameron & Coburn, 1984). Such after-hyperpolarizations are very similar to those displayed by tonic firing rat cells and are almost two orders of magnitude shorter than those reported in gut neurones. Furthermore, unlike enteric AH/type 2 cells (Nishi & North, 1973; Hirst & Spence, 1973), action potentials in the ferret trachea were blocked by TTX (Coburn, 1988). Therefore at present, it remains unclear whether the AH type cells of the ferret

trachea are really that similar to enteric AH/type 2 neurones. A second cell type distinguished in ferret ganglia (B cells) exhibited no somal action potentials, but on the basis of the presence of synaptic potentials, were suggested to include interneurones (Cameron & Coburn, 1984). No equivalent cell type has been distinguished in the rat trachea. In a subsequent study of ferret paratracheal neurones, an additional type of cell, that was found to be capable of generating highly damped trains of action potentials, was observed (Baker et al. 1986). Examination of recordings made from these cells suggests that they may have been damaged during impalement as they exhibited rather small action potentials (mean 64 mV) and low membrane potentials. Similar damped firing has been observed in injured, burst firing rat paratracheal neurones, suggesting that the damped firing cells in ferret ganglia may, under optimum conditions, also be capable of repetitive burst firing. In the rabbit, a brief abstract has reported the presence of two electrophysiologically distinct types of paratracheal neurone (Fowler & Weinreich, 1986). One type were highly refractory and exhibited prolonged post-spike hyperpolarizations, whilst the other cell type were capable of sustained action potential discharge, similar to the tonic firing rat paratracheal neurones.

Burst firing cells have been reported in a population of cat paratracheal neurones studied in vivo (Mitchell et al. 1987). These cells, like burst firing rat paratracheal neurones, all exhibited high levels of subthreshold, cholinergic fast synaptic potentials. In the cat, it has been suggested that burst firing of the ganglion cells requires synchronous multiple synaptic inputs from extrinsic nerve fibres (Mitchell et al. 1987). However, in the present study of rat paratracheal neurones, high levels of spontaneous synaptic activity were evident, even in the absence of extrinsic innervation (see Chapter 6 and Allen & Burnstock, 1990b),

suggesting that there may be intrinsic, as well as extrinsic synaptic inputs to these neurones. Furthermore, whilst no rat paratracheal neurones were observed to display spontaneous pace-maker activity, the fact that many neurones have inherent current-evoked burst firing characteristics suggests that the synaptic inputs to these cells may only trigger and/or modulate burst firing by these cells. The role of burst firing rat paratracheal neurones is as yet unknown. In the cat, burst firing of intrinsic ganglion cells has been found to occur with either an inspiratory or an expiratory rhythm and is related to activity in the phrenic nerve (Mitchell et al. 1987). Lucifer yellow staining of neurones firing with an inspiratory rhythm has demonstrated processes projecting from these cells into the trachealis muscle (Baker, 1986; Mitchell et al. 1987) and tension measurements made from the cervical trachea indicate that the trachealis muscle contracts with a similar inspiratory rhythm (Mitchell, Herbert & Baker, 1984). Therefore, it seems likely that a population of burst firing paratracheal neurones, at least in the cat, may be responsible for controlling the calibre of the trachea during the different phases of the respiratory cycle.

Studies of the synaptic interactions occurring within paratracheal ganglia have been very limited. Nicotinic cholinergic synaptic interactions have been directly demonstrated in the ferret, cat and rat ganglia (Cameron & Coburn, 1984; Mitchell et al. 1987; Allen & Burnstock, 1990b and Chapter 6). In addition, focal stimulation of the laryngeal nerve and interganglionic nerve trunks has revealed the presence of fast inhibitory and slow excitatory post-synaptic potentials in ferret paratracheal ganglia, but the mediators of these responses remains unknown (Cameron & Coburn, 1984). Studies of muscarinic receptor-mediated responses in the airways have revealed the presence of both M_1 and M_2 muscarinic receptor subtypes

on intrinsic neurones (Fryer & MacLagan, 1984; Bloom et al. 1987; Minette & Barnes, 1988; Lammers, Minette, McCusker & Barnes, 1989). M_1 receptors are thought to be involved in modulating vagally induced bronchoconstriction (Bloom et al. 1987; Lammers et al. 1989), whilst the M_2 receptors are thought to be autoreceptors acting to inhibit the release of acetylcholine from these neurones (Minette & Barnes, 1988). Autoradiographic studies have localised muscarinic receptors on almost all rat paratracheal neurones in culture (James et al. 1990). However, the actions of exogenously applied muscarinic agonists upon these neurones has not yet been investigated. In the guinea-pig, there is also evidence for M_1 receptors on the sympathetic nerves innervating the airways. Sympathetic nerve stimulation produces bronchodilation, and activation of the muscarinic receptors present on these nerves is believed to inhibit noradrenaline release and thereby indirectly increase the effect of vagally induced bronchoconstriction (MacLagan, Fryer & Faulkner, 1989). The precise location of these M_1 receptors is currently unknown. They may be in sympathetic ganglia, as with the M_1 receptors described in other sympathetic ganglia (Ashe & Yarosh, 1984), or they may be present on sympathetic nerves which are closely associated with airway cholinergic nerves or ganglia.

Noradrenaline acting at prejunctional α_2-adrenoceptors has been reported to inhibit the contraction of tracheal smooth muscle in the guinea-pig by inhibiting cholinergic neurotransmission (Grundström et al. 1981). Presynaptic inhibition mediated by α-adrenoreceptors has also been reported in ferret paratracheal ganglia (Baker et al. 1983) and more recently, the possible involvement of prejunctional β_2-adrenoceptors has been suggested (Skoogh & Svedmyr, 1989). However, at present, there is some debate as to whether there is sympathetic innervation of tracheal

ganglia. Noradrenergic nerves have been described around a small proportion of intrinsic ganglion cells in the cow lung (Jacobowitz, Kent, Fleisch & Cooper, 1973) and in cat bronchi (Knight, 1980), whereas a recent study of the mouse, rat and guinea-pig trachea did not detect noradrenergic fibres around tracheal ganglia (Baluk & Gabella, 1989a). In the absence of functional sympathetic innervation of tracheal ganglia, then circulating catecholamines may play an important role, since the ganglia have many small blood vessels within them (Baluk et al. 1985), or alternatively noradrenaline may be released from associated SIF cells.

GABA has previously been shown to depress cholinergic transmission in the airways through $GABA_A$ receptor-mediated inhibition of acetylcholine release (Tamaoki et al. 1987), but it may also play a role in modulating ganglionic neurotransmission through the activation of $GABA_A$ receptors present on intrinsic neurones (see Chapter 7 and Allen & Burnstock, 1990c). However, as with the effects of noradrenaline, an intrinsic source of GABA has yet to be identified (see Chapter 7). In addition to GABA and noradrenaline, a variety of other neurotransmitters have been shown to have prejunctional inhibitory actions upon vagal cholinergic neurotransmission. These include enkephalin, NPY and histamine (Russell & Simons, 1985; Stretton & Barnes, 1988; Ichinose, Stretton, Schwartz & Barnes, 1989). Whilst more recently, substance P and neurokinin A have been shown to facilitate neurotransmission in guinea-pig pulmonary parasympathetic nerves through NK_2 receptors (Hall, Barnes, Meldrum & MacLagan, 1989).

In conclusion, it would appear that paratracheal neurones and ganglia could potentially be the sites of complex interactions between the sympathetic and parasympathetic nerves innervating the airways. It is clear from the studies outlined

in the first two sections of this discussion that there is still much to learn about the intrinsic ganglia of the heart and trachea. In the following, final section of this discussion some ideas and suggestions for future work to help to further elucidate the properties and functions of these ganglia will be outlined.

Suggestions for future studies

The tissue culture and in vitro ganglion preparations employed in this thesis both offer a variety of advantages and disadvantages which could be exploited in future studies of intracardiac and paratracheal neurones. Some ideas for more experiments and possible developments to extend the uses of these preparations in order to facilitate further studies of these ganglia will now be discussed.

Culture preparations

From the studies carried out so far, it is clear that intracardiac neurones display considerable neurochemical complexity. However, there are many other potential neurotransmitters and neuromodulator substances localised in the heart, which may also act upon intracardiac neurones, and have yet to be studied. For example, autoradiographic studies of sections of the heart have localised SP binding sites over intracardiac ganglia (Hoover & Hancock, 1988) and in a brief abstract, SP has been reported to act upon a population of guinea-pig intracardiac neurones in situ (Konishi et al. 1984), but the proportion of intracardiac neurones expressing these, or any other neurokinin receptors has not yet been determined.

Studies of the neurochemical and electrophysiological properties of intracardiac neurones could also be combined with morphological and immunocytochemical techniques to help to build up a profile of the different cell types. Such a system of "chemical coding" has been proposed to help to clarify the innervation of the gut (Costa, Furness & Gibbins, 1986). Central to establishing whether a similar principle can be applied in the heart would be the demonstration of regional differences in

the projections and tissues innervated by the intracardiac neurones. There is evidence, from studies of canine and rat atria, of the selective innervation of different areas of the heart by discrete populations of intracardiac ganglia (Randall & Ardell, 1985a, b; Randall et al. 1986a, b; Blomquist et al. 1987; Pardini et al. 1987). Although many of the intracardiac ganglia are diffusely spread within the atria, there are concentrations of ganglia around the nodal regions, and it would be feasible to produce cultures containing neurones from these areas alone. By combining retrograde labelling and tissue culture techniques, we may also be able to gain some insight into the projections and properties of individual ganglion cells. In particular, the possibility of locally injecting areas of the heart with fluorescent rhodamine labelled microspheres could be particularly promising. These microspheres are taken up by nerves and retrogradely transported, but are not cytotoxic (Katz, Burkhalter & Dreyer, 1984). Furthermore, they remain within the labelled cell for considerable periods of time. Thus, after injecting the microspheres into a selected area of the heart and allowing a suitable period for their uptake and transport by intrinsic neurones, cultures could then be prepared in the usual way. Subsequently, the labelled neurones could then be identified and studied using electrophysiological, autoradiographical and immunocytochemical techniques.

Another very interesting line of investigation would be into possible synaptic interactions between intracardiac neurones in culture. The dissociation methods currently employed to produce these cell cultures do, by necessity, involve the disruption of all synaptic interactions. The electrophysiological studies carried out so far have been confined to atrial neurones maintained for 7 to 14 days in culture. The reasons for using this age range were twofold. Firstly, similar studies of neurones from other dissociated culture preparations, where it is possible to directly

correlate the properties of the cultured and the in situ ganglion cells, indicate that the basic electrophysiological characteristics of the cells are maintained even in very young cultures (see for example Bader, Bertrand & Kato, 1982). Secondly, cell proliferation during prolonged periods in culture, tended to result in the neurones being overgrown by other cells. Also, the increased density of cells in the cultures caused the medium to become exhausted and acidic very quickly, leading to further deterioration in the condition of the neurones. More frequent replacement of the medium helped in this respect, however this caused further cell proliferation and, in itself, disturbed the neurones. A possible solution to the excessive non-neuronal cell proliferation would be to use mitotic inhibitors, but it would be necessary to carry out experiments to test whether they altered the phenotype of the neurones. Previous studies of other ganglia suggest that functional synaptic interactions do not become fully established until between 3 and 5 weeks in culture (Baccaglini & Cooper, 1982). Even then, the nature of the innervation depends to a large extent upon the presence or absence of non-neuronal cells. In the present studies on cultures of less than 2 weeks of age, spontaneous synaptic potentials have been neither observed nor have they been evoked. This observation is supported at the ultrastructural level, where very few synapses have been observed at this age in culture (Kobayashi et al. 1986a). Therefore, in future studies, it would be interesting to investigate the possibility of synapse formation between intracardiac neurones when maintained for prolonged periods in culture. Such synaptic interactions could then be studied using focal stimulation techniques to determine whether, for example, postsynaptic muscarinic or purinergic responses could be evoked which are similar to the effects produced by the exogenously applied agonists at these receptors. Furthermore, the presence of synaptic interactions would also allow studies of prejunctional modulatory mechanisms to be carried out.

A dissociated cell culture preparation has recently been developed to study rat paratracheal neurones in culture. Using this preparation, muscarinic receptors have been localised on the vast majority of neurones (James et al. 1990). In addition, preliminary studies indicate that these cultures are suitable for electrophysiological studies and that they exhibit functional nicotinic receptors (Burnstock, Allen & Hassall, 1987). This preparation would be a very useful adjunct to the in situ tracheal preparation, as the neurones are free from overlying glial cells and could thus be used in patch-clamp studies. Furthermore, they could also be utilised in the same ways as outlined above for cultured intracardiac neurones.

Intact ganglion preparations

The in vitro preparation of the trachea developed as part of this thesis contains a largely intact plexus of nerves and intrinsic ganglia and, as such, is potentially ideal for studying the synaptic interactions occurring within paratracheal ganglia. The spontaneous synaptic responses observed so far were largely fast cholinergic excitatory post-synaptic potentials. However, by using repetitive nerve stimulation it may be possible to evoke slow excitatory and inhibitory responses, similar to those observed in the ferret trachea (Cameron & Coburn, 1984). Stimulation could be applied by either using field stimulation across the trachealis muscle or more focally by using sodium chloride filled microelectrodes placed on or close to selected nerve trunks. If synaptic responses can be evoked, then the underlying ionic nature of the responses and the neurotransmitters responsible could be investigated using selective agonists and antagonists. In addition to nerve stimulation, it may also be possible to impale two neurones and stimulate one, whilst recording any evoked responses from the other. Preliminary studies using focal

nerve stimulation have elicited slow excitatory synaptic responses in two paratracheal neurones and in one of these cells, the response was associated with a fall in membrane conductance. This slow synaptic response may arise as a result of the inhibition of the M-current in these cells. If this is so, then this response may be common to many paratracheal neurones.

As with studies of intracardiac neurones, there are still many neurotransmitters and neuromodulators, such as VIP and purines, that have potent actions in the airways, but have yet to be applied directly onto paratracheal neurones. In the case of drugs which act upon both the neurones and the muscle, some means of immobilising the trachea would have to be developed as contraction of the trachealis muscle would dislodge the recording electrode. This is likely to require selective drug treatments as the ganglia are too diffusely spread to be successfully immobilised using pinning techniques. Two possible drugs that could be of use are verapamil and nifedepine which block action potential discharge in smooth muscle.

Finally, the development of a similar intact ganglion preparation of intracardiac neurones would obviously be extremely important in future studies of the intrinsic innervation of the heart. Some preliminary attempts have been made to develop such a preparation, however, there are a number of problems which still need to be overcome. For example, unlike the trachealis muscle, the atria are much more three-dimensional structures and therefore it is difficult to pin them out so that the ganglia can be clearly visualised. Furthermore, when pinned out, the area of the atria is quite considerable (approximately 2-3 cm^2 in young rats). Therefore, unless only small areas of the atria are studied at one time, it would be almost impossible to achieve the low fluid levels required to visualise the ganglia with Hoffman

modulation optics and at the same time maintain superfusion of the tissue. Finally, and what to date has proven to be the most difficult problem to overcome, is the immobilisation of the spontaneously contracting myocardium to allow stable recordings to be made, without, at the same time, altering the properties of the intracardiac neurones. Some preliminary studies have enabled brief (< 5 min) recordings from rat intracardiac neurones (Allen, unpublished observation). From this very limited data, it would appear that, like guinea-pig intracardiac neurones, a population of rat neurones also exhibit a pronounced hump in the repolarization phase of their action potentials and a prolonged spike after-hyperpolarization.

In summary, the intramural ganglia of the heart and trachea display a high level of complexity and may be the sites for integration of parasympathetic, sympathetic and sensory innervation within these tissues. Together, the tissue culture and in situ ganglion preparations used in this thesis provide a unique means of studying the properties and roles of these neurones in the local innervation of the heart and trachea.

REFERENCES

Adams, P.R. & Brown, D.A. (1975). Actions of γ-aminobutyric acid on sympathetic ganglion cells. Journal of Physiology 250, 85-120.

Adams, P.R. & Brown, D.A. (1982). Synaptic inhibition of the M-current: slow excitatory post-synaptic potential mechanism in bullfrog sympathetic neurones. Journal of Physiology 332, 263-272.

Adams, P.R., Brown, D.A. & Constanti, A. (1982a). M-currents and other potassium currents in bullfrog sympathetic neurones. Journal of Physiology 330, 537-642.

Adams, P.R., Brown, D.A. & Constanti, A. (1982b). Pharmacological inhibition of the M-current. Journal of Physiology 332, 223-262.

Ahmed, Z. & Connor, J. (1979). Measurement of calcium influx under voltage clamp in molluscan neurones using the metallochromic dye Arsenazo III. Journal of Physiology 286, 61-82.

Akaike, N., Inomata, N. & Tokutomi, N. (1987). Contribution of chloride shifts to the fade of γ-aminobutyric acid-gated currents in frog dorsal root ganglion cells. Journal of Physiology 391, 219-234.

Akasu, T., Gallagher, J.P., Koketsu, K. & Shinnick-Gallagher, P. (1984). Slow excitatory post-synaptic currents in bull-frog sympathetic neurones. Journal of Physiology 351, 583-593.

Akasu, T., Hirai, K. & Koketsu, K. (1983). Modulatory actions of ATP on membrane potentials of bullfrog sympathetic ganglion cells. Brain Research 258, 313-317.

Akasu, T. & Koketsu, K. (1985). Effect of adenosine triphosphate on the sensitivity of the nicotinic acetylcholine-receptor in the bullfrog sympathetic ganglion cell. British Journal of Pharmacology 84, 525-531.

Akasu, T., Shinnick-Gallagher, P. & Gallagher, J.P. (1984). Adenosine mediates a slow hyperpolarizing synaptic potential in autonomic neurones. Nature 311, 62-65.

Allen, T.G.J. & Burnstock, G. (1987). Intracellular studies of the electrophysiological properties of cultured intracardiac neurones of the guinea-pig. Journal of Physiology 388, 349-366.

Allen, T.G.J. & Burnstock, G. (1990a). M_1 and M_2 muscarinic receptors mediate excitation and inhibition of guinea-pig intracardiac neurones in culture. Journal of Physiology (in press).

Allen, T.G.J. & Burnstock, G. (1990b). A voltage-clamp study of the electrophysiological characteristics of the paratracheal neurones of the rat trachea. Journal of Physiology (in press).

Allen, T.G.J. & Burnstock, G. (1990c). $GABA_A$ receptor-mediated increase in membrane chloride conductance in rat paratracheal neurones. British Journal of Pharmacology (submitted for publication).

Allen, T.G.J. & Burnstock, G. (1990d). The actions of adenosine 5'-triphosphate on guinea-pig intracardiac neurones in culture. British Journal of Pharmacology (submitted for publication).

Anwar-UL, S., Gilani, H. & Gobbin, L.B. (1986). The cardio-selectivity of himbacine: a muscarinic receptor antagonist. Naunyn Schmiedebergs Archives of Pharmacology 332, 16-20.

Ashe, J.H. & Yarosh, C.A. (1984). Differential and selective antagonism of the slow-inhibitory postsynaptic potential and slow excitatory postsynaptic potential by gallamine and pirenzepine in the superior cervical ganglion of the rabbit. Neuropharmacology 23, 1321-1329.

Baccaglini, P.I. & Cooper, E. (1982). Influences on the expression of acetylcholine receptors on rat nodose neurones in culture. Journal of Physiology 324, 441-451.

Bachelard, H., St-Pierre, S. & Rioux, F. (1986). The coronary vasodilation effect of neurotensin in the guinea-pig isolated heart. Peptides 7, 431-435.

Bader, C.R., Bertrand, D. & Kato, G. (1982). Chick cilary ganglion in dissociated cell culture. II. Electrophysiological properties. Developmental Biology 94, 131-141.

Baker, D.G. (1986). Parasympathetic motor pathways to the trachea: recent morphologic and electrophysiologic studies. Clinical Chest Medicine 7, 223-229.

Baker, D.G., Basbaum, C.B., Herbert, D.A. & Mitchell, R.A. (1983). Transmission in airway ganglia of ferrets: inhibition by norepinephrine. Neuroscience Letters 41, 139-143.

Baker, D.G., McDonald, D.M., Basbaum, C.B. & Mitchell, R.A. (1986). The architecture of nerves and ganglia of the ferret trachea as revealed by acetylcholinesterase histochemistry. Journal of Comparative Neurology 246, 513-526.

Baluk, P., Fujiwara, T. & Matsuda, S. (1985). The fine structure of the ganglia of the guinea-pig trachea. Cell and Tissue Research 239, 51-60.

Baluk, P. & Gabella, G. (1989a). Ganglion neurones in the rat trachea lack sympathetic input and some of them partially express a noradrenergic phenotype. Journal of Physiology 416, 16P.

Baluk, P. & Gabella, G. (1989b). Some intrinsic neurones of the guinea-pig heart contain substance P. Neuroscience Letters 104, 269-273.

Barlow, R.B., Berry, K.J., Glenton, P.A.M., Nikolaou, N.N. & Soh, K.S. (1976). A comparison of affinity constants for muscarine sensitive acetylcholine receptors in guinea-pig atrial pace-maker cells at 29^{o}C and in ileum at 29^{o}C and 37^{o}C. British Journal of Pharmacology 58, 613-620.

Barlow, R.B. & Shepherd, M.K. (1985). A search for selective antagonists at M_2-

muscarinic receptors. British Journal of Pharmacology 85, 427-435.

Barlow, R.B. & Shepherd, M.K. (1986). A further search for selective antagonists at M_2-muscarinic receptors. British Journal of Pharmacology 89, 837-843.

Barnes, P.J. (1986). Neural control of human airways in health and disease. State of the Art. American Review of Respiratory Diseases 134, 1289-1314.

Barnes, P.J. (1987). Vasoactive intestinal polypeptide and pulmonary function, In Current Topics in Pulmonary Pharmacology and Toxicology, ed. Hollinger, M.A., pp. 156-173. New York: Elsevier.

Barnes, P.J. (1989). Regulatory peptides in the respiratory system. In Regulatory Peptides, ed. Polak, J.M., pp. 317-333. Berlin: Birkhäuser Verlag.

Barrett, J.N., Magleby, K.L. & Pallotta, B.S. (1982). Properties of single calcium activated potassium channels in cultured rat muscle. Journal of Physiology 331, 211-230.

Baumgarten, H.G., Holstein, A.-F. & Owman, C. (1970). Auerbach's plexus of mammals and man: electron microscopic identification of the different types of neuronal processes in myenteric ganglia form Rhesus monkeys, guinea-pigs and man. Zeitschrift fur Zellforschung 106, 376-397.

Belluzzi, O., Sacchi, O. & Wanke, E. (1985). Identification of delayed potassium and calcium currents in the rat sympathetic neurone under voltage clamp. Journal of Physiology 358, 109-129.

Belvisi, M.G., Ichinose, M. & Barnes, P.J. (1989). Modulation of non-adrenergic, non-cholinergic neural bronchoconstriction in guinea-pig airways via $GABA_B$-receptors. British Journal of Pharmacology 97, 1225-1231.

Berne, R.M. (1980). The role of adenosine in the regulation of coronary blood flow. Circulation Research 47, 807-813.

Birdsall, N.J.M. & Hulme, E.C (1987). Characterisation of muscarinic acetylcholine

receptors and their subtypes. I.S.I. Atlas of Science: Pharmacology, 98-100.

Blackman, J.G. & Purves, R.D. (1969). Intracellular recordings from ganglia of the thoracic sympathetic chain of guinea-pig. Journal of Physiology 203, 173-198.

Blomquist, T.M., Priola, D.V. & Romero, A.M. (1987). Source of intrinsic innervation of canine ventricles: a functional study. American Journal of Physiology 252, H638-H644.

Bloom, J.W., Yamamura, H.I., Baumgartener, C. & Halonen, M. (1987). A muscarinic receptor with a high affinity for pirenzepine mediates vagally induced bronchoconstriction. European Journal of Pharmacology 113, 21-27.

Bonner, T.I. (1989). The molecular basis of muscarinic receptor diversity. Trends In Neurosciences 12, 148-151.

Bonner, T.I., Buckley, N.J., Young, A.C. & Brann, M.R. (1987). Identification of a family of muscarinic acetylcholine receptor genes. Science 237, 527-532.

Bonner, T.I., Young, A.C., Brann, M.R. & Buckley, N.J. (1988). Cloning and expression of the human and rat m5 muscarinic acetylcholine receptor genes. Neuron 1, 403-410.

Bormann, J., Hamill, O.P., Sakmann, B. (1987). Mechanism of anion permeation through channels gated by glycine and γ-aminobutyric acid in mouse cultured spinal neurones. Journal of Physiology 385, 243-286.

Bowery, N.G. & Brown, D.A. (1972). γ-Aminobutyric acid uptake by sympathetic ganglia. Nature 238, 89-91.

Brown, A.M. (1967). Cardiac sympathetic adrenergic pathways in which sympathetic transmission is blocked by atropine sulphate. Journal of Physiology 191, 271-288.

Brown, D.A. (1988). M currents. In Ion Channels, Vol. 1, ed. Narahashi, T., pp. 55-94. New York: Plenum Press.

Brown, D.A. & Adams, P.R. (1980) Muscarinic suppression of a novel voltage-sensitive K^+-current in a vertebrate neurone. Nature 283, 673-608.

Brown, D.A., Constanti, A. & Adams, P.R. (1983). Ca^{++}-activated potassium current in vertebrate sympathetic neurons. Cell Calcium 4, 407-420.

Brown, D.A. & DiFrancesco, D. (1980). Voltage-clamp investigations of membrane currents underlying pace-maker activity in rabbit sino-atrial node. Journal of Physiology 308, 331-351.

Brown, D.A., Fatherazi, S., Garthwaite, J. & White, R.D. (1980). Muscarinic receptors in rat sympathetic ganglia. British Journal of Pharmacology 70, 577-592.

Brown, D.A., Forward, A. & Marsh, S. (1980). Antagonist discrimination between ganglionic and ileal muscarinic receptors. British Journal of Pharmacology 71, 362-364.

Brown, D.A., Gähwiler, B.H., Marsh, S.J. & Selyanko, A.A. (1986). Mechanisms of muscarinic excitatory synaptic transmission in ganglia and brain. Subtypes of muscarinic receptors II. Trends in Pharmacological Sciences Supplement, 66-71.

Brown, D.A. & Galvan, M. (1977). Influence of neuroglial transport on the actions of γ-aminobutyric acid in mammalian ganglion cells. British Journal of Pharmacology 59, 373-378.

Brown, D.A. & Selyanko, A.A. (1985a). Two components of the muscarine-sensitive membrane current in rat sympathetic neurones. Journal of Physiology 365, 335-363.

Brown, D.A. & Selyanko, A.A. (1985b). Membrane currents underlying the cholinergic slow excitatory post-synaptic potential in the rat

sympathetic ganglion. Journal of Physiology 365, 365-387.

Brown, J.R., Hayes, A.G. Meecham, K.G. & Tyers, M.B. (1983). Effect of SP agonists and antagonists on guinea-pig isolated trachea preparation. British Journal of Pharmacology 79, Supplement 156P.

Burnstock, G. (1972). Purinergic nerves. Pharmacological Reviews 24, 509-581.

Burnstock, G. (1978). A basis for distinguishing two types of purinergic receptor. In Cell Membrane Receptors for Drugs and Hormones: A Multi-disciplinary Approach, ed. Straub, R.W. & Bolis, L., pp. 107-118. New York: Raven Press.

Burnstock, G. (1980). Purinergic receptors in the heart. Supplement I, Circulation Research 46, I175-I182.

Burnstock, G. (1985). Purinergic mechanisms broaden their sphere of influence. Trends in Neurosciences 8, 5-6.

Burnstock, G. (1986a). The changing face of autonomic neurotransmission. Acta Physiologica Scandaninavica 126, 67-91.

Burnstock, G. (1986b). Purines as cotransmitters in adrenergic and cholinergic neurones. Progress in Brain Research 68, ed. Hökfelt, T., Fuxe, K. & Pernow, B., Chapter 13, Amsterdam: Elsevier.

Burnstock, G. (1988). Autonomic neural control mechanisms. In The Airways Neural Control in Health and Disease, ed. Kaliner, M.A. & Barnes, P.J., pp. 1-22. New York, Basel: Marcel Dekker.

Burnstock, G., Allen, T.G.J. & Hassall, C.J.S. (1987). The electrophysiologic and neurochemical properties of paratracheal neurones in situ and in dissociated cell culture. American Review of Respiratory Disease 136, S23-S26.

Burnstock, G. & Kennedy, C. (1985). Is there a basis for distinguishing two types of

P_2-purinoceptor? General Pharmacology 16, 433-440.

Burnstock, G. & Warland, J.J.I. (1987). P_2-purinoceptors of two subtypes in the rabbit mesenteric artery: reactive blue 2 selectively inhibits responses mediated via the P_{2y}- but not P_{2x}-purinoceptor. British Journal of Pharmacology 90, 383-391.

Cadieux, A., Springall, D.R., Mulderry, P.K., Rodrigo, J., Ghatei, M.A., Terenghi, G., Bloom, S.R. & Polak, J.M. (1986). Occurrence, distribution and ontogeny of CGRP immunoreactivity in the rat lower respiratory tract: effect of capsaicin treatment and surgical denervations. Neuroscience 19, 605-627.

Calaresu, F.R. & St. Louis, A.J. (1967). Topography and numerical distribution of intracardiac ganglion cells in the cat. Journal of Comparative Neurology 131, 55-66.

Cameron, A.R. & Coburn, R.F. (1982). Calcium dependence of the afterhyperpolarization of type A cells of the ferret paratracheal ganglion. Federation Proceedings 41, 1356.

Cameron, A.R. & Coburn, R.F. (1984). Electrical and anatomical characteristics of the cells of the ferret paratracheal ganglion. American Journal of Physiology 246, C450-C458.

Cameron, A.R., Johnston, C.F., Kirkpatrick, C.T. & Kirkpatrick, M.C.A. (1983). The quest for the inhibitory neurotransmitter in bovine smooth muscle. Quarterly Journal of Experimental Physiology 68, 413-426.

Cassell, J.F. & McLachlan, E.M. (1987). Muscarinic agonists block five different potassium conductances in guinea-pig sympathetic neurones. British Journal of Pharmacology 91, 259-261.

Cherubini, E. & North, R.A. (1984a). Actions of γ-aminobutyric acid on neurones of the guinea-pig myenteric plexus. British Journal of Pharmacology 82, 93-100.

Cherubini, E. & North, R.A. (1984b). Inhibition of calcium spikes and transmitter release by γ-aminobutyric acid in guinea-pig myenteric plexus. British Journal of Pharmacology 82, 101-105.

Cheung, A., Polak, J.M., Bauer, F.E., Cadieux, A., Christofides, N.D., Springall, D.R. & Bloom S.R. (1985). Distribution of galanin immunoreactivity in the respiratory tract of the of pig, guinea-pig, rat and dog. Thorax 40, 889-896.

Chiang, C-H. & Gabella, G. (1986). Quantitative study of the ganglion neurons of the mouse trachea. Cell and Tissue Research 246, 243-252.

Christofides, N.D., Yiangou, Y., Piper, P.J., Ghatei, M.A., Sheppard, M.A., Tatemoto, K., Polak, J.M. & Bloom, S.R. (1984). Distribution of peptide histidine isoleucine in the mammalian respiratory tract and some aspects of its pharmacology. Endocrinology 115, 1958-1963.

Ciriello, J. & Calaresu, F.R. (1982). Medullary origin of vagal preganglionic axons to the heart of the cat. Journal of the Autonomic Nervous System 5, 9-22.

Coburn, R.F. (1988). Cholinergic neuroeffector mechanisms in airway smooth muscle. In The Airways Neural Control in Health and Disease, ed. Kaliner, M.A. & Barnes, P.J., pp. 159-186. New York: Marcel Dekker.

Coburn, R.F. & Kalia, M.P. (1986). Morphologic features of spiking and non-spiking cells in the paratracheal ganglion of the ferret. Journal of Comparative Neurology 254, 341-351.

Coburn, R.F. & Tomita, T. (1973). Evidence for noradrenergic inhibitory nerves in the guinea-pig trachealis muscle. American Journal of Physiology 224, 1072-1080.

Coleman, R.A. & Levy, G.P. (1974). A non-adrenergic inhibitory nervous pathway in guinea-pig trachea. British Journal of Pharmacology 52, 167-174.

Connor, J.A. & Stevens, C.F. (1971). Voltage clamp studies of a transient outward

membrane current in gastropod neural somata. Journal of Physiology 213, 21-30.

Constanti, A., Adams, P.R. & Brown, D.A. (1981). Why do barium ions imitate acetylcholine? Brain Research 206, 244-250.

Constanti, A. & Galvan, M. (1983). Fast inward-rectifying current accounts for anomalous rectification in olfactory cortex neurones. Journal of Physiology 385, 153-178.

Constanti, A. & Sim, J.A. (1987). Muscarinic receptors mediating suppression of the M-current in guinea-pig olfactory cortex neurones may be of the M_2 subtype. British Journal of Pharmacology 90, 3-5.

Costa, M. & Furness, J.B. (1982). Nervous control of intestinal motility. In Handbook of Experimental Pharmacology, Vol. 59, Mediators and Drugs in Gastrointestinal Motility I. Morphological Basis and Neurophysiological Control, ed. Bertaccini, G., pp. 279-382. Berlin: Springer.

Costa, M., Furness, J.B. & Gibbins, I.L. (1986). Chemical coding in enteric neurones. In Progress in Brain Research, Vol. 68, ed. Hökfelt, T., Fuxe, K. & Pernow, B., pp. 217-239. B.V. Amsterdam, New York, Oxford: Elsevier Scientific Publications.

Crepel, F. & Penit-Soria, J. (1986). Inward rectification and low threshold calcium conductance in rat cerebellar Purkinje cells. An in vitro study. Journal of Physiology 372, 1-23.

Crowcroft, K., Jessup, S. & Ramwell, P.W. (1967). Thin-layer chromatography of 1-dimethyl-aminonapthaline-5-sulphonyl derivatives of amino acids present in superfusates of the cat cerebral cortex. Biochemical Journal 103, 79-85.

Crowe, R. & Burnstock, G. (1982). Fluorescent histochemical localisation of quinacrine-positive neurones in the guinea-pig and rabbit atrium.

Cardiovascular Research, 16, 384-390.

Dalsgaard, C.-J., Franco-Cereceda, A., Lundberg, J.M., Theodorsson-Norheim, E. & Hökfelt, T. (1986). Distribution and origin of substance P and neuropeptide Y immunoreactive nerves in the guinea-pig heart. Cell and Tissue Research 243, 477-485.

Da Prada, M., Richards, J.G. & Lorez, H.P. (1978). Blood platelets and biogenic monoamines: Biochemical, pharmacological, and morphological studies. In Platelets: A Multidisciplinary Approach, ed. de Gaetano, G. & Garattini, S., pp. 331-353. New York: Raven Press.

Davies, F., Francis, E.T.B. & King, T.S. (1952). The conducting system of the vertebrate heart. Biological Reviews of the Cambridge Physiological Society 21, 173-188.

Dayer, A.M., DeMey, J. & Will, J.A. (1985). Localization of somatostatin-, bombesin- and serotonin-like immunoreactivity in the lung of the foetal rhesus monkey. Cell and Tissue Research 239, 621-625.

DeGroat, W.C. (1970). The actions of γ-aminobutyric acid and related amino acids on mammalian autonomic ganglia. Journal of Pharmacology and Experimental Therapeutics 172, 384-396.

DeGroat, W.C. & Saum, W.R. (1972). Sympathetic inhibition of the urinary bladder of pelvic ganglionic transmission in the cat. Journal of Physiology 220, 297-314.

Deisz, R.A. & Lux, H.D. (1985). γ-Aminobutyric acid-induced depression of calcium currents of chick sensory neurones. Neuroscience Letters 56, 205-210.

Dennis, M.J., Harris, A.J. & Kuffler, S.W. (1971). Synaptic transmission and its duplication by focally applied acetylcholine in parasympathetic neurons in the heart of the frog. Proceedings of the Royal Society B 177, 509-539.

Deschenes, M., Feltz, P. & Lamour, Y.C. (1976). A model for an estimate in vivo of the ionic basis of presynaptic inhibition: an intracellular analysis of the GABA-induced depolarization in rat dorsal root ganglia. Brain Research 118, 486-493.

Dey, R.D., Shannon Jr., W.A. & Said, S.I. (1981). Localization of VIP-immunoreactive nerves in airways and pulmonary vessels of dogs, cats and human subjects. Cell and Tissue Research 220, 231-238.

Diamond, L. & O'Donnell, M. (1980). A non-adrenergic inhibitory pathway to the feline airways. Science 208, 185-188.

Diamond, L., Szarek, J.L., Gillespie, M.N. & Altiere, R.J. (1983). In vivo bronchodilator activity of vasoactive intestinal polypeptide in the cat. American Review of Respiratory Disease 128, 827-832.

DiFrancesco, D. & Ojeda, C. (1980). Properties of the current i_f in the sino-atrial node of the rabbit compared with those of i_{k2} in Purkinje fibres. Journal of Physiology 308, 353-367.

Dodd, J., Dingledine, R. & Kelly, J.S. (1981). The excitatory action of acetylcholine on hippocampal neurones of the guinea-pig and rat in vitro. Brain Research 207, 109-127.

Dodd, J. & Horn, J.P. (1983). Muscarinic inhibition of sympathetic C neurones in the bullfrog. Journal of Physiology 334, 271-291.

Doidge, J.M. & Satchell, D.G. (1982). Adrenergic and non-cholinergic inhibitory nerves in mammalian airways. Journal of the Autonomic Nervous System 5, 83-99.

Dolphin, A.C., Forda, S.R. & Scott, R.H. (1986). Calcium-dependent currents in cultured rat dorsal root ganglion neurones are inhibited by an adenosine analogue. Journal of Physiology 373, 47-61.

Drury, A.N. & Szent-Györgyi, A. (1929). The physiological activity of adenine

compounds with special reference to their action upon mammalian heart. Journal of Physiology 68, 213-237.

Dunlap, K. (1981). Two types of γ-aminobutyric acid receptors on embryonic sensory neurones. British Journal of Pharmacology 74P, 579-585.

Dunlap, K. & Fischbach, G.D. (1981). Neurotransmitters decrease the calcium conductance activated by depolarization of embryonic chick sensory neurones. Journal of Physiology 317, 519-535.

Dutar, P. & Nicoll, R.A. (1988). Classification of muscarinic responses in hippocampus in terms of receptor subtype and second-messenger systems: Electrophysiological studies in vitro. Journal of Neuroscience 8, 4214-4224.

Egan, T.M. & North, R.A. (1986). Acetylcholine hyperpolarizes central neurones by acting on an M_2 muscarinic receptor. Nature 319, 405-407.

Ehinger, B., Falck, B., Persson, H. & Sporrong, B. (1968). Adrenergic and cholinesterase-containing neurones of the heart. Histochemie 16, 197-205.

Eimerl, J. & Feuerstein, G. (1986), The effect of μ, γ, K and ∈ opioid receptor antagonists on heart rate and blood pressure of the pithed rat. Neuropeptides 8, 351-358.

Elfman, A.G. (1943). The afferent parasympathetic innervation of the lungs and trachea of the dog. American Journal of Anatomy 72, 1-28.

Elfvin, L-G. (1983). Autonomic Ganglia, ed. Elfvin, L-G., Chichester, West Sussex: Wiley.

Ellis, J.L. & Farmer, S.G. (1989). Effect of peptidases on non-adrenergic, non-cholinergic inhibitory responses of tracheal smooth muscle: a comparison with the effects on VIP- and PHI-induced relaxation. British Journal of Pharmacology 96, 521-526.

Ellison, J.P. & Hibbs, R.G. (1974). Catecholamine-containing cells of the guinea-pig heart. An ultrastructural study. Journal of Molecular and Cellular Cardiology 6, 17-26.

Ellison, J.P. & Hibbs, R.G. (1976). An ultrastructural study of mammalian cardiac ganglia. Journal of Molecular and Cellular Cardiology 8, 89-101.

Erdo, S.L. & Bowery, N.G. (1986). GABAergic Mechanisms in the Mammalian Periphery. ed. Erdo, S.L. & Bowery, N.G., New York: Raven Press.

Fisher, A.W.F. (1964). The intrinsic innervation of the trachea. Journal of Anatomy 98, 117-124.

Forsgren, S. (1987). Marked sympathetic innervation in the regions of the bundle branches shown by catecholamine histofluorescence. Journal of Molecular and Cellular Cardiology 19, 555-568.

Fowler, J.C., Greene, R. & Weinreich, D. (1985). Two calcium-sensitive spike after-hyperpolarizations in visceral sensory neurones of the rabbit. Journal of Physiology 365, 59-75.

Fowler, J.C. & Weinreich, D. (1986). Electrophysiological membrane properties of paratracheal ganglion neurons of the rabbit. Neuroscience Abstracts 11, 1182.

Franco-Cereceda, A., Bengtsson, L. & Lundberg, J.M. (1987). Inotropic effects of calcitonin gene-related peptide, vasoactive intestinal polypeptide and serotonin in the right human atrium in vitro. European Journal of Pharmacology 134, 69-76.

Franco-Cereceda, A., Lundberg, J.M. & Hökfelt, T. (1986). Somatostatin an inhibitory parasympathetic transmitter in the human heart. European Journal of Pharmacology 132, 101-102.

Fryer, A.D. & MacLagan, J. (1984). Muscarinic inhibitory receptors on pulmonary parasymapthetic nerves in the guinea-pig. British Journal of

Pharmacology 83, 973-978.

Furness, J.B. & Costa, M. (1980). Types of nerves in the enteric nervous system. Neuroscience 5, 1-20.

Furness, J.B. & Costa, M. (1987). The Enteric Nervous System. Edinburgh: Churchill Livingstone.

Fujimoto, S., Yamamoto, K., Kuba, K., Morita, K. & Kato, E. (1980). Calcium localisation in the sympathetic ganglion of the bullfrog and the effects of caffeine. Brain Research 202, 21-32.

Fyffe, R.E.W. & Perl, E.R. (1984). Is ATP a central synaptic mediator for certain primary afferent fibers from mammalian skin? Proceedings of the National Academy of Science. U.S.A. 81, 6890-6893.

Gabella, G. (1972). Fine structure of the myenteric plexus in the guinea-pig ileum. Journal of Anatomy 111, 69-97.

Gabella, G. (1976). Structure of the Autonomic Nervous System. London: Chapman and Hall.

Gabella, G. (1979). Innervation of the gastrointestinal tract. International Review of Cytology 59, 129-193.

Gagliardi, M., Randall, W.C., Bieger, D., Wurster, R.D., Hopkins, D.A. & Armour, J.A. (1988). Activity of in vivo cardiac plexus neurons. American Journal of Physiology 255, H789-H800.

Gähwiler, B.H. & Brown, D.A. (1985a). $GABA_B$ receptor-activated K^+ current in voltage-clamped CA_3 pyramidal cells in hippocampal cultures. Proceedings of the National Academy of Science. U.S.A. 82, 1558-1562.

Gähwiler, B.H. & Brown, D.A. (1985b). Functional innervation of cultured hippocampal neurones by cholinergic afferents from co-cultured septal explants. Nature 313, 577-579.

Gallagher, J.P., Griffith, W.H. & Shinnick-Gallagher, P. (1982). Cholinergic transmission in cat parasympathetic ganglia. Journal of Physiology 332, 473-486.

Gallego, R. & Eyzaguirre, C. (1978). Membrane and action potential characteristics of A and C nodose ganglion cells studied in whole ganglia and in tissue slices. Journal of Neurophysiology 41, 1217-1232.

Galligan, J.J., North, R.A. & Tokimasa, T. (1989). Muscarinic agonists and potassium currents in guinea-pig myenteric neurones. British Journal of Pharmacology 96, 193-203.

Gay, L.A. & Stanfield, P.R. (1977). Cs^+ causes a voltage-dependent block of inward K^+ currents in resting skeletal muscle fibres. Nature 267, 169-170.

Gershon, M.D. (1981). The enteric nervous system. Annual Review of Neuroscience 4, 227-272.

Gerstheimer, F.P. & Metz, J. (1986). Distribution of calcitonin gene-related peptide-like immunoreactivity in the guinea-pig heart. Anatomy and Embryology 175, 255-260.

Gibbins, I.L., Furness, J.B., Costa, M., MacIntyre, I., Hillyard, C.J. & Girgis, S. (1985). Co-localisation of calcitonin gene-related peptide-like immunoreactivity with substance P in cutaneous, vascular and visceral sensory neurones of the guinea-pig. Neuroscience Letters 57, 125-130.

Giraldo, E., Hammer, R. & Ladinsky, H. (1986). Binding profile in rat brain of compound AF-DX 116, a novel cardioselective muscarinic receptor antagonist of the competitive type. Trends in Pharmacological Sciences 7, Supplement 80-81.

Gordon, J.L. (1986). Extracellular ATP: effects, sources and fate. Biochemical Journal 233, 309-319.

Grafe, P., Mayer, C.J. & Wood, J.D. (1980). Synaptic modulation of calcium-

dependent potassium conductance in myenteric neurones. Journal of Physiology 305, 235-248.

Grundström, N., Andersson, R.G.G. & Wikberg, J.E.S. (1981). Pharmacological characterization of the autonomous innervation of guinea-pig tracheobronchial smooth muscle. Acta Pharmacology and Toxicology 49, 150-157.

Gu, J., Polak, J.M., Allen, J.M., Huang, W.M., Sheppard, M.N., Tatemoto, K. & Bloom, S.R. (1984). High concentrations of a novel peptide, neuropeptide Y, in the innervation of the mouse and rat heart. Journal of Histochemistry and Cytochemistry 32, 467-472.

Gulbenkian, S., Wharton, J., Hacker, G.W., Varndell, I.M., Bloom, S.R. & Polak, J.M. (1985). Co-localization of neuropeptide tyrosine (NPY) and its C-terminal flanking peptide (C-PON). Peptides 6, 1237-1243.

Haas, H.L., & Greene, R.W. (1984). Adenosine enhances afterhyperpolarization and accommodation in hippocampal pyramidal cells. Pflügers Archiv 402, 244-247.

Hagiwara, S. & Takahashi, K. (1974). The anomalous rectification and cation selectivity of the membrane of a star-fish egg cell. Journal of Membrane Biology 18, 61-80.

Hagiwara, S., Miyazaki, S. & Rosenthal, N.P. (1976). Potassium current and the effect of cesium on this current during anomalous rectification of the egg cell membranes of a starfish. Journal of General Physiology 67, 621-638.

Hagiwara, S., Miyazaki, S., Moody, W. & Patlak, J. (1978). Blocking effects of barium and hydrogen ions on the potassium current during anomalous rectification in the starfish egg. Journal of Physiology 279, 167-185.

Hall, A.K., Barnes, P.J., Meldrum, L.A. & MacLagan, J. (1989). Facilitation by tachykinins of neurotransmission in guinea-pig pulmonary

parasympathetic nerves. British Journal of Pharmacology 97, 274-280.

Halliwell, J.V. & Adams, P.R. (1982). Voltage-clamp analysis of muscarinic excitation in hippocampal neurones. Brain Research 250, 71-92.

Hamill, O.P., Marty, A., Neher, E., Sakmann, B. & Sigworth, F. (1981). Improved patch-clamp techniques for high resistance recording from cells and cell free membrane patches. Pflügers Archiv 391, 85-100.

Hammer, R., Berrie, E.P., Birdsall, N.J.M., Burgen, A.S.V. & Hulme, E.E.C. (1980). Pirenzepine distinguishes between different subclasses of muscarinic receptors. Nature 283, 90-92.

Hammer, R., Giraldo, E., Schiavi, G.B., Monferini, E. & Ladinsky, H. (1986). Binding profile of a novel cardioselective muscarinic receptor antagonist AF-DX 116 to membranes of peripheral tissues and brain in the rat. Life Sciences 38, 1653-1662.

Hancock, J.C., Hoover, D.B. & Houghland, M.W. (1987). Distribution of muscarinic receptors of acetylcholine in the rat heart. Journal of the Autonomic Nervous System 19, 59-66.

Harris, A.J., Kuffler, S.W. & Dennis, M.J. (1971). Differential chemosensitivity of synaptic and extrasynaptic areas of the neuronal surface membrane in parasympathetic neurons of the frog, tested by microapplication of acetylcholine. Proceedings of the Royal Society B 177, 541-553.

Hartzell, H.C., Kuffler, S.W., Stickgold, R. & Yoshikami, D. (1977). Synaptic excitation and inhibition resulting from the direct action of acetylcholine on two types of chemoreceptor on individual amphibian parasympathetic neurones. Journal of Physiology 271, 817-846.

Hassall, C.J.S. & Burnstock, G. (1984). Neuropeptide Y-like immunoreactivity in cultured intrinsic neurones of the heart. Neuroscience Letters 52, 111-115.

Hassall, C.J.S. & Burnstock, G. (1986). Intrinsic neurones and associated cells of the guinea-pig heart in culture. Brain Research 364, 102-113.

Hassall, C.J.S. & Burnstock, G. (1987a). Evidence for uptake and synthesis of 5-hydroxytryptamine by a subpopulation of intrinsic neurones in the guinea-pig heart. Neuroscience 22, 413-423.

Hassall, C.J.S. & Burnstock, G. (1987b). Immunocytochemical localisation of neuropeptide Y and 5-hydroxytryptamine in a subpopulation of amine-handling intracardiac neurones that do not contain dopamine β-hydroxylase. Brain Research 422, 74-82.

Hassall, C.J.S., Buckley, N.J. & Burnstock, G. (1987). Autoradiographic localisation of muscarinic receptors on guinea-pig intracardiac neurones and atrial myocytes in culture. Neuroscience Letters 74, 145-150.

Haxhui, M.A., Deal Jr, E.C., Norcia, M.P., Lunteren, E.V., Mitra, J. & Cherniack, N.S. (1986). Medullary effects of nicotine and GABA on tracheal smooth muscle tone. Respiratory Physiology 64, 351-363.

Henri, J.L. & Calaresu, F.R. (1972). Distribution of cardio-acceleratory sites in the intermediolateral nucleus of the cat. American Journal of Physiology 222, 700-704.

Higashi, H., Morita, K. & North, R.A. (1984). Calcium dependent after-potentials in visceral afferent neurones of the rabbit. Journal of Physiology 355, 479-492.

Hirst, G.D.S., Holman, M.E. & Spence, I. (1974). Two types of neurones in the myenteric plexus of the duodenum in the guinea-pig. Journal of Physiology 236, 303-326.

Hirst, G.D.S., Johnson, S.M. & Van Helden, D.F. (1985). The slow calcium-dependent potassium current in a myenteric neurone of the guinea-pig ileum. Journal of Physiology 361, 315-337.

Hirst, G.D.S. & Spence, I. (1973). Calcium action potentials in mammalian peripheral neurones. Nature 243, 106-112.

Hoffman, R. (1977). The modulation contrast microscope: principles and performance. Journal of Microscopy 110, 205-222.

Holz, G.G., Rane, S.G. & Dunlap, K. (1986). GTP-binding proteins mediate transmitter inhibition of voltage-dependent calcium channels. Nature 319, 670-672.

Hoover, D.B. & Hancock, J.C. (1988). Distribution of substance P binding sites in guinea-pig heart and pharmacological effects of substance P. Journal of the Autonomic Nervous System 23, 189-197.

Hopwood, A.M. & Burnstock, G. (1987). ATP mediates coronary vasoconstriction via P_{2X}-purinoceptors and coronary vasodilatation via P_{2Y}-purinoceptors in isolated perfused rat heart. European Journal of Pharmacology 136, 49-54.

Honjin, R. (1954). On the ganglia and nerves of the lower respiratory tract of the mouse. Journal of Morphology 95, 263-288.

Honjin, R. (1956). On the nerve supply of the lungs of the mouse with special references to the structure of the peripheral vegetative nervous system. Journal of Comparative Neurology 105, 587-625.

Horn, J. & Dodd, J. (1981). Monosynaptic muscarinic activation of K conductance underlies the slow inhibitory postsynaptic potential in sympathetic ganglia. Nature 292, 625-627.

Houston, D.A., Burnstock, G & Vanhoutte, P.M. (1987). Different P_2-purinergic receptor subtypes of endothelium and smooth muscle in canine blood vessels. Journal of Pharmacology and Experimental Therapeutics 241, 501-506.

Huguenard, J.R. & Alger, B.E. (1986). Whole-cell voltage-clamp study of the fading of GABA-activated currents in acutely dissociated hippocampal neurones.

Journal of Neurophysiology 56, 1-18.

Hume, R.I. & Thomas, S.A. (1988). Multiple actions of adenosine 5'-triphosphate on chick skeletal muscle. Journal of Physiology 406, 503-524.

Ichinose, M., Stretton, C.D., Schwartz, J.-C. & Barnes, P.J. (1989). Histamine H_3-receptors inhibit cholinergic neurotransmission in guinea-pig airways. British Journal of Pharmacology 97, 13-15.

Irvin, J.L. & Irvin, E.M. (1954). The interaction of quinacrine with adenine nucleotides. Journal of Biological Chemistry 210, 45-56.

Ito, H. (1982). Evidence for initiation of calcium spikes in C cells of rabbit nodose ganglia. Pflügers Archiv 394, 106-112.

Ito, Y. & Takeda, K. (1982). Non-adrenergic inhibitory nerves and putative transmitters in smooth muscle of the cat trachea. Journal of Physiology 330, 497-511.

Iverson, L.L. & Kelly, J.S. (1975). Uptake and metabolism of γ-aminobutyric acid by neurones and glial cells. Biochemical Pharmacology 24, 933-938.

Jacobowitz, D. (1967). Histochemical studies of the relationship of chromaffin cells and adrenergic nerve fibres to the cardiac ganglia of several species. Journal of Pharmacology and Experimental Therapeutics 158, 227-240.

Jacobowitz, D.G., Kent, K.M., Fleisch, J.H. & Cooper, T. (1973). Histofluorescent study of catecholamine-containing elements in cholinergic ganglia from the calf and dog lung. Proceedings of the Society for Experimental Biology and Medicine 144, 464-466.

Jacobowitz, D.M. (1974). The peripheral autonomic system. In The Peripheral Nervous System, ed. Hubbard J.I., pp. 87-110. New York, London: Plenum Press.

Jahr, C.E. & Jessell, T.M. (1983). ATP excites a subpopulation of rat dorsal horn

neurones. Nature 304, 730-733.

James, S., Bailey, D.J. & Burnstock, G. (1990). Autoradiographic visualization of muscarinic receptors on rat paratracheal neurones in dissociated cell culture. Brain Research (in press).

Jansen, J.K.S. & Nicholls, J.G. (1973). Conductance changes, an electrogenic pump and the hyperpolarization of leech neurones following impulses. Journal of Physiology 229, 635-655.

Jessen, K.R. & Burnstock, G. (1982). The enteric nervous system in tissue culture: a new model for the study of complex nervous networks. In Trends in Autonomic Pharmacology, ed. Kalsner, S., pp. 95-115. Baltimore: Urban & Schwarzenburg.

Jessen, K.R., Hills, J.M. & Saffrey, M.J. (1986). Immunohistochemical demonstration of GABAergic neurons in the enteric nervous system. Journal of Neuroscience 6, 1628-1634.

Jessen, K.R., Mirsky, R., Dennison, M. & Burnstock, G. (1979). GABA may be a transmitter in the vertebrate peripheral nervous system. Nature 281, 71-74.

Karhula, T., Häppölä, O., Joh, T. & Wu, J.-Y. (1988). Localization of L-glutamine decarboxylase immunoreactivity in the major pelvic ganglia and the coeliac-superior mesenteric ganglion complex of the rat. Histochemistry 90, 255-260.

Katayama, K. & Morita, K. (1989). Adenosine 5'-triphosphate modulates membrane potassium conductance in guinea-pig myenteric neurones. Journal of Physiology 408, 373-390.

Kato, E. & Kuba, K. (1980). Inhibition of transmitter release in bullfrog sympathetic ganglion cells induced by γ-aminobutyric acid. Journal of Physiology 298, 271-283.

Kato, E., Morita, K., Kuba, K., Yamada, S., Kuhara, T., Shinka, T. & Matsumoto, I. (1980). Does γ-aminobutyric acid in blood control transmitter release in bullfrog sympathetic ganglia? Brain Research 195, 208-214.

Katz, L.C., Burkhalter, A. & Dreyer, W.J. (1984). Fluorescent latex microspheres as a retrograde neuronal marker for in vivo and in vitro studies of visual cortex. Nature 310, 498-500.

Kelly, J.S. & Beart, P.M. (1975). Amino acid receptors in the CNS II. GABA in supraspinal regions. In Handbook of Psychopharmacology. Amino Acid Neurotransmitters, Vol. 4, ed. Iverson, L.L., Iverson, S.D. & Snyder, S.H., pp. 129-210. New York: Plenum Press.

Kenny, S.L. & Ariano, M.A. (1986). The immunofluorescence localization of glutamine decarboxylase in the rat superior cervical ganglion. Journal of the Autonomic Nervous System 17, 211-215.

Kerr, D.I.B. & Krantis, A. (1979). A new class of ATP antagonist. Proceedings of the Australian Physiological and Pharmacological Society 10, 156P.

King, T.S. & Coakley, J.B. (1958). The intrinsic nerve cells of the cardiac atria of mammals and man. Journal of Anatomy 92, 353-376.

Knight, D.S. (1980). A light and electron microscopic study of feline intrapulmonary ganglia. Journal of Anatomy 131, 413-428.

Kobayashi, Y., Hassall, C.J.S. & Burnstock, G. (1986a). Culture of intramural cardiac ganglia of the newborn guinea-pig. I. Neuronal elements. Cell and Tissue Research 244, 595-604.

Kobayashi, Y., Hassall, C.J.S. & Burnstock, G. (1986b). Culture of intramural cardiac ganglia of the newborn guinea-pig. II. Non-neuronal elements. Cell and Tissue Research 244, 605-612.

Koketsu, K. (1969). Cholinergic potentials and the underlying ionic mechanisms. Federation Proceedings 28, 101-102.

Koketsu, K. & Yamada, M. (1982). Presynaptic muscarinic receptors inhibiting active acetylcholine release in bullfrog sympathetic ganglia. British Journal of Pharmacology 77, 75-82.

Konishi, S., Okamoto, T. & Otsuka, M. (1984). Synaptic transmission and effects of substance P and somatostatin on guinea-pig cardiac ganglia. IUPHAR Proceedings, 1604P.

Konopka, L.M., McKeon, T.W. & Parsons, R.L. (1989). Galanin-induced hyperpolarization and decreased membrane excitability of neurones in mudpuppy cardiac ganglion. Journal of Physiology 410, 107-122.

Krishtal, O.A., Marchenko, S.M. & Pidoplichko, V.I. (1983). Receptors for ATP in the membrane of mammalian sensory neurones. Neuroscience Letters 35, 41-45.

Krnjević, K., Pumain, R. & Renaud, L. (1971). The mechanism of excitation by acetylcholine in the cerebral cortex. Journal of Physiology 215, 247-268.

Kuba, K. (1980). Release of calcium ions linked to the activation of potassium conductance in a caffeine-treated sympathetic neurone. Journal of Physiology 298, 251-270.

Kuba, K. & Koketsu, K., (1976a). Analysis of the slow excitatory potential in bullfrog sympathetic ganglion cells. Japanese Journal of Physiology 26, 651-669.

Kuba, K. & Koketsu, K. (1976b). The muscarinic effects of acetylcholine on the action potential of bullfrog sympathetic ganglion cells. Japanese Journal of Physiology 26, 703-716.

Kuffler, S.W. (1980). Slow synaptic responses in autonomic ganglia and the pursuit of a peptidergic transmitter. Journal of Experimental Biology 89, 257-289.

Kuntz, A. (1953). Autonomic Nervous System, 4th edition. Philadelphia: Lea &

Febiger.

Lammers, J.-W.J., Minette, P., McCusker, M. & Barnes, P.J. (1989). The role of pirenzepine-sensitive (M_1) muscarinic receptors in vagally mediated bronchoconstriction in humans. American Review of Respiratory Disease 139, 446-451.

Landois, L. (1885). A Textbook of Human Physiology. Translated by W. Stirling, Vol. 1, 4th edition, pp. 217-225. London: Charles Griffin.

Langley, J.N. (1921). The Autonomic Nervous System. Cambridge: W. Heffer & Sons Ltd.

Larsell, O. (1922). The ganglia, plexuses and nerve-terminations of the mammalian lung and pleura pulmonalis. Journal of Comparative Neurology 35, 97-130.

Libet, B., Chichibu, S. & Tosaka, T. (1968). Slow synaptic responses and excitability in sympathetic ganglia of the bullfrog. Journal of Neurophysiology 31, 383-395.

Londos, C., Cooper, D.M.F. & Woolf, J. (1980). Subclasses of external adenosine receptors. Proceedings of the National Academy of Science. U.S.A. 77, 2551-2554.

Lundberg, J.M., Terenius, L., Hökfelt, T. & Goldstein, M. (1983). High levels of neuropeptide Y in peripheral noradrenergic neurons in various mammals including man. Neuroscience Letters 42, 167-172.

Lundberg, J.M., Fahrenkrug, J., Hökfelt, T., Martling, C.-R., Larsson, O., Tatemoto, K. & Änggärd, A. (1984). Coexistence of peptide HI (PHI) and VIP in nerves regulating blood flow and bronchial smooth muscle tone in various mammals including man. Peptides 5, 593-606.

Lundberg, J.M., Hua, X.-Y. & Franco-Cereceda, A. (1984). Effects of neuropeptide Y (NPY) on mechanical activity and neurotransmission in the heart, vas

deferens and urinary bladder of the guinea-pig. Acta Physiologica Scandaninavica 121, 325-332.

Lundberg, J.M. & Saria, A. (1982). Vagal substance P nerves involved in control of vascular permeability and smooth muscle tone in trachea and bronchi. British Journal of Pharmacology 77, Supplement 441P.

Lundberg, J.M. & Saria, A. (1987). Polypeptide-containing neurons in airway smooth muscle. Annual Review of Physiology 49, 557-572.

Luts, A., Uddman, R. & Sundler, F. (1989). Neuronal galanin is widely distributed in chicken respiratory tract and co-exists with multiple neuropeptides. Cell and Tissue Research 256, 95-103.

Luzzi, S., Franchi-Micheli, S., Folco, G., Rossoni, G., Cuiffi, M. & Zilletti, L. (1987). Effects of baclofen on different models of bronchial hyperreactivity in guinea-pig. Agents and Actions 20, 307-309.

MacLagan, J., Fryer, A.D. & Faulkner, D. (1989). Identification of M_1 muscarinic receptors in pulmonary sympathetic nerves in the guinea-pig by use of pirenzepine. British Journal of Pharmacology 97, 499-505.

Madison, D.V. & Nicoll, R.A. (1984). Control of repetive discharge in rat CA1 pyramidal neurones in vitro. Journal of Physiology 354, 319-331.

Manzini, S., Hoyle, C.H.V. & Burnstock, G. (1986). An electrophysiological analysis of the effect of reactive blue 2, a putative P_2-purinoceptor antagonist, on inhibitory junction potentials of rat caecum. European Journal of Pharmacology 127, 197-204.

Marty, A. (1981). Calcium dependent potassium channels with large unitary conductance in chromaffin cell membranes. Nature 291, 497-500.

Matsuzaki, Y., Hamasaki, Y. & Said, S.I. (1980). Vasoactive intestinal polypeptide; A possible transmitter of nonadrenergic relaxation of guinea pig airways. Science 210, 1252-1253.

Mayer, M.L., Higashi, H., Gallagher, J.P. & Gallagher, P.S. (1983). On the mechanism of action of GABA in pelvic vesical ganglia: biphasic responses evoked by two opposing actions on membrane conductance. Brain Research 260, 233-248.

Mayer, M.L., Higashi, H., Shinnick-Gallagher, P. & Gallagher, J.P. (1981). A hyperpolarizing GABA response associated with a conductance decrease. Brain Research 222, 204-208.

Mayer, M.L. & Westbrook, G.L. (1983). A voltage-clamp analysis of inward (anomalous) rectification in mouse spinal sensory ganglion neurones. Journal of Physiology 340, 19-45.

McAfee, D.A. & Yarowsky, P.T. (1979). Calcium dependent potentials in mammalian sympathetic neurones. Journal of Physiology 290, 507-523.

McCormick, D.A. & Prince, D.A. (1986). Acetylcholine induces burst firing in thalamic reticular neurones by activating a potassium conductance. Nature 319, 402-405.

McMahan, U.J. & Kuffler, S.W. (1971). Visual identification of synaptic boutons on living ganglion cells and of varicosities in postganglionic axons in the heart of the frog. Proceedings of the Royal Society B 177, 485-508.

McMahan, U.J. & Purves, D. (1976). Visual identification of two types of cells and their synaptic contacts in a living autonomic ganglion of the mudpuppy (Necturus Maculosus). Journal of Physiology 254, 405-425.

Meech, R.W. (1978). Calcium dependent potassium activation in nervous tissue. Annual Review of Biophysics and Bioengineering 7, 1-18.

Meech, R.W. (1980). Ca^{++}-activated K^{+} conductance. Cold Spring Harbor Reports in the Neurosciences, Vol. 1, Molluscan Nerve Cells: from Biophysics to Behaviour, ed. Koester, J. & Byrne, J.H., pp. 93-103. Cold Spring Harbor: Cold Spring Harbor Laboratory.

Meech, R.W. & Standen, N.B. (1975). Potassium activation in Helix aspera neurones under voltage clamp: a component mediated by calcium influx. Journal of Physiology 249, 211-240.

Minette, P.A. & Barnes, P.J. (1988). Prejunctional inhibitory muscarinic receptors on cholinergic nerves in human and guinea-pig airways. Journal of Applied Physiology 64, 2532-2537.

Mitchell, R.A., Herbert, D.A. & Baker, D.G. (1984). Inspiratory rhythm in airway smooth muscle tone. Journal of Applied Physiology 58, 911-920.

Mitchell, R.A., Herbert, D.A., Baker, D.G. & Basbaum, C.B. (1987). In vivo activity of tracheal parasympathetic ganglion cells innervating tracheal smooth muscle. Brain Research 437, 157-160.

Mochida, S. & Kobayashi, H. (1986a). Three types of muscarinic conductance changes in sympathetic neurones discriminately evoked by different concentrations of acetylcholine. Brain Research 383, 299-304.

Mochida, S. & Kobayashi, H. (1986b). Multiple muscarinic responses directly evoked in isolated neurones dissociated from rabbit sympathetic ganglia. Journal of the Autonomic Nervous System 17, 289-301.

Mochida, S. & Kobayashi, H. (1986c). Activation of M_2 muscarinic receptors causes an alteration in action potentials by modulation of Ca^{2+} entry in isolated sympathetic neurons of rabbits. Neuroscience Letters 72, 199-204.

Moravec, J. & Moravec, M. (1987). Intrinsic plexus of mammalian heart: Morphological basis of cardiac rhythmical activity? International Review of Cytology 106, 89-148.

Morita, K., North, R.A. & Tokimasa, T. (1982a). The calcium dependent potassium conductance in guinea-pig myenteric neurones. Journal of Physiology 329, 341-354.

Morita, K., North, R.A. & Tokimasa, T. (1982b). Muscarinic agonists inactivate potassium conductance of guinea-pig myenteric neurones. Journal of Physiology 333, 125-139.

Morita, K., Katayama, Y., Koketsu, K. & Akasu, T. (1984). Actions of ATP on the soma of bullfrog primary afferent neurones and its modulatory action on the GABA-induced response. Brain Research 293, 360-363.

Mutschler, E. & Lambrecht, G. (1984). Selective muscarinic agonists and antagonists in functional tests. Trends in Pharmacological Sciences supplement, 39-44.

Nadel, J.A. (1980). Autonomic regulation of airway smooth muscle. In Physiology and Pharmacology of the Airways, ed. Nadel, J.A., pp. 217-258. New York: Marcel Dekker.

Navaratnam, V. (1980). Anatomy of the mammalian heart. In Hearts and Heart-like Organs, Vol. 1. ed. Bourne, G.H., pp. 349-374. New York: Academic Press.

Neely, B.H., Hageman, G.R. & James, T.N. (1983). Effects of γ-aminobutyric acid on neural regulation of the canine sinus node. American Journal of Physiology 244, H266-H272.

Neild, T.O. (1978). Slow depolarisation of neurones in the guinea-pig inferior mesenteric ganglion following repetitive stimulation of preganglionic nerves. Brain Research 140, 231-239.

Nielsen, K.C. & Owman, Ch. (1968). Difference in cardiac innervation between hibernators and non-hibernating mammals. Acta Physiologica Scandaninavica Supplementum 316, 1-30.

Newberry, N.R. & Nicoll, R.A. (1984). Direct hyperpolarizing action of baclofen on hippocampal pyramidal cells. Nature 308, 450-452.

Nilsson, G., Dahlberg, K., Brodin, E., Sundler, F. & Strandberg, K. (1977).

Distribution and constrictor effect of substance P in guinea pig tracheobronchial tissue. In Substance P, ed. von Euler, U.S. & Pernow, B., pp. 75-81. New York: Raven Press.

Nishi, S. & Koketsu, K. (1968). Early and late after-discharges of amphibian sympathetic ganglion cells. Journal of Neurophysiology 31, 109-121.

Nishi, S. & North, R.A. (1973). Intracellular recording from the myenteric plexus of the guinea-pig ileum. Journal of Physiology 231, 471-491.

Noble, D. (1979). The Initiation of the Heart Beat. London, New York: Oxford University (Clarendon) Press.

North, R.A., Slack, B.E. & Surprennant, A. (1985). Muscarinic M_1 and M_2 receptors mediate depolarization and presynaptic inhibition in guinea-pig enteric nervous system. Journal of Physiology 368, 435-452.

North, R.A. & Tokimasa, T. (1982). Muscarinic synaptic potentials in guinea-pig myenteric plexus neurones. Journal of Physiology 333, 151-156.

North, R.A. & Tokimasa, T. (1983). Depression of calcium-dependent potassium conductance of guinea-pig myenteric neurones by muscarinic agonists. Journal of Physiology 342, 253-266.

Nozdrachev, A.D. & Pogorelov, A.G. (1982). Extracellular recording of neuronal activity of the cat heart ganglia. Journal of the Autonomic Nervous System 6, 73-81.

Osborne, L.W. & Silva, D.G. (1970). Histological, acetylcholinesterase, and fluorescence histochemical studies on the atrial ganglia of the monkey heart. Experimental Neurology 27, 497-511.

Pack, R.J., Al-Ugaily, L.H. & Widdicombe, J.G. (1984). The innervation of the trachea and extrapulmonary bronchi of the mouse. Cell and Tissue Research 238, 61-68.

Palmer, J.M., Wood, J.D. & Zafirov, D.H. (1987). Purinergic inhibition in the small intestinal myenteric plexus of the guinea-pig. Journal of Physiology 387, 357-369.

Papka, R.E. (1976). Studies of cardiac ganglia in pre- and postnatal rabbits. Cell and Tissue Research 175, 17-35.

Pardini, B.J., Patel, K.P., Schmid, P.G. & Lund, D.D. (1987). Location and distribution of parasympathetic ganglion cells in the rat heart. Society for Neuroscience 10, 607.

Parsons, R.L., Neel, D.S., Konopka, L.M. & McKeon, T.W. (1989). The presence and possible role of a galanin-like peptide in the mudpuppy heart. Neuroscience 29, 749-759.

Phillis, J.W. & Wu, P.H. (1981). The role of adenosine and its nucleotides in central synaptic transmission. Progress in Neurobiology 16, 187-239.

Polak, J.M. & Bloom, S.R. (1982). Regulatory peptides in the respiratory tract of man and other animals. Experimental Lung Research 3, 313-328.

Potter, E.K. (1985). Prolonged non-adrenergic inhibition of cardiac vagal action following sympathetic stimulation: Neuromodulation by neuropeptide Y. Neuroscience Letters 54, 117-121.

Randall, W.C. & Ardell, J.L. (1985a). Selective parasympathectomy of autonomic and conducting tissue of the canine heart. American Journal of Physiology 248, H61-H68.

Randall, W.C. & Ardell, J.L. (1985b). Differential innervation of the heart. In Cardiac Electrophysiology and Arrhythmias, ed. Zipes, D. & Jolife, J., pp. 137-144. New York: Grune & Stratton.

Randall, W.C., Ardell, J.L., Calderwood, D., Milosavljevic, M. & Goyal, S.C. (1986a). Parasympathetic ganglia innervating the canine atrioventricular nodal region. Journal of the Autonomic Nervous System 16, 311-323.

Randall, W.C., Milosavljevic, M., Wurster, R.D., Geis, G.S. & Ardell, J.L. (1986b). Selective vagal innervation of the heart. Annals of Clinical and Laboratory Science 16, 198-208.

Rang, H.P. & Ritchie, J.H. (1968). On the electrogenic sodium pump in a mammalian non-myelinated nerve fibre. Journal of Physiology 196, 183-221.

Reinecke, M. & Forssmann, W.G. (1984). Regulatory peptides (SP, NT, VIP, PHI, ENK) of autonomic neurones in guinea-pig heart. Clinical Experimental Hypertension - Theory and Practice A6, (10 & 11), 1867-1871.

Richardson, J.B. (1979). Nerve supply to the lungs. American Review of Respiratory Diseases 119, 785-802.

Richardson, J.B. & Beland, J. (1976). Nonadrenergic inhibitory nervous system in human airways. Journal of Applied Physiology 41, 764-771.

Richardson, J.B. & Bouchard, T. (1975). Demonstration of a nonadrenergic inhibitory nervous system in the trachea of the guinea-pig. Journal of Allergy and Clinical Immunology 56, 437-480.

Rogawski, M.A. (1985). The A-current: how ubiquitous a feature of excitable cells is it? Trends in Neurosciences 8, 214-219.

Roper, S. (1976). The acetylcholine sensitivity of the surface membrane of the multiply-innervated parasympathetic ganglion cells of the mudpuppy before and after partial denervation. Journal of Physiology 254, 455-473.

Russell, J.A. & Simons, E.J. (1985). Modulation of cholinergic neurotransmission in airways by enkephalin. Journal of Applied Physiology 58, 853-858.

Said, S.I. (1982). Vasoactive peptides in the lung, with special reference to vasoactive intestinal polypeptide. Experimental Lung Research 3, 343-348.

Said, S.I., Bosher, L.P., Spath, J.A. & Kontos, H.A. (1972). Positive inotropic action

of newly isolated vasoactive intestinal polypeptide (VIP). Clinical Research 20, 29.

Salt, T.E. & Hill, R.G. (1983). Excitation of single sensory neurones in the rat caudal trigeminal nucleus by ionophoretically applied adenosine 5'-triphosphate. Neuroscience Letters 35, 53-57.

Sargent, P.B. & Dennis, M.J. (1977). Formation of synapses between parasympathetic neurones deprived of preganglionic innervation. Nature 268, 456-458.

Schulman, J.A. & Weight, F.F. (1976). Synaptic transmission: long-lasting potentialism by a post-synaptic mechanism. Science 194, 1437-1439.

Segal, M. (1982). Intracellular analysis of a postsynaptic action of adenosine in the rat hippocampus. European Journal of Pharmacology 79, 193-199.

Shvalev, V.N. & Sosunov, A.A. (1985). A light and electronmicroscopic study of cardiac ganglia in mammals. Zeitschrift fur Zellforschung und Mikroskopische Anatomie 99, 676-694.

Skoogh, B.-E., Holtzman, M.J., Sheller, J.R. & Nadel, J.A. (1982). Barbiturates depress vagal motor pathways to ferret tracheal at ganglia. Journal of Applied Physiology 53, 253-257.

Skoogh, B.-E. & Svedmyr, N. (1989). Classification of beta-adrenoceptor in ferret tracheal smooth muscle by pharmacological response. Pulmonary Pharmacology 1, 173-177.

Smith, R.B. (1970). Binucleate neurones in the human foetal heart. Experientia 26, 772.

Smith, R.B. & Taylor, I.M. (1971). Observations on the intrinsic innervation of the guinea-pig tracheobronchial smooth muscle. Neuroscience Letters 34, 247-251.

Sneddon, P. & Burnstock, G. (1984). Inhibition of excitatory junction potentials in

guinea-pig vas deferens by α,β-methylene-ATP further evidence for ATP and noradrenaline as cotransmitters. European Journal of Pharmacology 100, 85-90.

Sneddon, P., Westfall, D.P. & Fedan, J.S. (1982). Cotransmitters in the motor nerves of the guinea-pig vas deferens: electrophysiological evidence. Science 218, 693-695.

Standen, N.B. & Stanfield, P.R. (1978). A potential- and time-dependent blockade of inward rectification in frog skeletal muscle fibres by barium and strontium ions. Journal of Physiology 280, 169-191.

Standen, N.B. & Stanfield, P.R. (1980). Rubidium block and rubidium permeability of the inward rectifier of frog skeletal muscle fibres. Journal of Physiology 304, 415-435.

Stjärne, L., Lundberg, J.M. & Åstrand, P. (1986). Neuropeptide Y- A cotransmitter with noradrenaline and adenosine 5'-triphosphate in the sympathetic nerves of the mouse vas deferens? A biochemical, physiological and electropharmacological study. Neuroscience 18, 151-166.

Stone, T.W. (1981). Physiological roles for adenosine and adenosine 5'-triphosphate in the nervous system. Neuroscience 6, 523-555.

Stretton, C.D. & Barnes, P.J. (1988). Modulation of cholinergic neurotransmission in guinea-pig trachea by neuropeptide Y. British Journal of Pharmacology 93, 672-678.

Su, C. (1983). Purinergic neurotransmission and neuromodulation. Annual Review of Pharmacology and Toxicology 23, 397-411.

Tamaoki, J., Graf, P.D. & Nadel, J.A. (1987). Effect of γ-aminobutyric acid on neurally mediated constriction of guinea-pig trachealis smooth muscle. Journal of Pharmacology and Experimental Therapeutics 243, 86-90.

Tay, S.S.W., Wong, W.C. & Ling, E.A. (1984). An ultrastructural study of the

neuronal changes in the cardiac ganglia of the monkey (Macaca fascularis) following unilateral vagotomy. Journal of Anatomy 138, 67-80.

Tokimasa, T. (1984). Muscarinic agonists depress calcium-dependent G_K in bullfrog sympathetic neurones. Journal of the Autonomic Nervous System 10, 107-116.

Tokimasa, T. (1985). Spontaneous muscarinic suppression of the Ca-activated K-current in bullfrog sympathetic neurones. Brain Research 344, 134-141.

Tosaka, T., Chichibu, S. & Libet, B. (1968). Intracellular analysis of slow inhibitory and excitatory postsynaptic potentials in sympathetic ganglia of the frog. Journal of Neurophysiology 31, 396-408.

Trussell, L.O. & Jackson, M.B. (1985). Adenosine activated potassium conductance in cultured striatal neurones. Proceedings of the National Academy of Science. U.S.A. 182, 4857-4861.

Uddman, R., Alumets, J., Densert, O., Håkanson, R. & Sundler, F. (1978). Occurrence and distribution of VIP nerves in the nasal mucosa and tracheobronchial wall. Acta Otolaryngology 86, 443-448.

Uddman, R., Sundler, F. & Emson, P. (1984). Occurrence and distribution of neuropeptide Y-immunoreactive nerves in the respiratory tract and middle ear. Cell and Tissue Research 237, 321-327.

Uddman, R., Ekblad, E., Edvinsson, L., Håkanson, R. & Sundler, F. (1985). Neuropeptide Y-like immunoreactivity in perivascular nerve fibres of the guinea-pig. Regulatory Peptides 10, 243-257.

Urban, L. & Papka, R.E. (1985). Origin of small primary afferent substance P-immunoreactive nerve fibres in the guinea-pig heart. Journal of the Autonomic Nervous System 12, 321-331.

Van Calker, D., Müller, M. & Hamprecht, B. (1979). Adenosine regulates via two different types of receptors, the accumulation of cyclic AMP in cultured

brain cells. Journal of Neuroscience 33, 999-1005.

Vance, W.H. & Bowker, R.C. (1983). Spinal origins of cardiac afferents from the region of the left anterior descending artery. Brain Research 258, 96-100.

Wanke, E., Ferroni, A., Margaroli, A., Ambrosini, A., Pozzan, T. & Meldolesi, J. (1987). Activation of a muscarinic receptor selectively inhibits a rapidly activated Ca^{2+} current in rat sympathetic neurons. Proceedings of the National Academy of Science. U.S.A. 84, 4313-4317.

Watson, M., Yamamura, M.I. & Roeske, W.R. (1983). A unique regulatory profile and regional distribution of [^{3}H] pirenzepine binding in the rat provide evidence for distinct M_1 and M_2 receptor subtypes. Life Sciences 32, 3001-3011.

Weight, F.F. & Votava, J. (1970). Slow synaptic excitation in sympathetic ganglion cells: evidence for synaptic inactivation of K^+ conductance. Science 170, 755-757.

Weihe, E., McKnight, A.T., Corbett, A.D., Hartschuh, W., Reinecke, M. & Kosterlitz, H.W. (1983). Characteristics of opioid peptides in the guinea-pig heart and skin. Life Sciences 33, Supplement, Vol. 1, 711-714.

Weihe, E., Reinecke, M. & Forssmann, W.G. (1984). Distribution of vasoactive intestinal polypeptide-like immunoreactivity in the mammalian heart. (Interrelation with neurotensin and substance P-like immunoreactive nerves). Cell and Tissue Research 236, 527-540.

Welford, L.A. & Anderson, W.H. (1988). Purine receptors and guinea-pig trachea: evidence for a direct action of ATP. British Journal of Pharmacology 95, 689-694.

West, G.A. & Bellardinelli, L. (1985). Correlation of sinus slowing and pacemaker shift caused by adenosine in rabbit SA node. Pflügers Archiv 403, 66-74.

Westfall, D.P., Stitzel, R.E. & Rowe, J.N. (1978). The postjunctional effects of neural release of purine compounds in the guinea-pig vas deferens. European Journal of Pharmacology 50, 27-38.

Wharton, J., Polak, J.M., Bloom, S.R., Will, J.A. & Brown, M.R. (1979). Substance P-like immunoreactive nerves in the mammalian lung. Investigative Cell Pathology 2, 3-10.

Widdicombe, J.G. (1987). Nervous control of airway tone. In Bronchial Hyperresponsiveness, ed. Nadel, J.A., Pauwels, R. & Snashhall, P.D., pp. 46-67. Oxford: Blackwell Scientific Publications.

Williams, M. (1987). Purinergic receptors and central nervous system function. In Psychopharmocology: The Third Generation of Progress, ed. Meltzer, Y., pp. 289-301. New York: Raven Press.

Wood, J.D. (1984). Enteric neurophysiology. American Journal of Physiology 247, G585-G598.

Wood, J.D. & Mayer, C.J. (1979). Adrenergic inhibition of serotonin release from neurons in guinea pig Auerbachs plexus. Journal of Neurophysiology 4, 594-603.

Yamauchi, A. (1973). Ultrastructure of the innervation of the mammalian heart. In Ultrastructure of the Mammalian Heart, ed. Challice C.E. & Virágh, S., pp. 127-178. New York, London: Academic Press.

Yamauchi, A., Fujimaki, Y. & Yokota, R. (1975a). Reciprocal synapses between cholinergic postganglionic axons and adrenergic innervation in the cardiac ganglion of the turtle. Journal of Ultrastructural Research 50, 47-57.

Yamauchi, A., Yokota, R. & Fujimaki, Y. (1975b). Reciprocal synapses between cholinergic axons and small granule-containing cells in the rat cardiac ganglion. Anatomical Record 181, 195-210.

Yasui, S., Ishizuka, S. & Akaike, N. (1985). GABA activates different types of chloride-conducting receptor ionophore complexes in a dose-dependent manner. Brain Research 344, 176-180.

Yatani, A., Goto, M. & Tsuda, Y. (1978). Nature of catecholamine-like actions of ATP and other energy rich nucleotides on the bullfrog atrial muscle. Japanese Journal of Physiology 28, 47-61.

Yeh, J.Z., Oxford, G.S., Wu, C.H. & Narahashi, T. (1976a). Interactions of aminopyridines with potassium channels in squid axon membranes. Biophysics Journal 16, 77-81.

Yeh, J.Z., Oxford, G.S., Wu, C.H. & Narahashi, T. (1976b). Dynamics of aminopyridine block of potassium channels in squid axon membrane. Journal of General Physiology 68, 519-535.

Yip, P., Palombini, B. & Coburn, R.F. (1981). Inhibitory innervation to the guinea-pig trachealis muscle. Journal of Applied Physiology: Respiratory and Environmental, Exercise Physiology 50, 374-383.